The Spatio-Temporal Influence of Atmospheric Circulations on Hydroclimate in Great Britain

HARRY WEST

A thesis submitted in partial fulfilment of the requirements of the University of the West of England, Bristol for the degree of Doctor of Philosophy.

Department of Geography & Environmental Management, Faculty of Environment and Technology, University of the West of England, UK.

March 2023

Abstract

Atmospheric circulations have an important influence on regional climate. Understanding the relationships between circulations, rainfall and streamflow at a regional and catchment scale is therefore of interest to water and environmental managers. However previous work exploring circulation-climate relationships across Great Britain have been limited spatially and temporally or have been restricted by data availability and in the number of circulations assessed.

This PhD research aims to address these limitations and contribute to our understanding of the relationship between atmospheric circulations and British hydroclimate at a high spatio-temporal resolution over long (50-100 years) historic time periods. This research finds that strong rainfall and flow relationships are present with the North Atlantic Oscillation (NAO), in particular in the north-west where strong positive correlations (r=0.6-0.9) and spatially significant precipitation hotspots persist during winter (e.g. there is a >70% likelihood of significant wet/dry conditions in some NW areas related to the phase of the NAO). However, the strength and consistency of the NAO-rainfall-flow relationship varies spatially and temporally, and in some regions the occurrence of significant wet/dry conditions is almost equally likely under both NAO+ and NAO- phases. In response, this research explores the combined influence of various other atmospheric circulations, revealing the role of circulations such as the East Atlantic Pattern (EA) in influencing hydroclimate in particular across the southern, central and eastern regions (R^2=0.6-0.8). This research presents a new high spatio-temporal resolution understanding of the effect of atmospheric circulations and how they influence rainfall and streamflow both individually and in combination (e.g. in some catchments concurrent NAO+/EA- conditions are associated with >50% of severe meteorological drought events).

This research has implications for the inclusion of circulation indices in water and environmental management practice. NAO forecasting work has developed in recent years, and the findings of this research suggest there is potential to factor these forecasts into water management planning in the north-western region which has strong NAO-rainfall-flow relationships. However even accurate NAO forecasts may have a limited role in management in the southern and central regions, where this research shows the EA and other circulations may be more influential. If (improved) monthly forecasts of these circulations were possible, then these indices would potentially have value for water/environmental managers across Great Britain.

Table of Contents

Common Acronyms

- CEH: Centre for Ecology & Hydrology
- EA: East Atlantic Pattern
- EAWR: East Atlantic Western Russia Pattern
- GEAR: Gridded Estimates of Aerial Rainfall
- IHU: Integrated Hydrological Unit
- NCAR: National Centre for Atmospheric Research
- NOAA: National Oceanic and Atmospheric Administration
- NAO: North Atlantic Oscillation
- NAO+: North Atlantic Oscillation Positive Phase (same applies for EA+, SCA+, EAWR+ and POL+)
- NAO-: North Atlantic Oscillation Negative Phase (same applies for EA-, SCA-, EAWR- and POL-)
- NAOI: North Atlantic Oscillation Index
- $NAOI_{PC}$: North Atlantic Oscillation Index (Principal Components Based)
- $NAOI_{ST}$: North Atlantic Oscillation Index (Station Based)
- POL: Polar/Eurasia Pattern
- SC: Standardised Coefficient
- SCA: Scandinavian Pattern
- SLP: Sea Level Pressure
- SPI: Standardised Precipitation Index
- SPI-1: Standardised Precipitation Index calculated with a one-month accumulation period (same applies for any number following SPI, e.g. SPI-3, SPI-12).
- SSI: Standardised Streamflow Index
- SSI-1: Standardised Streamflow Index calculated with a one-month accumulation period (same applies for any number following SSI, e.g. SSI-3, SSI-12).

Introduction

The Influence of Atmospheric Circulations on Hydroclimate in Great Britain

Atmospheric-oceanic circulations (also referred to as teleconnections) have a significant influence on regional climate. Across the North Atlantic and Europe a number of circulations were identified by Barnston and Livezey (1987). The most historically well-researched circulation is the North Atlantic Oscillation (NAO) - the primary mode of climate variability in the region (Hurrell et al. 1997; Rodwell et al. 1999). The NAO represents the difference in sea level pressure (SLP) between two dipoles: the Icelandic Low and Azores High (Hurrell et al. 2003). Previous studies have explored the relationship between the phase and strength of the NAO and regional climate in Great Britain. Strong positive correlations between the NAO and rainfall have been reported in the north-western regions (Wilby et al. 1997; Simpson & Jones 2014; Afzal et al. 2015; Rust et al. 2018). Relationships between summer rainfall and the NAO have also been noted, however these are generally weaker and more spatially consistent across Great Britain than winter rainfall correlations (Folland et al. 2009; Hall & Hanna 2018).

As the NAO has an influence on rainfall, it stands to reason that river flows may also have a relationship to the phase and strength of the circulation, as changing rainfall distributions propagate through catchments (Kingston et al. 2006). NAO-rainfall-flow relationships have been found across the North Atlantic and Europe (Kingston et al. 2007; 2009; Wrzesinski & Paluszkiewicz 2011; Berton et al. 2017) and in Great Britain specifically (Phillips et al. 2003; Burt & Howden 2013; Rust et al. 2021a). Beyond river flow control, associations between the NAO and groundwater levels (Lavers et al. 2015; Rust et al. 2019) and water temperatures (Wilby & Johnson 2020) have also been found. Studies have also related the phase of the NAO to hydrological extremes (Burt & Howden 2013; Rust et al. 2019; Chen et al. 2021). However, the propagation of NAO-rainfall deviations through the hydrological cycle is moderated by catchment characteristics such as terrain, landcover and geology (Phillips et al. 2003; Rust et al. 2021a).

Continuing to develop an understanding of the effect of the NAO on climate, and subsequently hydrology and water resources, is timely as in recent years advances have been made in our ability to predict the circulation several months in advance, especially during winter (Parker et al. 2019; Athanasiasdis et al. 2020; Smith et al. 2020). Although forecasting potential at monthly timescales remains limited, with better predictions for longer timescales (Kent et al. 2022). There is also potential to include the NAO in streamflow modelling and flood predication (Wedgbrow et al. 2005; Donegan et al. 2021; Moulds et al. 2022), and weather generators used by water companies (Serinaldi & Kilsby 2012; Dawkins et al. 2022). However, spatio-temporal variability and non-stationarity in NAO-rainfall relationships may be a limiting

factor in the inclusion of even highly accurate NAO forecasts in water and environmental management decision making (Hall & Hanna 2018; Rust et al. 2021b).

Beyond the NAO, a number of other atmospheric circulations exist in the North Atlantic and European region (Barnston & Livezey 1987), including the East Atlantic Pattern (EA), Scandinavian Pattern (SCA), East-Atlantic West-Russia Pattern (EAWR) and the Polar/Eurasia Pattern (POL). Whilst these circulations are arguably less influential than the NAO, studies have found relationships with European climate, which vary across spatial and temporal scales (Bueh & Nakamura 2007; Moore & Renfrew 2012; Casanueva et al. 2014; Ionita 2014; Zubiate et al. 2014; Mellado-Cano et al. 2019; Gao et al. 2019). This suggests that the strength and phase of these other circulations may explain some of the NAO-rainfall signature variability discussed above. Studies have also explored how different combinations of atmospheric circulation indices may allow for a more complete understanding of climate variability (Moore et al. 2013; Comas-Bru & McDermott 2014). Recent research also suggests that the EA in particular may become predictable in late autumn/early winter (Thornton et al. 2023).

Figure 1 presents the NOAA (National Oceanic and Atmospheric Administration) monthly indices for the NAO, EA, SCA, EAWR and POL circulations between 1950-2015 (NOAA 2021a). All five circulations show variability in their strength and phase (positive/negative) over the period. All indices have an average value ~0 (i.e. close to neutral conditions) (Table 1). The EA index is unique in that it shows a weak positive trend over the period 1950-2015 (also reported by Mikhailova & Yurovsky 2016) highlighting a general shift towards more frequent positive phases of the circulation from ~1990 onwards. The other circulation indices show no temporal trend.

Table 1: Descriptive statistics of the five atmospheric circulations.

	Mean	Standard Deviation
NAO	-0.09	1.08
EA	-0.25	1.08
SCA	0.14	0.99
EAWR	0.04	1.10
POL	0.04	1.03

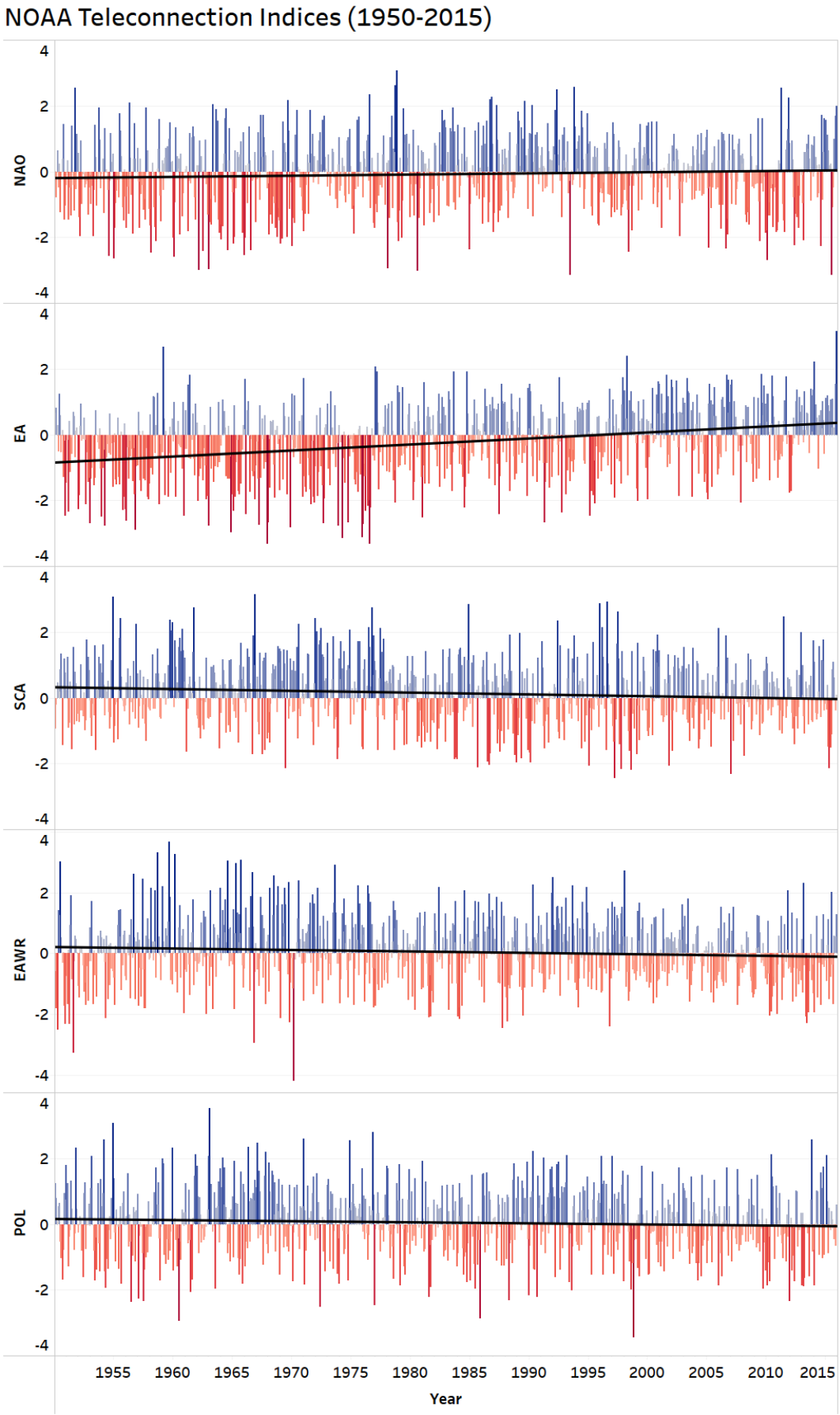

Figure 1: *NOAA Teleconnection Indices for the five atmospheric circulations (1950-2015). Linear trend lines shown in black.*

Limitations of Previous Research & Opportunities for Further Study

As referenced above previous studies have explored, to various extents, the relationship between atmospheric circulations and hydroclimate. However, limitations in previous research present opportunities to continue to develop our understanding of these relationships, and how they vary over space and time in Great Britain.

- **Spatial resolution**: Historically, many studies relied on hydroclimatological variables from relatively few monitoring stations/catchments (Wilby et al. 1997; Folwer & Kilsby 2002; Phillips et al. 2003; Kingston et al. 2013; Kosanic et al. 2014; Lavers et al. 2015) limiting the spatial footprint of any analyses. Further, studies which have used spatially continuous modelled rainfall, have tended to use coarse resolution data and a focus on the wider North Atlantic and European region (Folland et al. 2009; Moore et al. 2013; Comas-Bru & McDermott 2014; Ionita 2014; Mellado-Cano et al. 2019). This limits the ability to infer local/regional scale circulation-rainfall-flow relationships.
- **Temporal resolution**: Many studies have only explored circulation-rainfall-flow relationships during the winter (Moore et al. 2013; Comas-Bru & McDermott 2014; Mellado-Cano et al. 2019). This is despite significant summer circulation-rainfall relationships also being identified (Folland et al. 2009; Hall & Hanna 2018).
- **Data record length**: As a result of relying on station-measured datasets, some previous research has been limited by data record length, with studies exploring relationships over 30-50 year periods (Wilby et al. 1997; Folwer & Kilsby 2002; Kingston et al. 2013; Lavers et al. 2015).
- **Number of circulations**: Many studies have only focused on NAO-climate-flow relationships (Phillips et al. 2003; Burt & Howden 2013; Rust et al. 2018; 2021a), and whilst others have explored various combinations of atmospheric circulation indices and how they influence rainfall and other climatic variables, they have been limited in number (two/three circulations) and by the spatial/temporal resolution considerations above (Moore et al. 2013; Comas-Bru & McDermott 2014; Mellado-Cano et al. 2019).

Research Aim and Objectives

This research aims to contribute to our understanding of the relationship between atmospheric circulations and the hydroclimate of Great Britain at a high spatio-temporal resolution and over long historic time-periods.

To address this aim research objectives were established to:

1. **Quantify the influence of the NAO on rainfall and streamflow across long-term (50-100 years) historic spatio-temporal signatures.**
2. **Investigate the extent to which catchment characteristics moderate circulation-rainfall deviations propagating to streamflow.**
3. **Assess long-term variability in monthly NAO-rainfall signatures.**
4. **Assess the influence of a range of other circulations on rainfall and evaluate the relative importance of the NAO over space and time.**
5. **Assess the explanatory potential of atmospheric circulation combinations for the British hydroclimate and explore the implications for water/environmental management decision making.**

In this research high spatial resolution refers to the use of 1-5km gridded precipitation datasets and modelled flows for a large number (291) of catchments. Meanwhile high temporal resolution refers to monthly scale analysis, whereas many other studies have been conducted at longer multi-year, annual or seasonal timescales.

Methodological Overview

Hydroclimatological Datasests

Over the past 5-10 years there has been an increase in the number of historic modelled hydroclimatological datasets being published for Great Britain by the Centre for Ecology and Hydrology (CEH). These datasets have high spatial and temporal resolutions and cover long historic time periods. Standardised indicators calculated from these datasets allow evaluation of wet/dry and high/low flow conditions (and severity) relative to a standard baseline period. When combined with monthly circulation indices from NCAR and NOAA, these datasets, including gridded rainfall (Tanguy et al. 2016) and Standardised Precipitation Index (SPI) time series (Tanguy et al. 2017a; 2017b), modelled flows for a large number (~300) of catchments and associated Standardised Streamflow Indices (Smith et al. 2018; Barker et al. 2018), offer an opportunity to explore circulation-rainfall-streamflow associations across Great Britain at high resolution and over long time periods, which was not previously possible.

Table 2 presents an overview of the different secondary datasets used in this research and provides and assessment of quality indicators and potential limitations of each.

Table 2: Details of the secondary datasets used in this research.

Dataset	Source	Key Details	Quality Indictors/Limitations
Circulation Indices			
NAO Index (Station Derived) ($NAOI_{ST}$)	NCAR	• Monthly NAOI (1864-2015) calculated using station-measured SLP data.	• An advantage of ST indices is they have few modelling/analytical assumptions and have long record lengths. • The main limitation is that the stations are fixed locations and so indices may not capture conditions as the NAO dipoles move across the year.
NAO Index (Principal Components Derived) ($NAOI_{PC}$)	NCAR	• Monthly NAOI (1899-2015) calculated through a principal components analysis of gridded SLP data.	• PC derived indices better represent circulations across the year as they are calculated using gridded SLP datasets (in other words they are not limited by dipole mobility). • The NOAA indices are simultaneously modelled allowing for direct comparisons in circulation phase/strength to be made. • A limitation of the NOAA indices for multiple circulations is they have a shorter record length than the NCAR NAO indices (1950-present).
NOAA Circulation Indices (NAO/EA/SCA/EAWR/POL)	NOAA	• Monthly circulation indices (1950-2015) calculated using the PC-based approach of Barnston & Livezey (1987).	
Precipitation			
Gridded Estimates of Aerial Rainfall (GEAR)	UK CEH (Tanguy et al. 2016)	• 1km gridded monthly rainfall dataset (1890-2015). • Calculated by interpolating observed rainfall at gauged sites. • The GEAR dataset has been developed according to the guidance provided in BS 7843-4:2012 (Tanguy et al. 2016).	• GEAR data is sensitive to the number of, and distance between, rainfall gauges used in the interpolation. • A distance threshold of 100km is set between stations - where this is exceeded no interpolated rainfall value is calculated. • Higher uncertainty is found in older rainfall grids due to fewer observations available as model inputs. This also results in a greater number of 1km pixels where the 100km threshold for calculation is exceeded.

Gridded Standardised Precipitation Index (SPI)	UK CEH (Tanguy et al. 2017)	• 5km gridded monthly SPI dataset – calculated for multiple accumulation periods (1862-2015). • Standard period of 1961-2010. • Gamma distribution fitted to historic rainfall in calculation (the European standard – Stagge et al. 2015). • Underlying rainfall dataset is the Met Office 5km rainfall grids.	• The SPI is calculated using the Met Office rainfall grids; therefore there is less historic variability in the interpolation due to the addition of recovered historic rainfall records. • The SPI data has a coarser spatial resolution than GEAR. Although over large regions this is unlikely to cause notable differences in any spatial calculations. This may be an important consideration for smaller catchments. • IHU's are administrative groupings of catchments used in the organisation of flow measurement and hydrometric data management (Kral et al. 2015). They therefore represent a practical unit of analysis for understanding circulation-hydroclimate associations.
Standardised Precipitation Index for IHU Groups	UK CEH (Tanguy et al. 2017)	• As above, however calculated for the IHU Groups of Great Britain. • IHU's are derived from the CEH Integrated Hydrological Digital Terrain Model (IHDTM) (Kral et al. 2015).	
Streamflow			
Historic Modelled Daily Flows for Great Britain	UK CEH (Smith et al. 2018)	• Daily reconstructed flows for 303 catchments (1891-2015). • Generated using the GR4J model. • Dataset used represents the best performing run of 500 ensemble members.	• GR4J model parameters were assessed against observed flows from NRFA. Modelled data found to be a quality representation of flows (Smith et al. 2019). • Model was calibrated using multiple evaluation metrics (500,000 runs). • Flow time series derived for the top performing 500 ensemble members. • Smith et al. (2019) note the potential of this dataset to allow for long-term investigations which were not previously possible. • This research uses the best performing flow estimate, and therefore does not consider the minimum/maximum flow estimates.

Standardised Streamflow Index (SSI)	UK CEH (Barker et al. 2018)	• SSI for 303 catchments – calculated for multiple accumulation periods. • Standard period of 1961-2010. • Tweedie distribution fitted to historic flows in calculation. • Underlying flow data is the Historic Modelled Daily Flows described above (based on the top performing flow estimate)	• The SSI was derived from the historic flows noted above and so the same quality measures apply. • Tweedie distribution was applied after an evaluation of different distributions for UK flows (Svensson et al. 2017).

Analytical Methods

The secondary datasets outlined in Table 2 are used throughout the work presented in this thesis. A number of (spatial) statistical analyses are undertaken using these datasets. This section presents an overview of these different techniques.

Standard Statistical Analysis

- **Correlation analysis**: Correlation analysis is a common tool for exploring the association between teleconnections and hydroclimate (Almendra-Martín 2022). Pearson correlation analysis evaluates the linear relationship between two variables whilst Spearman's rank correlation quantifies the association between two ranked variables (Rogerson 2014). The correlation coefficient is a measure of the strength of association between two variables and is often mapped to explore the spatiality in the relationship (e.g. Folland et al. 2009; Burt & Howden 2013; Rust et al. 2018). Alongside the correlation coefficient the probability that the result of that test might have occurred by chance (the p-value) is also calculated. The smaller this value, the more statistically significant the result is, and there is higher confidence that the result of the test is true. A significance threshold of 5% (p=0.05) is commonly used (Rogerson 2014). However, when undertaking multiple tests on a dataset there is a higher potential of Type I errors (false significant positives) occurring. To address this, p-value adjustments for multiple testing can be used. A simple adjustment is the Bonferroni correction ($Bonferroni\ corrected\ p = \frac{\alpha}{n}$), however this approach is conservative in its nature and can result in the removal of many significant results. An alternative approach when undertaking many tests with the same dataset is to use a False Discovery Rate (FDR) corrected p-value (Benjamini & Hochberg 1995) which is less conservative and designed for use with large datasets (Haynes 2013).

- **Regression analysis**:
    - **Univariate regression**: A univariate regression describes the relationship between an independent variable and one explanatory variable. The R^2 value is used to report the strength of the relationship and the extent to which the explanatory variable explains the variability of the independent variable.
    - **Multivariable regression**: Multivariable regression describes the relationship between an independent variable and multiple explanatory variables. As above the R^2 value reports the strength of any relationship. Standardised coefficient (SC) values for each explanatory variable can be used compare the relative size of the effects of the explanatory variables. SC values have been used to identify the dominant circulations affecting hydroclimate (e.g. Chun et al. 2019).
    - **Quantile regression**: Linear regression assumes a linear relationship between the independent and explanatory variables. Quantile regressions allows for an assessment of the relationship at different quantiles of the dependent variable and has been used in hydroclimatic research (e.g. Amini et al. 2019).

Spatial Statistics

Spatial statistical methods allow for an assessment of significance in the spatial distribution of values within a dataset. Their application to the field of hydroclimatology is relatively novel, with several having origins in health and crime GIS applications (Ord & Getis 1995; Scott & Warmerdam 2021).

- **Moran's I**: The Moran's I statistic is a measure of spatial autocorrelation. It determines whether a spatial distribution of values is significantly clustered/dispersed or randomly distributed (Esri 2022b). In the calculation of the Moran's I a conceptualisation of spatial relationships is required. This is a definition of the spatial relationship between features in a dataset; guidance by software developers in determining this is provided to achieve optimal results (Esri 2022c).
- **Space-time analysis**:
    - **Getis-Ord Gi***: The Getis-Ord Gi* statistic (Getis & Ord 2010) identifies clusters of significantly high/low values within a spatial dataset - identified as hot or cold spots with varying confidence (90, 95 or 99%). The statistic indicates whether the spatial clustering of high/low values is more pronounced than would be expected in a random distribution (Esri 2021a). A conceptualisation of spatial relationships is required. The Getis-Ord Gi* statistic can be calculated at multiple time intervals to allow for an assessment of the consistency of significant spatial patterns.

    - **Space-Time Clustering**: This analysis groups features with similar values across space-time using a k-means clustering algorithm (Esri 2020). The clustering algorithm can determine the optimal number of clusters to maximise within cluster value similarity and between cluster differences. This is evaluated using the pseudo-F statistic (Esri 2020).
- **Similarity analysis**: Similarity analysis determines the similarity of features to a specified candidate feature based on a number of attributes. A similarity index is calculated for each feature by standardising the attributes using a z-score transformation where the mean of all of the attributes is subtracted from the attributes of the candidate feature, the differences are then squared and totalled (Esri 2022a).

Research Outputs

Peer-Reviewed Journal Articles

The main body of this thesis is comprised of six peer-reviewed journal articles, published between 2019-2022. The six papers are listed below and variably draw on the datasets and analytical approaches outlined in the previous section:

- **Paper 1**: West, H., Quinn, N. & Horswell, M. (2019). Regional Rainfall Response to the North Atlantic Oscillation in Great Britain. *Hydrology Research*, Vol.50(6), 1549-1563.
- **Paper 2**: West, H., Quinn, N. & Horswell, M. (2022). Spatio-Temporal Propagation of North Atlantic Oscillation (NAO) Rainfall Deviations to Streamflow in British Catchments. *Hydrological Sciences Journal*, Vol.67(5), 676-688.
- **Paper 3**: West, H., Quinn, N. & Horswell, M. (2021). Spatio-Temporal Variability in North Atlantic Oscillation Monthly Rainfall Signatures in Great Britain. *Atmosphere*, Vol.12(6), 763.
- **Paper 4**: West, H., White, P., Quinn, N. & Horswell, M. (2022). The Spatio-Temporal Influence of Atmospheric Circulations on Monthly Precipitation in Great Britain. *Atmosphere*, Vol.13(3), 429.
- **Paper 5**: West, H., Quinn, N. & Horswell, M. (2021). Monthly Rainfall Signatures of the North Atlantic Oscillation & East Atlantic Pattern in Great Britain. *Atmosphere*, Vol.12(11), 1533.
- **Paper 6**: West, H., Quinn, N. & Horswell, M. (2022). The Influence of the North Atlantic Oscillation & East Atlantic Pattern on Drought in British Catchments. *Frontiers in Environmental Science*, Vol.10, 754597.

Table 3 below maps how each of the six research papers presented in the thesis address the overall projects aim and objectives outlined in the previous section.

Table 3: Mapping the Research Objectives against the six published articles.

Research Objective	Paper	Papers Aims & Objectives
1. Quantify the influence of the NAO on rainfall and streamflow across long-term (50-100 years) historic spatio-temporal signatures.	• **Paper 1**: Regional Rainfall Response to the North Atlantic Oscillation in Great Britain. • **Paper 2**: Spatio-Temporal Propagation of North Atlantic Oscillation (NAO) Rainfall Deviations to Streamflow in British Catchments.	• To quantify long-term effects of the NAO on rainfall and streamflow using high resolution data. • To quantify differences in rainfall/streamflow under NAO+/NAO- conditions. • To evaluate the effect of the choice of NAOI on resultant rainfall signatures.
2. Investigate the extent to which catchment characteristics moderate circulation-rainfall deviations propagating to streamflow.	• **Paper 2**: Spatio-Temporal Propagation of North Atlantic Oscillation (NAO) Rainfall Deviations to Streamflow in British Catchments.	• To compare rainfall and streamflow NAO signatures across a large number of catchments. • To identify the characteristics of catchments with similar/different NAO rainfall and flow signatures. • To classify catchments based on their resilience to NAO-rainfall deviations propagating to flow.
3. Assess long-term variability in monthly NAO-rainfall signatures.	• **Paper 3**: Spatio-Temporal Variability in North Atlantic Oscillation Monthly Rainfall Signatures in Great Britain.	• Assess the statistical significance and consistency of NAO-rainfall spatial signatures. • Establish the spatial distribution of consistent or variable monthly NAO-rainfall responses.
4. Assess the influence of a range of other circulations on rainfall and evaluate the relative importance of the NAO over space and time.	• **Paper 4**: The Spatio-Temporal Influence of Atmospheric Circulations on Monthly Precipitation in Great Britain.	• Quantify the individual relationship between different circulations and monthly rainfall. • Assess the combined influence of circulations on monthly rainfall. • Identify the relative importance of each circulation in influencing monthly rainfall and how this varies over space/time.

5. Assess the explanatory potential of atmospheric circulation combinations for the British hydroclimate and explore the implications for water/environmental management decision making.	• **Paper 5**: Monthly Rainfall Signatures of the North Atlantic Oscillation & East Atlantic Pattern in Great Britain. • **Paper 6**: The Influence of the North Atlantic Oscillation & East Atlantic Pattern on Drought in British Catchments.	• Quantify the combined effect of the NAO and EA on rainfall volume/distribution using high resolution datasets. • Understand the effect of the NAO and EA on drought conditions, and how deficits propagate through catchments. • Evaluate how using the NAO and EA in combination might lead to an enhanced understanding of rainfall/flow distribution. • Discuss the potential utility of circulation index forecasts for water/environmental management.

Additional Conference Papers

In addition to the peer-reviewed articles which comprise the main body of this thesis, the following papers have been presented at national and international conferences between 2018-2023:

- West, H., Quinn, N. & Horswell, M. (2023). Atmospheric Circulations and Drought Conditions in British Catchments: Highlighting the Role of the East Atlantic Pattern. *European Geosciences Union General Assembly*, Vienna, Austria, April 2023.
- West, H., Quinn, N. & Horswell, M. (2021). Mapping Spatio-Temporal Variability in NAO Rainfall Signatures. *vEGU2021: Gather Online,* April 2021.
- West, H., Quinn, N. & Horswell, M. (2020). Mapping wet-dry signatures of the North Atlantic Oscillation (NAO) in British catchments. *EGU2020: Sharing Geoscience Online,* May 2020.
- West, H., Quinn, N. & Horswell, M. (2019). Spatio-Temporal Linkages between the North Atlantic Oscillation (NAO), Rainfall and Streamflow in Great Britain: Evidence from New Historic Datasets. *American Geophysical Union Fall Meeting,* San Francisco, California, USA, Dec 2019.
- West, H., Quinn, N. & Horswell, M. (2019). Spatial Variations in the Relationship Between Precipitation and Streamflow in Great Britain. *International Union of Geophysics & Geodesy General Assembly,* Montreal, Canada, July 2019.
- West, H., Quinn, N. & Horswell, M. (2019). A Space-Time Geostatistical Approach to Exploring the Stationarity of North Atlantic Oscillation Driven Wet/Dry Conditions in Great Britain. *European Geosciences Union General Assembly,* Vienna, Austria, April 2019.

- West, H., Quinn, N. & Horswell, M. (2019). Examining Spatial Variations in the Utility of SPI as a 1 to 3 Month Ahead Streamflow Indicator. *UK Drought & Water Scarcity Conference: Addressing Current & Future Challenges,* University of Oxford, UK, 20-21 March 2019.
- West, H., Quinn, N. & Horswell. M. (2018). The Spatial Signature of the North Atlantic Oscillation in Monthly Rainfall Patterns in Great Britain (1899/1900-2014/2015). *British Hydrological Society National Symposium,* London, UK, 12-13 September 2018.
- West, H., Quinn, N., Horswell, M. (2018). Regionalising the Influence of the North Atlantic Oscillation in Seasonal Hydrological Extremes in Great Britain. *European Geosciences Union General Assembly,* Vienna, Austria, April 2018.

Paper 1: Regional rainfall response to the North Atlantic Oscillation (NAO) across Great Britain

Citation: West, H., Quinn, N. & Horswell, M. (2019). Regional Rainfall Response to the North Atlantic Oscillation in Great Britain. *Hydrology Research*, Vol.50(6), 1549-1563.

Published: 25th May 2019.

Contributions: This paper was produced during the early stages of the PhD process. During these early stages a large variety of new datasets were released by UK CEH, and NQ suggested that the NAO would be an interesting phenomenon to explore. HW undertook the data preparation, spatial analysis and the presentation of the results. HW led on the writing of the initial draft, which was shared for feedback with NQ and MH and finalised for submission.

Changes to Original Paper:

- Figure 1: Minor edits have been made to the placement of the labels to enhance clarity and closer align with the text.

Abstract

The North Atlantic Oscillation (NAO) has been long studied as the primary teleconnection affecting the British and European climate. However, previous studies have focused on extremes or have been spatially and temporally limited. In recent years, our ability to predict the NAO has improved. Also, new research is emerging, suggesting that the NAO is a key driver of hydrological extremes. These factors mean that there is a renewed value in enhancing our understanding of how the NAO influences general rainfall patterns. In this study, we spatially analyse correlations between NAO indices and monthly rainfall data and the Standardised Precipitation Index. We also map mean monthly rainfall differences under NAO-positive and -negative conditions. Based on our results, we identify three main observations: (I) there is sensitivity in the rainfall patterns to the chosen NAO index; (II) there is a clear winter north/west and south/east divide in rainfall patterns; and (III) the NAO does have an effect on summer rainfall patterns, although the spatiality of these patterns is less distinctive than in winter. As far as we are aware, this is the first national scale, monthly NAO–rainfall analysis undertaken for a long period.

Introduction

Climate change is expected to significantly alter hydro-meteorological and climatological processes and patterns in Great Britain (Garner et al. 2017; Kendon et al. 2018), and understanding the characteristics and impacts of wet and dry extreme events remains a challenge (Jones et al. 2014; Watts et al. 2015; Parry et al. 2016; Van Loon et al. 2016). Oceanic–atmospheric circulation interactions (also referred to as teleconnections) have a key influence on regional climate (Wilby et al. 1997; Rust et al. 2018). Given the close interconnectedness of the climate and hydrological system, floods and droughts are inherently driven by larger-scale meteorological processes and their interactions with local-scale catchment characteristics (Wilby & Quinn 2013; Van Loon & Laaha 2015; Barker et al. 2016; De Luca et al. 2017; Huang et al. 2017). Furthering our understanding of the influence of teleconnections on local and regional climate is therefore key in water and climate resilience planning.

Weather in Great Britain is highly variable, often fluctuating between wet and dry conditions (e.g. the very wet winter of 2013/2014 and the dry summer of 2018). The North Atlantic Oscillation (NAO) characterises some of the variability of the North Atlantic jet stream and has been acknowledged as the primary teleconnection affecting the British climate (Wilby et al. 1997; Hurrell et al. 2003). For example, Rodwell et al. (1999) suggested that the NAO is the single most important teleconnection influencing climate variability in the Northern Hemisphere, and Sweeney & O'Hare (1992) linked variations in precipitation to large-scale NAO fluctuations across Europe. More recent studies continue to emphasise the influence of the NAO on British and European climatic patterns (Comas-Bru & McDermott 2014; Varouchakis et al. 2018). In a review of studies relating to hydro-meteorological signal control of the NAO, Rust et al. (2018) highlight the strong relationship (positive correlations) between the NAO and precipitation during winter months across Northern Europe.

The NAO can be defined in various ways but generally represents the sea level pressure (SLP) fluctuation between Iceland and the Azores that has been well defined in meteorology since the 19th century (Hur rell et al. 2003). Many studies use the NAO Index (NAOI) as a quantitative measure of the pressure gradient between Iceland and the Azores (e.g. Simpson & Jones 2014; Bonaccorso et al. 2015; Spencer & Essery 2016).

The NAO fluctuates between a positive and negative state; each state is known to produce characteristic climatic patterns over Great Britain and mainland Europe (Hall & Hanna 2018; Rust et al. 2018). A positive NAO (which represents stronger than the usual difference in the SLP between Iceland and the Azores) is generally associated with stormy and wet winter conditions as winds from the west dominate bringing warmer air and storms across the North Atlantic region. A negative NAO represents the reverse with a weaker than usual difference in the SLP. Winds from the east and north-east are more frequent, bringing with them cold air,

while the adjusted position of the jet stream leads to weaker and less frequent storms. As a result, Europe is more likely to experience cold, calm and dry winters (Hurrell et al. 2003; Baker et al. 2017). Many studies have associated fluctuations of the NAO to precipitation patterns in Great Britain specifically (Figure 1).

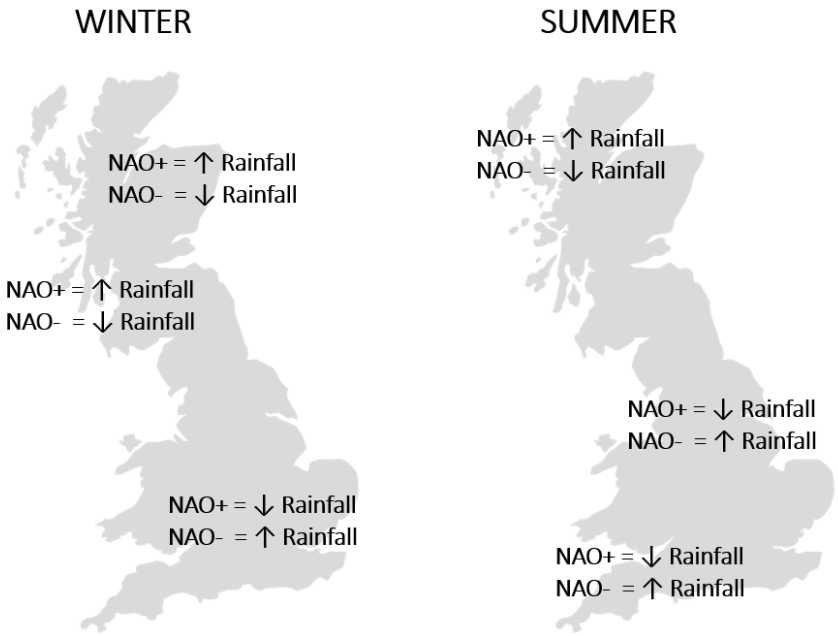

Figure 1*: Generalised NAO winter and summer rainfall patterns from previous studies (Wilby et al. 1997; Fowler & Kilsby 2002; Burt & Howden 2013; Kosanic et al. 2014; Simpson & Jones 2014; Afzal et al. 2015; Hall & Hanna 2018). A more detailed summary of these findings can be found in Table S1 in the Supplemental Material.*

The impact of the NAOI phase during winter and summer is known to differ significantly (Folland et al. 2009; del Rio et al. 2011; Sun & Wang 2012). While the strength of regional correlations with rainfall of the winter (December, January, February (DJF)) NAO Index ($NAOI_W$) and summer (June, July, August (JJA)) NAO Index ($NAOI_S$) vary across Great Britain, a general relationship is evident, particularly for the north/west of the country. There is a positive correlation between positive NAOIW values and winter precipitation, and a negative correlation between positive $NAOI_S$ values and summer precipitation. Conversely, negative $NAOI_S$ values are correlated with higher summer precipitation, and negative $NAOI_W$ values are associated with lower winter precipitation (Folland et al. 2009; Simpson & Jones 2014; Hall & Hanna 2018).

Earlier analyses of relationships between NAOI and precipitation are typically based on precipitation data from relatively few sites (e.g. Wilby et al. 1997; Fowler & Kilsby 2002) and short record lengths (e.g. Fowler & Kilsby 2002; Afzal et al. 2015). Studies have also tended to focus on extremes rather than more general wet/dry patterns (e.g. Simpson & Jones 2014) and have had a clear emphasis on the relationship between the NAO and winter climate (e.g. Comas-Bru & McDermott 2014; Rust et al. 2018). This seems an understandable focus as intense and more frequent rainfall is typically associated with low pressure systems coming

from the tropics – the movement of these systems being directly associated with the NAO phase (Wilby et al. 1997; Fowler & Kilsby 2002). While relationships between winter rainfall and the NAO are now well defined, the influence of the NAO on regional summer climates is less clear (Folland et al. 2009) and is limited to some evidence, suggesting negative correlations between the NAOI and summer precipitation in all regions apart from the far north-west Scotland (Hall & Hanna 2018).

The availability of nationally consistent gridded precipitation datasets, such as the Centre for Ecology and Hydrology (CEH) Gridded Estimates of Areal Rainfall (GEAR) dataset (Tanguy et al. 2016), now provides new opportunities for analysis of teleconnection drivers of rainfall. Similarly, the recent publication of the gridded Standardised Precipitation Index (SPI) time series (Tanguy et al. 2017a) offers an additional advantage as the data are conveniently scaled in relation to relative wetness and dryness over a specified rainfall accumulation period (Hannaford et al. 2011). As a result, the SPI has been used to assess the spatial signature of teleconnections in rainfall in regions worldwide (Irannezhad et al. 2015; Kingston et al. 2015). The availability of these datasets is particularly important in helping develop a deeper understanding of the spatial structure of associations between North Atlantic teleconnections and precipitation, and any time-related/seasonal trends in this structure. Previous studies using similar spatially consistent data have tended to rely on UKCP09 estimates (e.g. Spencer & Essery 2016), which are known to have limitations/pre-conditions for estimates of summer rainfall (Met Office 2016). New understanding of the relationships between hydrological extremes and the NAO (Rust et al. 2019), coupled with improvements in long-range NAO prediction ability (Scaife et al. 2014; Smith et al. 2016; Baker et al. 2017; Weisheimer et al. 2017) and the potential for the NAOI to be used in hindcasting (Smith et al. 2019), also means that there is now a renewed value in developing a more complete understanding of how the NAO influences the spatial distribution of seasonal rainfall across Great Britain. Being able to infer more detailed regional rainfall responses in relation to predicted teleconnection behaviour would be of significant value in helping inform strategic responses to weather extremes (Palin et al. 2016; Bell et al. 2017; Clark et al. 2017).

In this study, we aim to examine the spatial distribution of rainfall (using both GEAR monthly rainfall estimates and the SPI) under positive and negative NAOI conditions. This represents the first monthly, nationally consistent spatial analysis undertaken for a long record (1899–2015, 117 water years) addressing the full wet/dry continuum.

Methods

Data

To represent the NAO condition, the NAOI was used. This study makes use of two commonly used NAOI calculation methods: the station-based method ($NAOI_{ST}$) which calculates the index based on the fixed SLP station measured data, and the principal component analysis method ($NAOI_{PC}$) comprising a time series of the leading empirical orthogonal function of Atlantic SLP (Hurrell et al. 2003). Both datasets were obtained from the US National Centre for Atmospheric Research (https://climatedataguide.ucar.edu/climate-data) at a monthly interval for the water years October 1899–September 2015.

Monthly total rainfall values (1899–2015) were obtained from the CEH GEAR dataset (Tanguy et al. 2016). GEAR provides interpolated monthly estimates of total rainfall on a 1 km grid and has a relatively complete spatial coverage of Great Britain. The rainfall estimates are derived from the Met Office national database of observed precipitation. The GEAR dataset was selected due to its high spatial resolution and long record period (when compared to similar UK rainfall datasets). The SPI, as defined by Mckee et al. (1993), was also sourced from CEH at monthly intervals (1899–2015) with a 1-month rainfall accumulation period (SPI-1) (Tanguy et al. 2017a). This dataset is provided at 5 km gridded spatial resolution and is derived based on the monthly GEAR dataset. The SPI is calculated by fitting a gamma distribution (Stagge et al. 2015) to historical precipitation time series. The years 1961–2010 are used as the baseline for SPI calculation. The SPI is a standardised index, with positive values representing wetter than normal conditions for a given period, and negative values representing drier than normal conditions. The SPI is normally distributed with a mean of 0 (i.e. near-normal conditions) and a standard deviation of 1. Theoretically, values can range from −5 (extremely dry) to +5 (extremely wet), although approximately 95% of values occur within the range of −2 to +2, and 68% within the range of −1 to +1 (Tanguy et al. 2017a).

Regional rainfall/SPI and NAOI correlations

The Met Office Climate Districts are commonly used in similar studies (e.g. Wilby et al. 1997; Simpson & Jones 2014) and, as they represent areas of relatively homogeneous climate, were the chosen spatial unit of analysis for the correlation of regional mean monthly total rainfall/SPI-1 and the NAOI. Mean monthly rainfall (based on GEAR data) and SPI-1 were calculated by spatially averaging all gridded values within each climate district. The mean monthly rainfall/SPI-1 for the study period are then correlated with the NAOI calculated using both the ST and PC method for Great Britain. Exploratory analysis established normality and linear relationships, so a Pearson correlation was deemed appropriate. In our analysis, we defined seasons as winter (DJF), spring (MAM), summer (JJA) and autumn (SON).

Calculation of the deviation of mean monthly rainfall and mean SPI-1

The monthly NAOI was classified into a state of positive, negative or neutral NAO phase. In light of the known limitations of the $NAOI_{ST}$ method of calculation, especially in the summer months (see Discussion), only the $NAOI_{PC}$ method was used for further analysis. The NAO phase was defined as half the standard deviation plus/minus the long-term mean (after Berton et al. 2017). The NAO-positive phase was calculated to be NAOI >0.502 and -negative phase <−0.503. Months with a $NAOI_{PC}$ between these values represent an NAO neutral state. Each month in the GEAR and SPI-1 dataset was categorised using these values into being in either an NAO-positive, NAO-negative or NAO-neutral state (Figure 3). For each month, all datasets for a given phase were averaged on a cell-by-cell basis to produce a mean dataset for each month under each NAO condition. For the GEAR data, the NAO-positive/-negative mean monthly datasets were then subtracted from the NAO neutral dataset for that month. This produced a final dataset to show deviation in mean monthly rainfall in the given phase compared to when NAO is neutral.

The deviations in mean monthly rainfall and mean SPI-1 values were then spatially averaged using the Met Office Climate Districts. In order to examine how similar each region's response to the NAO was over the study period, the mean deviation from neutral NAO conditions/mean monthly SPI of each district was then correlated against values from the other districts. Regions which are positively correlated suggest areas where rainfall displays a similar NAO response and vice versa for negatively correlated regions.

Results

Regional mean correlations

Figure 2 shows the results of the regional mean SPI correlation analysis with $NAOI_{ST}$ and $NAOI_{PC}$. Similar seasonal variations were produced using both rainfall measures (SPI and monthly GEAR data). Positive correlations suggest high SPI/GEAR values (i.e. high rainfall) when under NAO-positive conditions and vice versa for NAO-negative. Negative correlations are indicative of low SPI/GEAR values (i.e. low rainfall) when NAO is positive and vice versa for NAO negative. Significant positive correlations between $NAOI_{ST}$ and monthly rainfall are found in the west of Great Britain, and particularly in the north, for all months between October and April. While significant correlations persist in ‘Scotland North’ and ‘Scotland West’ in spring (MAM), they are largely absent in England and Wales. June is characterised by a marked gradient with most of England showing significant negative correlations. July and August are characterised by a notable lack of significant correlations between $NAOI_{ST}$ and the rainfall measures, with July largely having weak positive correlations and August a combination of weak positive and negative correlations. September to November sees a change in the correlation strength; such

as that by November, 'England East and North East' is the only region not showing a significant positive correlation.

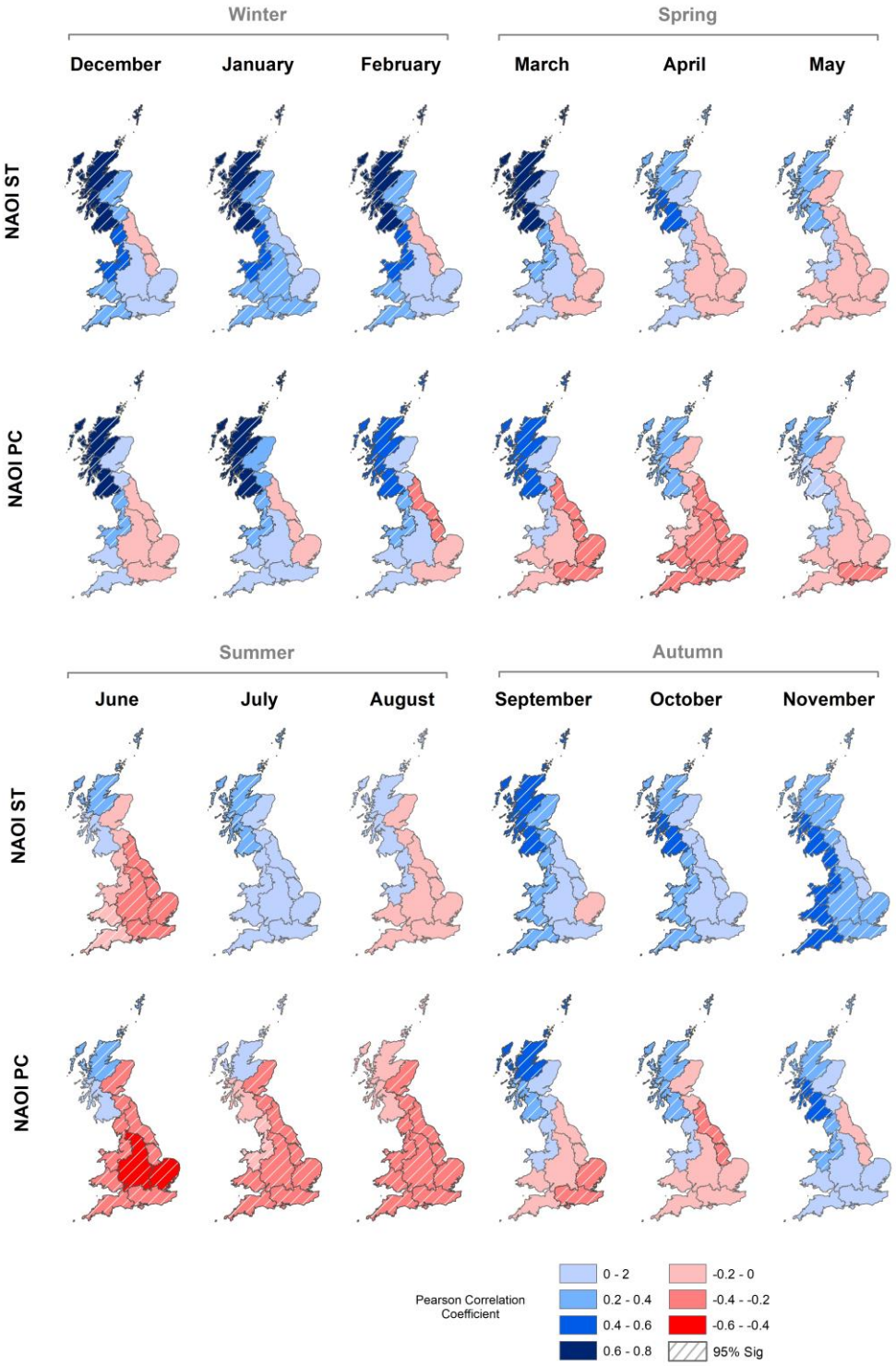

***Figure 2**: Correlations between $NAOI_{ST}$ and $NAOI_{PC}$ with regional mean SPI-1. The two NAOI methods show similar patterns in the winter months (DJF), with strong positive correlations in the North. However, note that the significant differences observed between the two NAOIs in the summer months where stronger negative correlations are observed using $NAOI_{PC}$.*

$NAOI_{PC}$ produces similar spatial patterns to those described above; significant positive correlations are found for the north and west for the months of September to May. During this time, the central and southern regions fluctuate between positive and negative correlations (of varying significance). $NAOI_{PC}$ correlations vary from those gained through using $NAOI_{ST}$ in spring (MAM), where more pronounced negative correlations are present in the central and southern regions. This signal is enhanced moving into the summer months where all of England, Wales and 'Scotland East' see significant negative correlations between SPI and $NAOI_{PC}$.

NAO-phase definition

Figure 3 shows the results of the NAO-phase classification process using the method of Berton et al. (2017) on the $NAOI_{PC}$ time series. Based on our definition of phases, the NAO was in a positive or negative phase for approximately 53% of the time between October 1899 and September 2015. The NAO-phase occurrence and intensity were clearly more pronounced during the winter (DJF) rather than summer (JJA) months, especially for NAO-positive.

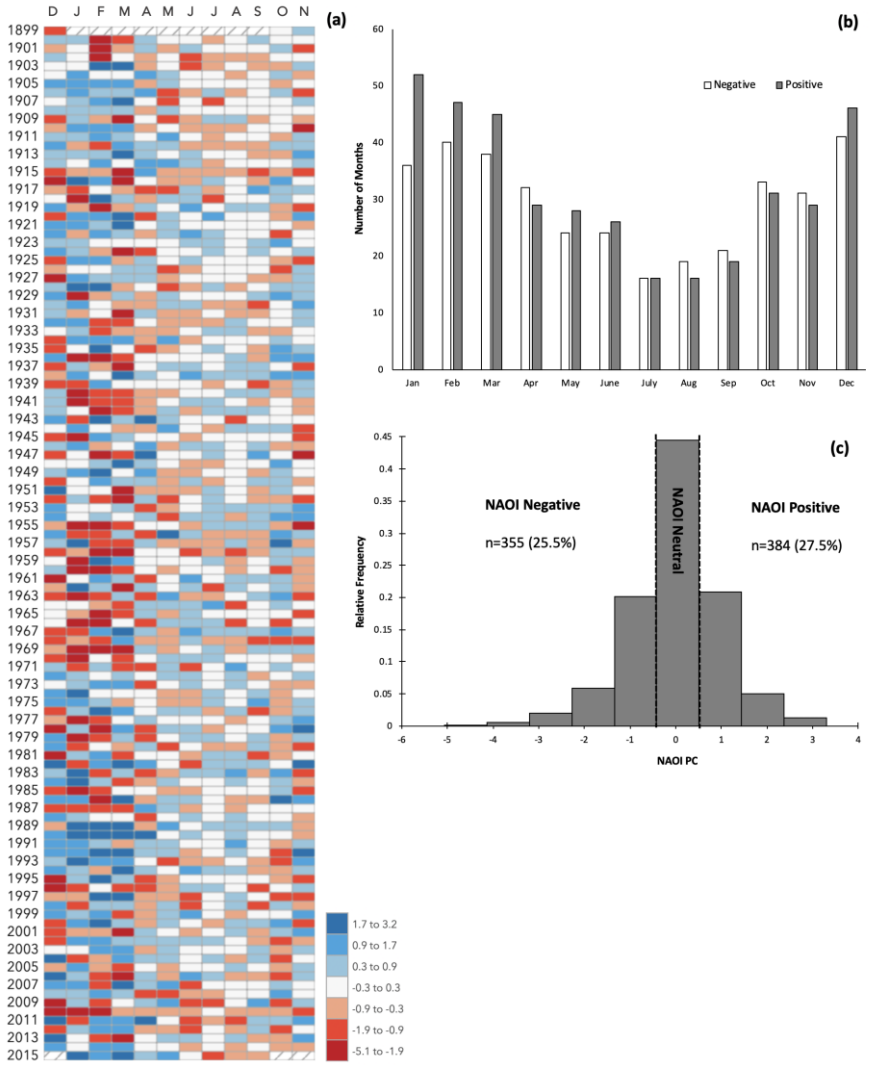

***Figure 3**: (a) Heatmap showing the temporal distribution of NAO-phase occurrence and intensity, (b) the frequency of occurrence of each NAO phase per month and (c) the distribution of $NAOI_{PC}$ classification over the study period (1899–2015).*

Spatial patterns of deviation in mean monthly rainfall and mean SPI-1 under NAO phase

Figure 4 shows the NAO phase-dependent deviation in mean monthly rainfall (calculated as the difference from mean monthly rainfall under NAO neutral conditions). Clear regional and seasonal differences are observed in both NAO-positive and -negative phases. The most notable deviations in rainfall occur in the north of Great Britain during the winter months (DJF) (in particular in Scotland North and Scotland West). These regions receive significantly more or less rainfall under NAO-positive or -negative conditions, respectively. These conditions are inverted in the south/east of Great Britain, with these regions seeing decreases/increases under NAO-positive/-negative, however to a lesser extent compared to the north. This creates a strong winter spatial signal in rainfall under the two NAO conditions, with the north/west and south/east showing clear regional differences. The magnitude of the deviation is also different in terms of enhanced wetness/dryness; NAO-positive tends to produce wetter conditions than NAO-negative does dry. This suggests that the enhancing effect on rainfall is more marked than the dampening effect. Only small changes in rainfall under NAO conditions were found in southern Great Britain throughout winter. Moving into spring (MAM), this spatial pattern is largely retained, although the magnitude of the deviation in rainfall decreases with time.

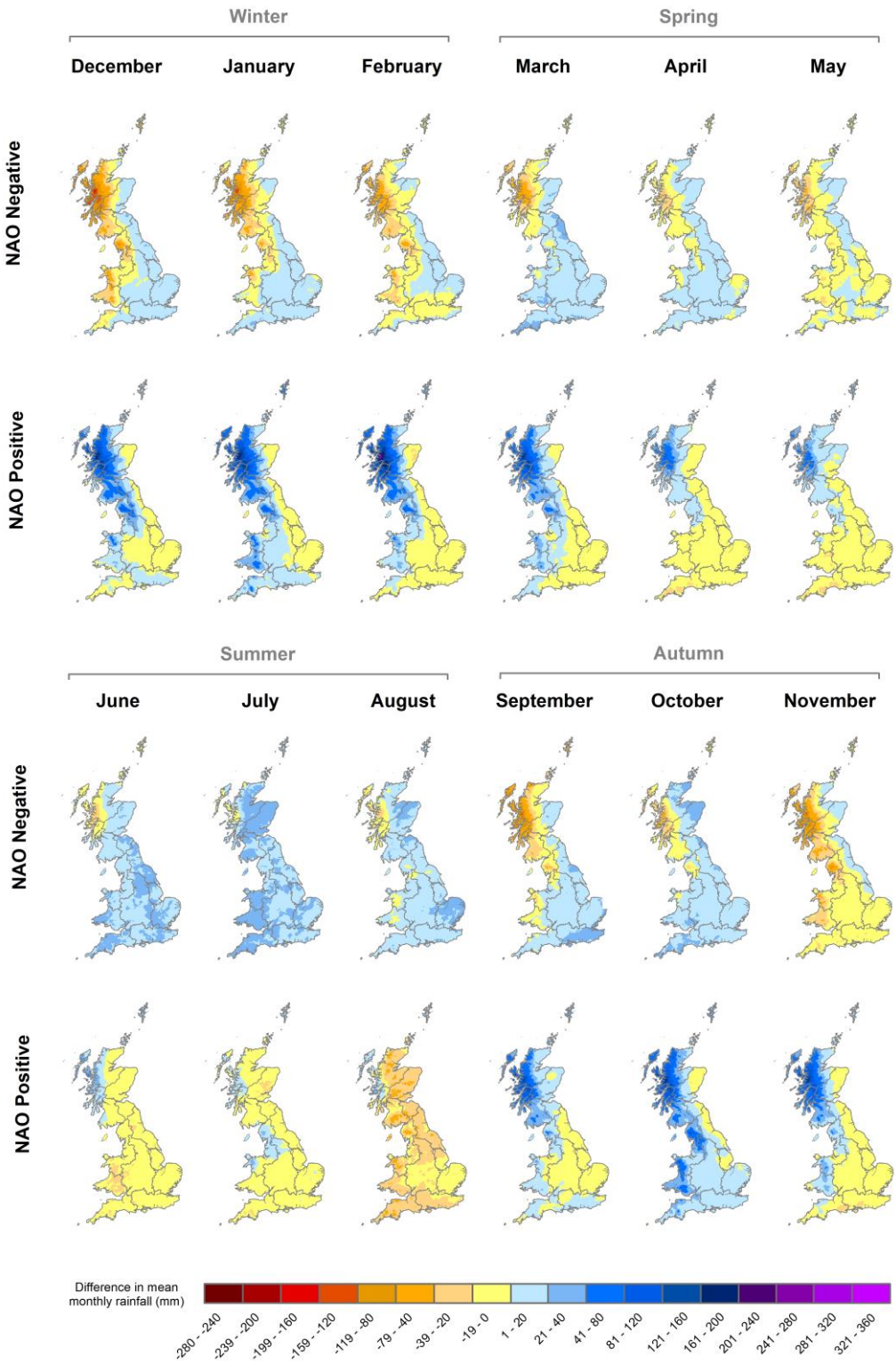

***Figure 4**: Difference in mean monthly rainfall values (mm) under the NAO phase for the period October 1899–September 2015. Note the significant increase/decrease in rainfall in the north/west during the winter months and the wetter/drier conditions observed during the summer months under NAO-positive/negative (GEAR data from Tanguy et al. 2016).*

Significant differences in rainfall are also observed during the summer months (JJA). However, the relative increases/decreases in rainfall under NAO-positive/-negative are broadly inverted

when compared to the winter months (DJF). The NAO spatial signature now seems more apparent in the southern and central regions, with NAO-positive resulting in notably drier conditions, and NAO-negative producing wetter conditions (up to approximately ±30 mm), most notably in July and August in South West England and South Wales. The clear north/west and south/east spatial divide in rainfall patterns observed in the winter months becomes less pronounced, with the central and southern regions of Great Britain being more homogeneous in their rainfall response, and much of the country displaying a similar rainfall deviation to these regions. In the autumn months (SON), the patterns in rainfall deviation start to invert again becoming more similar to those described above in winter and the regional differences in the NAO rainfall response become more discernible.

Figure 5 shows the comparable analysis undertaken using mean monthly SPI-1 data. As with the deviation in monthly rainfall analysis discussed above, notable seasonal and spatial patterns in wet/dry conditions are present when NAO is in either a positive or negative phase. During the winter (DJF), the north has significantly high/low SPI values, representing wetter than normal/drier than normal conditions under positive/negative NAO. Mean SPI-1 values follow a similar winter spatial pattern to the monthly deviation analysis – a clear north/west and south/east difference in the NAO response. While during the summer months (JJA) this pattern is broadly inverted and more homogeneous spatially so that the central and southern regions experience the most notable drier/wetter conditions under NAO positive/negative, with the rest of the country experiencing similar conditions.

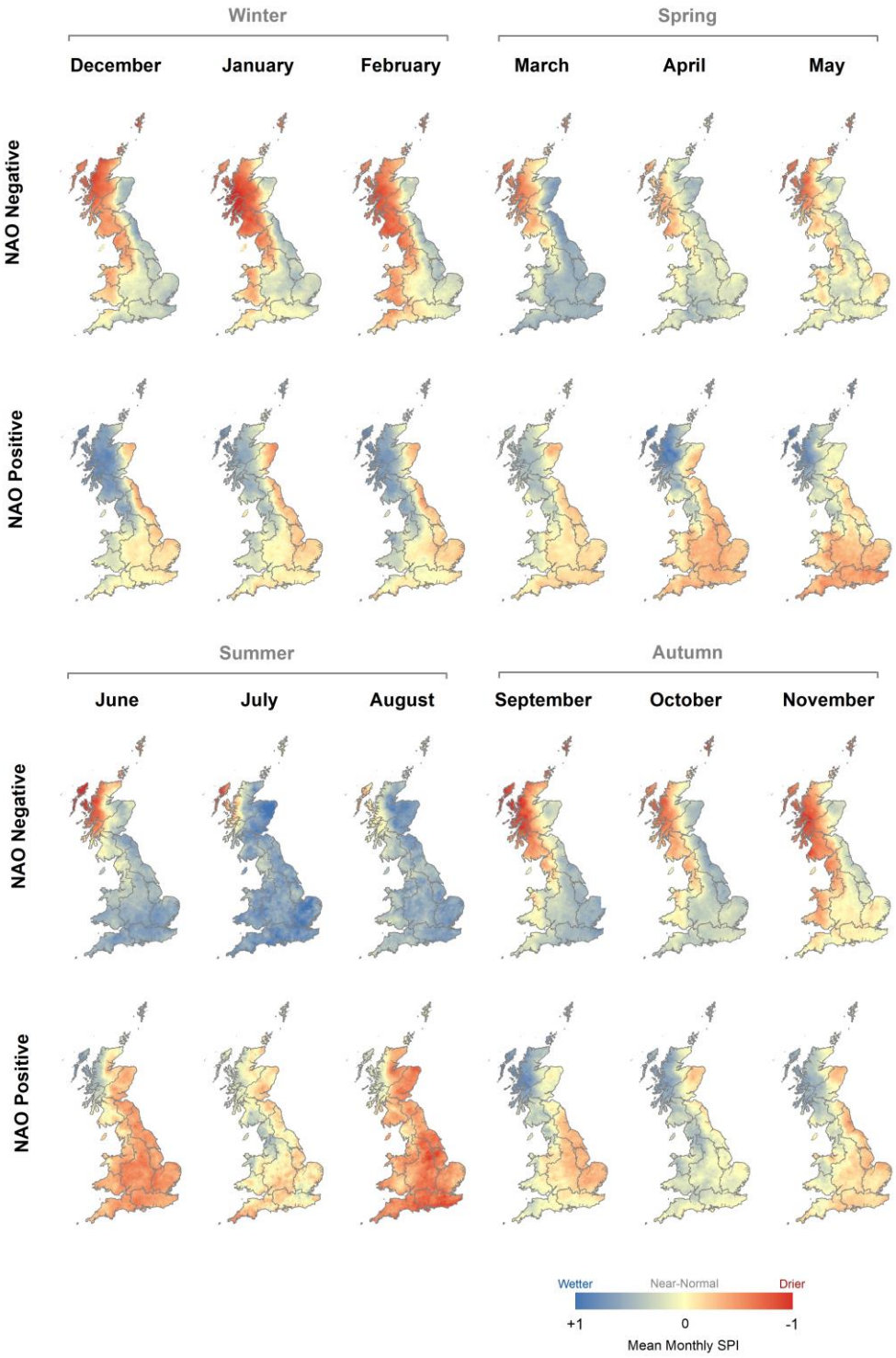

***Figure 5**: Mean monthly SPI-1 under NAO conditions for the period October 1899–September 2015. Note the significantly wetter/drier conditions in the north/west during the winter months and the wetter/ drier conditions observed during the summer months under NAO positive/negative. (SPI data from Tanguy et al. 2017a).*

Figure 6 shows the results of the correlation analysis to assess the similarity of each region's response to NAO-positive/-negative conditions (derived using both the mean monthly rainfall deviation data and mean SPI-1 data). Regions which show positive correlations in their spatial

mean rainfall deviation or SPI-1 respond to the NAO in a similar way (i.e. they are wetter or drier by a similar magnitude), while regions which are negatively correlated show where differences occur in the regional response to NAO fluctuation. Similar spatial patterns in correlation are present using both mean monthly rainfall deviation (from the GEAR dataset) and mean monthly SPI-1.

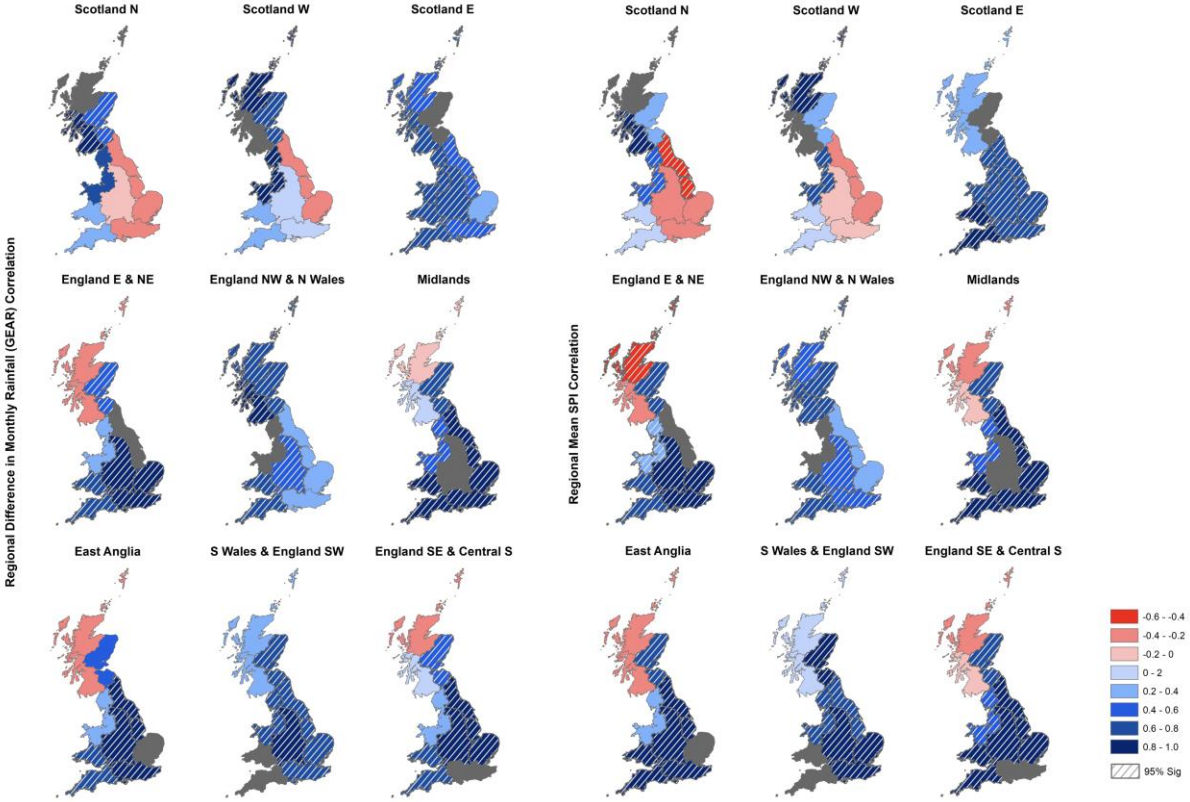

***Figure 6**: Spatial representation of Pearson correlation coefficient values for assessing the similarity of rainfall response across the nine Met Office Climate Districts. Note the positive correlations of the north-western/south-eastern regions and the negative correlations between Scotland and the Southern/Central regions. Block grey areas indicate the region used as the independent variable in the correlation analysis.*

'Scotland North' and 'Scotland West' are strongly positively correlated at the 95% confidence level; these regions are also positively correlated with 'England North West and North Wales'. This suggests that these regions respond to the NAO in a similar manner. A clear grouping is also evident in the positive correlations around the South East of Great Britain, with 'East Anglia' and 'England South East and Central South' showing similar responses. Based on these regional groupings of positive correlations, the north/west and south/east divide present in the previous analysis is clearly shown in the correlation maps, most notably in the southern regions' negative correlation with 'Scotland North' and 'Scotland West'.

However, the clear spatial signature is only evident in the correlations between certain regions. Some regions, such as 'Scotland East', 'South Wales and England South West', and the 'Midlands', show consistent significant positive correlations with almost all other regions. This

suggests that these regions respond in a similar way to the NAO and tend to follow the general pattern in deviation/mean SPI-1 as the rest of the country.

Discussion

This research sets out to examine the spatiality of rainfall patterns under NAO-positive and -negative conditions using nationally consistent, high-resolution datasets (Tanguy et al. 2016, 2017a). This extends previous NAO rainfall studies based in Great Britain as it considers the full wet/dry continuum, rather than just weather extremes, across a full year, rather than just the winter months, and is not restricted in terms of available data as we use spatially consistent gridded datasets rather than analysis based on selected stations/regions. A range of methods were implemented to achieve this, and based on the convergence of evidence in the results, we identify three main observations: (I) the sensitivity of spatial rainfall analysis to the chosen NAOI calculation method; (II) the clear north/west and south/east divide in rainfall signatures under NAO-positive and -negative conditions during the winter months; and (III) the NAO does appear to have some influence over summer (JJA) rainfall, although the spatiality of these patterns is less distinctive when compared to winter. These will now be discussed in turn.

The first observation relates to the use of different NAOI measures; in our study, namely the decision to use $NAOI_{ST}$ or $NAOI_{PC}$. Pearson correlation analysis was undertaken using both SPI-1 and monthly GEAR data against both NAOI measures (Figure 2). While the two measures generally produced similar spatial patterns in correlation strength during the winter months, notable differences were observed during spring (MAM) and summer (JJA). $NAOI_{PC}$ produced significant strong negative correlations in the southern and central regions during this period, while the $NAOI_{ST}$ method produced much weaker correlations which were not significant. This implies that if $NAOI_{ST}$ is used, then under positive NAO much of the country is wetter than average, and drier under NAO negative. However, if $NAOI_{PC}$ is used, then this pattern is the opposite. Therefore, had the later analysis to examine rainfall spatiality been undertaken using the $NAOI_{ST}$ method, it is likely that the results would have been far less conclusive as those gained from the $NAOI_{PC}$ method (Kosanic et al. 2014).

The poor representation of summer NAO has been noted as a key limitation of the station-based method of NAOI calculation (Pokorná & Huth 2015). The main limitation is the mobility of the dipoles of the NAO across any given year (Jung et al. 2003; Beranová & Huth 2008). During the summer months, the main pressure 'action points' of the NAO (the Azores high and Icelandic low) move away from the position of the in situ monitoring stations, measurements from which are used to calculate $NAOI_{ST}$, due to a combination of factors including the East Atlantic and Scandinavian teleconnections (Hurrell & Van Loon 1997; Moore et al. 2013) which have also been attributed to UK meteorological patterns (Comas-Bru & McDermott 2014; Zubiate et al. 2017). Based on our correlation analysis and the potential

misrepresentation of summer rainfall patterns under NAO conditions, we support the conclusions of Hurrell & Deser (2009) who suggest that there is no unique or universally accepted way to define the NAO, and those of Pokorná & Huth (2015) who advise caution in the selection of NAO representative indices and recommend non-station-based methods of calculation for summer NAO representation due to circulation spatial variability.

The spatial analysis of rainfall patterns under NAO-positive and -negative phase informs our second and third main observations. The accepted general understanding of NAO impact on rainfall across Great Britain during the winter months is to associate winter storms with NAO-positive and colder/drier winters with NAO-negative indices (Visbeck et al. 2001). Our analysis of both deviations in mean monthly rainfall and mean SPI-1 values shows a clear north/west and south/east spatial divide in response to NAO during the winter months, implying a less spatially generalisable response than suggested above. The north/west of Great Britain, in particular, sees rainfall patterns significantly alter under different NAO phases. Under NAO positive, these regions see notable increases in monthly rainfall, while under NAO negative there is a notable decrease. Although to a smaller magnitude, the opposite response is observed in the southern and eastern regions. This clear winter spatial pattern in rainfall under NAO positive/negative conditions is also evident in the regional correlation analysis, where the northern and western regions are positively correlated with each other, but negatively correlated with the southern and eastern regions. This winter spatial pattern has been observed in other studies over shorter timescales using station-based measurements of rainfall, thus indicating some long-term consistency in this pattern (Wilby et al. 1997; Fowler & Kilsby 2002; Burt & Howden 2013; Simpson & Jones 2014). Although this winter pattern coincides with upland/lowland topographic patterns, which may enhance rainfall under NAO-positive conditions (Burt & Howden 2013), the notable dry conditions under NAO-negative suggest that the interaction between NAO and local characteristics is far more complex. Having an understanding of the generalisable winter NAO rainfall pattern is significant given that in recent years notable advances have been made in our ability to predict winter NAO-phase months in advance (Baker et al. 2017; Hall et al. 2017; Weisheimer et al. 2017). For example, being able to say with some degree of confidence that the NAO will remain in a negative condition over the winter months will allow for early warning water shortage systems in Scotland to be triggered to ensure consistent supply in the upcoming dry period.

The clear spatial pattern during winter which reverses under the two different NAO conditions is likely associated with the location of storm tracks due to altered jet stream location (Visbeck et al. 2001). Long-term storm track analysis (mid-Holocene) suggests that a NAO-positive phase is characterised by a stronger and more northerly/easterly storm track across the Atlantic (Trigo 2006; Brayshaw et al. 2010). This NAO-driven pattern is evident in both precipitation and wind speed records (Burningham & French 2013).

Our analysis shows that the NAO winter spatial pattern continues into spring (MAM), gradually decreasing in discernibility over time; this is explainable by the SLP anomalies associated with winter NAO tending to persist into spring across the Atlantic region (Herceg-Bulić & Kucharski 2014). This change in the NAO rainfall signature over time brings into focus our final main observation. Moving into summer (JJA), the spatial pattern of rainfall under both positive and negative NAO is far less distinctive and more homogenous (Figures 4 and 5). Some regional differences are observable, with the central and southern regions showing the most notable deviation from normal conditions. However, the general direction of this deviation under NAO-positive and -negative conditions is broadly inverted during summer when compared to winter. NAO-positive now produces relatively homogenous dry conditions, and NAO-negative produces wetter conditions. Alongside the NAO, it is likely that high SPI values (high rainfall) are associated with convective storms during the summer months (Kendon et al. 2014). As these systems are small in their spatial influence, this may partly explain the dispersed summer rainfall patterns in Figures 4 and 5.

Conclusion

As the primary teleconnection affecting the British climate, the NAO has been well researched (Wilby et al. 1997; Fowler & Kilsby 2002; Burt & Howden 2013). However, many studies have focused on winter climate and weather extremes and have been based on a limited number of in situ measurements/regions. This study sets out to examine the spatial signatures of NAO phase-dependent precipitation, using nationally consistent datasets. Through correlation and spatial analysis, we draw attention to three observations regarding regional response in rainfall patterns to the NAO: (I) the sensitivity of any analysis to the chosen NAOI; (II) the clear north/west and south/east divide in rainfall signatures during the winter months; and (III) the NAO does appear to have some influence over summer rainfall, although the spatiality of these patterns is less distinctive when compared to winter patterns.

Our results extend the understanding of the NAO's influence on rainfall patterns in Great Britain and suggest that, now more than ever, there is potential to improve our predictive ability of teleconnections and precipitation, allowing for better informed water management decisions. This is important given the potential future impacts of climate change on hydro-meteorological conditions in Great Britain (Watts et al. 2015). In relation to seasonal forecasting and climate projections, this work shows some potential and adds to the growing evidence finding value of including the NAOI in model simulations (Baker et al. 2017; Smith et al. 2019).

It is important to note that our work uses gridded rainfall from the CEH-GEAR dataset, which over the period shows variability in the number of rainfall stations used for interpolation. Therefore, an avenue for future research would be to repeat similar analysis using more temporally consistent Met Office MIDAS (Met Office Integrated Data Archive System) rainfall.

The use of the new CEH SPI data (Tanguy et al. 2017a) also has potential for future research in this area, due to the calculation of multiple accumulation periods ranging from 3 to 24 months. Future research could utilise these longer periods to establish whether there is any lagged effect of the NAO on rainfall patterns. It is also important to note that the NAO cannot explain all of the rainfall spatio-temporal patterns in the UK. NAO rainfall spatial signatures have been found to show variable levels of consistency over long records (West et al. 2019a), and extreme events have been found to occur due to the interaction of multiple teleconnections (Rust et al. 2019). There is therefore still a future need to consider the NAO's interaction with and the general influence of other teleconnections on weather and climate in Great Britain to further improve our predictive capability of seasonal rainfall patterns (Comas-Bru & McDermott 2014; Hall & Hanna 2018).

Supplemental Material

***Table S1**: Findings of previous studies examining the influence of the NAO on precipitation in Great Britain.*

Study	Geographic area	Period	Northern and Scotland, north-west England	Central, southern, north eastern England
Wilby *et al.,* 1997	9 homogeneous precipitation zones as defined after Gregory *et al*. (1991). 7 rainfall stations per region used to spatially average rainfall	1931-1989	Positive correlations between winter NAOI and regional rainfall amounts. All UK regions produced positive correlations in Autumn expect central and southern England.	Negative correlations between winter NAOI and regional rainfall amounts.
Folwer & Kilsby, 2002	Northern England (7 rainfall stations)	1961-1990	Strong correlation between winter precipitation and positive NAO, particularly in western areas.	NA
Burt & Howden, 2013	UK Upland Areas (90 rainfall stations)	Site dependent – between 24 and 181 years (mean =74 years)	Strong positive correlations in the North during winter. Much weaker negative or non-significant	Some small positive correlations in winter, mostly non-significant. Significant negative

			correlations during summer.	correlations in summer.
Kosanic *et al.,* 2014	South West England (5 rainfall stations)	Site dependent - between 1880-2011	NA	Measured precipitation data is negatively correlated with NAO.
Simpson & Jones, 2014	9 homogeneous precipitation zones after Jones & Conway (1997). UKCP09 5km gridded rainfall (Perry & Hollis, 2005).	1766-2011	Positive correlations between winter NAOI and extreme rainfall indices/percentiles. Negative correlations between summer NAOI and extreme rainfall.	Weak negative correlations between winter NAOI and extreme rainfall indices/percentiles. Stronger negative correlations between summer NOAI and extreme rainfall.
Afzal *et al.,* 2015	Scotland (40 rainfall stations)	1961-2000	Suggests positive trends in rainfall are associated with an increase in positive NAO intensity during winter.	NA
Spencer & Essery, 2016	Scotland UKCP09 snow lying grid (Perry & Hollis, 2005)	1875-2013	Scottish snow cover is generally negatively correlated with the NAO index. The strongest correlations between the NAO index and snow cover are found in eastern and southern Scotland.	NA
Hall & Hanna, 2018	11 UK geographic regions UKCP09 5km gridded rainfall (Perry & Hollis, 2005)	1951-2014	Significant positive correlations between NAO and precipitation in winter. Significant negative correlations in summer.	Significant negative correlations between NAO and precipitation in eastern and southern England in winter.

Paper 2: Spatio-Temporal Propagation of North Atlantic Oscillation (NAO) Rainfall Deviations to Streamflow in British Catchments

Citation: West, H., Quinn, N. & Horswell, M. (2022). Spatio-Temporal Propagation of North Atlantic Oscillation (NAO) Rainfall Deviations to Streamflow in British Catchments. *Hydrological Sciences Journal*, Vol.67(5), 676-688.

Published: 3rd March 2022.

Contributions: Initial analysis exploring the spatio-temporal relationships between the NAO and streamflow was undertaken for assessment within the Catchment Hydrology module completed by HW as part of this PhD. This followed a similar analytical framework to Paper 1. Following feedback from NQ and MH this analysis was refined and finalised. HW led on the writing of the initial draft, which was shared for feedback with NQ and MH and finalised for submission.

Changes to Original Paper:

- Figure 2: A spelling error has been resolved.
- Minor edits have been made to the text interpreting Figures 3 and 4 in the Results section. These edits have been made to enhance clarity and align the figures and text,

Abstract

The North Atlantic Oscillation (NAO) teleconnection is often cited as the leading mode of climate variability in Great Britain. The NAO has been found to produce significant rainfall deviations that vary in space and time. This study sought to analyse the effect of the NAO at the catchment scale across a large number of catchments in Great Britain across a long study period (1900–2015). We first quantify the effect of the NAO on rainfall and streamflow at a monthly scale, revealing distinctive spatio-temporal patterns under positive and negative phases of the NAO. Through a comparison of correlation analyses we also explore whether catchment characteristics moderate the propagation of NAO–rainfall deviations to streamflow, and classify catchments based on their resilience and susceptibility to NAO–rainfall deviations. In summary, our analyses combined contribute to an improved understanding of the hydrometeorological impact of the NAO in British catchments.

Introduction

The North Atlantic Oscillation (NAO) characterizes some of the variability in the speed and latitude of the North Atlantic Jet Stream (Woollings et al. 2014) and has long been understood as the primary atmospheric–oceanic circulation (teleconnection) affecting climate in Great Britain (Hurrell and Van Loon 1997, Rodwell et al. 1999, Folland et al. 2009, Rust et al. 2018). The NAO is commonly defined by the sea level pressure variation between the Icelandic low-pressure action point and the Azores anticyclone. Depending on conditions at these locations the NAO fluctuates between positive (NAO+) and negative (NAO−) phases, quantified by the North Atlantic Oscillation Index (NAOI). An NAO+ phase represents a stronger than usual difference between the Icelandic Low and Azores High, whilst an NAO− phase represents a weaker than usual difference (Hurrell et al. 2003).

Variability in the NAO can be explored across different temporal scales – multi-annual or sub-annual (daily/monthly/seasonal). Studies have examined the influence of sub-annual variations in the NAO on precipitation patterns in Great Britain, finding good correlations between the two (Wilby et al. 1997, Fowler and Kilsby 2002, West et al. 2019b). Spatial patterns in the strength and direction of correlations vary seasonally. In the winter months rainfall in the northwestern regions of Great Britain is strongly positively correlated with the NAO, while rainfall in the southern and eastern regions is generally negatively correlated (Simpson and Jones 2014, Rust et al. 2018). Therefore, NAO+ phases typically result in higher rainfall in the northwest, whilst NAO− phases result in drier conditions (West et al. 2019b). Whilst the winter months are marked by this northwest/southeast NAO rainfall signature, in summer the rainfall response is more spatially consistent (West et al. 2019b). Correlations are also typically negative between the NAOI and summer rainfall. This indicates that NAO+/− phases typically result in drier/wetter conditions, respectively, across the country (Folland et al. 2009, Hall and Hanna 2018); the inverse response is seen in winter rainfall in the northwestern regions.

As the NAO influences rainfall, it stands to reason that there may also be a relationship between NAO phase and streamflow, as the changing rainfall distributions propagate through catchments (Kingston et al. 2006). Investigating such climate–rainfall–streamflow relationships is necessary to improve our understanding of hydrological responses and how these might change in the future (Laize and Hannah 2010, Lavers et al. 2010).

Studies have found NAO–flow relationships across the North Atlantic region. In North America, Kingston et al. (2007) and Berton et al. (2017) report significant correlations between the NAO and discharge in New England (alongside the Atlantic Multi-Decadal Oscillation). Significant NAO–flow relationships have also been identified in Europe. Generally, positive winter correlations are found in northern Europe, in particular in the northwestern UK and Scandinavia, and negative correlations are found in southern areas across the southeast of

the UK, France and the Mediterranean basin (Kingston et al. 2009, Wrzesinski and Paluszkiewicz 2011, Burt and Howden 2013, Rust et al. 2021a). NAO signals have also been identified in groundwater hydrographs (Lavers et al. 2015). For example, Rust et al. (2019) report an average of 21.7% of groundwater storage variability across various aquifers in Britain is relatable to seven-year NAO cycles, with stronger relationships found in chalk and sandstone borehole locations in southern England where the NAO periodicity is linked with up to 40% of the groundwater variability. Wilby and Johnson (2020) also report associations between the NAO and water temperatures, which vary in space and time across England.

However, there is also evidence that NAO–rainfall patterns do not propagate into discharge because the characteristics of the catchment's moderate the rainfall-flow transfer, making them less susceptible to NAO-driven rainfall variability. For example, Rust et al. (2021a) note that their identified seven-year NAO–flow relationship was found to be influenced by the response time of subsurface hydrological pathways. Phillips et al. (2003) investigated the relationship between atmospheric–oceanic circulations and discharge in two British catchments: the chalk-dominated Itchen in southern England and the impermeable Ewe in Scotland. The strongest significant NAO–flow relationships were found in the Ewe catchment, especially in winter. Phillips et al. (2003) proposed this was due to its location in the northwest and the dominance of surface runoff pathways. In contrast, the signal of the NAO in the Itchen was limited to the winter months, indicating that for the rest of the year its permeable bedrock and higher storage capacity mean that the catchment is less susceptible to NAO-related rainfall variability due to a more sustained baseflow contribution.

Catchments that lack moderating characteristics, such as permeable bedrock, are more susceptible to NAO-driven rainfall variability, which can be further amplified by topography. Burt and Howden (2013) refer to the "double orographic enhancement" effect, where the NAO significantly increases the natural orographic enhancement of rainfall in upland areas of Britain. These enhanced NAO–rainfall signatures cascade down to streamflow; significant positive correlations were found across 86 flow gauge stations between the NAOI and seasonal river flow totals in winter, spring and autumn (Burt and Howden 2013). The most significant correlations were found in upland areas in northwest Scotland. These close NAO–flow relationships suggest that catchments with certain characteristics lack the ability to moderate NAO-driven rainfall variability. These characteristics include steep topography, low infiltration rates (Sibley 2010) and impermeable bedrock, as in the Ewe described previously (Phillips et al. 2003).

Given the variation in catchment characteristics across Great Britain (Chiverton et al. 2015), improving our understanding of the influence of the NAO on streamflow may allow for more effective water management decisions to be taken. Furthering our understanding of NAO–flow spatio-temporal relationships is also timely because:

1. Our ability to predict NAO variability across multiple temporal scales has notably improved in recent years (Baker et al. 2018; Parker et al. 2019, Athanasiadis et al. 2020, Smith et al. 2020).
2. Research continues to highlight the NAO's role in influencing hydrometeorological extreme events (Burt and Howden 2013, Kingston et al. 2013, Rust et al. 2019, Tsanis and Tapoglou 2019). Catchments with moderating characteristics may prove to be more resilient to NAO-related hydrometeorological extremes.
3. Research by the UK Centre for Ecology and Hydrology (CEH) suggests that the NAOI may be a useful addition to flow forecasting models and could improve forecasting skill particularly in the north and west of Britain (UK Hydrological Outlook 2020). Similar evidence is developing in Irish flow modelling research (Donegan et al. 2021).

As far as we are aware, no study has yet explored NAO–rainfall–flow propagation in British catchments at a high spatial and temporal resolution. The recent release of historical hydrometeorological modelled datasets from CEH offers a new opportunity to undertake such an analysis, which has not previously been possible over long historical time periods for a large number of catchments. There is therefore value in using these new long-term and large-scale datasets to enhance our spatio-temporal understanding of sub-annual relationships between the NAO and streamflow in Britain, and a need to assess the extent to which catchment characteristics can moderate the effect of NAO-related rainfall deviations on discharge.

This study aims to meet this need by:

- Quantifying long-term spatio-temporal relationships between the monthly NAO and rainfall and flows across 291 catchments in Great Britain.
- Evaluating spatio-temporal NAO–rainfall and NAO–flow relationships and identifying the moderating effect of catchment characteristics.
- Defining a classification that identifies catchments most resilient and most susceptible to NAO–rainfall deviations, to improve catchment understanding.

Methods

Many sub-annual NAO studies have focused on winter (e.g. Hurrell 1995, Kingston et al. 2006). However, Bower et al. (2004) noted the importance of examining catchment sensitivity to climatic drivers across a whole annual cycle, and West et al. (2019b) identify that the NAO rainfall spatial signature can vary markedly on a monthly basis. To avoid the recognized dilution of signatures across larger temporal scales, our study initially undertakes a monthly-scale analysis. A summary of the data and methods used in this study is shown in Figure 1

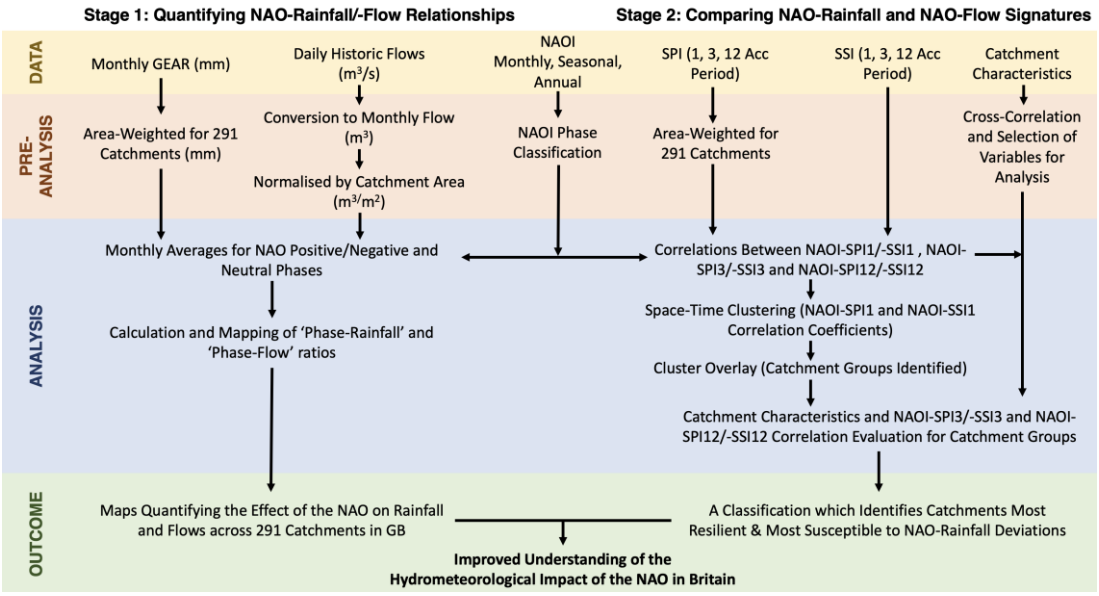

***Figure 1**: Flowchart summarizing the key stages of the analysis.*

Data and Pre-Analysis

NAOIs have long been used in similar research to quantify the NAO (Wilby et al. 1997, Folland et al. 2009, Hall and Hanna 2018, Rust et al. 2018); however, there is no fixed approach to defining the NAO (Hurrell and Deser 2009), and the choice of NAOI can have a notable influence on subsequent analyses. To avoid the known limitations of summer NAOIs calculated using measured sea level pressure data (station-based indices) (Pokorná and Huth 2015), an NAOI derived from a principal components (PC) analysis of the leading empirical orthogonal function of sea level pressure anomalies in the Atlantic region was used (Hurrell et al. 2003). PC-based indices are more accurate representations of spatial patterns of the NAO across a year (National Center for Atmospheric Research (NCAR) 2020). PC-based NAOIs calculated at the monthly, seasonal (December–January–February, DJF and June–July–August, JJA) and annual scales were used in this study, downloaded for the period January 1900–November 2015 from the National Center for Atmospheric Research (NCAR 2020).

The phase of the NAO can be defined in various ways, and classifying the monthly NAOI into positive, negative and neutral phases allows for the identification of clear NAO positive/negative signals as weaker "neutral" conditions can be removed (Berton et al. 2017). In this study the NAO phase was defined as half the standard deviation plus/minus the long-term mean of the NAOI (Berton et al. 2017). NAO+ phases were defined as having an NAOI > 0.502, and NAO− were defined as NAOI < −0.503. Months falling within this range were classified as NAO neutral months.

In Stage 1 of our analysis the NAO signal in rainfall and flows at the catchment scale was quantified. For rainfall, the monthly 1 km Gridded Estimates of Areal Rainfall (GEAR) dataset (Tanguy et al. 2016) from CEH was spatially averaged for each of the 291 catchments across

the analysis period (average rainfall was calculated by area-weighting the 1 km gridded rainfall dataset (Equation 1):

$$R = \sum_{i=1}^{n} r_i \left(\frac{a_i}{A}\right) \quad \text{(Equation 1)}$$

where ri is the rainfall value of the 1 km pixel, ai is the area of the 1 km pixel that overlaps with the catchment boundary, and A is the total catchment area (ai/A is the proportion of the catchment covered by each 1 km pixel).

To represent streamflow a long-term historical dataset, also from CEH, was used. Reconstructions of daily river flows using the GR4J model for the 291 catchments across the analysis period (January 1900–November 2015) were extracted from a larger dataset (Smith et al. 2018). This dataset has been evaluated for high, medium and low flows and was found to produce quality representations of historical flows (Smith et al. 2019). The data used in this study represent the best-performing model from a 500-member ensemble (Smith et al. 2018). Given its long historical record this dataset has been noted as allowing for large-scale and long-term spatio-temporal investigations which have previously not been possible (Smith et al. 2019). The daily reconstructed flows (m^3/s) were converted into monthly volumes (m^3) and normalized by catchment area (m^3/m^2) for each month in the 116-year record. We will refer to this value, representing monthly runoff volume per unit area, as the "monthly flow index."

In Stage 2, standardized indices for both precipitation and flows were used alongside the NAOI. Standardized indices were chosen for this stage of the analysis as they are scaled in relation to relative wetness/dryness (or high flows/low flows) over a specified accumulation period, and have been used in previous studies exploring the teleconnections between atmospheric–oceanic circulations and hydrometeorological signatures (Irannezhad et al. 2015, Kingston et al. 2015, West et al. 2019b). To represent precipitation, we use the CEH 5 km gridded Standardized Precipitation Index (SPI) dataset. The SPI dataset is normally distributed and has a standard period of 1961–2010 (Tanguy et al. 2017a). Area-weighted SPI values, with one-month, three-month and 12-month accumulation periods, were initially calculated for each of the 291 catchments (following Equation (1) and substituting the 1 km gridded rainfall values for the 5 km gridded SPI). For flows, a similar Standardized Streamflow Index (SSI) dataset (Barker et al. 2018) was used. This SSI data was calculated using the reconstructed flow dataset described above (Smith et al. 2018), fitting a Tweedie distribution for a standard period of 1961–2010 (aligning with the SPI) (Barker et al. 2018). As with the SPI data, accumulation periods of one month, three months and 12-months were used. The range of datasets used, and the pre-analysis work, are summarized in Table 1.

Table 1: Datasets used in this study and associated pre-analysis work

Name	Source	Pre-Analysis	Scale
Stage 1:			
North Atlantic Oscillation Index (NAOI)	National Center for Atmospheric Research (NCAR, 2020)	Monthly data categorised into Positive, Negative and Neutral phases.	National scale, monthly index.
Gridded Estimates of Aerial Rainfall (GEAR) (1km x 1km grid)	(Tanguy *et al.,* 2016)	Area weighted per catchment.	Catchment scale, monthly data.
Historic Flows (at gauging station site)	(Smith *et al*., 2019)	Converted to monthly volumes and catchment area-normalised (referred to as the 'monthly flow index')	Catchment scale, monthly data.
Stage 2:			
North Atlantic Oscillation Index (NAOI)	National Center for Atmospheric Research (NCAR, 2020)	NA	National scale, monthly, seasonal (DJF and JJA) and annual indices.
Standardised Precipitation Index (SPI) (5km x 5km grid)	(Tanguy *et al.,* 2017a)	Area weighted per catchment.	Catchment scale, 1-month, 3-month and 12-month accumulation periods.
Standardised Streamflow Index (SSI) (at gauging station site)	(Barker *et al*., 2018)	NA	Catchment scale, 1-month accumulation period.
Various Catchment Characteristics Data	National River Flow Archive	Catchment characteristics were cross-correlated and any factors significantly and strongly related to one-another were removed from the analysis.	Catchment scale.

The first two research aims identified above lend themselves to two distinct analytical stages. The combined outputs of these stages allow for a comprehensive assessment of NAO–rainfall–flow propagation at a monthly scale across a large number of catchments, and an improved understanding of the hydrometeorological impact of the NAO across Great Britain.

Stage 1: Quantifying NAO-Rainfall and NAO-Flow Relationships

The first stage of the analysis sought to quantify NAO–rainfall and NAO–flow relationships across the 291 catchments using the monthly GEAR rainfall and monthly flow index (m^3/m^2) datasets described above:

1. The area-weighted rainfall for each month and each catchment was averaged under NAO positive, negative and neutral conditions.

2. The average rainfall depth under NAO+ conditions was then divided by the average rainfall depth under NAO− conditions for the respective catchments and months.
3. This "phase–rainfall" ratio represents the change in rainfall depth between NAO+ and NAO− phases. A value close to 1 indicates that the catchment-averaged rainfall does not vary between phases, whereas increasing deviations on either side of 1 indicate successively larger rainfall differences between the two phases. A phase–rainfall ratio of 2 would mean that rainfall doubles in NAO+ relative to NAO− phases, and conversely a ratio of 0.5 would mean NAO+ rainfall is half that of NAO− conditions.
4. A similar "phase–flow" ratio was constructed on the basis of the ratio of the catchment area normalized flow (i.e. the monthly flow index defined above) between NAO+ and NAO− phases.

These phase ratios quantify the relative influence of the NAO on rainfall and flows for each month and across all 291 catchments, allowing for the identification of spatio-temporal NAO–rainfall and NAO–flow signatures.

Stage 2: Comparing NAO-Rainfall and NAO-Flow Signatures

Stage 2 of the analysis sought to compare rainfall and flow responses to the NAO to assess whether catchment characteristics moderate the propagation of NAO–rainfall deviations through to streamflow, and to explore how this varies in space and time. Spearman rank correlation tests were undertaken between the monthly NAOI and catchment-weighted SPI1 (SPI with a one-month accumulation period) and NAOI and SSI1.

These two sets of monthly correlations for the 291 catchments were used as separate inputs to a space–time clustering algorithm (Esri 2020). This analysis grouped together catchments with similar monthly NAOI–SPI1/NAOI–SSI1 correlation coefficients across the year. The clustering used a k-means algorithm, with spatially random starting seeds. The similarity in correlation coefficient values across catchments was assessed using the Euclidean distance between the time series values (the square root of the sum of squared differences in coefficient values across time) (Esri 2020). Rather than specify a fixed number of clusters to classify the catchments, the algorithm determined an optimal number of clusters. To do this, 90 space–time clustering solutions were produced, each containing between two and 10 catchment clusters. These clustering solutions were then evaluated using the pseudo-F statistic. This value is a measure of within-cluster similarity and between-cluster difference – in other words, how distinct each cluster is from another. The clustering solution with the highest pseudo-F statistic was identified as the optimal clustering output (Esri 2020). For both sets of correlation time series, the algorithm determined the optimal number of clusters to be four.

The outputs of these analyses were two datasets that presented clusters of catchments with similar NAOI–SPI1/NAOI–SSI1 correlations across the year. These datasets were spatially

overlaid to identify unique combinations of clusters from the two space–time clustering analyses. This resulted in a final classification where "catchment groups" could be identified based on similar NAO–rainfall (represented by the NAOI–SPI1 correlation cluster membership) and NAO–flow (represented by the NAOI–SSI1 correlation cluster membership) responses.

The local catchment characteristics of each catchment group (the unique combination of SPI and SSI clustering results) were then explored. Catchment characteristics influence the hydrological processes within each catchment, and the efficiency of the rainfall–streamflow transfer – for example, impermeable geology increasing the speed of runoff resulting in shorter flow response times. Box plots presenting the range of various catchment characteristics (including altitude, landcover, geology and the baseflow index (BFI)) were produced for each catchment group. We acknowledge that in this study we have only looked at catchment size, landcover, topography and geology and have not accounted for the potential compounding effects of inter-basin transfers, flood attenuation measures or other human alterations of the catchment system.

It stands to reason that in catchments with similar NAOI–SPI and NAOI–SSI correlations the characteristics potentially have little moderating effect on runoff – therefore flows in these catchments are likely to be susceptible to NAO–rainfall deviations. Meanwhile, in catchments where NAOI–SPI correlations are not replicated between NAOI and SSI, the characteristics have a potentially greater effect on moderating runoff and slowing the flow response time – these catchments are therefore likely to be less susceptible/more resilient to NAO–rainfall deviations (Figure 2).

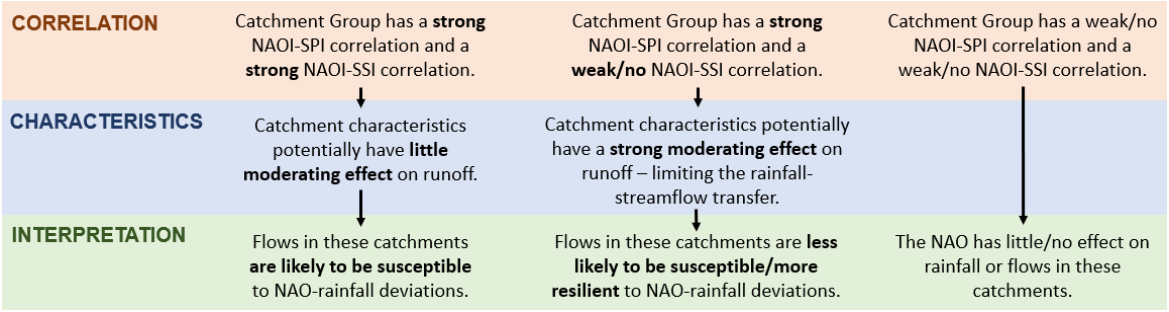

***Figure 2**. Interpretation of the correlation results in relation to the effect of local catchment characteristics.*

The final stage of the analysis sought to establish whether the spatio-temporal patterns in NAO response identified at the monthly scale were present at other (sub-)annual time scales. To explore relationships at the seasonal (three-monthly) time scale, Spearman correlations were run between the winter NAOI (DJF) and February SPI3/SSI3 and between the summer NAOI (JJA) and August SPI3/SSI3. At the annual scale a final set of correlations were run between the annual NAOI and SPI12/SSI12 for December. These additional sets of correlations were

plotted for the catchment groups identified earlier, allowing an evaluation of consistency in NAO rainfall and flow responses across multiple time scales.

Results

Stage 1: Quantifying NAO-Rainfall and NAO-Flow Relationships

Figures 3 and 4 present the monthly phase–rainfall and phase–flow ratios, which quantify the influence of NAO+ and NAO− phases. The results show clear monthly and seasonal differences in the strength and distribution of the NAO's hydrometeorological signature. In both figures, values greater than 1 indicate that average monthly rainfall/flows are higher under NAO+ than NAO−, while values less than 1 indicate average rainfall/flows are lower under NAO+. Catchments where the NAO± change is minimal are shaded yellow.

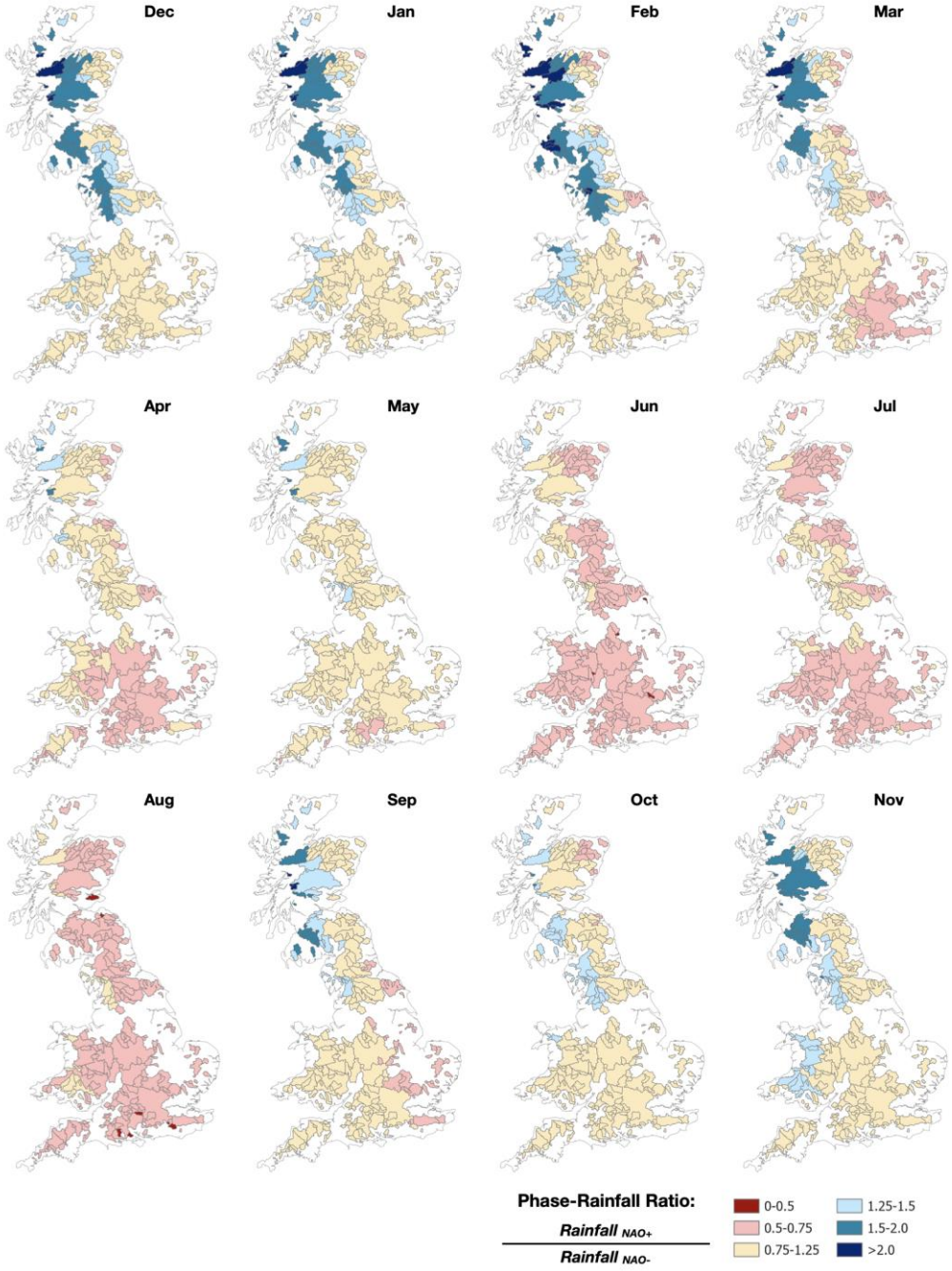

***Figure 3**: Monthly phase–rainfall ratios showing change in catchment area-weighted rainfall between NAO+ and NAO− phases.*

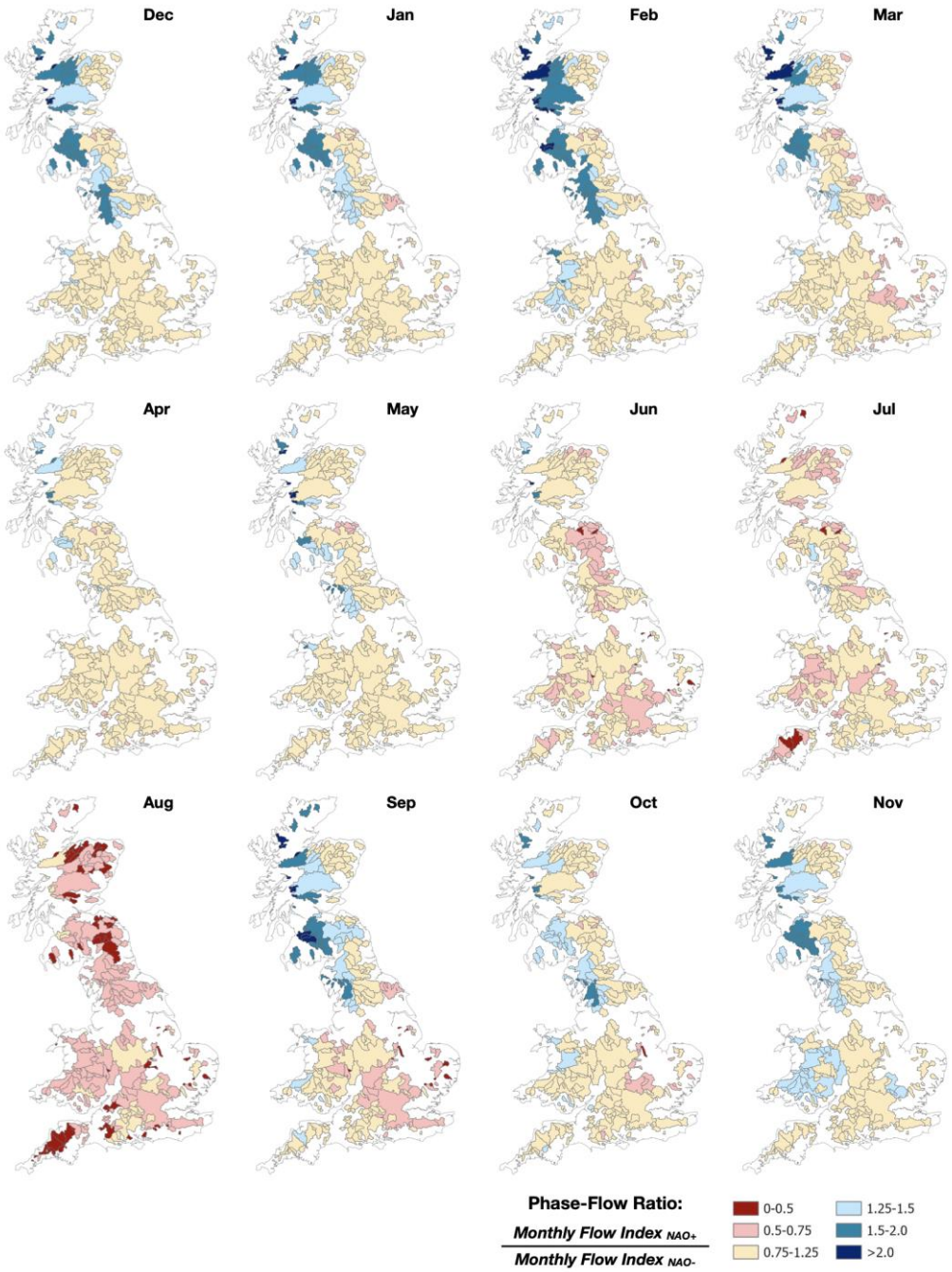

***Figure 4**: Monthly phase–flow ratios showing change in runoff per unit area (m^3/m^2) (Monthly Flow Index) between NAO+ and NAO− phases.*

During the winter months a general northwest and southeast pattern can be observed in the rainfall and flow response to NAO+ and NAO− phases. Catchments in the northwest see a significant uplift in rainfall under NAO+ phases which cascades down to streamflow in catchments. During winter some northwest catchments see flows 1.5–2.0 times higher during NAO+ phases, while flows in the majority of the southern/eastern catchments experience less notable change between the two NAO phases.

In spring and early summer, the rainfall and flow signatures start to differ, and the distinct winter spatial pattern generally becomes more homogeneous. Throughout summer, an NAO+

phase results in consistent reductions in rainfall compared to an NAO− phase. Whilst this is reflected in some catchments, many experience smaller flow deviations, and catchments where flows are more notably reduced in June and July are dispersed throughout the country. However, in August the majority of the 291 catchments see a flow reduction related to NAO+ conditions, with some catchments where flows are more than halved (0–0.5) under an NAO+ phase compared to NAO−.

Stage 2: Comparing NAO-Rainfall and NAO-Flow Patterns

Figure 5 presents two sets of time-series clusters, representing monthly correlations between the NAOI and SPI1, and between NAOI and SSI1. As in the phase–rainfall analysis above, the correlations between NAOI and SPI1 show a clear spatio-temporal response to the NAO in rainfall patterns. Across all months there is a clustering of values northwest/southeast across the country, with the greatest between-cluster differences observed in the winter months (represented by the average value plot for the NAOI–SPI1 correlations). In winter a similar space–time signal can be observed in the NAOI–SSI1 correlations. In summer the between-cluster differences are minimal for the NAOI–SSI1 correlations, resulting in a less spatially distinctive space–time clustering, in particular in the central and southern region.

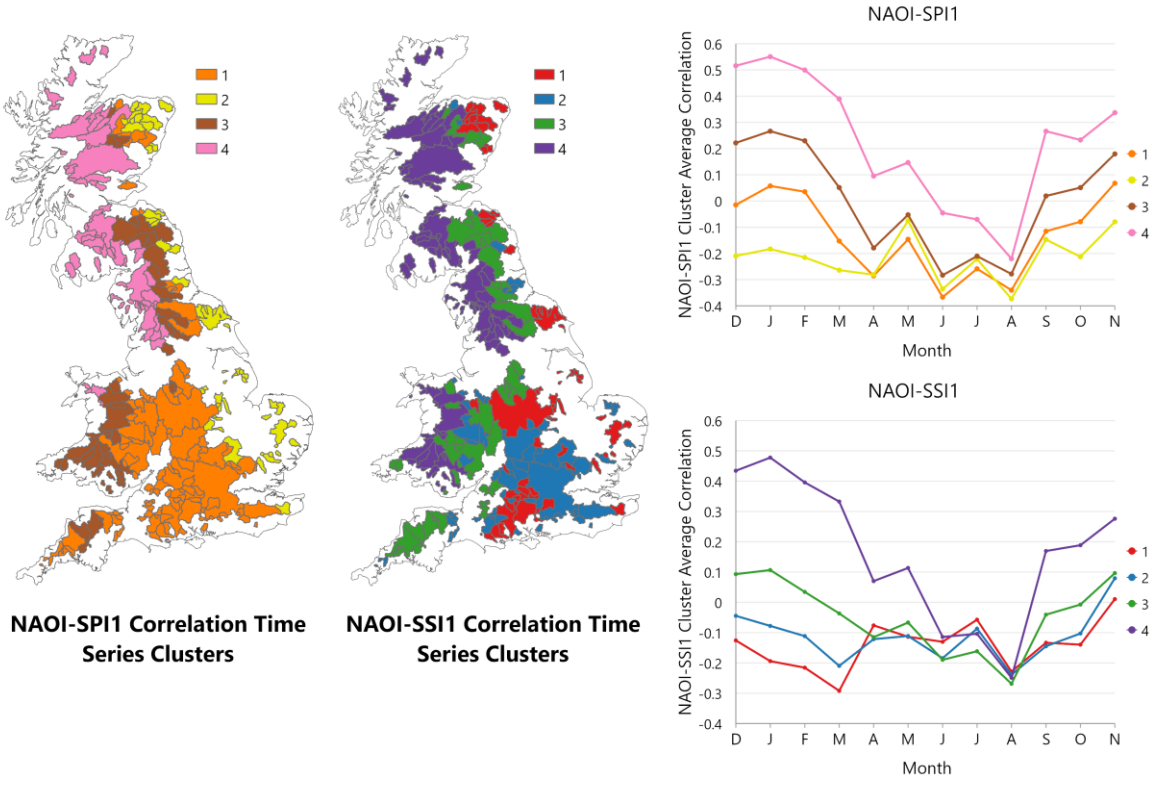

***Figure 5**: Space–time clusters for the NAOI–SPI1 and NAOI–SSI1 correlation analyses. The cluster colour on each map is the colour of the line in the respective graph. The plots represent the average value per cluster for each calendar month.*

The two cluster datasets mapped in Figure 5 were combined to identify unique combinations of clusters from the two space–time clustering analyses (Table 2). In total eight combinations

(out of a possible 16) were found, which we refer to as “catchment groups.” Catchment groups represent a collection of catchments with similar NAOI–SPI and NAOI–SSI correlation time series. These groupings are mapped in Figure 6, alongside box plots presenting the range of the monthly NAOI–SPI1 and NAOI–SSI1 correlations for each group.

***Table 2**: Cluster combinations identified in the catchment group analysis.*

NAOI-SPI Cluster	NAOI-SSI Cluster	Catchment Group Identifier	Number of Catchments
3	3	1	21
4	3	2	43
3	4	3	57
4	4	4	12
3	2	5	37
2	2	6	23
2	1	7	29
1	1	8	69

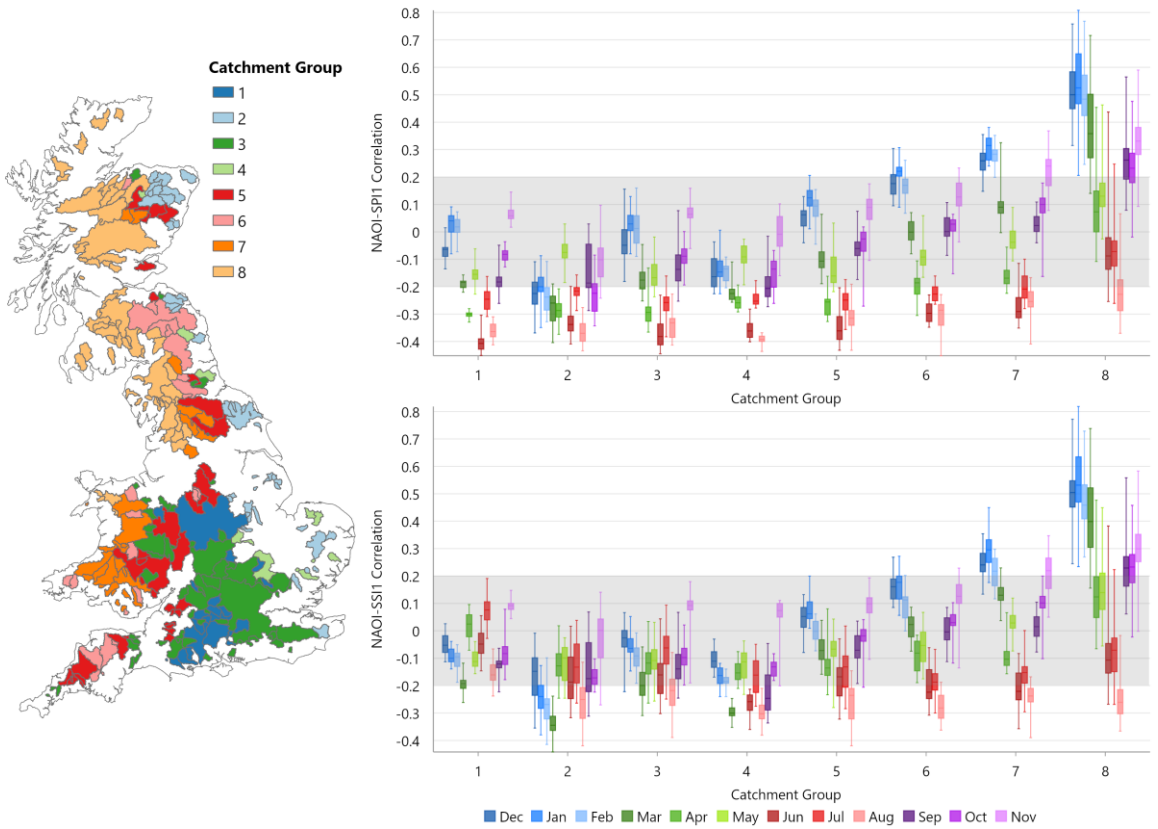

***Figure 6**: Catchment groupings identified in Table 2. Box plots represent the range of NAOI–SPI1/–SSI1 correlations for each grouping. There is no association between the symbology of the catchment groups and box plots. Low correlations (−0.2 to +0.2) are greyed out.*

Within each group, similar winter NAO–rainfall and NAO–flow responses can be observed. For example, the largest catchment group (Group 8) is concentrated along the northwestern coastline. As previously described, these areas see significant increases/decreases in winter flows under NAO± conditions, which tend to mirror the NAO–rainfall signatures. However, notable differences across other catchment groups (in particular, Groups 1–5) can be seen in the summer months. For example, catchments within Group 1, concentrated in central/southern England, have negative correlations between NAOI and SPI1, which are not replicated in the NAOI–SSI1 correlations.

Seasonal and Annual Correlation Analysis

To evaluate the consistency of the monthly NAO–rainfall and NAO–flow responses at seasonal and annual scales, further sets of correlations were calculated and evaluated for the catchment groups (Figure 7). Winter correlations between the three-month NAOI (DJF) and February SPI3/SSI3 show a very similar response to the monthly NAO–SPI/–SSI correlations (Figure 6), with the most notable positive correlations being observed in Group 8 in the northwest. In the summer months, moderately stronger and relatively consistent NAOI–SPI3 negative correlations are observed across Groups 1–7. At the annual scale the NAO–rainfall and NAO–flow correlations show a similar pattern to that observed in winter – catchments in Group 8 continue to show positive correlations with the NAOI, while catchments for the majority of the country, in Groups 1–6, show weak annual correlations for both SPI12 and SSI12.

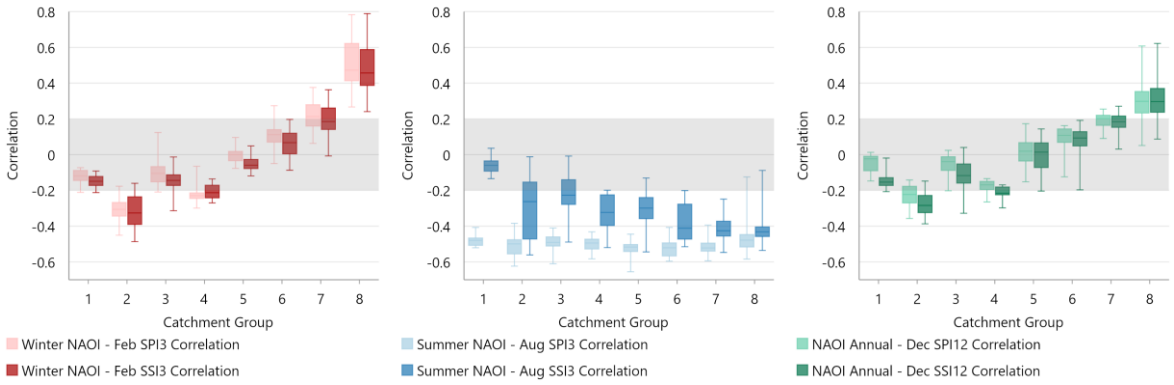

***Figure 7**: Seasonal and annual correlations for the eight catchment groups between the three-monthly/annual NAOI and SPI/SSI with longer accumulation periods.*

Discussion

Monthly NAO-Rainfall and NAO-Flow Relationships

The first aim of this study was to quantify the sub-annual spatio-temporal relationships between the NAO, rainfall and streamflow in Great Britain. This was analysed through the

calculation and mapping of two ratios (phase–rainfall and phase–flow), representing the change in average monthly rainfall or flows between NAO+ and NAO− phases, respectively.

The magnitude of the NAOI is notably strong in the winter months, and these strong NAO+ and NAO− phases result in characteristic hydrometeorological patterns in Great Britain (Wilby et al. 1997, Fowler and Kilsby 2002, Folland et al. 2009, West et al. 2019b). Winter months are characterized by a northwest/southeast divide in the relationship between NAO and rainfall/streamflow, which we quantify using our phase–rainfall and phase–flow ratios. Catchments in the northwest see significant uplift in rainfall under NAO+ conditions (relative to NAO− conditions) which propagates through to higher streamflow. In some catchments, flows are as much as doubled when the NAO is positive compared to when it is negative. Less discernible differences between the two NAO phases are observed in both rainfall and flows in the southeast.

Whilst the magnitude of the NAOI is weaker in the summer months compared to winter (Folland et al. 2009), our phase–rainfall and phase–flow ratios show that the NAO also has a quantifiable effect on rainfall and streamflow in the summer months. However, the NAO± wet/dry response is the opposite of that in winter. NAO+ conditions can result in lower summer flows, with the strongest NAO+ summer flow signature being observed in August. During August, under average NAO+ conditions, a large number of catchments see lower flows compared to when the NAO is negative, and in some catchments, flows are more than halved.

The Moderating Effect of Catchment Characteristics

The second aim of this study was to compare correlations between the NAOI and rainfall (quantified by the SPI) and NAOI and streamflow (quantified by the SSI). We also explored whether catchment characteristics moderate the propagation of NAO–rainfall deviations through the hydrological cycle to influence discharge. The transfer of rainfall to streamflow is influenced by a number of different variables in British catchments (Chiverton et al. 2015, Barker et al. 2016, Rust et al. 2021a) and Figure 8 explores a range of catchment characteristic datasets for the catchment groups identified in Figure 6 and Table 2.

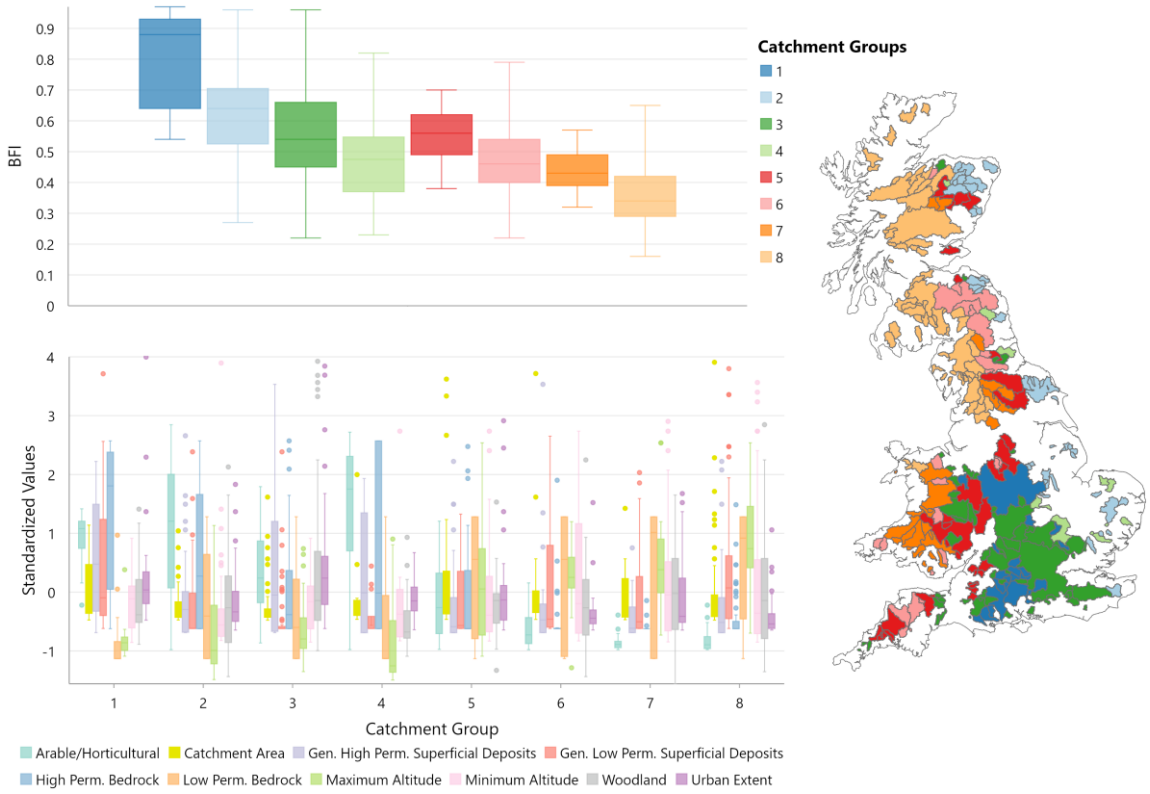

Figure 8: *The baseflow index (BFI) and a range of local characteristics of the catchment groupings in Fig. 5. Colours for the characteristics are not associated with the BFI or the map of catchment groups. Catchment characteristics with variable units and values are plotted using a z-score standardization.*

Catchments in the northwestern regions, as discussed earlier, are highly responsive to winter NAO-driven rainfall (generally in Groups 7 and 8). This is partly associated with their geographic location in relation to the influence of the NAO in the North Atlantic region. The phase of the NAO has been found to drive the location of storm tracks across the Atlantic (Visbeck et al. 2001; Brayshaw et al. 2010). Given their location along the northwestern coastline these catchments are likely to have strong NAO–rainfall relationships, as have been noted in previous studies (e.g. Rust et al. 2018, West et al. 2019b). In terms of their physical characteristics these catchments have low-medium BFI values. This is likely a result of their relatively high low-permeability bedrock coverage, restricting slower groundwater flow pathways and catchment storage capacity. Notably, these catchments are also high altitude (Fig. 8) which is significant given that the NAO has been found to amplify the natural orographic enhancement of rainfall in upland regions of Great Britain (Burt and Howden 2013). These factors suggest that in the winter months these catchments do not have the characteristics necessary to moderate NAO–rainfall deviations, therefore the NAO–rainfall and NAO–flow patterns are similar (Figures 3–6).

In contrast to Group 8, catchments in Group 1, which are located in central/southern England, have very weak NAO–rainfall and NAO–flow correlations. During the summer months moderate and consistent negative correlations between NAOI and SPI1 are present. This is also observed in the GEAR rainfall analysis, where much of the country sees a 25–50% reduction in rainfall

under NAO+ phases relative to NAO−, a pattern also observed in other studies (Folland et al. 2009, West et al. 2019b). However, these negative NAOI–SPI1 correlations are not replicated in flows. Summer NAOI–SSI1 correlations for Group 1 are very weak. These catchments have high/very high BFI values, are low-lying and have high coverage of highly permeable superficial deposits and bedrock geologies. We suggest as a result of these local characteristics they are able to moderate the propagation of NAO–rainfall deviations through the catchment. For example, a 25–50% decrease in rainfall under NAO+ conditions described above is not transferred to a similar reduction in discharge.

Comparison across Temporal Scales

While catchments in the north and west typically show strong SSI1 relationships with short SPI accumulation periods, catchments in the central and southern regions (generally Catchment Groups 1, 3 and 4) have been found to have the strongest SPI–SSI1 correlations when SPI accumulation periods greater than one month have been used (Barker et al. 2016, West et al. 2019c). This raises the question as to whether the catchments identified as being able to moderate monthly NAO rainfall deviations (especially in the summer months) remain able to do so at longer seasonal/annual scales.

In winter the similarity in the seasonal and monthly analyses (Figures 6 and 7) suggests that these catchments in the northwest remain unable to moderate to winter NAO rainfall deviations across temporal scales. In the summer, the majority of catchments in the central and southern regions were identified as being able to moderate monthly NAO–rainfall deviations due to their characteristics (notably, NAO+ low-rainfall summers). These catchments show similar moderating ability at the seasonal scale, as the three-month NAOI (JJA) negative correlations with August SPI3 are not replicated in the NAOI–SSI3 correlations. In other words, the moderating characteristics of these catchment groups (such as their altitude, elevation and geologies – Figure 8) result in limited propagation of summer NAO rainfall signatures at both the monthly and three-monthly time scales.

The annual scale correlations between the annual NAOI and SPI12/SSI12 showed similar patterns to those observed in the winter months. This reinforces the importance of looking across a full annual cycle when exploring climate signatures in rainfall and flow datasets discussed in the introduction (Bower et al. 2004), as the summer patterns in rainfall, which are variably replicated in flows, are not fully represented at this temporal scale. This observation also reinforces the growing evidence base of distinct NAO summer signatures in Great Britain (Folland et al. 2009, Hall and Hanna 2018, West et al. 2019b). Table 3 provides a summary of the multi-scale correlation analyses for the catchment groups.

Table 3: Summary of the multi-scale correlation analyses for the 8 Catchment Groups (Groups are mapped Figure 5, and characteristics inferred from Figure 7).

Catchment Group	Correlation Patterns/Characteristics
1 (Higher Summer Resilience)	• In winter and at the annual scale there is little evidence of NAO signatures in rainfall or flows in these catchments. • In the summer months (and seasonal scale) moderate negative correlations with rainfall are not replicated in flows. • Suggests geology and altitude characteristics are able to the moderate NAO rainfall influence in summer months.
2 (Higher Summer Resilience)	• In winter and at an annual scale there are some weak-moderate negative correlations between the NAO and rainfall. This is generally well replicated in flows. • In the summer months (and seasonal scale) moderate negative correlations with rainfall are not replicated in flows. • Suggests geology and altitude moderate NAO rainfall deviations in summer, however this is not the case in winter.
3 and 4 (Higher Summer Resilience)	• In winter and at an annual scale there is little evidence of NAO signatures in rainfall or flows in these catchments. • In the summer months (and seasonal scale) moderate negative correlations with rainfall are not (fully) replicated in flows. • Suggests geology (deposits) and altitude moderate NAO rainfall influence in summer months.
5 (Higher Summer Resilience)	• In winter and at an annual scale there is little evidence of NAO signatures in rainfall or flows in these catchments. • In summer months (and seasonal scale) moderate negative correlations with rainfall are not (fully) replicated in flows. There are moderate SSI correlations in August at the monthly scale however. • Suggests variable geology and altitude (high BFI) offer moderating ability in early summer.
6 (Potential Summer Resilience)	• In winter and at an annual scale there is some, but little, evidence of NAO signatures in rainfall and flows in these catchments. • In early summer moderate negative correlations with rainfall are not (fully) replicated in flows. In August and when looking seasonally some moderate correlations are replicated. • Suggests these catchments have some moderating properties in summer. Although location and altitude might overcome this in late summer or after persistent NAO influence.
7 (Higher Susceptibility)	• In winter and at the annual scale similar weak-positive correlations are observed in both rainfall and flows. • Weak-moderate negative rainfall correlations in summer are relatively well replicated in flows.

	• Suggests catchment characteristics and location results in limited ability to moderate to NAO rainfall deviations, and monthly flows follow rainfall.
8 (Higher Susceptibility)	• In winter and at the annual scale similar moderate/strong correlations are observed in both rainfall and flows. • In early summer rainfall and flow correlations are weak. Some moderate August correlations. • Suggests catchment characteristics and location results in limited or no ability to moderate to NAO rainfall deviations, and monthly flows follow rainfall.

It should be noted that spatio-temporal variability in NAO rainfall signatures has been observed in other studies (Rust et al. 2021b, West et al. 2021a) and deviations in rainfall across Great Britain and Europe have also been attributed to other atmospheric circulations, such as the East Atlantic Pattern and Scandinavian Pattern (Comas-Bru and McDermott 2014, Mellado-Cano et al. 2019). There is therefore scope to apply the long-term historical flow datasets used in this study to further understand NAO signature variability and the impact of other circulations on regional hydrology in Great Britain.

Conclusion

This study sought to firstly explore sub-annual NAO hydrometeorological signatures in 291 catchments across Great Britain. Through comparative analyses based on historical rainfall and flow datasets, we identify distinctive spatio-temporal flow responses of the NAO at the monthly scale across a long time period (1900–2015). In particular we note the spatial divide in NAO–flow response in winter compared with the more spatially consistent summer patterns.

Secondly, we sought to understand the extent to which local catchment characteristics might be able to moderate sub-annual NAO–rainfall–flow propagation. Through comparative analysis of rainfall and flow datasets we present a new understanding of the spatio-temporally variable nature of the propagation of NAO variability to flows as a result of the moderating effect of catchment characteristics. For example, catchments in the northwestern regions of Britain, due their location, topography and geology, typically show strong relationships between NAOI and rainfall, which persist during winter as correlations between NAOI and flows. The similarity of the two responses leads to the conclusion that these catchments have a limited ability to moderate NAO–rainfall deviations in winter. Meanwhile, during summer, we note that NAO rainfall signatures are present, for example lower rainfall under NAO+ phases relative to NAO− phases. However, for a large number of catchments in the central and southern regions of Britain, these signatures are not replicated in flows. These catchments are relatively flat and low-lying and have highly permeable geologies. We therefore conclude that these catchment characteristics moderate the propagation of NAO–rainfall deviations during the summer. As far

as we are aware, this study represents the first spatially and temporally large-scale analysis of the sub-annual influence of the NAO on streamflow in Britain and presents new evidence as to the variable nature of the propagation of NAO variability to flows as a result of moderating catchment characteristics.

Paper 3: Spatio-Temporal Variability in North Atlantic Oscillation Monthly Rainfall Signatures in Great Britain

Citation: West, H., Quinn, N. & Horswell, M. (2021). Spatio-Temporal Variability in North Atlantic Oscillation Monthly Rainfall Signatures in Great Britain. *Atmosphere*, Vol.12(6), 763.

Published: 13th June 2021.

Contributions: New analytical functionality added to ArcGIS Pro over the course of the PhD project enabled an extension of the work undertaken in Paper 1 to investigate the consistency/variability in spatial rainfall signatures associated with the NAO. HW undertook the analysis and data presentation. This was refined with NQ and MH. HW produced the first draft of this paper which was shared with NQ and MH for comment prior to submission.

Changes to Original Paper:

- No changes have been made between this version and that published in June 2021.

Abstract

The North Atlantic Oscillation (NAO) is the primary atmospheric-oceanic circulation/teleconnection influencing regional climate in Great Britain. As our ability to predict the NAO several months in advance increases, it is important that we improve our spatio-temporal understanding of the rainfall signatures that the circulation produces. We undertake a high resolution spatio-temporal analysis quantifying variability in rainfall response to the NAO across Great Britain. We analyse and map monthly NAO-rainfall response variability, revealing the spatial influence of the NAO on rainfall distributions, and particularly the probability of wet and dry conditions/extremes. During the winter months, we identify spatial differences in the rainfall response to the NAO between the NW and SE areas of Britain. The NW area shows a strong and more consistent NAO-rainfall response, with greater probability of more extreme wet/dry conditions. However, greater NAO-rainfall variability during winter was found in the SE. The summer months are marked by a more spatially consistent rainfall response; however, we find that there is variability in both wet/dry magnitude and directionality. We note the implications of these spatially and temporally variable NAO-rainfall responses for regional hydrometeorological predictions and highlight the potential explanatory role of other atmospheric-oceanic circulations.

Introduction

Weather in Great Britain can be highly variable, fluctuating between wet and dry extremes. The North Atlantic Oscillation (NAO) atmospheric-oceanic circulation has long been cited as the leading mode of climate variability in the North Atlantic region (Wilby et al. 1997; Rodwell et al. 1999; Hurrell et al. 2003) due to its influence on the location and amplitude of the North Atlantic Jet Stream (Woollings et al. 2014). The NAO teleconnection is commonly defined by the sea level pressure (SLP) variation between two meridional dipoles: the Icelandic low-pressure action point and the Azores anticyclone. Fluctuations in the difference in SLP between Iceland and the Azores leads to the occurrence of NAO positive (NAO+) phases, representing a greater than normal difference in SLP between the two dipoles, or NAO negative (NAO−) phases representing a weaker than normal difference in SLP. The strength and phase of the NAO can be quantified by the North Atlantic Oscillation Index (NAOI) (Hurrell et al. 2003).

Previous work has explored the influence of sub-annual variability and phase of the NAO on weather and climate in Great Britain. Strong positive correlations are often reported between the NAOI and winter rainfall in the north-western areas of the country (Folwer & Kilsby 2002; Afzal et al. 2015; Rust et al. 2018), whilst weaker negative winter correlations have been found in the south-east and central areas (Simpson & Jones 2013; Kosanic et al. 2014). Previous work has quantified these opposing regional rainfall responses to NAO+ and NAO− phases relative to when the NAO is in a weak neutral state, finding that in winter, average monthly rainfall increases under NAO+ and decreases under NAO− conditions can be as much as 200–300 mm in the north-west (West et al. 2019b). Negative correlations between the winter NAOI and modelled snow cover have also been found in the north-west of Scotland (Spencer & Essery 2016), suggesting that winter NAO− phases are associated with higher snowfall in these regions.

Whilst the magnitude of the NAOI is weaker in the summer months (Folland et al. 2009), significant NAOI-rainfall correlations have been reported (Hall & Hanna 2018). However, the correlation coefficients are generally weaker in summer than during the winter months (West et al. 2019b). In winter, the NAO-rainfall response is characterised by a north-west/south-east spatial divide as described above, whilst in summer the spatial signature is more homogenous across the country (Folland et al. 2009; Hall & Hanna 2018). In summer months, average monthly rainfall increases under NAO− conditions and decreases under NAO+ conditions are approximately 50–100 mm, compared to NAO neutral conditions (West et al. 2019b).

These NAO rainfall signatures propagate through the hydrological cycle, with NAO responses observed across Great Britain in catchment runoff (Phillips et al. 2003; Burt & Howden 2013; Rust et al. 2021a), groundwater (Lavers et al. 2015; Rust et al. 2019) and fluvial water temperatures (Wilby & Johnson 2020), although this propagation can be moderated by

catchment characteristics such as topography, landcover and geology (Burt & Howden 2013; Rust et al. 2021a). Ongoing research is exploring whether this understanding of NAO-rainfall-flow propagation can be incorporated into seasonal streamflow modelling and forecasting (UK Hydrological Outlook 2020; Donegan et al. 2021).

As discussed above, the NAO has been found to influence hydrometeorology across the country, and its spatial signature is evident in monthly average rainfall datasets (West et al. 2019). However, several studies have reported inconsistency in seasonal NAO-rainfall responses across Great Britain. Hall and Hanna (2018) present three winter rainfall anomaly maps produced by the UK Met Office for 2013/2014, 2014/2015 and 2015/2016 (see their Figure 1). The reported NAOI values all indicate an NAO+ phase of varying magnitudes. However, only in the winter of 2014/2015 was the typical north-west/south-east winter NAO-rainfall response (as described above) observed. This study concluded by foregrounding the role of other North Atlantic teleconnections as secondary modes of climate variability, such as the East Atlantic Pattern (EA) and Scandinavian Pattern, in influencing regional rainfall (and temperatures) in Britain (Hall & Hanna 2018). Variability in winter NAO-rainfall signatures, both in terms of strength and spatiality, has also been attributed to other atmospheric teleconnections, in particular positive and negative phases of the EA, in other work (Comas-Bru & McDermott 2014; Mellado-Cano et al. 2019).

Our ability to predict the NAO, especially during its stronger phases during the winter months (Weisheimer et al. 2017; Parker et al. 2019), has improved. In particular, recent research from the National Center for Atmospheric Research (NCAR) and the UK Met Office suggests that winter NAO prediction several months in advance may be increasingly possible (Athanasiadis et al. 2020; Smith et al. 2020). As NAO forecasting skill improves, it is important that we continue to develop our spatial and temporal understanding of the rainfall signatures associated with the circulation, especially as evidence of the propagation of NAO rainfall deviations to other hydrometeorological variables, such as runoff and groundwater, continues to emerge.

Whilst previous studies have explored average monthly and seasonal NAO-rainfall responses across Great Britain (Wilby et al. 1997; Hall & Hanna 2018; West et al. 2019b) as far as we are aware, no study has quantified the spatial influence of the NAO on rainfall distributions, and particularly the probability of wet and dry conditions/extremes. Understanding NAO-rainfall variability is important as it underpins the potential application of NAO forecasts in water management decision making. This study responds to this need through the novel application of spatio-temporal statistics and high spatial and temporal resolution Standardised Precipitation Index (SPI) data. Specifically, we aim to:

1. Assess the statistical significance and consistency of NAO-rainfall spatial signatures.

2. Establish the spatial distribution of consistent or variable monthly NAO-rainfall responses.

Methods

Figure 1 summarises the key stages of this analysis to explore space-time variability in monthly NAO-rainfall response across Great Britain, which are explained in full below.

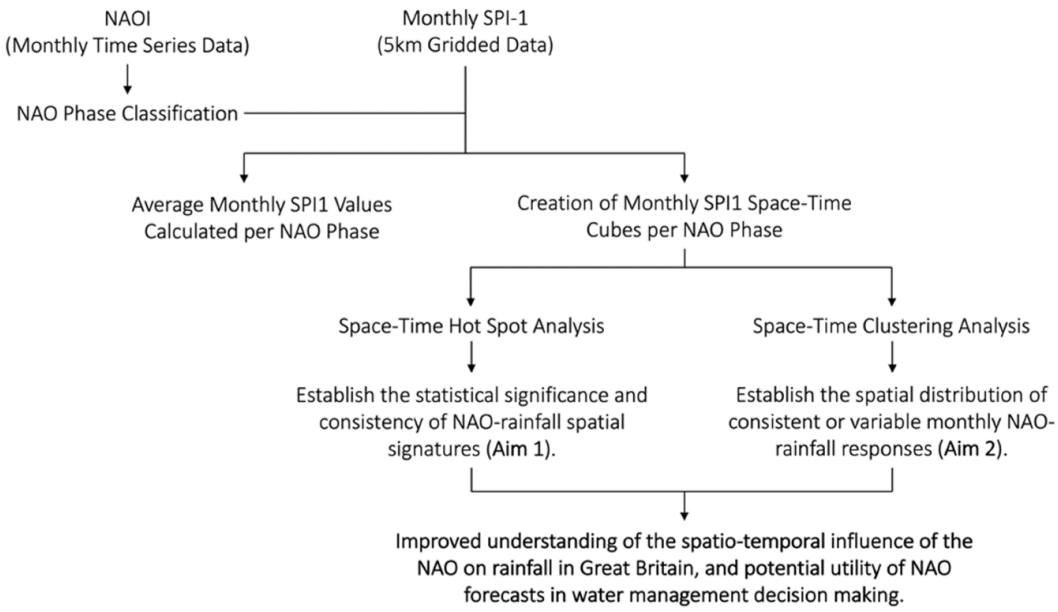

***Figure 1**: Flow chart of the analytical stages of this study.*

Data

A range of indices have been used in previous work to quantify the phase and strength of the NAO (Wilby et al. 1997; Folland et al. 2009; Rust et al. 2019; West et al. 2019b), and the choice of NAOI can have a notable influence on subsequent analyses (Pokorná & Huth 2015). As this study focuses on quantifying monthly NAO-rainfall response variability across a full year, an NAOI calculated using a principal components (PC) analysis of the leading empirical orthogonal function of sea level pressure anomalies in the North Atlantic region was used (Hurrell et al. 2003). These NAO indices avoid the limitation of indices directly derived using station-measured data in the summer months when the NAO dipoles can move away from the monitoring stations (Pokorná & Huth 2015). As a result, the use of station-based NAO indices in summer months can produce weaker and non-significant NAOI-rainfall correlation analyses (West et al. 2019b). Monthly PC-based NAOI data were downloaded for the period January 1900–December 2015 from NCAR (NCAR 2020).

Previous studies have used different approaches to defining NAO+ and NAO− phases using the NAOI. In this study, the NAO phase was defined as half the standard deviation plus/minus the long-term mean of the NAOI dataset (Berton et al. 2017). By identifying NAO phases in this way, we could remove months where the NAO signal is weak, allowing only clear NAO+ and

NAO− rainfall responses to be considered. NAO+ phases were defined as having a NAOI > 0.502 and NAO− < −0.503 (data between this range were classified as NAO neutral and removed). Table 1 shows the distribution of NAO phase and months for the period January 1900–December 2015.

Table 1. *Frequency Distribution of NAO Phases per Month (January 1900–December 2015).*

Period	NAO+ Frequency	NAO− Frequency	NAO Neutral Frequency
Dec	47	40	29
Jan	52	36	28
Feb	47	40	29
WINTER	**146**	**116**	**86**
Mar	45	38	33
Apr	29	32	55
May	28	24	64
SPRING	**102**	**94**	**152**
Jun	26	24	66
Jul	16	16	84
Aug	16	19	81
SUMMER	**58**	**59**	**231**
Sep	19	21	76
Oct	31	33	52
Nov	29	31	56
AUTUMN	**79**	**85**	**184**

We used the 5 km gridded Standardised Precipitation Index (SPI) dataset from the UK Centre for Ecology and Hydrology (CEH) (Tanguy et al. 2017a) to represent precipitation. Standardised indices have been widely used in research exploring the hydrometeorological response to atmospheric-oceanic teleconnections (Irannezhad et al. 2014; Kingston et al. 2015; West et al. 2091b). The SPI dataset from CEH was calculated by fitting a gamma distribution to modelled historical rainfall using a standard period of 1961–2010 (Tanguy et al. 2017a). For this study, the SPI calculated with a one-month accumulation period (SPI-1) was used to give a relative indication of wetness/dryness compared to the standard period at a monthly scale. The SPI-1 data for the same period as the monthly NAOI from NCAR (January 1900–December 2015) were downloaded from CEH.

The SPI-1 values are normally distributed and can range from −5 to 5, although approximately 95% of values occur within the range of −2 (extremely dry) to 2 (extremely wet), and 68% within the range of −1 to 1 (Tanguy et al. 2017a). We use a qualitative classification of SPI-1

thresholds to indicate the relative degree of wetness/dryness (Table 2) in the interpretation of our results.

***Table 2**: Qualitative Descriptors for SPI-1 Values adapted from (McKee et al. 1993).*

Qualitative Descriptor	SPI-1 Value Range
Extremely Wet	2.0–5.0
Very Wet	1.5–1.99
Moderately Wet	1.0–1.49
Near Normal	−0.99–0.99
Moderately Dry	−1.49– −1.0
Severely Dry	−1.99– −1.5
Extremely Dry	−5.0– −2.0

Calculation of Monthly Average SPI-1 Values

To provide a point of comparison, before undertaking the NAO-rainfall space-time variability analysis described below, we mapped the average monthly SPI-1 values under NAO+ and NAO− phases over the period January 1900–December 2015. The average monthly SPI-1 value under each phase was calculated for each 5km pixel. This analysis provided a dataset of average rainfall conditions (represented by the SPI-1) for each calendar month under NAO+ and NAO− conditions.

Space-Time Data Array

To undertake the spatio-temporal analyses, the monthly SPI-1 data were structured into a series of data arrays (a space-time cube). Each array contained the monthly 5 km gridded SPI-1 data stacked in time ascending order for each NAO phase. The number of time steps in each space-time cube equalled the monthly-phase frequency values in Table 1. A space-time cube was created for each month under NAO+ and NAO− conditions using Esri ArcGIS Pro software (Version 2.6).

Space-Time Hot Spot Analysis (Getis Ord Gi Statistic)*

The Getis-Ord Gi* statistic (Getis & Ord 2010) identifies clusters of significantly high and low values within a spatial dataset—identified as hot or cold spots with varying significance levels (90, 95 or 99%). The statistic indicates whether the spatial clustering of high/low values is more pronounced than would be expected in a random spatial distribution of those same values (Esri 2021a). The Getis-Ord Gi* statistic is commonly used in spatial statistical analyses in health and crime applications (Ord & Getis 1995; Scott & Warmerdam 2021). This study's application of it in the field of hydrometeorology/climatology is novel.

As the Getis-Ord Gi* statistic has a spatial component, its calculation requires consideration of how pixels are spatially related, so that high/low value clusters can be identified (i.e., a

conceptualisation of spatial relationships between the 5km SPI-1 pixels). Because of the spatially continuous gridded SPI-1 data, we used the 'edges and corners' or 'queens' contiguity rule, where each pixel's statistical neighbourhood included the eight pixels which share a boundary or point of contact in the four cardinal and diagonal directions. Hot spots in this context represent clusters of pixels where the SPI-1 values are significantly high, whilst cold spots represent the inverse (low SPI-1 values). The Getis-Ord Gi* statistic therefore allows for the identification of statistically significant wet or dry (high SPI-1/low SPI-1) spatial patterns.

The Getis-Ord Gi* statistic was calculated for each time step (SPI-1 dataset) in the space–time cubes for NAO+ and NAO− conditions. The output is a multi-variate dataset, indicating the percentage time each pixel is in either a significant hot (high SPI-1 value—wet) or cold spot (low SPI-1 value—dry). This enables an evaluation of the statistical significance and consistency of the spatial rainfall (wet/dry) response to the NAO across Great Britain and provides an assessment as to the spatial probability of significant wet/dry conditions under NAO+ and NAO− phases.

Space-Time Clustering Analysis

The second spatio-temporal analysis was a space-time clustering process (Esri 2020), which grouped 5 km pixels with similar SPI-1 values across space, time, and NAO phase for each month. The clustering used a k-means algorithm with spatially random starting seeds. During the cluster calculation, SPI-1 time series similarity was assessed using the Euclidean distance between the SPI-1 time series values (the square root of the sum of squared differences in SPI-1 values across time) (Esri 2020). The algorithm produced 90 space-time clustering solutions, with potential results between two and ten output clusters. The optimal clustering solution was identified as that which had the highest pseudo-F statistic. This statistic describes the within-cluster SPI-1 time series similarity and between-cluster SPI-1 time series difference—the larger the pseudo-F statistic of the clustering solution, the greater the distinctiveness of each individual cluster in space and time (Esri 2020).

The range of the average SPI-1 values within each space-time cluster was investigated using box plots, frequency histograms and descriptive statistics, quantifying the distribution of SPI-1 within clusters and providing a measure of the consistency/variability in space-time rainfall response to the phase of the NAO.

Results

Average Monthly SPI-1 Values

Figure 2 and Figure 3 present the average monthly SPI-1 values under NAO+ and NAO− conditions. Whilst these are average monthly SPI-1 values and mask extreme values, clear spatial and temporal signatures of the NAO can be detected. In the winter months, the NAO

rainfall response described in the introduction can be observed (Wilby et al 1997; Folland et al. 2009; Rust et al. 2018; Hall & Hanna 2018). Under NAO+ conditions, the north-west areas have higher/positive average SPI-1 values, indicating wet conditions, and under NAO− conditions, the region is typically dry (negative SPI-1 values). The inverse average wet/dry response, albeit weaker, is seen in the southern and eastern areas.

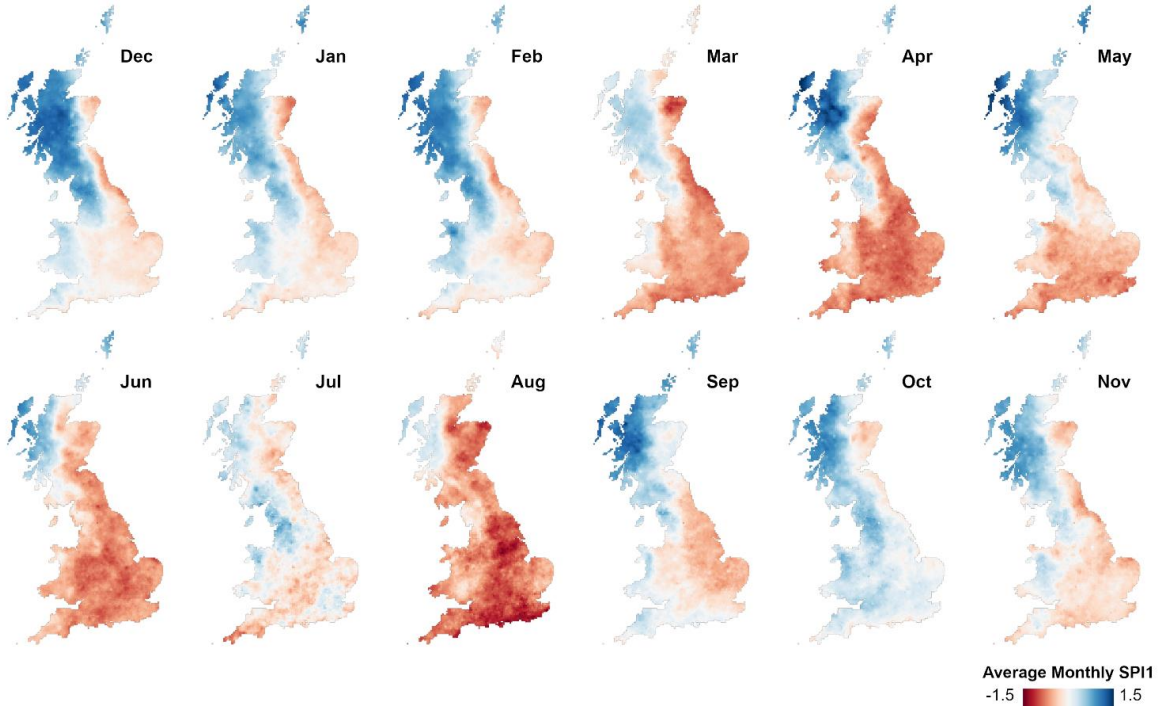

***Figure 2**: Average monthly SPI-1 values under NAO+ conditions (January 1900–December 2015).*

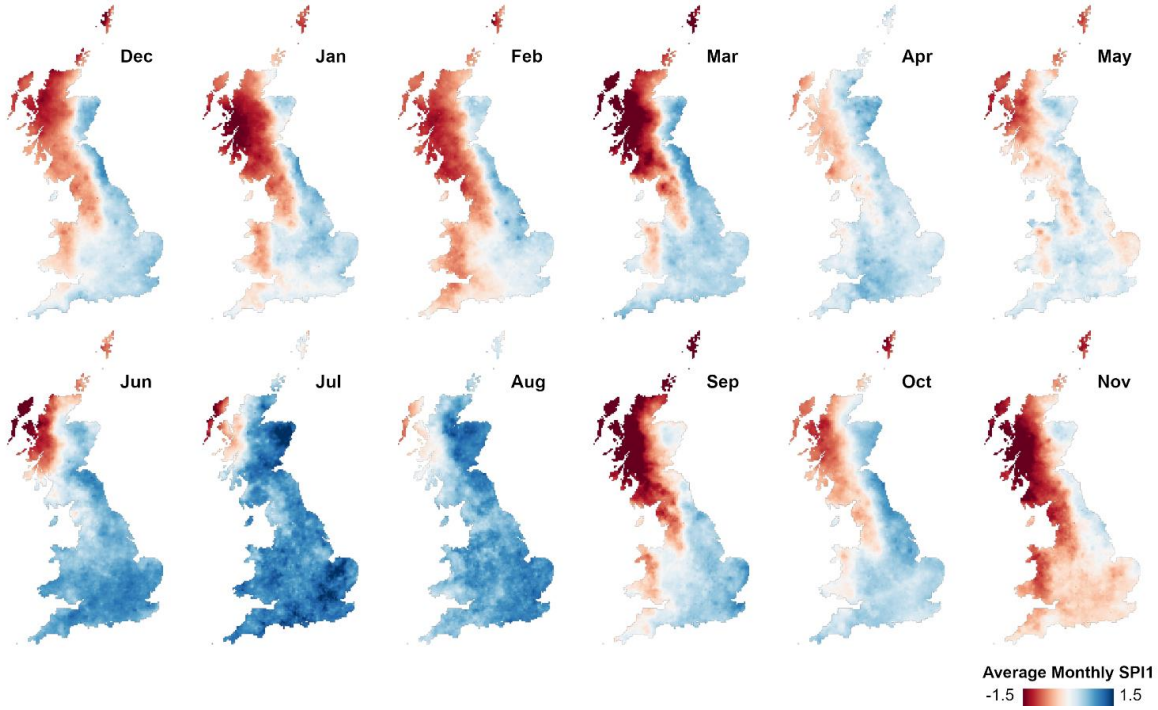

***Figure 3**: Average monthly SPI-1 values under NAO− conditions (January 1900--December 2015).*

Moving through to the summer months, the average NAO-rainfall response becomes more spatially homogeneous (i.e., there is less difference between the different areas of the country), and the wet/dry response in the north-west during winter is inverted; a spatio-temporal pattern also noted in other studies (Folland et al. 2009; Hall & Hanna 2018; West et al. 2019b).

Space-Time Hot Spot Results

Figure 4 and Figure 5 show the results of the space-time hot spot analysis. This analysis involved calculating the Getis-Ord Gi* for each time step (SPI-1 dataset) of the month/phase space–time cubes as described in Section 2.3, allowing us to examine the statistical significance and consistency of the patterns discussed above. The mapped results in Figure 4 and Figure 5 below show the percentage of time each 5 km pixel was in a statistically significant hot spot (i.e., a cluster of pixels with high/wet SPI-1 values) or cold spot (i.e., a cluster of pixels low/dry SPI-1 values). These maps indicate the spatial probability of significant wet/dry conditions under NAO+ and NAO− phases. Averages of these results for the nine Met Office Climate Districts for Great Britain are shown in Figure 6.

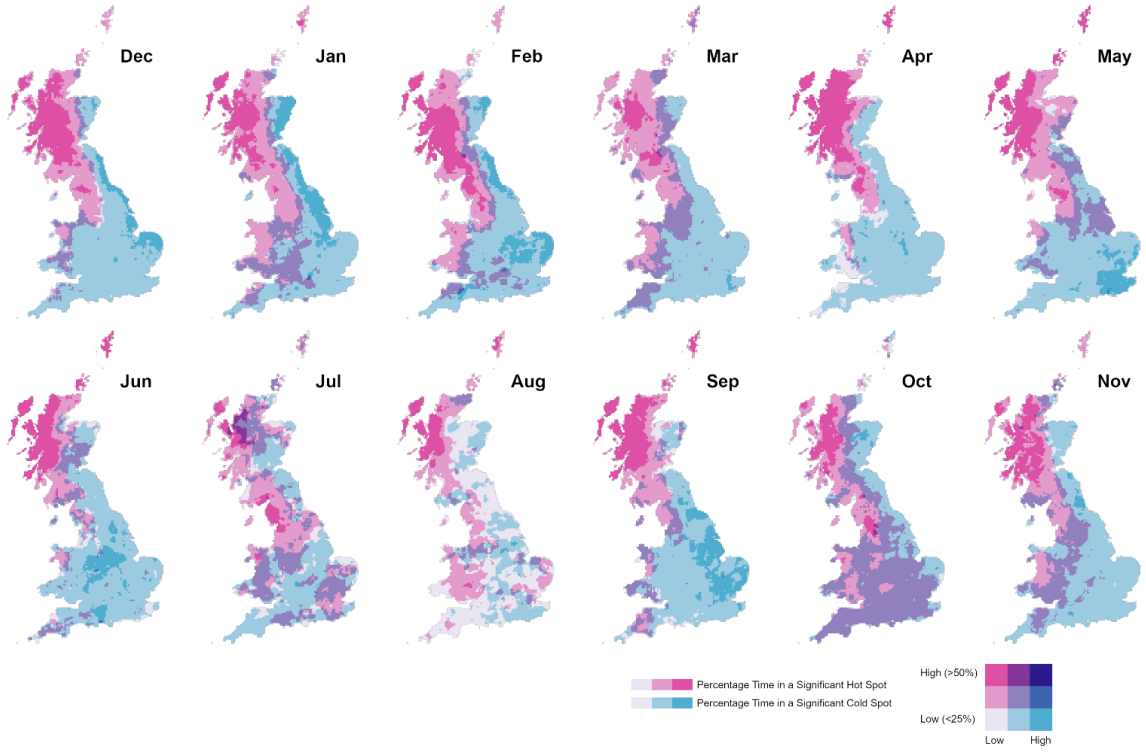

***Figure 4**: Space-time hot spot results under NAO+ conditions. Pinks indicate where the percentage of time in a significant (95%) hot spot is high (indicating wetter conditions), and light blues where the percentage of time in a significant (95%) cold spot is high (indicating drier conditions). Light grey indicates low occurrence of both hot and cold spots, whilst mixed shades indicate occurrence of both hot and cold spots. Disaggregated versions of these maps can be found in Appendix A.*

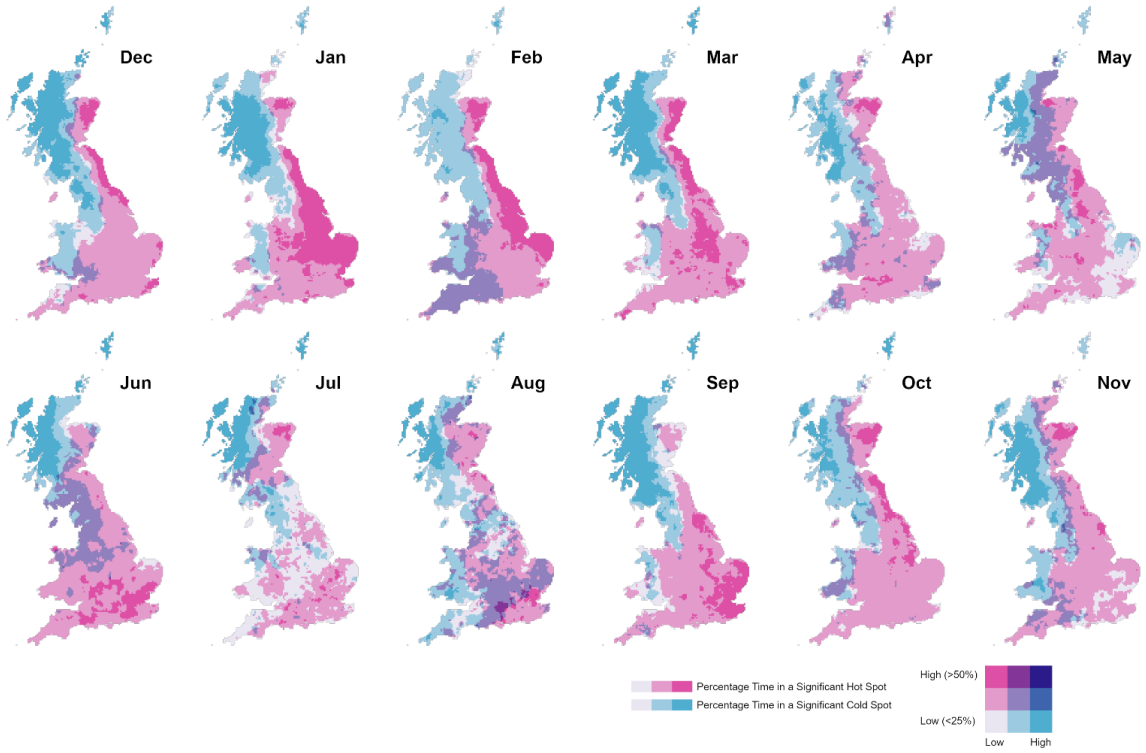

***Figure 5**: As per Figure 4 but under NAO− conditions.*

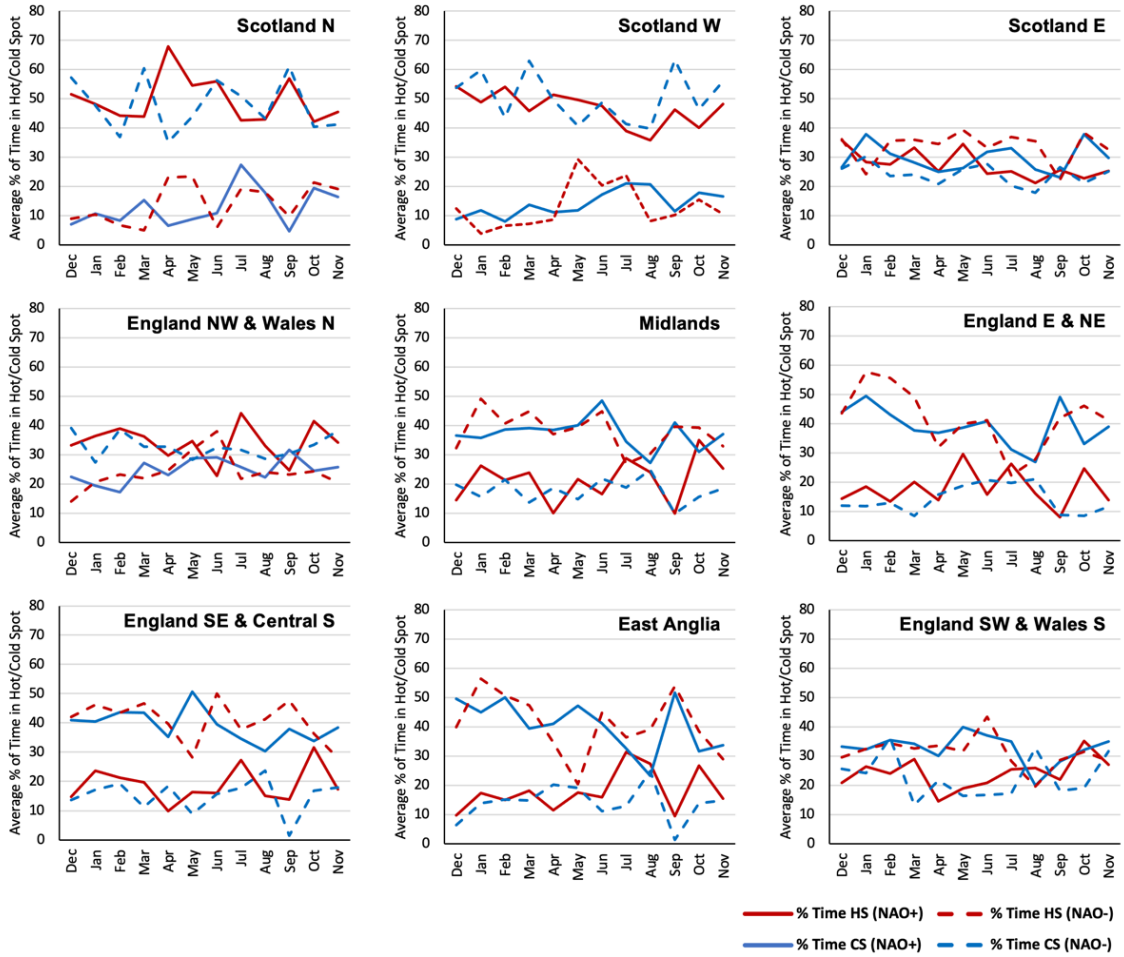

***Figure 6**: Regional average percentage of time in a significant hot/cold spot (based on the mapped results in Figures 4 and 5). Regions based on the Met Office Climate Districts for Great Britain.*

The space-time hot spot analysis reveals statistically significant spatio-temporal patterns in the NAO-rainfall response across Great Britain. The winter months are marked by the previously noted north-west/south-east spatial divide of opposing wet/dry responses to the NAO, as identified in other studies (Wilby et al. 1997; Rust et al. 2018; West et al. 2019b). In our analysis (Figure 4 and Figure 5), this pattern is shown by the location of widespread hot and cold spots in the NW and SE areas, indicating significant clusters of pixels with high/low (wet/dry) SPI-1 values. This suggests that the wet/dry spatial pattern we detect in winter rainfall associated with the phase of the NAO is statistically significant.

Looking across the record, this NW/SE opposing response appears to have a relatively high degree of consistency in some areas, for example, Scotland North and West, and to a slightly lesser extent England South West and Central South and East Anglia are in a statistically significant wet/dry cluster (hot/cold spot) for a relatively high proportion of the analysis period (Figure 6). This suggests that there is a higher probability that the NAO+ and NAO− phases will result in this statistically significant winter NW/SE spatial pattern. However, it should be noted that in winter, some areas, for example Scotland East and England North West and Wales North, show little or no difference between the occurrence of significant clusters of wet/dry SPI-1 values (hot/cold spots). Therefore, the effect of the NAO in producing significant wet/dry spatial patterns in these Climate Districts is more limited.

Figure 2 and Figure 3 show that the spatial rainfall response to the NAO is on average more homogeneous in the summer months (Folland et al. 2009; Hall & Hanna 2018; West et al. 2019b). As a result, less discernible patterns are found in the hot spot analysis, and the occurrence of statistically significant hot/cold spots (i.e., significant clusters of high/low SPI-1 values) is more variable in space and time (Figure 4 and Figure 5). Most Climate Districts show minor differences in the occurrence of significant clusters of wet/dry SPI-1 values in summer, except for Scotland North and West (Figure 6).

Space-Time Clustering Results

Figure 7 and Figure 8 present the space-time clustering results. This analysis explored the variability around the average NAO responses identified in Figure 2 and Figure 3 (discussed above). Each cluster represents spatial groupings of 5km pixels which have a similar response to the NAO phase during that month across the temporal record. The optimal number of clusters based on the pseudo-F statistic was consistently three. In Figure 7 and Figure 8, the more saturated the blue/red colour, the more distinctive the space-time cluster wet/dry response to the NAO (i.e., the space-time median value is wetter/drier). Less saturated clusters indicate a space-time median SPI-1 value closer to 0, suggesting a less distinctive wet/dry average rainfall response to the NAO across the temporal record. The distributions of cluster median SPI-1 values per time step are plotted in Figure 9, and the associated descriptive statistics are shown in Figure 10. Figure 11 and Figure 12 show frequency

histograms of the cluster median SPI-1 values and the percentage of time each cluster experiences wet/dry conditions.

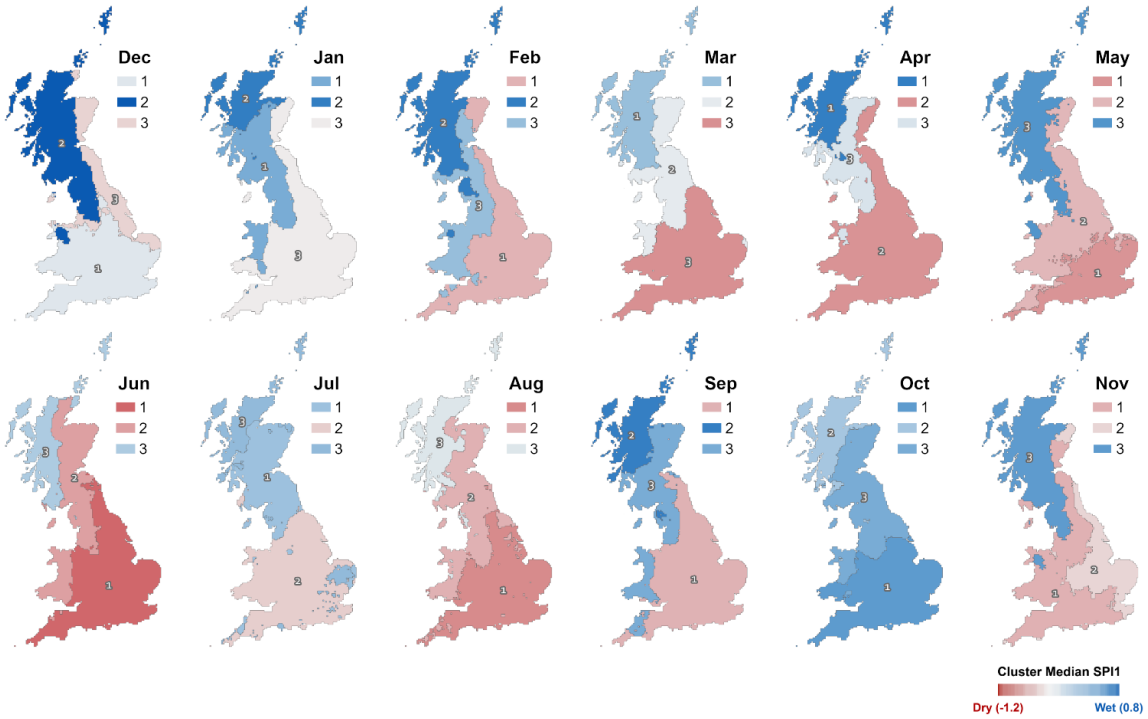

***Figure 7**: Monthly space-time clusters of SPI-1 values under NAO+ conditions. The clusters are coloured based on the median SPI-1 value of the cluster in space and time. Blue indicates a wetter median, whereas red indicates a drier median. Less saturated clusters indicate median SPI-1 values closer to 0.*

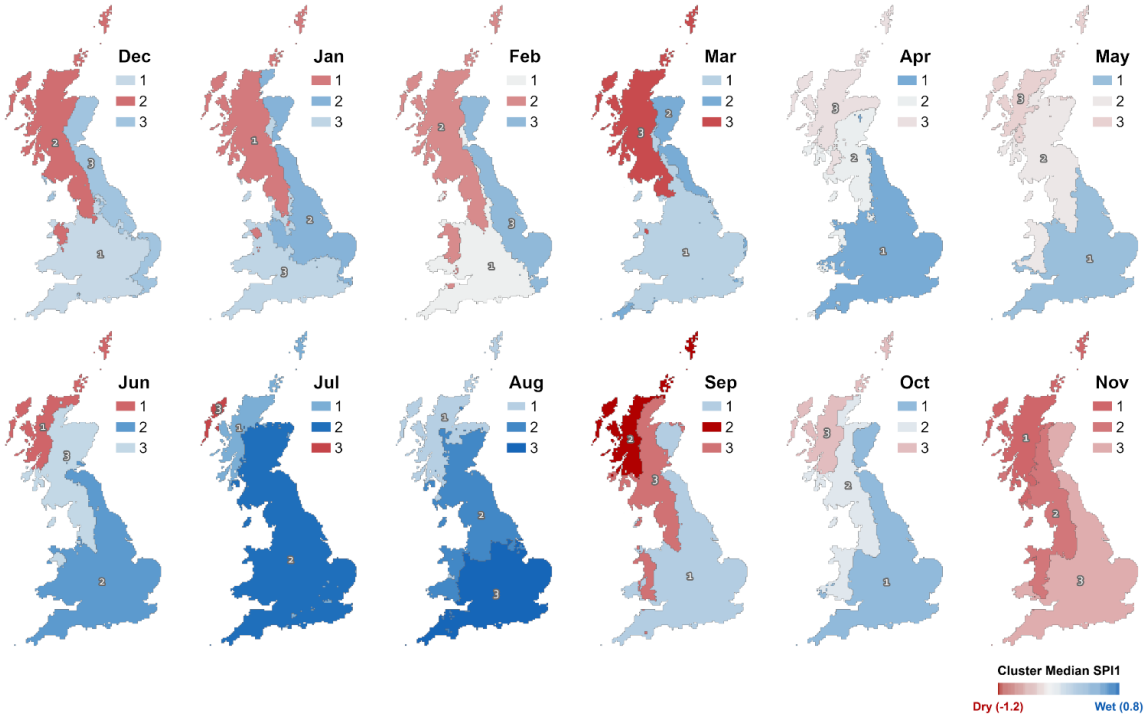

***Figure 8**: As per Figure 7 but showing the monthly space-time clusters of SPI-1 values under NAO− conditions.*

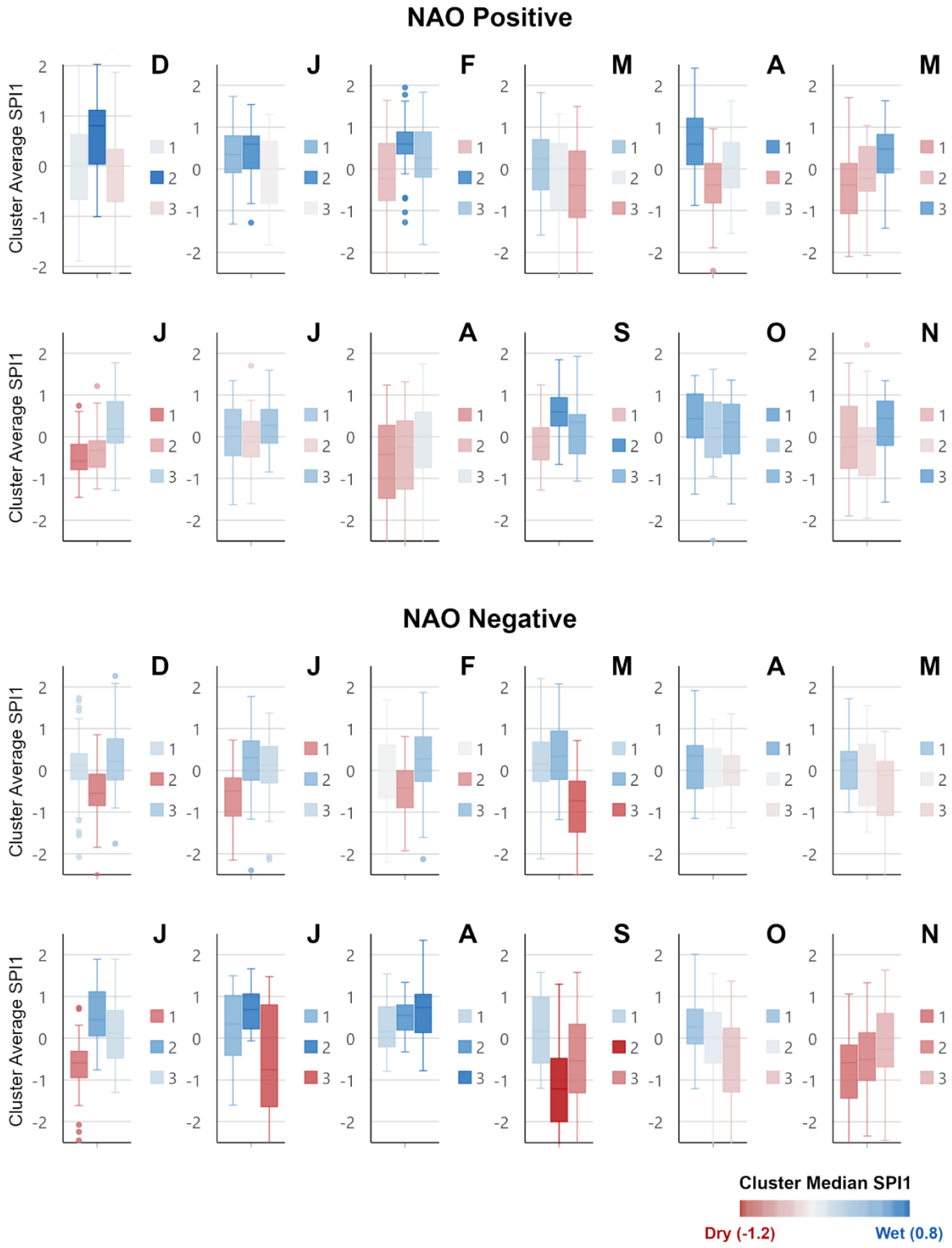

Figure 9: *Box plots representing the distribution of cluster median SPI-1 values for the space–-time clusters mapped in Figures 7 and 8. As with Figures 7 and 8 the box plots are coloured based on the median SPI-1 value of the cluster in space and time. Individual points represent outlier values.*

	Dec NAO Positive			Dec NAO Negative		
	1	2	3	1	2	3
Median	0.044	0.802	-0.114	0.115	-0.551	0.219
Mean	-0.018	0.567	-0.101	0.072	-0.518	0.250
Minimum	-1.891	-1.009	-2.134	-0.208	-2.516	-1.755
Maximum	2.010	2.028	1.868	1.733	0.852	2.263
Range	3.901	3.037	4.002	1.941	3.367	4.018
First Quartile	-0.667	0.037	-0.711	-0.219	-0.844	-0.229
Third Quartile	0.631	1.114	0.335	0.400	-0.093	0.757
IQR	1.298	1.078	1.046	0.619	0.751	0.986
STD	0.966	0.740	0.920	0.905	0.742	0.822
Variance	0.933	0.547	0.846	0.819	0.551	0.675

	Jun NAO Positive			Jun NAO Negative		
	1	2	3	1	2	3
Median	-0.581	-0.326	0.184	-0.591	0.441	0.119
Mean	-0.468	-0.268	0.269	-0.684	0.530	0.172
Minimum	-1.453	-1.249	-1.286	-2.449	-0.762	-1.301
Maximum	0.742	1.213	1.770	0.726	1.895	1.897
Range	2.195	2.461	3.055	3.175	2.657	3.198
First Quartile	-0.788	-0.732	-0.150	-0.943	0.051	-0.479
Third Quartile	-0.183	-0.101	0.842	-0.312	1.110	0.658
IQR	0.605	0.631	0.992	0.631	1.060	1.137
STD	0.540	0.636	0.763	0.840	0.757	0.841
Variance	0.291	0.405	0.583	0.705	0.574	0.707

	Jan NAO Positive			Jan NAO Negative		
	1	2	3	1	2	3
Median	0.345	0.597	-0.010	-0.497	0.304	0.130
Mean	0.318	0.450	-0.093	-0.646	0.215	-0.037
Minimum	-1.321	-1.289	-1.821	-2.655	-2.395	-2.797
Maximum	1.736	1.541	1.305	0.719	1.771	1.373
Range	3.057	2.830	3.126	3.374	4.166	4.170
First Quartile	-0.089	0.004	-0.823	-1.097	-0.237	-0.301
Third Quartile	0.793	0.784	0.658	-0.179	0.707	0.571
IQR	0.882	0.780	1.481	0.918	0.944	0.872
STD	0.678	0.601	0.852	0.751	0.833	0.914
Variance	0.459	0.362	0.726	0.565	0.695	0.835

	Jul NAO Positive			Jul NAO Negative		
	1	2	3	1	2	3
Median	0.233	-0.133	0.268	0.338	0.683	-0.758
Mean	0.025	-0.072	0.087	0.265	0.656	-0.772
Minimum	-1.624	-1.603	-3.140	-1.606	-0.065	-4.827
Maximum	1.347	1.696	1.593	1.493	1.662	1.474
Range	2.971	3.298	4.733	3.099	1.727	6.300
First Quartile	-0.452	-0.484	-0.158	-0.413	0.223	-1.646
Third Quartile	0.655	0.363	0.652	1.023	1.060	0.796
IQR	1.107	0.848	0.809	1.436	0.836	2.442
STD	0.846	0.849	1.089	0.933	0.534	1.826
Variance	0.716	0.720	1.186	0.871	0.285	3.335

	Feb NAO Positive			Feb NAO Negative		
	1	2	3	1	2	3
Median	-0.240	0.598	0.250	0.005	-0.421	0.274
Mean	-0.117	0.568	0.286	-0.112	-0.541	0.232
Minimum	-2.610	-1.279	-0.257	-2.980	-3.149	-2.123
Maximum	1.642	1.950	1.835	1.682	0.813	1.864
Range	4.252	3.230	2.092	4.663	3.962	3.987
First Quartile	-0.758	0.359	-0.198	-0.667	-0.891	-0.261
Third Quartile	0.608	0.881	0.886	0.611	-0.006	0.804
IQR	1.367	0.522	1.084	1.279	0.885	1.065
STD	0.966	0.656	0.910	1.102	0.877	0.875
Variance	0.933	0.430	0.829	1.214	0.768	0.765

	Aug NAO Positive			Aug NAO Negative		
	1	2	3	1	2	3
Median	-0.422	-0.250	0.049	0.156	0.540	0.732
Mean	-0.568	-0.441	-0.087	0.242	0.487	0.556
Minimum	-2.837	-2.565	-2.554	-0.792	-0.330	-0.782
Maximum	1.238	1.314	1.739	1.539	1.337	2.344
Range	4.075	3.879	4.293	2.331	1.667	3.125
First Quartile	-1.478	-1.260	-0.744	-0.206	0.199	0.132
Third Quartile	0.271	0.379	0.588	0.756	0.796	1.050
IQR	1.749	1.639	1.333	0.963	0.597	0.918
STD	1.085	1.055	1.163	0.618	0.484	0.732
Variance	1.178	1.114	1.352	0.382	0.234	0.536

	Mar NAO Positive			Mar NAO Negative		
	1	2	3	1	2	3
Median	0.246	0.028	-0.394	0.153	0.342	-0.729
Mean	0.166	-0.190	-0.396	0.152	0.342	-0.819
Minimum	-1.587	-2.561	-2.899	-2.119	-1.180	-2.505
Maximum	1.826	1.313	1.495	2.198	2.071	0.716
Range	3.413	3.874	4.393	4.317	3.250	3.220
First Quartile	-0.496	-0.971	-1.164	-0.259	-0.218	-1.479
Third Quartile	0.704	0.607	0.426	0.677	0.941	-0.259
IQR	1.200	1.578	1.590	0.936	1.159	1.220
STD	0.803	0.995	1.097	0.848	0.721	0.818
Variance	0.644	0.990	1.204	0.718	0.520	0.669

	Sep NAO Positive			Sep NAO Negative		
	1	2	3	1	2	3
Median	-0.246	0.590	0.343	0.172	-1.219	-0.537
Mean	-0.169	0.581	0.161	0.193	-1.257	-0.502
Minimum	-1.280	-0.665	-1.064	-1.201	-3.027	-2.651
Maximum	1.238	1.840	1.923	1.575	1.295	1.574
Range	2.518	2.505	2.988	2.776	4.323	4.226
First Quartile	-0.556	0.255	-0.407	-0.589	-2.002	-1.306
Third Quartile	0.214	0.935	0.527	0.980	-0.483	0.334
IQR	0.770	0.680	0.934	1.569	1.518	1.640
STD	0.684	0.565	0.733	0.864	1.029	1.127
Variance	0.467	0.319	0.537	0.746	1.058	1.270

	Apr NAO Positive			Apr NAO Negative		
	1	2	3	1	2	3
Median	0.590	-0.380	0.062	0.349	0.010	-0.057
Mean	0.606	-0.459	0.052	0.215	0.007	-0.036
Minimum	-0.875	-2.754	-1.543	-1.150	-1.171	-1.375
Maximum	2.414	0.958	1.622	1.911	1.237	1.350
Range	3.289	3.712	3.165	3.061	2.408	2.725
First Quartile	0.100	-0.813	-0.456	-0.439	-0.392	-0.356
Third Quartile	1.215	0.134	0.632	0.593	0.514	0.352
IQR	1.116	0.947	1.088	1.032	0.906	0.708
STD	0.826	0.862	0.796	0.764	0.624	0.589
Variance	0.682	0.743	0.634	0.583	0.389	0.347

	Oct NAO Positive			Oct NAO Negative		
	1	2	3	1	2	3
Median	0.435	0.206	0.344	0.269	0.042	-0.197
Mean	0.428	0.106	0.161	0.306	-0.128	-0.503
Minimum	-1.375	-2.658	-1.610	-1.209	-2.646	-3.936
Maximum	1.467	1.617	1.355	2.014	1.550	1.368
Range	2.842	4.275	2.965	3.224	4.196	5.304
First Quartile	-0.028	-0.495	-0.406	-0.137	-0.591	-1.289
Third Quartile	1.023	0.829	0.781	0.691	0.621	0.240
IQR	1.051	1.323	1.186	0.828	1.213	1.529
STD	0.718	0.993	0.844	0.724	0.899	1.165
Variance	0.515	0.985	0.713	0.524	0.808	1.356

	May NAO Positive			May NAO Negative		
	1	2	3	1	2	3
Median	-0.377	-0.223	0.475	0.243	-0.027	-0.117
Mean	-0.384	-0.163	0.347	0.090	-0.046	-0.485
Minimum	-2.096	-2.072	-1.421	-1.007	-1.474	-2.544
Maximum	1.708	1.040	1.634	1.717	1.547	0.935
Range	3.804	3.111	3.056	2.724	3.021	3.479
First Quartile	-1.073	-0.534	-0.094	-0.452	-0.841	-1.081
Third Quartile	0.130	0.532	0.826	0.452	0.628	0.216
IQR	1.202	1.066	0.920	0.904	1.468	1.297
STD	0.901	0.852	0.705	0.648	0.881	0.985
Variance	0.811	0.725	0.497	0.421	0.776	0.971

	Nov NAO Positive			Nov NAO Negative		
	1	2	3	1	2	3
Median	-0.249	-0.101	0.434	-0.587	-0.512	-0.268
Mean	-0.075	-0.225	0.286	-0.815	-0.537	-0.131
Minimum	-1.899	-1.952	-1.568	-3.504	-3.628	-2.448
Maximum	1.766	2.201	1.344	1.058	1.327	1.634
Range	3.664	4.152	2.913	4.563	4.955	4.083
First Quartile	-0.763	-0.927	-0.209	-1.434	-1.013	-0.686
Third Quartile	0.723	0.216	0.849	-0.162	0.129	0.593
IQR	1.486	1.143	1.059	1.273	1.141	1.279
STD	0.902	0.937	0.734	1.032	1.115	0.972
Variance	0.814	0.879	0.538	1.066	1.244	0.944

***Figure 10**: Descriptive statistics for the space-time cluster median SPI-1 box plots in Figure 9 (IQR = interquartile range; STD = standard deviation). Formatting of colours is applied per statistical measure. Blue indicates wetter mean/median SPI-1 values, red indicates drier mean/median SPI-1 values. Green graduated shading indicates greater range/IQR values.*

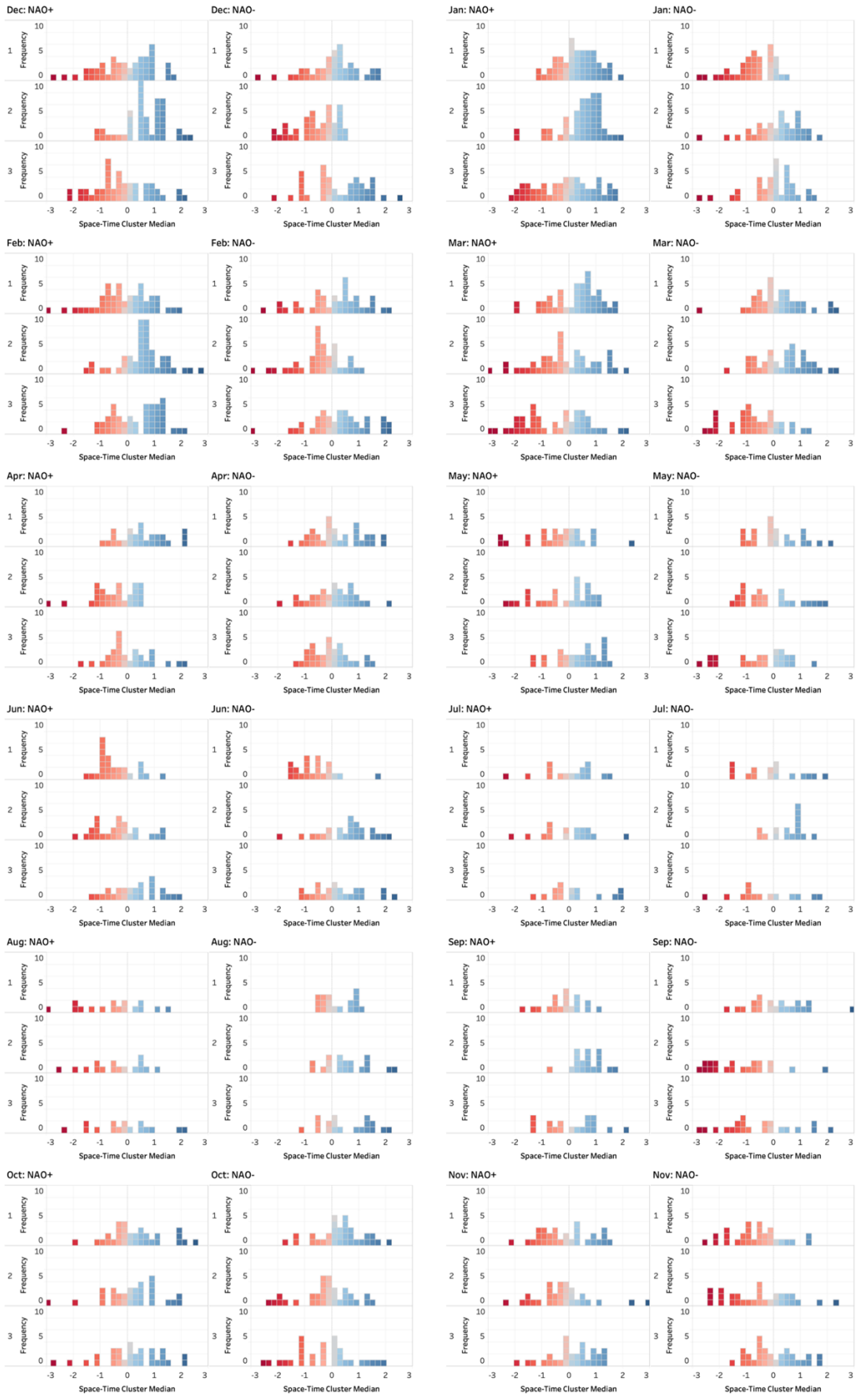

***Figure 11**: Frequency histograms of median SPI-1 values for the space–time clusters mapped in Figures 7 and 8.*

	Cluster	Dry Conditions (%)	Wet Conditions (%)	Difference (%)
Dec NAO-	1	42.5	57.5	-15.0
	2	72.5	27.5	45.0
	3	45.0	55.0	-10.0
Dec NAO+	1	50.0	50.0	0.0
	2	17.4	82.6	-65.2
	3	60.9	39.1	21.7
Jan NAO-	1	83.3	16.7	66.7
	2	38.9	61.1	-22.2
	3	41.7	58.3	-16.7
Jan NAO+	1	30.8	69.2	-38.5
	2	21.2	78.8	-57.7
	3	51.9	48.1	3.8
Feb NAO-	1	40.0	60.0	-20.0
	2	70.0	30.0	40.0
	3	40.0	60.0	-20.0
Feb NAO+	1	53.2	46.8	6.4
	2	19.1	80.9	-61.7
	3	36.2	63.8	-27.7
Mar NAO-	1	47.4	52.6	-5.3
	2	36.8	63.2	-26.3
	3	78.9	21.1	57.9
Mar NAO+	1	33.3	66.7	-33.3
	2	57.8	42.2	15.6
	3	60.0	40.0	20.0
Apr NAO-	1	46.9	53.1	-6.3
	2	43.8	56.3	-12.5
	3	56.3	43.8	12.5
Apr NAO+	1	27.6	72.4	-44.8
	2	65.5	34.5	31.0
	3	55.2	44.8	10.3
May NAO-	1	50.0	50.0	0.0
	2	58.3	41.7	16.7
	3	54.2	45.8	8.3
May NAO+	1	60.7	39.3	21.4
	2	46.4	53.6	-7.1
	3	32.1	67.9	-35.7

	Cluster	Dry Conditions (%)	Wet Conditions (%)	Difference (%)
Jun NAO-	1	87.5	12.5	75.0
	2	29.2	70.8	-41.7
	3	41.7	58.3	-16.7
Jun NAO+	1	76.9	23.1	53.8
	2	73.1	26.9	46.2
	3	38.5	61.5	-23.1
Jul NAO-	1	50.0	50.0	0.0
	2	18.8	81.3	-62.5
	3	62.5	37.5	25.0
Jul NAO+	1	43.8	56.3	-12.5
	2	50.0	50.0	0.0
	3	50.0	50.0	0.0
Aug NAO-	1	50.0	50.0	0.0
	2	33.3	66.7	-33.3
	3	27.8	72.2	-44.4
Aug NAO+	1	68.8	31.3	37.5
	2	62.5	37.5	25.0
	3	62.5	37.5	25.0
Sep NAO-	1	47.6	52.4	-4.8
	2	90.5	9.5	81.0
	3	71.4	28.6	42.9
Sep NAO+	1	63.2	36.8	26.3
	2	5.3	94.7	-89.5
	3	42.1	57.9	-15.8
Oct NAO-	1	27.3	72.7	-45.5
	2	60.6	39.4	21.2
	3	51.5	48.5	3.0
Oct NAO+	1	45.2	54.8	-9.7
	2	38.7	61.3	-22.6
	3	38.7	61.3	-22.6
Nov NAO-	1	79.3	20.7	58.6
	2	62.1	37.9	24.1
	3	55.2	44.8	10.3
Nov NAO+	1	56.7	43.3	13.3
	2	66.7	33.3	33.3
	3	43.3	56.7	-13.3

***Figure 12**: Percentage of time the cluster median SPI-1 value is wet (positive SPI-1 values) and dry (negative SPI-1 values) based on the frequency histograms in Figure 11. The difference value represents the difference between the per-centage of time under dry conditions and wet conditions.*

Examples of Consistent Monthly NAO-Rainfall Responses

In the space-time clustering analysis, the NAO-rainfall response observed in the average monthly SPI-1 analysis (Figure 2 and Figure 3) comes through clearly. For example, the north-west/south-east spatial divide in winter rainfall response (West et al. 2019b) can be seen in Figure 4 and Figure 5. During the winter months (DJF), the north-western areas experience the greatest change in rainfall under NAO+ and NAO− phases. In December, for example, the extremes of this response can be seen in NAO+ Cluster 2, which has a maximum cluster median SPI-1 value of 2 (extremely wet), and NAO− Cluster 2 which has a minimum cluster median SPI-1 value of −2.5 (extremely dry) (Figure 9 and Figure 10).

Clusters covering these north-western areas in winter also show a relatively more consistent NAO-rainfall response compared to other parts of the country. For example, Dec NAO+ Cluster 2 has a 65% chance of being relatively wetter than drier, whilst the similarly located Dec NAO− Cluster 2 has a 45% probability of experiencing drier rather than wetter conditions (Figure 11 and Figure 12). The interquartile range (IQR) of these two clusters also only include wet/dry cluster median SPI-1 values (Figure 9). Similar results for the north-western areas can be seen in January, for example the IQR for NAO− Cluster 1 only includes negative SPI-1 (dry) values (Figure 9).

In spring (MAM), similar spatial patterns to those described above can be seen, but with a north/south gradient in the clustering. As in winter, the median responses (Figure 7 and Figure

8) match with the average monthly values mapped in Figure 2 and Figure 3. For example, March NAO− Cluster 3 in north-western Scotland typically experiences notably dry conditions (Figure 8), with a 57% probability of experiencing drier rather than wetter conditions (Figure 11 and Figure 12). This cluster also has a notably low minimum cluster median value of −2.5 representing extremely dry conditions.

In summer (JJA), the more spatially homogeneous wet/dry NAO−/NAO+ responses in Figure 2 and Figure 3 can be seen in the cluster median values. Notably, the wet/dry directionality is the opposite to the NAO-rainfall response seen in the north-western areas during winter. For example, in June, NAO+ Clusters 1 and 2 which cover most of Great Britain (except for a cluster in the far north-west-Figure 7) show a relatively consistent dry response, with interquartile ranges (IQR) covering negative/dry SPI-1 values (Figure 9) and a 53% and 46% probability of drier rather than wetter conditions (Figure 11 and Figure 12).

Examples of Variable Monthly NAO-Rainfall Responses

The space-time clustering analysis also reveals that whilst typical and relatively consistent NAO response signals can be observed, there is also significant NAO-rainfall response variability within some of the space-time clusters.

Even in areas that show relative consistency, variability in the cluster median SPI-1 values can still be observed (Figure 9). For example, in December, NAO− Cluster 2 in the north-western region (Figure 8), the minimum cluster median SPI-1 value is −2.5 which represents extremely dry conditions; however, the maximum is an SPI-1 value representing near-normal conditions (0.8). Whilst drier conditions are more likely in this cluster (72.5%), wet conditions were present for 27.5% of the time period analysed (Figure 11 and Figure 12). In February, NAO+ Cluster 2, similarly covering the north-western area, the maximum cluster median SPI-1 value is 1.9 (severely wet) and the IQR covers positive values only. Whilst wetter than average conditions were found in this cluster for the majority of the time period (80%), the cluster did experience relatively dry conditions for 20% of the time period (Figure 11 and Figure 12). These findings suggest that whilst the typical winter NAO responses can be observed in the north-western area, there is also some variability in both the magnitude of the NAO-rainfall response and the directionality (i.e., positive/wet, or negative/dry SPI-1 values).

The rainfall response in clusters covering the central, southern and eastern areas of Great Britain support the average winter NAO-rainfall response mapped in Figure 2 and Figure 3. However, in comparison to the north-west, the winter rainfall response to NAO+ and NAO− phases is much more variable in clusters spanning these areas (Figure 7 and Figure 8). For example, NAO+ Cluster 1 in December, has a notably large value range, with cluster median SPI-1 values ranging from a maximum of 2 (extremely wet) to −1.8 (severely dry) (Figure 9 and Figure 10). The cluster median SPI-1 histograms also show a more normal distribution with

more equal probability of relatively wet and dry conditions in this cluster (Figure 11). Similar variability in these areas can also be seen in January and February. Clusters spanning the central and southern areas of Britain (Figure 7 and Figure 8) also show more variability in comparison to the north-west in spring.

In summer, some of the clusters covering the north-west exhibit more variability than similarly located clusters during the winter months. For example, June NAO+ Cluster 3 has a large cluster SPI-1 value range of −1.2 (moderately dry) to 1.7 (severely wet). Compared to the winter months in clusters covering the north-western area, the difference between the probability of wet and dry conditions associated with the phase of the NAO is reduced. In the example of June NAO+ Cluster 3, there is a 23% likelihood of experiencing wetter rather than drier conditions (Figure 11 and Figure 12). Some clusters during the summer months have large SPI-1 value ranges (Figure 9), and the likelihood of relative wet/dry conditions is equally likely (Figure 12), for example July NAO+ Cluster 2 and August NAO+ Cluster 1, which span the central, southern and eastern areas of Great Britain.

In late summer, the average NAO-rainfall response across Great Britain can be notably strong in comparison to June and July (West et al. 2019b). Whilst this can be observed in the clustering analysis, there is variability in the magnitude of the NAO-rainfall response. For example, August NAO− Cluster 3 shows a 45% likelihood of wetter rather than drier conditions (Figure 12). However, the magnitude of these wet events can vary—the cluster average SPI-1 range varies from −0.7 (slightly dry, but near-normal) to 2.3 (extremely wet) (Figure 10), and the frequency histograms show a wider spread across positive SPI-1 values (Figure 11). This demonstrates that even when there are clear average signals, as mapped in Figure 2 and Figure 3, there can be significant spatio-temporal variability in the NAO-rainfall response.

Discussion

This study sought to evaluate the variability in NAO-rainfall response across Great Britain at high spatial and temporal scales. Average 5 km gridded SPI-1 values were mapped under NAO+ and NAO− conditions for the period January 1900–December 2015 (Figure 2 and Figure 3). This revealed distinctive spatial signatures of the NAO in average monthly rainfall, such as the winter north-west/south-east spatial divide and more spatially homogeneous summer rainfall responses also observed in other studies (Wilby et al. 1997; Folland et al. 2009; Hall & Hanna 2018; Rust et al. 2018; West et al. 2019b). The key spatio-temporal differences in NAO-rainfall response and relative consistency/variability between winter and summer revealed by our space-time analyses are summarised in Figure 13.

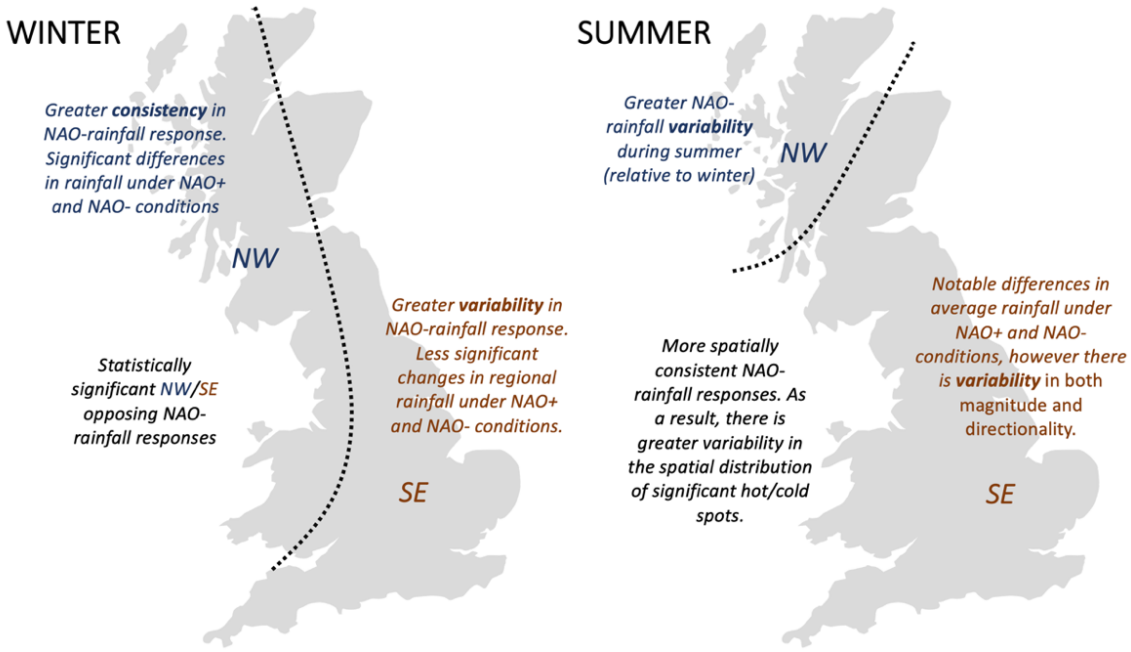

***Figure 13**: Schematic representation of the key spatio-temporal differences observed in NAO−-rainfall response during the winter and summer months.*

In the winter months, the results of the Getis-Ord Gi* space-time hot spot analysis confirm that the NW/SE spatial pattern (i.e., the spatial distribution of SPI-1 values) is statistically significant and consistent over the temporal record analysed (Figure 4 and Figure 5). The space-time clustering analysis (Figure 7 and Figure 8) also show these clear spatial patterns in the mean and median cluster average values, with clear differences as well in the frequency distribution of SPI-1 values related to NAO phase and region (Figure 11 and Figure 12). This indicates a more spatially reliable estimate of monthly rainfall volume under NAO+ and NAO− phases may be possible during the winter months.

In the north-western areas of Great Britain, the space-time clustering and hot spot analyses reveal rainfall is very responsive to the phase of the NAO. There are clear differences in rainfall response between the two NAO phases, with values markedly fluctuating between wet (positive SPI- values) and dry (negative SPI-1 values) (Figure 9). Significant wet conditions occur under NAO+ conditions and dry conditions under NAO−, which supports the significant NAOI-rainfall correlations found in other studies (Wilby et al. 1997; Afzal et al. 2015; Rust et al. 2018; West et al. 2019b). Our space-time analyses show that the NAO-rainfall response in the north-western area during winter also shows greater consistency in these significant NAO+/NAO− wet/dry rainfall deviations. In some space-time clusters, the frequency histograms show that the probability of relative wetness/dryness differs significantly in the north-west during winter, for example Jan NAO− Cluster 1 has an 83% likelihood of experiencing dry conditions, whilst the similarly located NAO+ Clusters 1 and 2 have a 69% and 78% likelihood of wetter than average conditions (Figure 11 and Figure 12). This indicates that we can have greater confidence in how the monthly rainfall volume in the north-western

area will change with the phase of the NAO during the winter months. Improved winter NAO forecasting skill (Parker et al. 2019; Athanasiadis et al. 2020; Smith et al. 2020) may therefore allow for effective water management decisions to be taken if we are able utilise this forecasting skill to predict an upcoming period of rainfall surplus (NAO+) or deficit (NAO−). However, it is important to note that even with these more consistent NAO-rainfall responses, our analysis shows the wet/dry response magnitude can still vary in the north-west (Figure 9 and Figure 11).

The southern, eastern and central areas of Great Britain have a consistent opposing (wet/dry) NAO-rainfall response to the north-west during the winter months (Figure 4 and Figure 5). However, the relative change in monthly average rainfall under NAO+ and NAO− conditions is notably less (Figure 2 and Figure 3), with median space-time cluster values in these areas being closer to 0 (Figure 9 and Figure 10). There is also greater variability in the NAO-rainfall response—the median SPI-1 histograms for clusters in these areas are typically more distributed across wet/dry values (Figure 11). The differences in the likelihood of relative wet/dry conditions associated with the phase of the NAO are notably reduced, being within approximately 20–30% (Figure 12). These findings suggest clear variability in both wet/dry event magnitude and directionality. As a result, it can be concluded that the NAO has a weaker and more variable influence on rainfall in the southern, eastern, and central areas, and as such, NAO forecasts might be of less practical use in water management decision making in comparison to the north-western area.

Differences in average monthly SPI-1 values during the summer months were found between the two NAO phases (Figure 2 and Figure 3), and less distinctive spatial differences between the north-western and southern/central areas of the country were found (Folland et al. 2009; Hall & Hanna 2018; West et al. 2019b) (Figure 4 and Figure 5). The more spatially consistent rainfall patterns during summer may be associated with greater convective rainfall generation (West et al. 2019b), compared to orographic rainfall during winter (Burt & Howden 2013). However, an area of future research would be to explore the physical processes resulting in the difference between NAO winter and summer rainfall patterns. On average, NAO+ conditions result in drier summer months, and NAO− wetter summer months (Figure 2 and Figure 3) aligning with negative NAOI-rainfall correlations observed in other studies (Folland et al. 2009; Hall & Hanna 2018; West et al. 2019b). The median space-time cluster values corroborate this (Figure 10), and in some cases clusters show more distinctive wet/dry summer responses, with the differences in the likelihood of relative wetness/dryness being approximately 50% for some clusters over the time period analysed (Figure 12). However, other clusters across the country also show notable variability in terms of magnitude and directionality in the NAO-rainfall response (Figure 9), with the relative probability of relative wetness/dryness being equal in some clusters (Figure 12). These findings demonstrate that even with clear average monthly signals (Figure 2 and Figure 3), there can be significant

variability in the NAO-rainfall (wet/dry) response, which may limit the practicality of NAO forecasts for water management decision making during summer.

In summary, our space-time analyses reveal that whilst typical NAO-rainfall signatures can be observed across the year, there is also significant NAO-rainfall response variability in space and time. This variability in both rainfall magnitude and wet/dry directionality may be a limiting factor in the utility of incorporating NAO forecasts into water management decision making (Rust et al. 2021b), even though the accuracy of these NAO forecasts has improved in recent years (Parker et al. 2019; Athanasiadis et al. 2020; Smith et al. 2020). The exception being in the north-western area during winter, where significant and more consistent changes in rainfall (Rust et al. 2018; West et al. 2019b) and subsequently catchment hydrology (Burt & Howden 2013), can be found relatable to the phase and strength of the NAO.

Variability in NAO-rainfall response in space and time across Britain might be explained by other North Atlantic and European atmospheric-oceanic circulations (teleconnections) moderating or enhancing the rainfall effect of the NAO and/or being potentially more dominant in driving regional rainfall in areas where the NAO's effect is weaker or when the NAO is in a neutral phase. As discussed above, in our analysis, the central, southern and eastern regions of Great Britain frequently had relatively variable NAO-rainfall responses under NAO+ and NAO− phases. The East Atlantic pattern in particular has been found to be positively correlated with rainfall these regions (Casanueva et al. 2014; Hall & Hanna 2018) and depending on its phase and strength may moderate or enhance the effect of the NAO on rainfall distribution and magnitude (Comas-Bru & McDermott 2014; Mellado-Cano et al. 2019).

Our research supports the findings of Hall and Hanna (2018), who suggest that even highly accurate NAOI forecasts might not provide enough information on their own to predict regional rainfall in Britain, and potentially subsequently catchment hydrology, several months in advance, without also considering the phase and magnitude of other atmospheric-oceanic circulations and climatic variables. As far as we are aware, no study has yet mapped at a high spatial and temporal (monthly) resolution the signature of these other North Atlantic/European circulations in regional rainfall across Great Britain.

In this study, the NAO was quantified using a PC-based NAOI, with phases defined using an approach adopted in previous work (Berton et al. 2017; West et al. 2019b). However, it is important to note that there is no universal approach to defining the NAO (Hurrell & Deser 2009), and there is an opportunity for future work to explore the sensitivity of these results to the chosen NAOI and phase definition method. We have demonstrated the effectiveness of high resolution spatio-temporal analytical methods in exploring the meteorological impact of atmospheric circulations and revealing spatio-temporal climatic patterns. For example, the Getis-Ord Gi* statistic allowed for the identification of statistically significant spatial wet/dry patterns in the SPI-1 data in the winter months, although we acknowledge its limitation in

detecting significant high/low value clusters in summer due to the more spatially consistent rainfall response. The space-time clustering analysis allowed us to look beyond average conditions and explore spatial and temporal consistency of the average and well-established NAO rainfall signatures in Great Britain. However, it is important to note that due to the random nature of the initial seed locations for the space-time clusters, modestly different results may be produced with a re-running of the analysis. This may be the case for locations (5km pixels) where the spatial differences in the SPI-1 time series values are smaller and so may switch cluster membership between model runs, for example in the Midlands area between the more distinctive NW/SE zones during winter.

Conclusion

This study presents a novel application of space-time analyses to understand the variability in NAO-rainfall signatures at a high spatial (5km) and temporal (monthly) resolution in Great Britain. Our analyses confirm that statistically significant NAO-rainfall signatures can be observed, and some regions show relatively high consistency in rainfall response to the phase of the NAO over time. However, our analyses also reveal that there is significant spatio-temporal variability in the rainfall response to the NAO, especially in the central, southern, and eastern areas of Great Britain. This has implications for the practical application of the NAOI in regional hydrometeorological forecasting as it is important to consider the variability in regional NAO-rainfall response under positive and negative phases of the NAO across Great Britain.

We suggest that such spatio-temporal variability might be explained by also considering the phase and magnitude of other atmospheric-oceanic teleconnections such as the East Atlantic Pattern. There is a need for high spatial and temporal resolution exploration of the hydrometeorological impact of these secondary modes of climate variability/teleconnections on rainfall in Great Britain, and in particular, the extent to which they might moderate or enhance the regional rainfall response to the NAO.

Appendix A

***Figure A1**: Disaggregated space-time hot spot results (DJFM). Values indicate percentage of time in a statistically significant hot/cold spot.*

Figure A2: Disaggregated space-time hot spot results (AMJJ). Values indicate percentage of time in a statistically significant hot/cold spot.

*Figure A3: Disaggregated space-time hot spot results (ASON). Values indicate percentage of time in a statistically significant hot/*cold *spot.*

Paper 4: The Spatio-Temporal Influence of Atmospheric Circulations on Monthly Precipitation in Great Britain

Citation: West, H., White, P., Quinn, N. & Horswell, M. (2022). The Spatio-Temporal Influence of Atmospheric Circulations on Monthly Precipitation in Great Britain. *Atmosphere*, Vol.13(3), 429.

Published: 7th March 2022.

Contributions: The analysis presented in this paper was developed in collaboration and with specialist advice provided by PW. HW completed the work with support by PW, the finished work was then shared with NQ and MH for feedback. HW led on the initial draft paper with comments offered by PW, NQ and MH prior to submission.

Changes to Original Paper:

- No changes have been made between this version and that published in March 2022.

Abstract

It has long been understood that the North Atlantic Oscillation (NAO) is a key driver of regional climate in Great Britain and across Europe. However, studies have also noted that there is spatio-temporal variability in NAO-rainfall signatures which arguably limits its practical inclusion in water management. In this study we quantify, at high spatio-temporal resolution, the influence of a broader set of atmospheric circulations on monthly precipitation. Using Standardised Precipitation Indices for the Integrated Hydrological Unit (IHU) Groups of Great Britain we apply univariate and multivariate regression models to understand the potential of five atmospheric circulation indices to explain precipitation variability. As far as we are aware this represents the first high spatial and temporal resolution analysis quantifying the influence of a broad set of atmospheric circulations, both individually and in combination. We highlight the influence of each circulation and establish that the NAO only partially explains precipitation variability, especially in the southern regions and during the summer months, where circulations, such as the East Atlantic Pattern, also have an important influence. In summary, we suggest that there is significant explanatory value in looking beyond the NAO when seeking to understand hydroclimatological variability in Great Britain, and there is potential for future work to explore how this understanding can translate into the practical application of atmospheric circulation indices in water management.

Introduction

Barnston and Livezey (1987) identified a number of large-scale atmospheric-oceanic circulations (teleconnections) in the North Atlantic and European region. Subsequent studies have continued to explore how they interact and influence climate across various spatial and temporal scales. In particular, the North Atlantic Oscillation (NAO) has been identified as a key climatic driver (Hurrell & Van Loon 1997; Rodwell et al. 1999), and strong associations between the phase and strength of the NAO and regional rainfall in Great Britain have been reported (Wilby et al. 1997; Fowler & Kilsby 2002; Rust et al. 2018). The NAO is defined by the difference in sea level pressure (SLP) between Iceland and the Azores (Hurrell et al. 2003) and fluctuates between positive (a greater than usual difference in SLP between Iceland the Azores) and negative (a weaker than usual difference in SLP between Iceland and the Azores) phases, quantified by North Atlantic Oscillation Indices (NAOI). Each phase of the NAO results in characteristic rainfall signatures in Great Britain (West et al. 2019b). Winter rainfall in the north-western regions, in particular, has a strong positive correlation with the NAOI (Wilby et al. 1997; Rust et al. 2018; Simpson & Jones 2014; Hall & Hanna 2018), and whilst the NAO is weaker during the summer (Folland et al. 2009), negative NAOI-rainfall correlations across Great Britain have been reported (Folland et al. 2009; Hall & Hanna 2018; West et al. 2019b). The rainfall effect of the NAO propagates through the hydrological system (Kingston et al. 2006) and relationships have been found with streamflow (Kingston et al. 2009; Wrzesinski & Paluszkiewicz 2011; Burt & Howden 2013; Rust et al. 2021a; West et al. 2022a), groundwater (Lavers et al. 2015; Rust et al. 2019) and water temperatures (Wilby & Johnson 2020). There is also potential to include the NAO into seasonal streamflow modelling and forecasting (UK Hydrological Outlook 2020; Donegan et al. 2021).

Whilst there are strong relationships between the NAO and rainfall (and subsequent hydrological variables), West et al. (2021a) found that NAO-rainfall signatures across Great Britain can vary over space and time. Whilst more temporally consistent and significant rainfall patterns were found in the north-west during winter, there was greater rainfall variability in the south and east (West et al. 2021a). Despite recent advancements in the skill of winter NAO forecasts (Athanasiadis et al. 2020; Smith et al. 2020), spatio-temporal variability in the NAO-rainfall effect is one of the limiting factors in the inclusion and application of the NAOI in water management (Hall & Hanna 2018; West et al. 2021a; Rust et al 2021b).

Variability in NAO-rainfall signatures may be associated with other atmospheric circulations also influencing regional climate (West et al. 2021a). Based on the method of Barnston and Livezey (1987), NOAA provide modelled monthly indices for different northern hemisphere circulations (NOAA 2021a). These have been used globally in studies exploring the impact of atmospheric circulations on climate, hydrology and the environment (Casanueva et al. 2014; Irannezhad et al. 2015; Bednorz et al. 2018; 2021; Amini et al. 2020; Uvo et al. 2021).

The East Atlantic Pattern (EA) is often defined as a monopole system, south of Iceland and west of Great Britain (≈55° N; 20–35° W) (Barnston & Livezey 1987; Moore & Renfrew 2012; Mellado-Cano et al. 2019). The EA is cited as the second most influential circulation affecting climate in the North Atlantic region, after the NAO (Mikhailova & Yurovsky et al. 2016; Maidens et al. 2021). Positive correlations between the EA and rainfall have been reported which are generally stronger in the southern regions of Great Britain and during winter [10,28,38] (Casanueva et al. 2014; Hall & Hanna 2018; West et al. 2021b). The EA can influence the strength and location of the NAO dipoles (Moore et al. 2011; 2013) which results in different spatial distributions and volume of rainfall across Europe (Mellado-Cano et al. 2019; West et al. 2021b; Rodrigo et al. 2021) and the likelihood of hydrological extremes (Chen et al. 2021; West et al. 2022b). Comas-Bru & McDermott (2014) conclude that a combination of the NAO and EA may be able to explain winter climate variability more accurately across the North Atlantic region.

The Scandinavian Pattern (SCA) has a primary centre of action around the Scandinavian Peninsula and two secondary, oppositely signed, centres over the north-eastern Atlantic and central Siberia (Bueh & Nakamura 2007). Originally referred to as the Eurasia-1 pattern, the SCA is the third leading mode of North Atlantic climate variability (Barnston & Livezey 1987; Comas-Bru & McDermott 2014). During winter, a positive SCA phase results in increased precipitation over southern Europe and the United Kingdom, and decreased precipitation over Scandinavia (Bueh & Nakamura 2007). Like the EA, the SCA can affect the location and strength of the Azores High and Icelandic Low dipoles (Moore et al. 2013), subsequently influencing climatic variables such as temperature, rainfall and windspeed (Comas-Bru & McDermott 2014; Zubiate et al. 2017). Rainfall deviations as a result of the phase of the SCA also propagate to streamflow in Scandinavia (Uvo et al. 2021).

Two arguably lesser studied atmospheric circulations in the North Atlantic and European region include the East Atlantic-West Russia Pattern and the Polar/Eurasia Pattern. The East Atlantic-West Russia Pattern (EAWR) was originally referred to as the Eurasia-2 pattern by Barnston and Livezey (Barnston & Livezey 1987). Strong relationships between the EAWR and rainfall have been reported across the East Atlantic, Europe and the Mediterranean (Krichak & Alpert 2002; 2005; Caroletti et al. 2021). A positive phase of the EAWR results in drier conditions across Europe and the Mediterranean, whilst negative phases result in wetter conditions (Ionita 2014). This relationship is strongest during the winter and decreases into late spring where there is no significant relationship (Ionita 2014). The Polar/Eurasia Pattern (POL) is associated with variations in the circumpolar circulation with positive (negative) phases reflecting a stronger (weaker) polar vortex (Barnston & Livezey 1987). During winter POL has two action centres, over the Kara Sea and East Asia, and during summer an additional third centre over midlatitude Europe (Barnston & Livezey 1987; Gao et al. 2019).

The POL influences climate predominately over Asia and eastern Europe (Gao et al. 2019) and may be linked to the NAO (Balling & Goodrich 2011).

Whilst studies have explored the climatic effects of each of these atmospheric circulations, both individually and in various combinations, many have been undertaken at coarse spatial resolution across Europe and the North Atlantic, or have been restricted to the winter months (e.g., Moore et al. 2013; Comas-Bru & McDermott 2014; Mellado-Cano et al. 2019). As far as we are aware, no study has yet explored at high resolution, the influence of all five of these circulations on monthly precipitation in Great Britain. This study aims to address this by firstly exploring how the circulations, both individually and in combination, are related to precipitation variability, and secondly how the relative importance of each circulation in influencing rainfall varies across space and time.

Methods

Data

As noted above, the NOAA Climate Prediction Centre (NOAA 2021a) models monthly teleconnection indices, from 1950 onwards, based on the rotated principal component analysis approach of Barston and Livezey (1987). Such modelling approaches avoid limitations associated with indices derived from station-measured SLP data (Pokorná & Huth 2015), principally the mobility of circulation action centres (Moore et al. 2013). Monthly indices for the NAO, EA, SCA, EAWR and POL circulations were downloaded from NOAA for the period January 1950–December 2015, corresponding to the availability of the SPI time series described below.

To represent rainfall variability, Standardised Precipitation Index (SPI) time series were downloaded from the UK Centre for Ecology and Hydrology (CEH) aggregated for the Integrated Hydrological Unit (IHU) Groups of Great Britain (Tanguy et al. 2017b). These 105 IHU Groups are catchment-based zones and represent a useful basis for exploring spatial patterns, whilst retaining scale for water management relevance. The SPI time series had a one-month accumulation period (SPI-1), and were calculated by fitting a gamma distribution to historical Met Office 5 km rainfall grids with a standard period of 1961–2010 (Tanguy et al. 2017b). Monthly data (i.e., SPI with a one-month accumulation period) was chosen as to avoid the intra-/inter-seasonal dilution of teleconnection rainfall patterns (West et al. 2022a). The SPI-1 data are scaled from relative wetness (positive values) to dryness (negative values) allowing for an assessment of relative rainfall magnitude, or wet/dry severity, in a given month. The analysis period (January 1950–December 2015) therefore represents the greatest overlap across precipitation and circulation indices.

Regression Analysis

Stage 1 of the analysis quantifies the potential of each individual atmospheric circulations ability to infer precipitation variability across Great Britain. Univariate linear regression models were used to understand the strength of the relationship between the teleconnection index and SPI-1 time series for each calendar month across the IHU Groups. Based on these univariate models, the R^2 values were used to assess the strength of the relationship.

Stage 2 of the analysis explores whether atmospheric circulation indices, in combination, offer additional explanatory ability across space and time than indices in isolation. To do this a multiple linear regression model of all five atmospheric circulation indices was developed, with SPI-1 as the dependent variable. This was also undertaken for each calendar month and for all IHU Groups. Similar multiple regression models have been applied in understanding the combined effect of circulations in previous research (Chun et al. 2021). As above, the R^2 values were used to evaluate the strength of the relationship, whilst the standardised coefficient (SC) (or beta coefficient) values for each teleconnection index gave an indication of the relative influence of each circulation in the model and the nature/directionality of the relationship with SPI-1. The SC values therefore identify the most influential atmospheric circulation affecting precipitation, its dominance relative to the other four circulations, and how this varies in space and time. Figure 1 describes the analytical stages undertaken in this study.

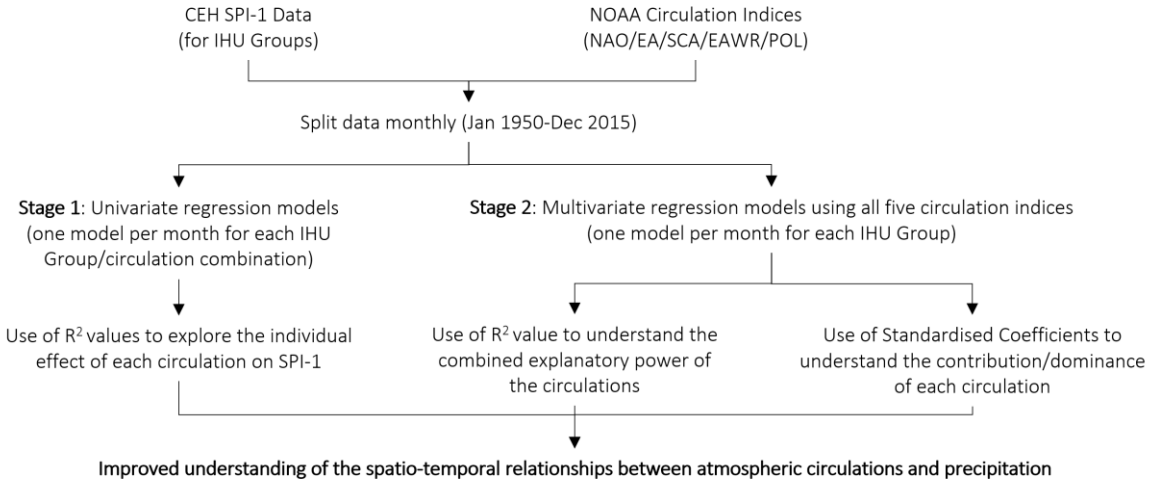

***Figure 1**: Flow chart summarizing the methodological stages of this study.*

Results

Univariate Regression Models

Figure 2 shows the strength of the relationship (R^2 values) between the NAO index and SPI-1, which distinctly changes in space and time. The relationship between the NAO and SPI-1 is

strongest during the winter months and in northern England and Wales and the Scottish regions. During summer the strength of the NAO SPI-1 relationship is weaker. Figure 3 shows the comparable R^2 values for the univariate EA regression model. Generally, the EA has a spatially and temporally consistent moderate relationship between the circulation index and SPI-1, which is weakest in the far north during winter and across large parts of the country in March, June and July.

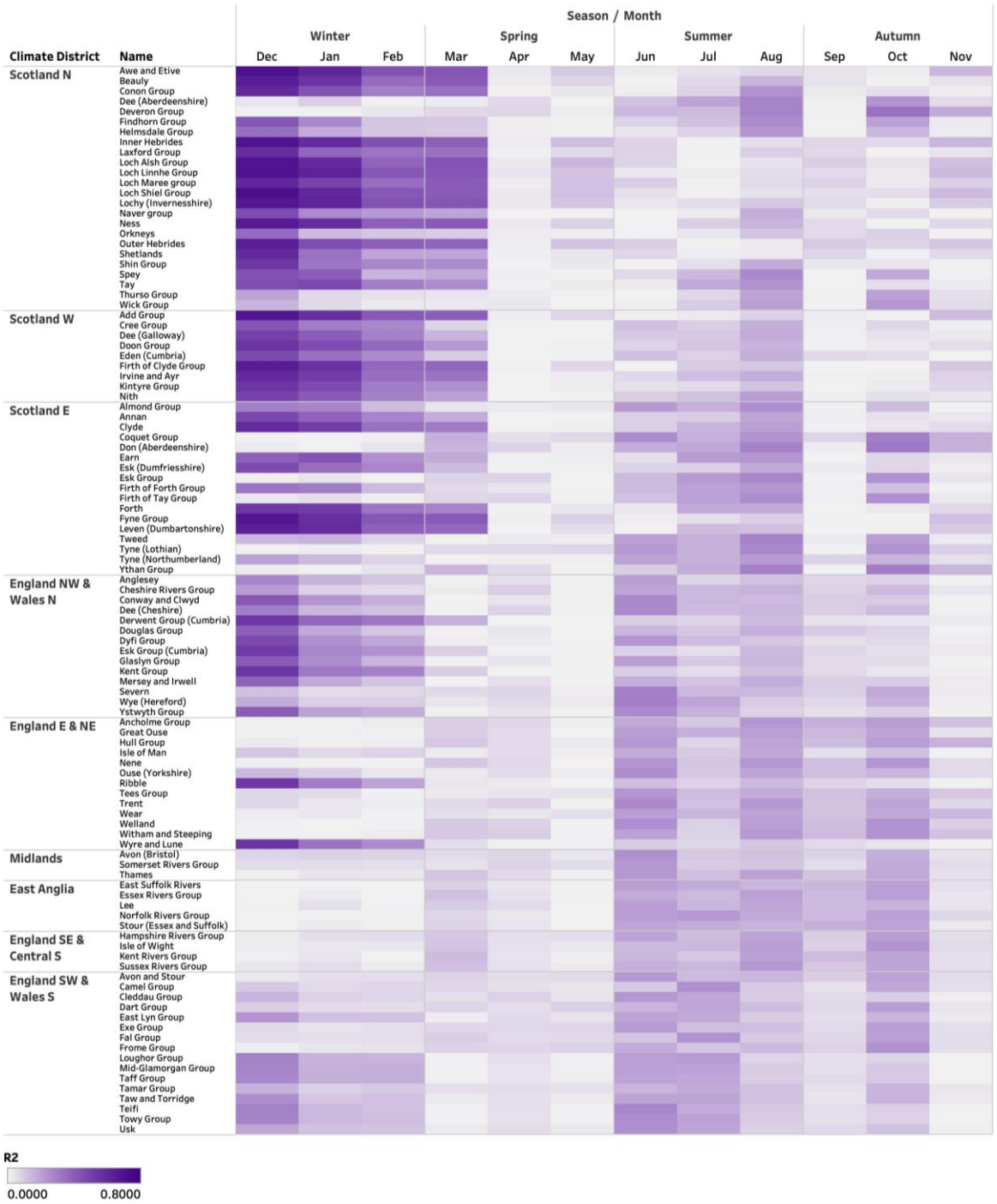

***Figure 2**: R^2 values of the univariate regression model exploring the relationship between the NAO index and SPI-1 values across the IHU Groups. Climate Districts relate to the nine Met Office Climate Distracts of Great Britain–a spatial unit used in previous research (Wilby et al. 1997; Simpson & Jones 2014; West et al. 2019b; 2021a).*

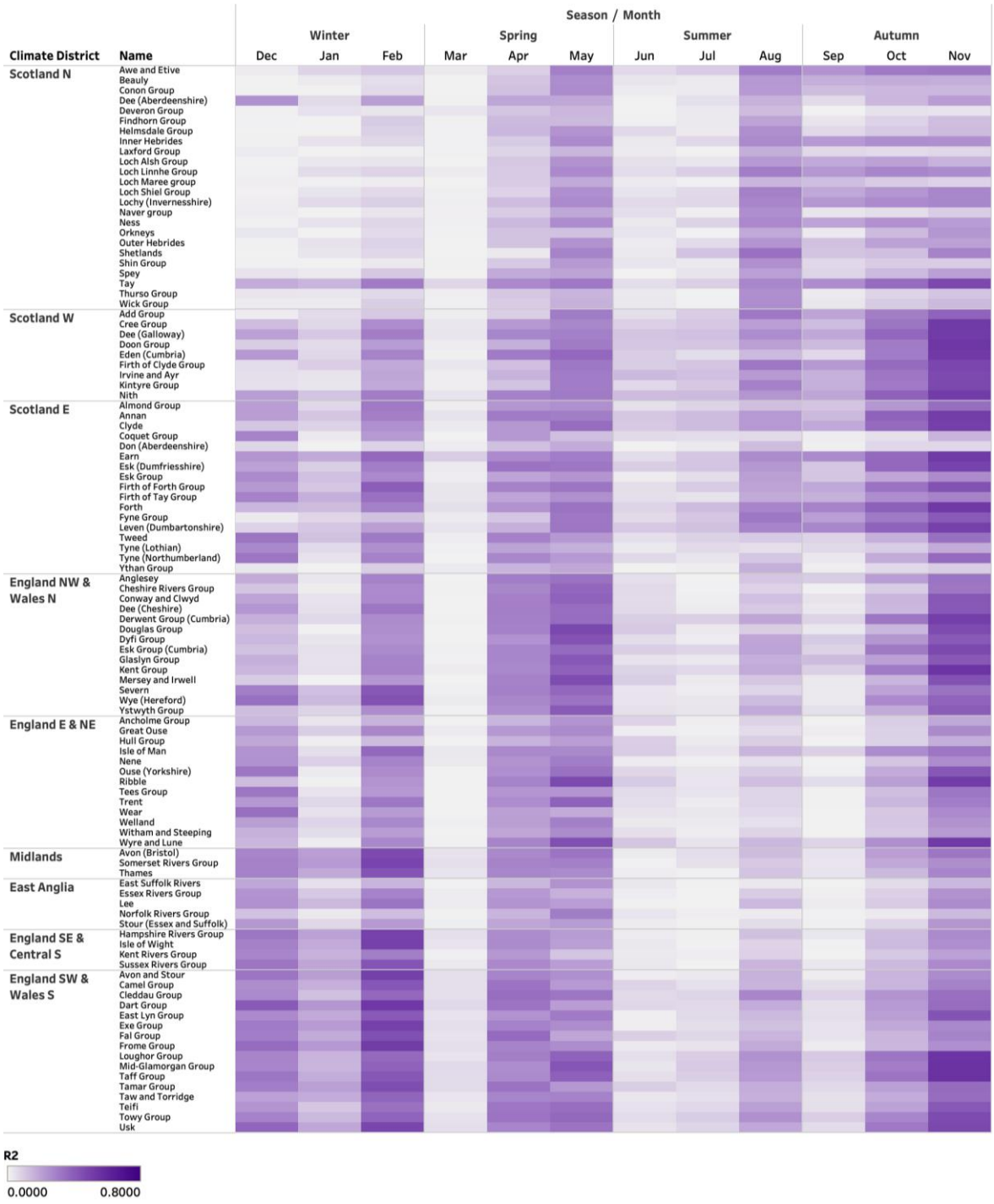

Figure 3: R2 values of the univariate regression model exploring the relationship between the EA index and SPI-1 values across the IHU Groups.

The NAO and EA models have the strongest R^2 values between the circulation indices and SPI-1, relative to the univariate models for the SCA, EAWR and POL circulations-figures for which can be found Appendix A. The SCA generally has a weak relationship with SPI-1 across most of the country, with the exception of late winter–early autumn in the north of Scotland (Figure A1). Likewise, the EAWR R^2 values are generally weak, especially during the summer months. However, the EAWR does have a strong relationship with SPI-1 in the southern regions in

January (Figure A2). The POL has a very weak relationship with SPI-1 across most of the year, especially during late spring and early summer (Figure A3).

Multivariate Regression Model

The results of the univariate regression analyses show that the ability of each circulation to explain precipitation varies in space and time, with the NAO and EA circulations generally having a stronger relationship with SPI-1. This stage of the analysis explores whether looking at the atmospheric circulation indices in combination offers greater explanatory ability than using the indices in isolation. Figure 4 shows the R^2 values of the multivariate regression model describing the strength of the relationship between a linear combination of the five circulation indices and SPI-1. In comparison to the univariate model outputs in Figure 2 and Figure 3, and Figure A1, Figure A2 and Figure A3 (Appendix A), the multivariate model has more spatially and temporally consistent and stronger R^2 values. This indicates that there is additional value in looking at the combined effects of the atmospheric circulations in explaining precipitation variability, rather than considering circulations in isolation. The multiple regression model is notably stronger during the winter months across Great Britain, and there is improved performance in summer as well. The weakest relationship between the combined circulation indices and SPI-1 is found in March across England and Wales.

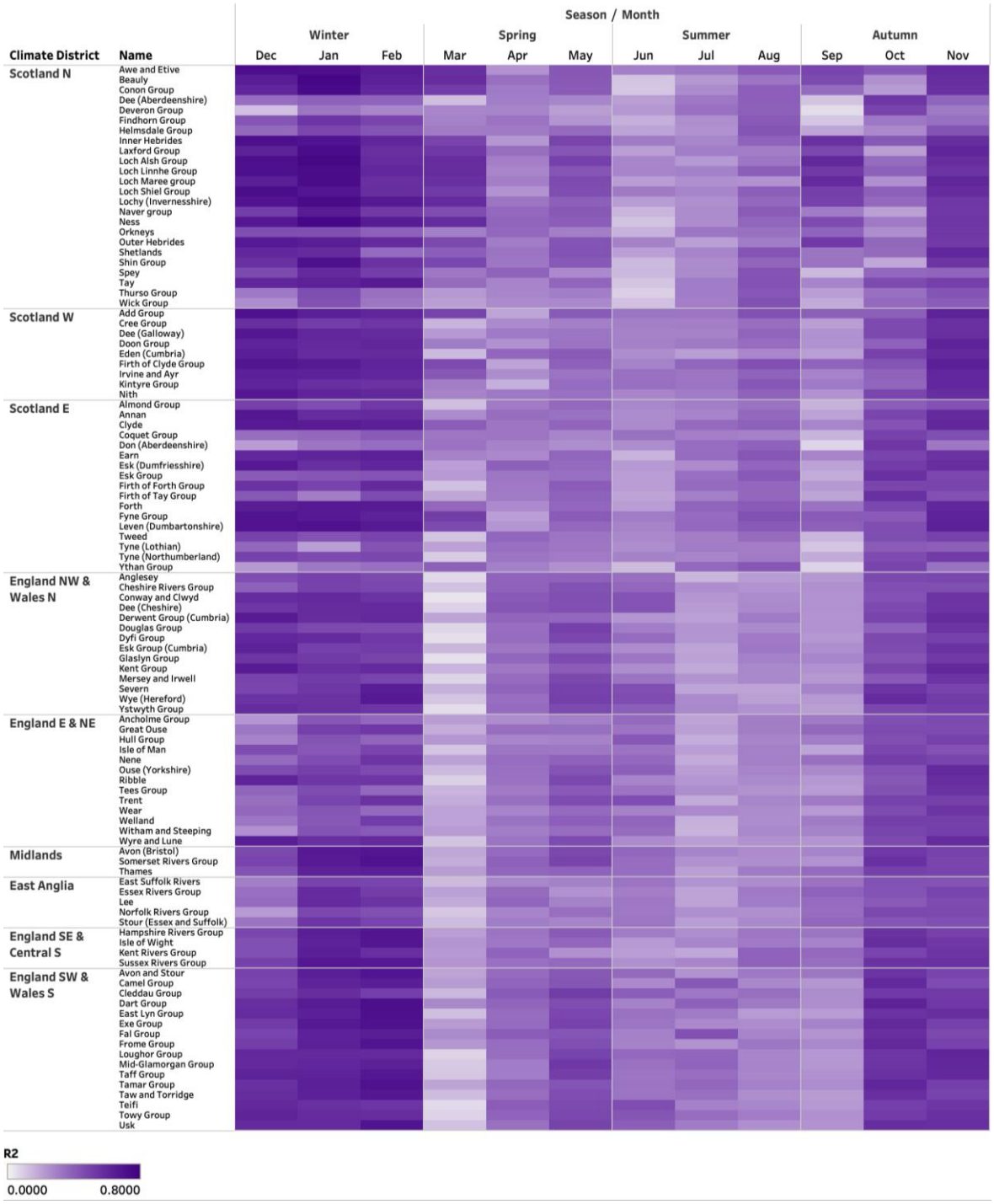

***Figure 4**: R^2 values of the multivariate regression model exploring the relationship between a combination of all five circulation indices and SPI-1 values across the IHU Groups.*

Using the standardised coefficients (SC) of the circulation indices from the multiple regression analyses enables exploration of the strength and directionality (positive/negative) of these relationships. Figure 5, Figure 6, Figure 7, Figure 8 and Figure 9 show the SC for each circulation index. The SC for the NAO (Figure 5) show the spatially and temporally variable nature of its relationship with precipitation. In the winter there is a positive relationship (green) with SPI-1, which is strongest in the north-western regions (also shown in the Figure 1). This indicates that positive phases of the NAO are associated with wetter conditions, and drier

conditions with NAO negative phases. In Spring and Autumn more of a north-west/south-east spatial difference is observed, with positive SC in the north and negative SC (purple) in the south. Finally, the summer months show a negative relationship across most of the country between the NAO and SPI-1. This indicates the effect of the phase of the NAO on precipitation is opposite to winter in the summer months; with NAO positive (negative) phases associated with drier (wetter) conditions. For most of the year, the relationship remains relatively strong compared to the other indices.

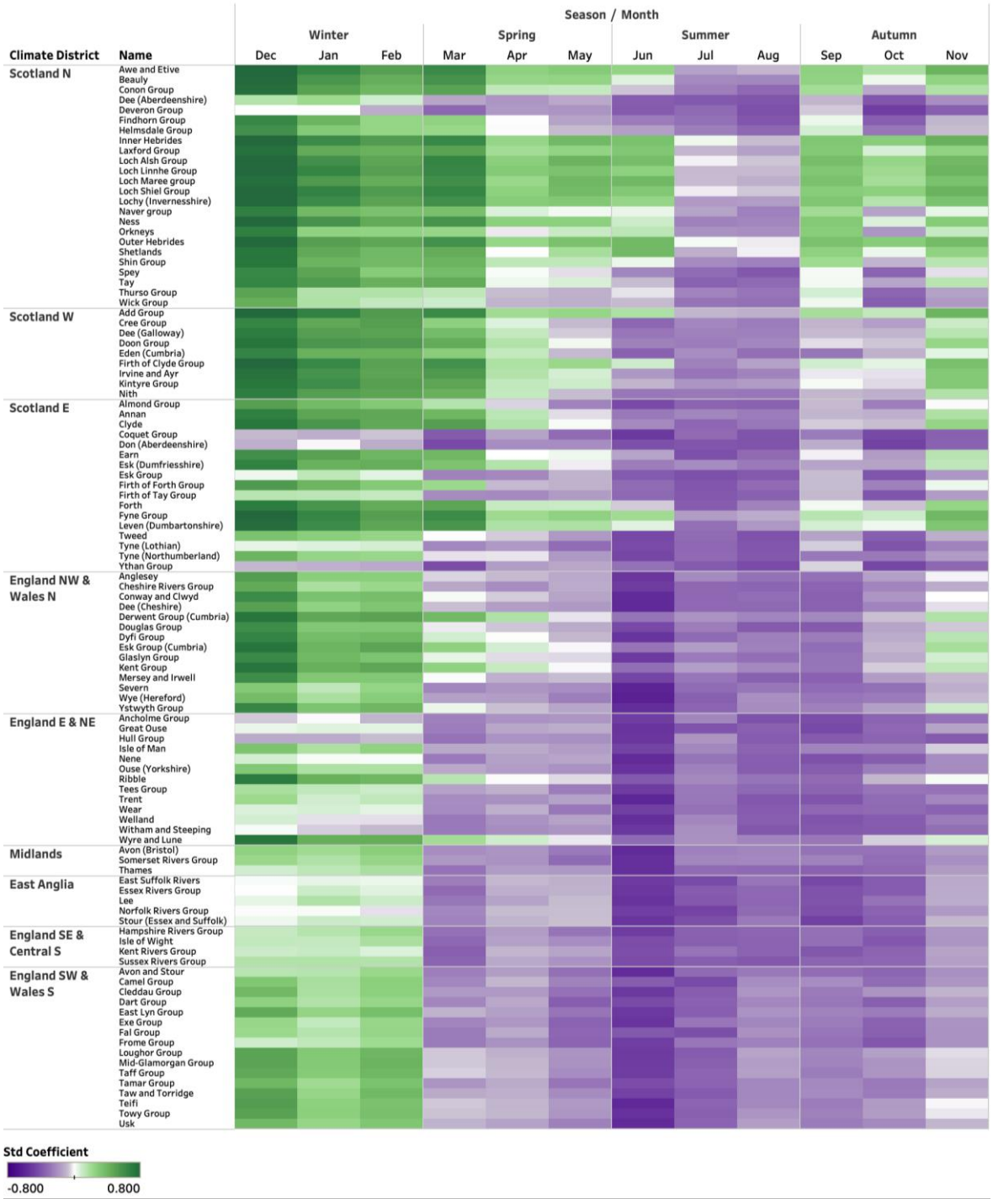

Figure 5: Standardised coefficient values for the NAO index from the multivariate regression model.

Figure 6 shows the SC from the EA multivariate regression model. Whilst the relationship between the NAO and SPI-1 varies in directionality across space and time (Figure 5), the strength and the directionality of the EA's relationship with SPI-1 is more consistent. Figure 6 shows that the EA generally has a positive relationship with precipitation across most of the country; in other words, EA positive (negative) phases are associated with wetter (drier) conditions. The exception to this is in the north of Scotland during winter where weak and negative SC are observed (Figure 6).

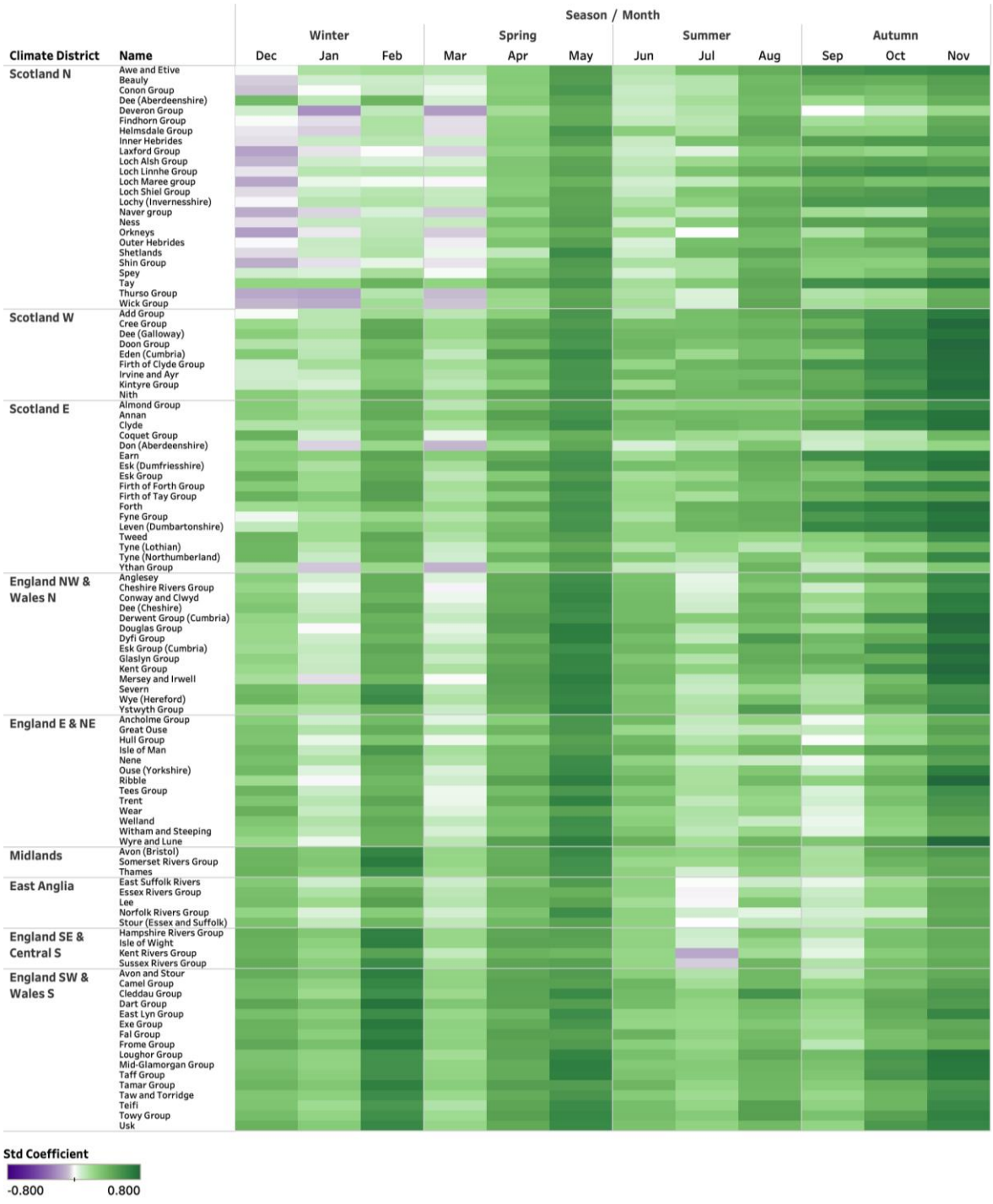

***Figure 6**: Standardised coefficient values for the EA index from the multivariate regression model.*

Like the NAO, the nature of the relationship between the SCA and precipitation has distinctive spatial differences across the year (Figure 7). For most of Great Britain, the relationship between the SCA and SPI-1 is positive, suggesting that SCA positive (negative) phases produce wetter (drier) conditions. However negative SC are observed in the north of Scotland, therefore indicating the opposite SCA phase-precipitation relationship. This negative pattern is observed in all months with consistent strength, except in December which has a weak positive directionality. Negative SC are also found in southern regions in January, February and July, although these are weaker than SC in Scotland.

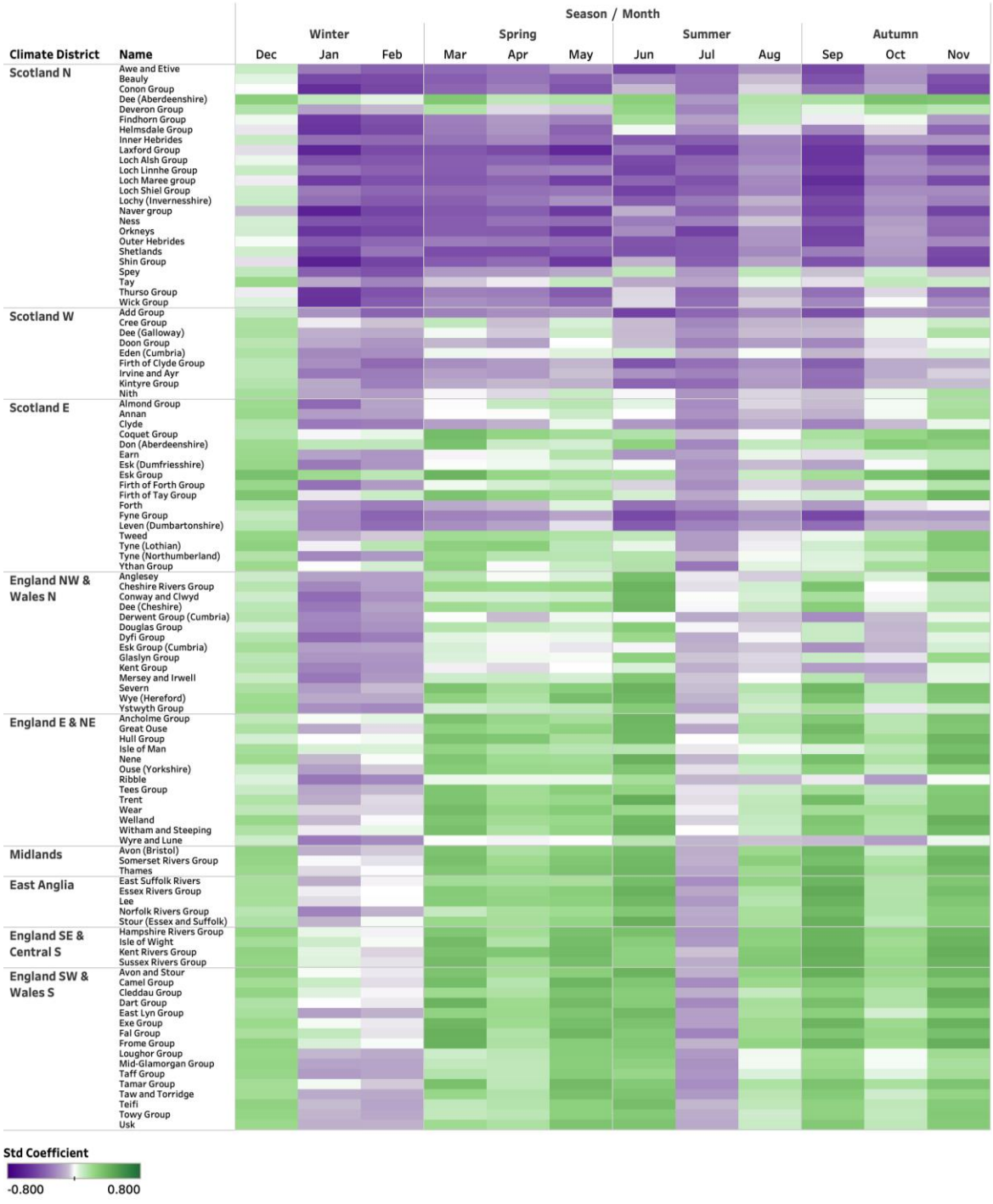

Figure 7: Standardised coefficient values for the SCA index from the multivariate regression model.

Figure 8 and Figure 9 show the SC for the EAWR and POL respectively. For the majority of the year both circulations have a negative relationship with precipitation, therefore positive phases of the EAWR and POL are more likely to result in drier conditions, and negative phases wetter conditions. Some months do have consistent positive SC, for example July and August in Figure 8, however these are weak. The EAWR has a stronger positive relationship in January and October, notably in the English and southern regions, and a weaker relationship during summer (similar to the pattern observed in the univariate analysis for the EAWR). The weaker POL SC (Figure 9) indicate that this circulation has a lesser influence on the model performance, and by inference precipitation variability, than the four other circulations (Figure 9). However, the POL SC are generally stronger in the summer than in the winter months.

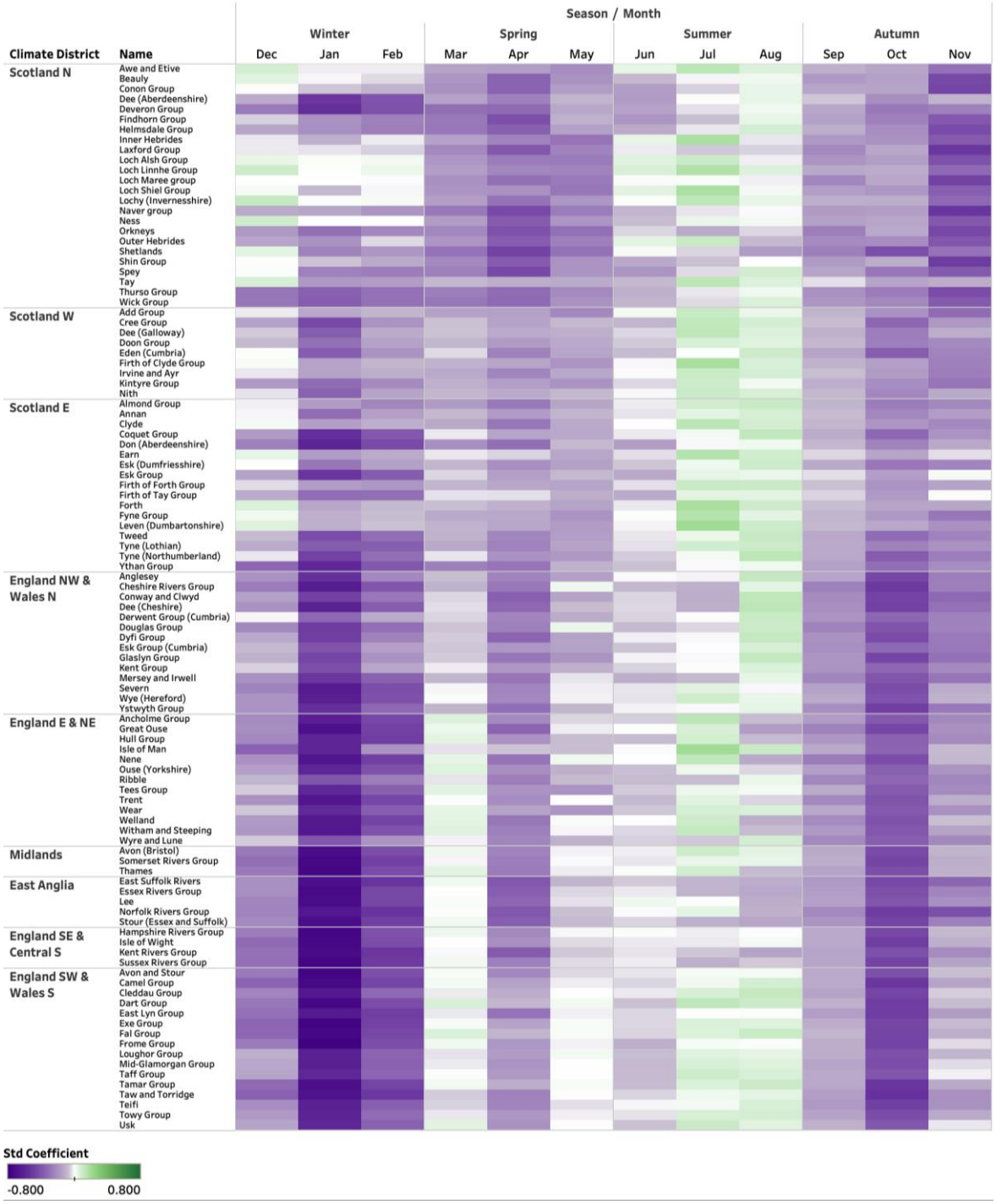

Figure 8: Standardised coefficient values for the EAWR index from the multivariate regression model.

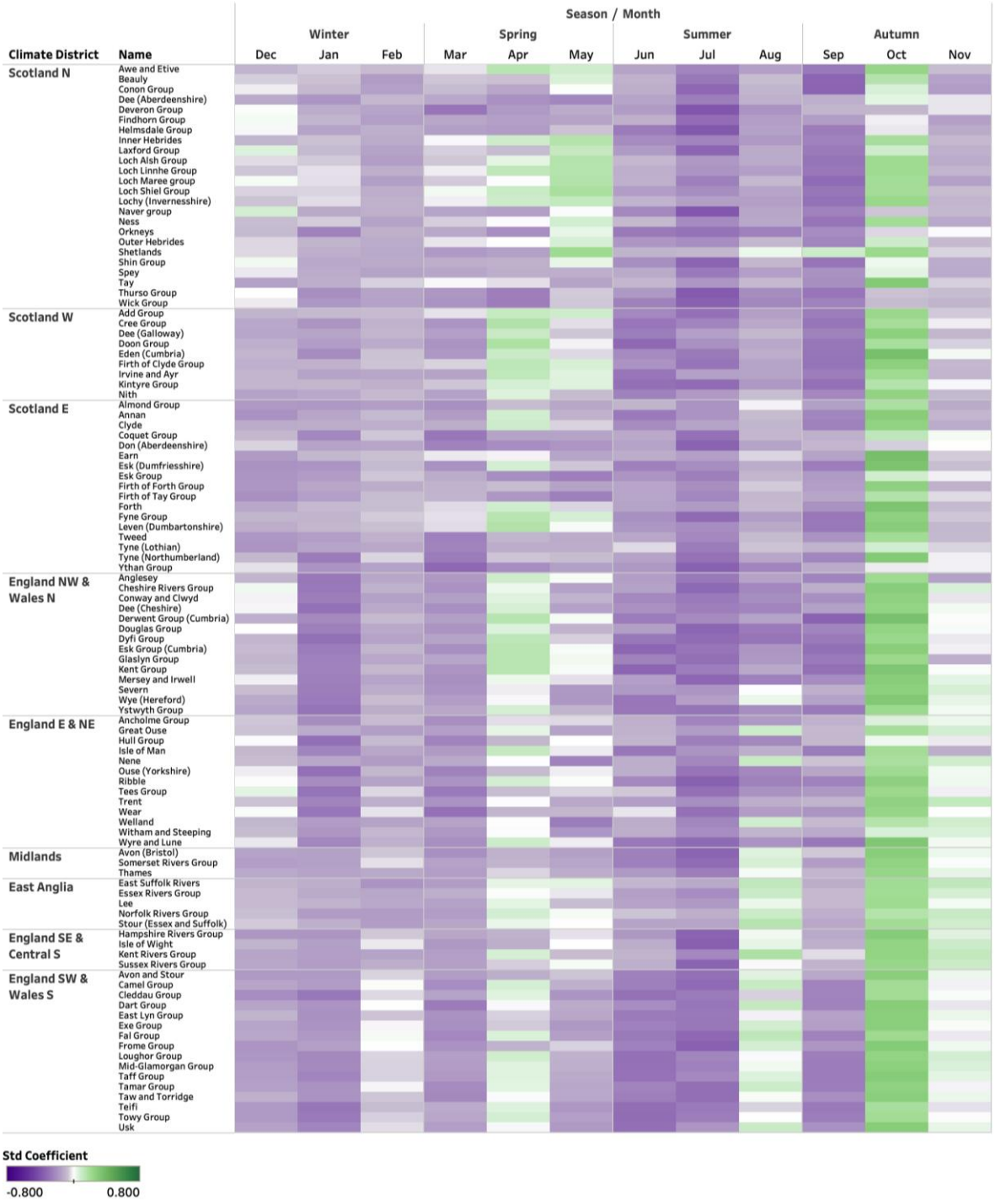

***Figure 9**: Standardised coefficient values for the POL index from the multivariate regression model.*

Exploring the absolute SC values for each of the five atmospheric circulations in the multivariate regression model also enables evaluation of the relative dominance of each circulation, and how this varies in space and time. Figure A4, Figure A5, Figure A6, Figure A7 and Figure A8 in Appendix A show the SC plots, but with the colour indicative of the rank of the circulation relative to the other four (determined by the strength of the absolute SC). This is summarised in Figure 10, where the categorical colour classification shows the circulation with the strongest (highest ranking) absolute SC across the IHU Groups and all months.

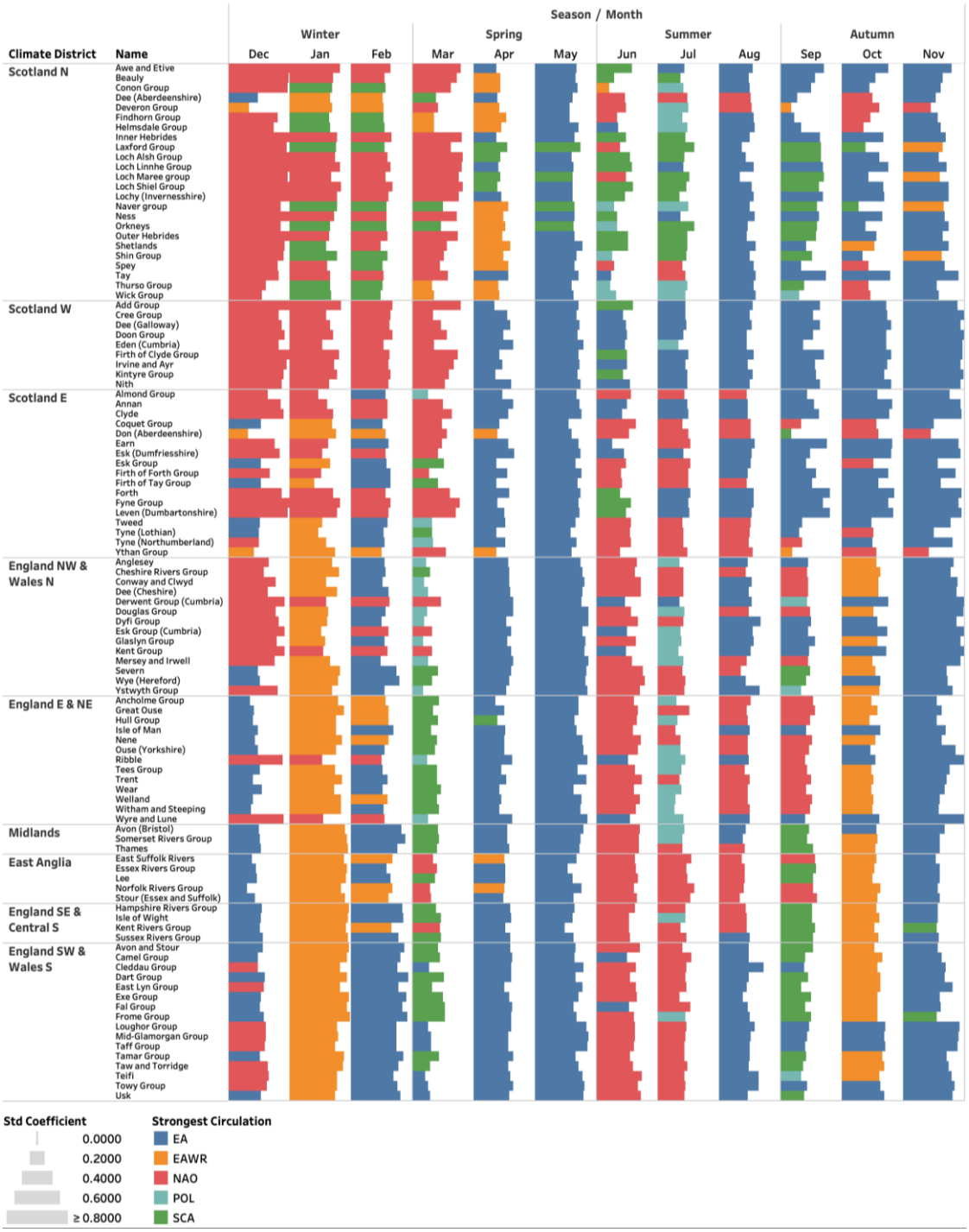

***Figure 10**: The strongest standardised coefficient values from Figure 5, Figure 6, Figure 7, Figure 8 and Figure 9. Colour indicates which circulation is the most influential in the multivariate regression (i.e., the circulation with the strongest absolute SC value). The size of the bar is based on the absolute SC value.*

During the winter months and early spring, the NAO is generally the dominant circulation influencing precipitation in the north west, with the SCA also having an influence in late winter and into spring and summer. In the southern and English regions, the EA is more influential. In the south, the EAWR is the most dominant circulation in January, with very strong (negative–as shown in Figure 8) absolute SC. In late spring the EA is the most influential pattern across most of the country, with the EAWR and SCA having a greater effect in a limited number of IHU Groups in the north. In the north, during summer, the SCA is more commonly the dominant

circulation, with the EA and POL indices also being the most influential in some IHU Groups. In autumn, the EA is frequently the dominant pattern across large parts of Great Britain, with the EAWR also having a notable influence in the southern regions during October.

As in Figure 10, Figure 11 shows the strongest standardised coefficient values from Figure 5, Figure 6, Figure 7, Figure 8 and Figure 9. Note that the size of the bar now indicates how dominant the circulation is relative to the circulation with the second highest SC (i.e., the absolute SC value of the dominant circulation minus the absolute SC of the second highest ranking circulation). The R2 values of the multivariate regression model are typically stronger in the winter months than during summer (Figure 4). This is reflected in the plots where the magnitude of the SC (Figure 10), and the difference between circulation's relative influence (Figure 11), is lower in summer than in winter. For example, in Figure 10 it was identified that the most dominant circulation in the north-west during the winter months is the NAO. In Figure 11 we can see that the SC of the NAO are notably stronger than that of the other circulations. Therefore, the NAO has a clear and isolated influence on precipitation in this region. In contrast the NAO and EA typically play an important role across the country during the summer months (Figure 10). However, the relative dominance of each is much less than in winter (Figure 11).

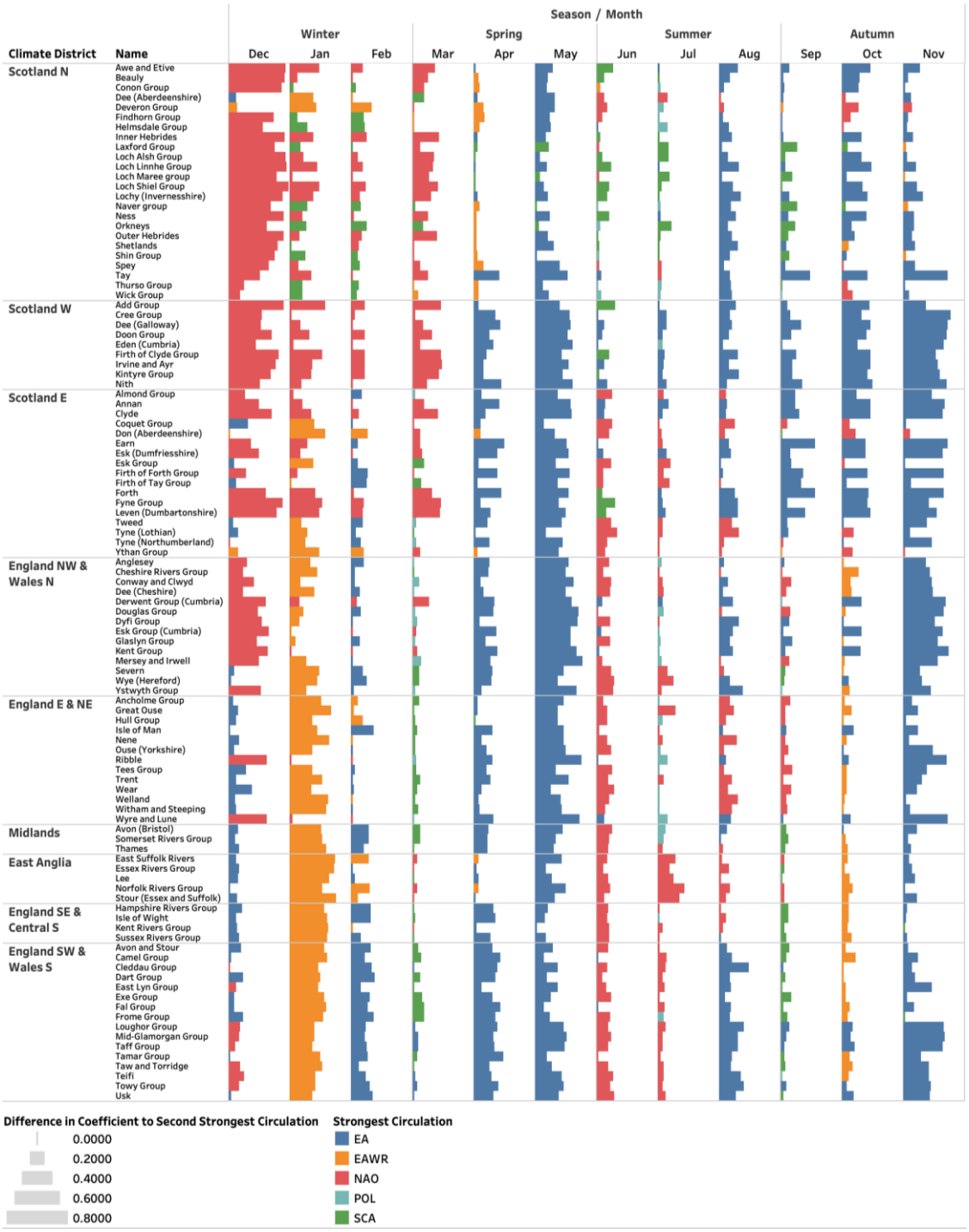

***Figure 11**: The strongest standardised coefficient values from Figure 5, Figure 6, Figure 7, Figure 8 and Figure 9. Colour indicates which circulation is the most influential in the multivariate regression (i.e., the circulation with the strongest absolute SC value). The size of the bar is based on the difference in absolute SC between the dominant and second most influential circulation.*

Consequently, during the winter months individual circulations can have a dominant and significant impact on regional precipitation, such as the NAO in the north west and EAWR in the southern regions during January. However, in the southern regions throughout most of the year, and in Scotland during spring, summer and autumn, precipitation variability is potentially better explained through looking at a combination of atmospheric circulations.

Discussion

This study explores, at a high spatial and temporal resolution, the relative influence North Atlantic/European atmospheric circulations on precipitation variability in Great Britain. Previous studies have either tended to focus on only one or a small number of these circulations, have been limited temporally to the winter, or undertaken using station-based or coarse spatial resolution modelled datasets (e.g., Burt & Howden 2013; Moore et al. 2013; Casanueva et al. 2014; Comas-Bru & McDermott 2014; Hall & Hanna 2018; Mellado-Cano et al. 2019). To address these limitations, we considered five key atmospheric circulations, using high resolution SPI-1 data for the IHU Groups of Great Britain (Tanguy et al. 2017b), at a monthly scale. Through univariate and multivariate regression models we show the spatial and temporal variation in the relative influence of five atmospheric circulations on precipitation in Great Britain – the NAO, EA, SCA, EAWR and POL.

The NAO influences regional rainfall across Great Britain, particularly in the north-west (Wilby et al. 1997; Rust et al. 2018; West et al. 2019b) where local topography can also enhance the NAO-rainfall effect (Burt & Howden 2013). This is shown in our analyses where strong positive relationships between the NAO and SPI-1 are observed in winter (Figure 2 and Figure 5). The phase of the NAO influences the location and strength of the North Atlantic jet stream (Hurrell et al. 2003); positive phases result in southerly jet stream bringing warm and moist conditions to Great Britain, meanwhile negative phases result in a northerly jet stream, resulting in colder and drier winters (Hurrell et al. 2003) with greater snowfall in the north-west (Spencer & Essery 2016). This understanding of physical processes corresponds with the positive (Figure 5) and dominant relationship (Figure 10) between the NAO and precipitation in the north-west during winter.

Whilst the dominance of the NAO in the north-west during winter is well-known (Wilby et al. 1997; Burt & Howden 2013; Rust et al. 2018; West et al. 2019b) the influence of the other circulations is much less understood, especially during the NAO's weaker summer state (Folland et al. 2009). This study highlights a consistent and moderately strong positive EA-precipitation relationship (Figure 6) and negative EAWR-precipitation relationship (Figure 8), which corroborates findings exploring the impact of these two circulations (Casanueva et al. 2014; Ionita 2014; Hall & Hanna 2018; West et al. 2021b). This reinforces the EA's role as the second leading mode of climate variability (Barnston & Livezey 1987; Moore et al. 2013; Comas Bru & McDermott 2014) and therefore its strong influence on precipitation across Great Britain throughout the year (Figure 10).

In this study we find that the SCA can also have a dominant and important influence on rainfall in Great Britain (Figure 10), with a weak positive and stronger negative relationship in the southern and far northern regions, respectively. Bueh & Nakamura (2007) reported positive relationships between the SCA and precipitation over southern Europe and negative

relationships over Scandinavia; corresponding to our observed north/south SC variation for the SCA (Figure 7). Our analysis of the SC values, however, indicates that the SCA is more frequently the dominant circulation in the north compared to the south (Figure 10), however it is relatively less influential compared to the NAO and EA (Figure 11). This demonstrates the SCA's role as the third mode of climate variability (Barnston & Livezey 1987; Moore et al. 2013; Comas Bru & McDermott 2014). The SC values for the POL circulation are consistently low throughout the year in our analysis (Figure 9), although they are moderately stronger in the summer, possibly associated with the additional and third centre of action of the circulation over midlatitude Europe (Barnston & Livezey 1987).

Our analysis shows that each circulation has a spatially and temporally variable influence on regional precipitation in Great Britain. Importantly, the results from the multiple regression analysis indicate that by looking at the atmospheric circulations in combination, rather than in isolation (for example the univariate regression models in Figure 2 and Figure 3), will provide a more complete description of precipitation variability. This is particularly true of the NAO and EA circulations (Mellado-Cano et al. 2019; West et al. 2021b), and for the southern regions in winter and across the country during summer, where there is notably less difference between the dominant and second most influential circulation (Figure 11).

Research has long highlighted the importance of the NAO in driving regional climate (Wilby et al. 1997; Hurrell et al 2003; Rust et al. 2018) However significant variability in NAO-rainfall signatures has also been reported, in particular, for southern England (West et al. 2021a). Despite advancements in our understanding of how NAO-rainfall deviations propagate through the hydrological cycle (Rust et al. 2021a; West et al. 2022a), such variability in NAO-rainfall signatures is a limiting factor in being able to use the NAOI in water and environmental management decision making, even as more skillful forecasts are increasingly available (Hall & Hanna 2018). We suggest that some of this spatio-temporal variability may be explained by looking at the strength and phase of other atmospheric circulations such as the EA. Consequently, there is the potential to incorporate and apply a broader range of monthly climate indices to explain, and possibly predict, precipitation variability (and subsequently hydrological variability). However, additional research is required to translate the findings of this study into useful predictive tools for application in water management. However, at present the utility of this may be limited given that recent advancements in teleconnection forecasting have been reported for the NAO (Athanasiadis et al. 2020; Smith et al. 2020).

Conclusion

As far as we are aware this study represents the first attempt to explore at high resolution the relative influence of five atmospheric circulations on monthly precipitation variability across Great Britain, both individually and in combination. Historically, many studies have focused on the NAO as the key driver of regional precipitation, and subsequently streamflow and

groundwater levels. However, our analyses reveal the variable influence of a broader range of circulations on regional precipitation, and by inference, catchment hydrology.

Importantly this study demonstrates how the NAO may only partially explain precipitation variability, especially in the southern regions and during the summer months, where circulations such as the EA also have an important influence. There is scope for future research to continue to develop our understanding of the impact of these circulations on rainfall (and its propagation through the hydrological cycle) at high spatial and temporal resolution using increasingly available long-term atmospheric circulation and hydrometeorological datasets. There is also potential to explore how circulation-driven precipitation interacts with local precipitation influences, such as topography (Burt & Howden 2013) and landcover which might also influence the spatio-temporal rainfall patterns observed in this study.

We suggest that there is significant explanatory value in looking beyond the NAO when seeking to explore climatological and hydrological variability in Great Britain. An aim of future research might be to explore how the understanding presented in this study may be used in a predictive capacity in water management practice; however, we acknowledge the associated limitations, most notably the lack of accurate annual forecasts for all five atmospheric circulations.

Appendix

***Figure A1**: R^2 values of the univariate regression model exploring the relationship between the SCA index and SPI-1 values across the IHU Groups.*

***Figure A2**: R^2 values of the univariate regression model exploring the relationship between the EAWR index and SPI-1 values across the IHU Groups.*

***Figure A3**: R^2 values of the univariate regression model exploring the relationship between the POL index and SPI-1 values across the IHU Groups.*

***Figure A4**: Rank of the NAO Standardised Coefficient. Colour represents the rank, with darker colours signifying greater influence (higher rank). Size is dependent on the magnitude of the SC.*

***Figure A5**: Rank of the EA Standardised Coefficient. Colour represents the rank, with darker colours signifying greater influence (higher rank). Size is dependent on the magnitude of the SC.*

Figure A6: *Rank of the SCA Standardised Coefficient. Colour represents the rank, with darker colours signifying greater influence (higher rank). Size is dependent on the magnitude of the SC.*

Figure A7: *Rank of the EAWR Standardised Coefficient. Colour represents the rank, with darker colours signifying greater influence (higher rank). Size is dependent on the magnitude of the SC.*

Figure A8: *Rank of the POL Standardised Coefficient. Colour represents the rank, with darker colours signifying greater influence (higher rank). Size is dependent on the magnitude of the SC.*

Paper 5: Monthly Rainfall Signatures of the North Atlantic Oscillation & East Atlantic Pattern in Great Britain

Citation: West, H., Quinn, N. & Horswell, M. (2021). Monthly Rainfall Signatures of the North Atlantic Oscillation & East Atlantic Pattern in Great Britain. *Atmosphere*, 12(11), 1533.

Published: 20th November 2021.

Contributions: Analytically this paper has a similar framework to Paper 1 which was developed collaboratively in the early stages of the PhD. HW undertook the various spatial analysis and first drafts of the presentation of the results. This was shared with NQ and MH for feedback and refined. HW produced the draft paper which was passed to NQ and MH for commentary prior to submission.

Changes to Original Paper:

- No changes have been made between this version and that published in November 2021.

Abstract

Atmospheric-oceanic circulations (teleconnections) have an important influence on regional climate. In Great Britain, the North Atlantic Oscillation (NAO) has long been understood as the leading mode of climate variability, and its phase and magnitude have been found to influence regional rainfall in previous research. The East Atlantic Pattern (EA) is also increasingly recognised as being a secondary influence on European climate. In this study we use high resolution gridded rainfall and Standardised Precipitation Index (SPI) time series data for Great Britain to map the monthly rainfall signatures of the NAO and EA over the period January 1950–December 2015. Our analyses show that the influence of the two teleconnections varies in space and time with distinctive monthly signatures observed in both average rainfall/SPI-1 values and incidences of wet/dry extremes. In the winter months the NAO has a strong influence on rainfall and extremes in the north-western regions. Meanwhile, in the southern and central regions stronger EA-rainfall relationships are present. In the summer months opposing positive/negative phases of the NAO and EA result in stronger wet/dry signatures which are more spatially consistent. Our findings suggest that both the NAO and EA have a prominent influence on regional rainfall distribution and volume in Great Britain, which in turn has implications for the use of teleconnection forecasts in water management decision making. We conclude that accounting for both NAO and EA influences will lead to an enhanced understanding of both historic and future spatial distribution of monthly precipitation.

Introduction

The North Atlantic Oscillation (NAO) has long been recognised as the first mode of climate variability in the North Atlantic region (Hurrell & Van Loon 1997; Rodwell et al. 1999). The NAO teleconnection is defined by the sea level pressure (SLP) variation between the Icelandic low-pressure action point and the Azores anticyclone. When the SLP difference between these two meridional dipoles is greater than normal, the NAO is described as being in a positive phase (NAO+), whilst a NAO negative phase (NAO−) represents a weaker than usual difference in SLP between the Icelandic Low and Azores High (Hurrell et al. 2003).

North Atlantic Oscillation Indices (NAOIs) are calculated to quantify the phase and magnitude of the NAO at monthly, seasonal and annual scales, and have been used to assess the influence of the NAO on spatial distributions and deviations in rainfall, temperature and other hydrometeorological variables. In Great Britain, significant correlations which vary in space and time have been found between the NAOI and measured and modelled rainfall. During the winter in the north-west of the country positive correlations are often reported, indicating that NAO+ phases result in higher rainfall in these regions, and NAO− phases result in drier conditions (Wilby et al. 1997; Fowler & Kilsby 2002; Burt & Howden 2013; Afzal et al. 2015; Rust et al. 2018). West et al. (2019b) used high resolution gridded rainfall datasets to quantify the deviation in average monthly rainfall under NAO+/− phases compared to weak NAO neutral conditions, finding that during the winter months deviations in average monthly rainfall volume can be as high as 200–300 mm in the north-west. Meanwhile in the southern and eastern regions weaker negative correlations between the NAOI and rainfall are found (Kosanic et al. 2014; Rust et al. 2018).

Typically, the magnitude of the NAOI is weaker in the summer months compared to winter (Folland et al. 2009). Despite this, significant correlations between the summer NAOI and rainfall have also been reported. These correlations are typically negative for most of Great Britain (Simpson & Jones 2014; Hall & Hanna 2018), with NAO+ phases resulting in drier conditions and NAO− phases in wetter conditions (West et al. 2019b). Although it should be noted that NAOI-rainfall correlations can be sensitive to the method of NAOI calculation, notably the choice between indices derived from station-measured or modelled SLP data (Pokorná & Huth 2015). Additionally, studies have explored how these NAO-rainfall deviations variably propagate through catchments to influence streamflow (Phillips et al. 2003; Lavers et al. 2010; Burt & Howden 2013; Rust et al. 2021a), groundwater (Lavers et al. 2015; Rust et al. 2019) and fluvial water temperatures (Wilby & Johnson 2020).

However, West et al. (2021a) observe that whilst average and relatively consistent rainfall responses to the NAO across Great Britain can be observed in line with the above descriptions, there can also be significant spatio-temporal variability in regional NAO-rainfall responses. For example, whilst in the north-west of the country more consistent NAO+/− wet/dry rainfall

responses in winter were found, significant NAO-rainfall variability can occur in the central, southern and eastern areas, with some regions having equal likelihood of wetter/drier conditions and extremes (West et al. 2021a). The spatial and temporal variability in the rainfall response to the NAO across Great Britain has been noted as a potentially limiting factor in the inclusion of even highly accurate monthly/seasonal NAO forecasts in water management decision making (Hall & Hanna 2018; West et al. 2021a; Rust et al. 2021b).

NAO-rainfall response variability may be associated with the phase and magnitude of other North Atlantic/European atmospheric-oceanic circulations which may enhance or moderate the effect of the NAO in influencing regional rainfall in Great Britain (Hall & Hanna 2018; West et al. 2021a). Research continues to highlight the importance of the East Atlantic Pattern (EA) in influencing European climate. The EA was first described by Wallace and Gutzler (1981) and is cited as the second mode of climate variability in the North Atlantic following the NAO (Comas Bru & McDermott 2014; Mikhailova & Yurovsky 2015). Barnston and Livezey (1987) identified a well-defined EA monopole south of Iceland and west of the United Kingdom (approximately 55° N; 20–35° W), a definition frequently used in research (Moore & Renfrew 2011; Comas Bru & McDermott, 2014; Mellado-Cano et al. 2019) and by NOAA in the calculation of their EA teleconnection index (NOAA 2021b).

The influence of the EA on rainfall distribution and deviations in Great Britain is less well defined than it is for the NAO; however, associations in both winter and summer have been identified. Significant positive correlations between the EA and rainfall have been reported across Great Britain (Comas-Bru & McDermott 2014; Casanueva et al. 2014) with precipitation anomalies in the central, southern and eastern regions possibly associated with varying phases of the EA (Hall & Hanna 2018). Interestingly, these are the same regions West et al. (2021a) note as having greater variability in NAO-rainfall response. In the summer months positive EA-rainfall correlations persist, albethey of a weaker strength (Hall & Hanna 2018).

Given the variability that can be observed in NAO rainfall signatures (West et al. 2021a; Rust et al. 2021b), interactions between the NAO and EA and their combined effect on spatial rainfall distributions across the North Atlantic and Europe have been explored. Moore et al. (2011; 2013) found that the EA has the potential to influence the location and magnitude of the NAO dipoles. Analysis using long-term indices derived from ship logbooks (Mellado-Cano et al. 2020) shows that winter precipitation distribution and magnitude (and temperatures) across Europe is sensitive to the phase and strength of both the NAO and EA (Mellado-Cano et al. 2019). The EA in particular was identified as the dominant pattern in approximately 50% of winters in the last three centuries (Mellado-Cano et al. 2019). This reinforces Comas-Bru and McDermott (2014) who suggested that through a combination of the NAO and EA we may be more able to accurately describe winter climate variability in Europe.

To date, studies which identify the combined effect of the NAO and EA on rainfall in Great Britain have been based on relatively coarse spatial resolution datasets (due to having a focus across the wider North Atlantic/European region) or have been temporally restricted to specific seasons (notably winter). This study aims to contribute to research seeking to identify the effect of the NAO and EA (and their interaction) on rainfall patterns in Great Britain by using relatively high resolution rainfall datasets to map the spatio-temporal monthly rainfall signatures of the NAO and EA over a 65-year period (January 1950–December 2015).

Methods

Data

Monthly indices for the NAO and EA were sourced from the NOAA Climate Prediction Center (NOAA 2021a) for the time period January 1950–December 2015. This time period was chosen as it represents the longest period with available data for both the teleconnection indices and rainfall datasets (described below). The CPC use the rotated principal component analysis (RPCA) approach of Barnston and Livezey (1987) to identify and quantify northern hemisphere teleconnection patterns at a monthly scale, including the NAO and EA. Teleconnection indices calculated through modelling approaches such as RPCA avoid the limitations associated with station-measured indices (Pokorná & Huth 2015). The modelled monthly teleconnection indices from the NOAA CPC are frequently used in similar research assessing the hydrometeorological and climatological impact of atmospheric-oceanic circulations globally (Comas-Bru & McDermott 2014; Casanueva et al. 2014; Irammezhad et al. 2015; Bednorz et al. 2018; Amini et al. 2020; Bednorz & Tomczyk 2021).

Two precipitation datasets were used to assess the influence of the NAO and EA on regional rainfall in Great Britain. Monthly rainfall totals were obtained from the UK Centre for Ecology and Hydrology (CEH) Gridded Estimates of Areal Rainfall (GEAR) dataset (Tanguy et al. 2016) for the period January 1950–December 2015. This dataset has a spatial resolution of 1 km and is based on interpolation of rainfall observations from the Met Office national database (Tanguy et al. 2016). Alongside the GEAR data, Standardised Precipitation Index (SPI) time series with a one-month accumulation period (SPI-1) were also downloaded for the study period from CEH. The SPI was calculated by fitting a gamma distribution to historical rainfall estimates with a standard period of 1961-2010, using the Met Office 5 km rainfall grids (Tanguy et al. 2017a; 2017b). Two variants of the SPI-1 data were used in this analysis: a 5 km gridded monthly dataset (Tanguy et al. 2017a), and aggregated monthly SPI-1 values for the Integrated Hydrological Unit Groups (IHU) of Great Britain (Tanguy et al. 2017b). In both variants of the SPI-1 dataset, positive values indicate wetter conditions, whilst negative values indicate drier conditions. The theoretical maximum/minimum of the dataset is 5/−5, representing significant wet/dry extremes; however, 95% of the values are within the range −2 to 2 (Tanguy et al. 2017a; 2017b).

IHU Group Correlation Analysis

Initially the relationships between the teleconnection indices and rainfall were explored individually, in other words the NAO-rainfall effect and EA-rainfall effect were analysed separately. Spearman correlation coefficients were calculated between the two teleconnections indices from the NOAA CPC and the SPI-1 values for the IHU Groups. Correlations were calculated for each calendar month and mapped. This correlation analysis allowed for the identification of the individual relationship between the NAO/EA and rainfall (represented by the IHU Group SPI-1 values) in Great Britain, and how these relationships vary in space and time.

Mean SPI-1 and Rainfall Analysis

The phase of both the NAO and EA was identified for each calendar month across the study period (January 1950–December 2015). Removing these weak monthly teleconnection index values allowed for the identification of clear monthly NAO/EA phase-rainfall signatures (Comas-Bru & McDermott 2014; Berton et al. 2017). NAO/EA Positive phases were identified where the respective teleconnection index was greater than 0.25, whilst NAO/EA Negative phases were identified where the index was less than −0.25. Months with either NAO or EA index values between these two thresholds were removed from subsequent analyses. Figure 1 shows the frequency of NAO/EA positive and negative phase combinations for each month.

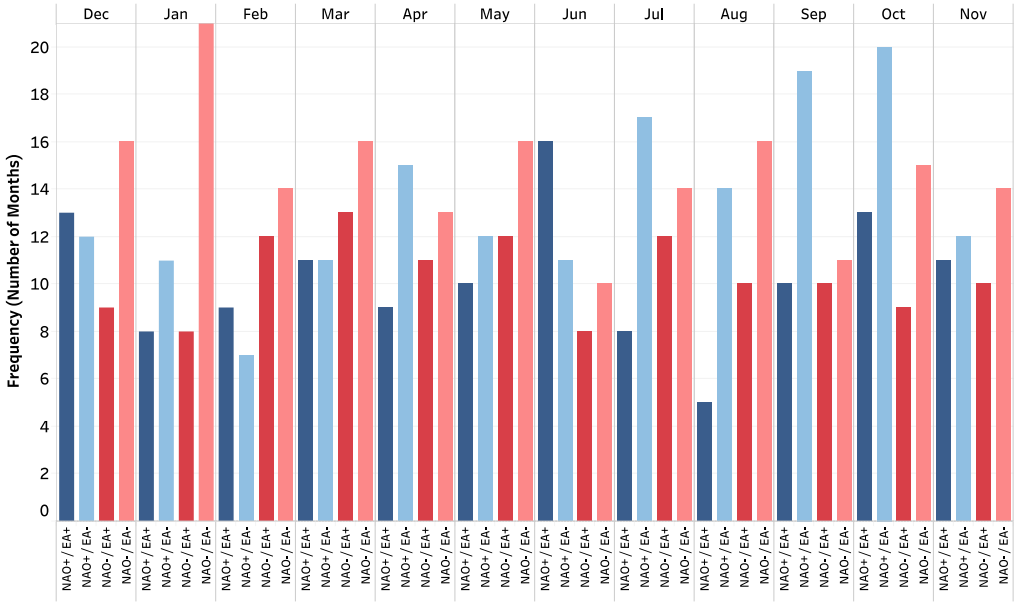

***Figure 1**: Frequency Analysis of NAO/EA Positive and Negative Phases*

Based on the monthly classification of teleconnection phases, we then explored the combined effect of the NAO and EA. For each month-phase combination (of both the same and opposing +/− sign) the average monthly rainfall from the CEH GEAR dataset (1 km gridded resolution) and average monthly SPI-1 value (5 km gridded resolution) was calculated. Descriptive statistics were also calculated for the nine Met Office Climate Districts. The Met Office Climate

Districts were chosen as they represent areas of relatively homogenous climate and have been used as a spatial unit of analysis in similar studies (Wilby et al. 1997; Simpson & Jones 2014; West et al. 2019b).

SPI-1 Threshold Frequency Analysis

The SPI-1 data is conveniently scaled between positive and negative values indicating wetness/dryness relative to a standard period (1961–2010 for the datasets used in this study). A common approach to interpreting the SPI, and similar standardised hydrometeorological/hydrological indices, is to classify the values using qualitative descriptors to indicate the severity of the wet/dry conditions (Table 1).

***Table 1**: Qualitative Descriptors and Associated SPI-1 Value Classification (McKee et al. 1993).*

Qualitative Descriptor	SPI-1 Value Range
Extremely Wet	≥2.0
Very Wet	1.5 - 1.99
Moderately Wet	1.0 - 1.49
Near Normal	-0.99 - 0.99
Moderately Dry	-1.49 - -0.99
Severely Dry	-1.99 - -1.5
Extremely Dry	≤ -2.0

To identify the relationship between the NAO and EA and significant wet and dry meteorological events, we map the percentage of time for each NAO/EA phase combination different SPI-1 thresholds are exceeded (i.e., the frequency of occurrence divided by the number of times that NAO/EA phase combination occurs—see Figure 1). In this analysis we identified the percentage of time extremely wet, very wet, severely dry and extremely dry thresholds (Table 1) were exceeded. This was undertaken using the 5 km gridded SPI-1 dataset, identifying for each calendar month any spatial and temporal patterns in the distribution of extreme wet and dry events across Great Britain.

Results

IHU Group Correlation Analysis

Figure 2 presents the results of the monthly correlation analyses between each of the teleconnection indices and the SPI-1 data at IHU Group level. In these correlation time series, positive correlations (shaded in blue) indicate that NAO/EA+ phases result in higher (wetter) SPI-1 values, meanwhile NAO/EA− phases result in lower (drier) SPI-1 values. Negative correlations (shaded in red) indicate the opposite teleconnection wet/dry relationship.

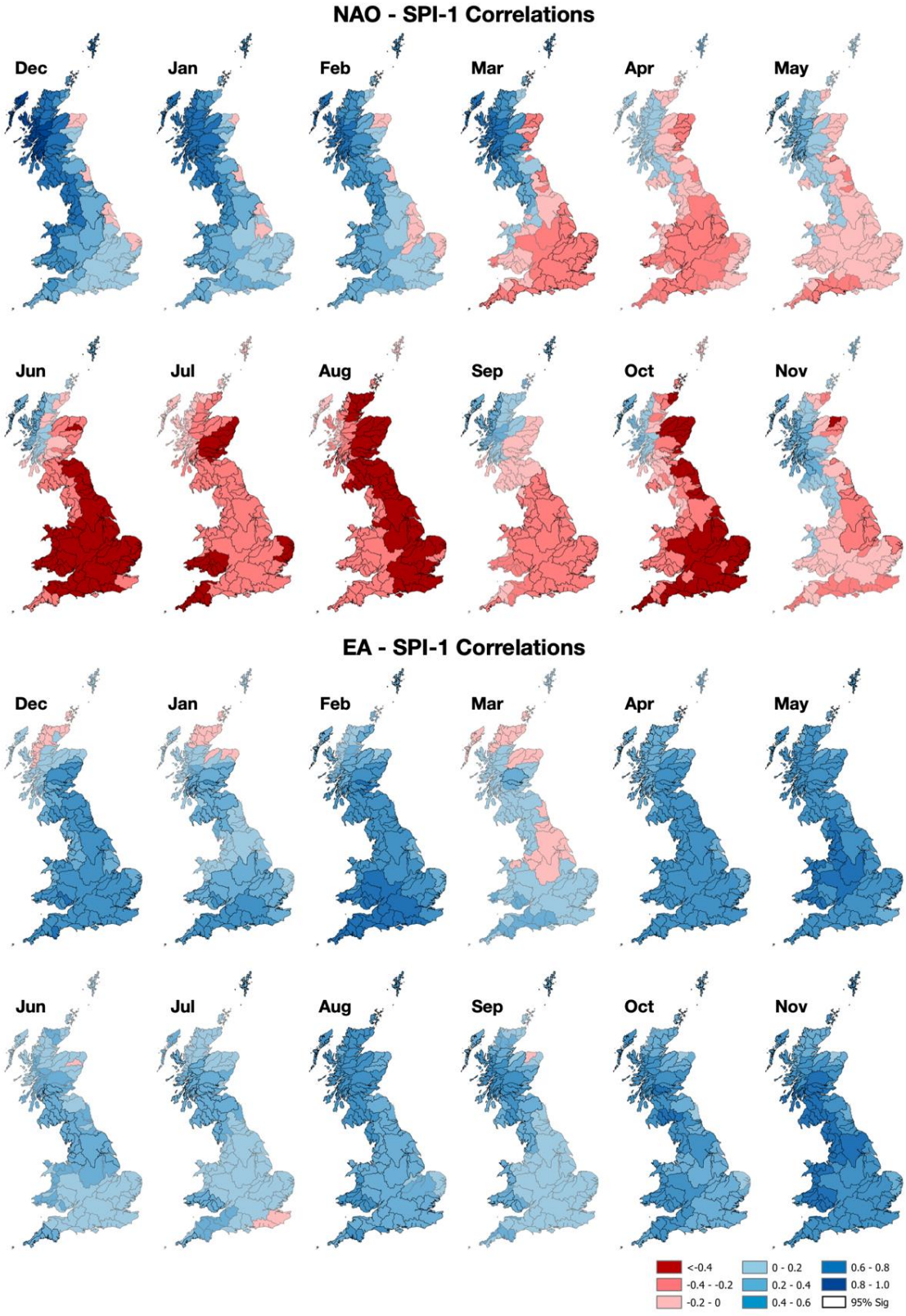

Figure 2: *Monthly correlation coefficients for the period January 1950–December 2015 between the NAO and EA teleconnection indices and the SPI-1 values at the IHU Group level. IHUs with a darker outline indicate 95% significance (p value ≤ 0.05).*

Noteworthy spatio-temporal differences can be observed between the NAO and EA correlation time series. In the winter months (DJF), strong positive correlations were found between the NAO and SPI-1 in the north-western regions of the country, with weaker and some negative

correlations in the southern and eastern IHUs. Spring (MAM) is marked by a transition from positive to negative NAO/SPI-1 correlations, which persist and strengthen in the summer months (JJA). The negative correlations between the SPI-1 and NAO are significant in most IHUs, with the exception of the far north-west.

Whilst the NAO correlation time series are marked by the positive-negative winter-summer transition described above, the EA has a more consistent positive relationship with the IHU SPI-1 values across the year. Stronger correlations between the EA and SPI-1 were found in the winter months, particularly in the southern and central regions of the country. Winter EA correlations in the north-west, where the NAO was strongly positively correlated with SPI-1, were weak and non-significant. Fewer significant correlations were found in the summer months, with the exception of August; however, the relationship remains positive.

Average Monthly Rainfall and SPI-1 Analysis

Figure 3 shows the average monthly rainfall based on the GEAR dataset under each NAO/EA phase combination for the nine Met Office Climate Districts for Great Britain. Figure 4 shows the same data; however, the months/phase combination are ranked from highest to lowest average monthly rainfall volume. Mapped averages of the 1 km GEAR dataset can be found in Appendix A. Figure 5 shows the average monthly SPI-1 value for each 5 km pixel, and Figures 6 and 7 plot the winter and summer NAO and EA monthly indices with the points symbolised based on the average SPI-1 value for that Climate District.

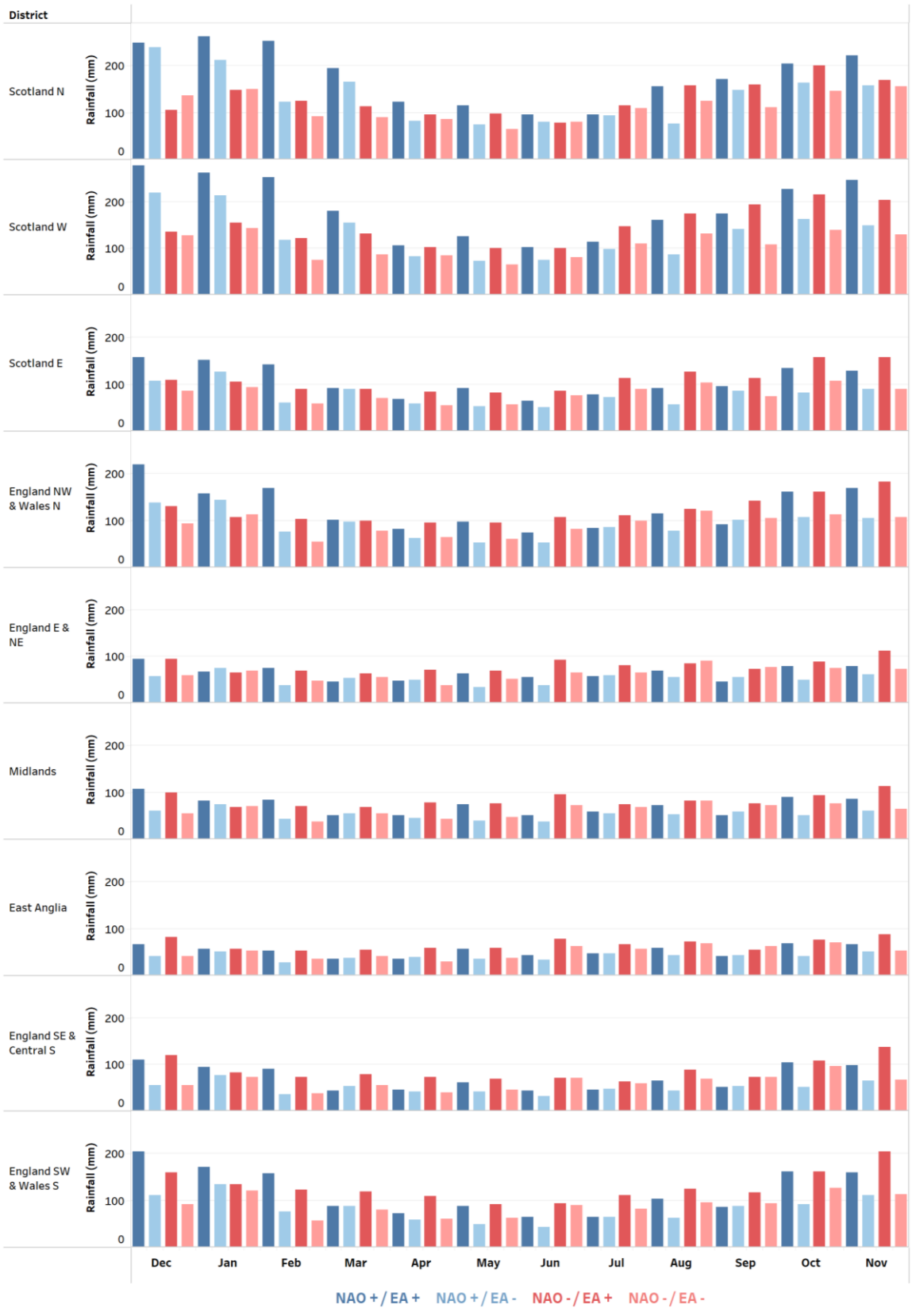

Figure 3: *Monthly average rainfall (based on the CEH GEAR dataset) for each NAO/EA phase combination for the nine Met Office Climate Districts.*

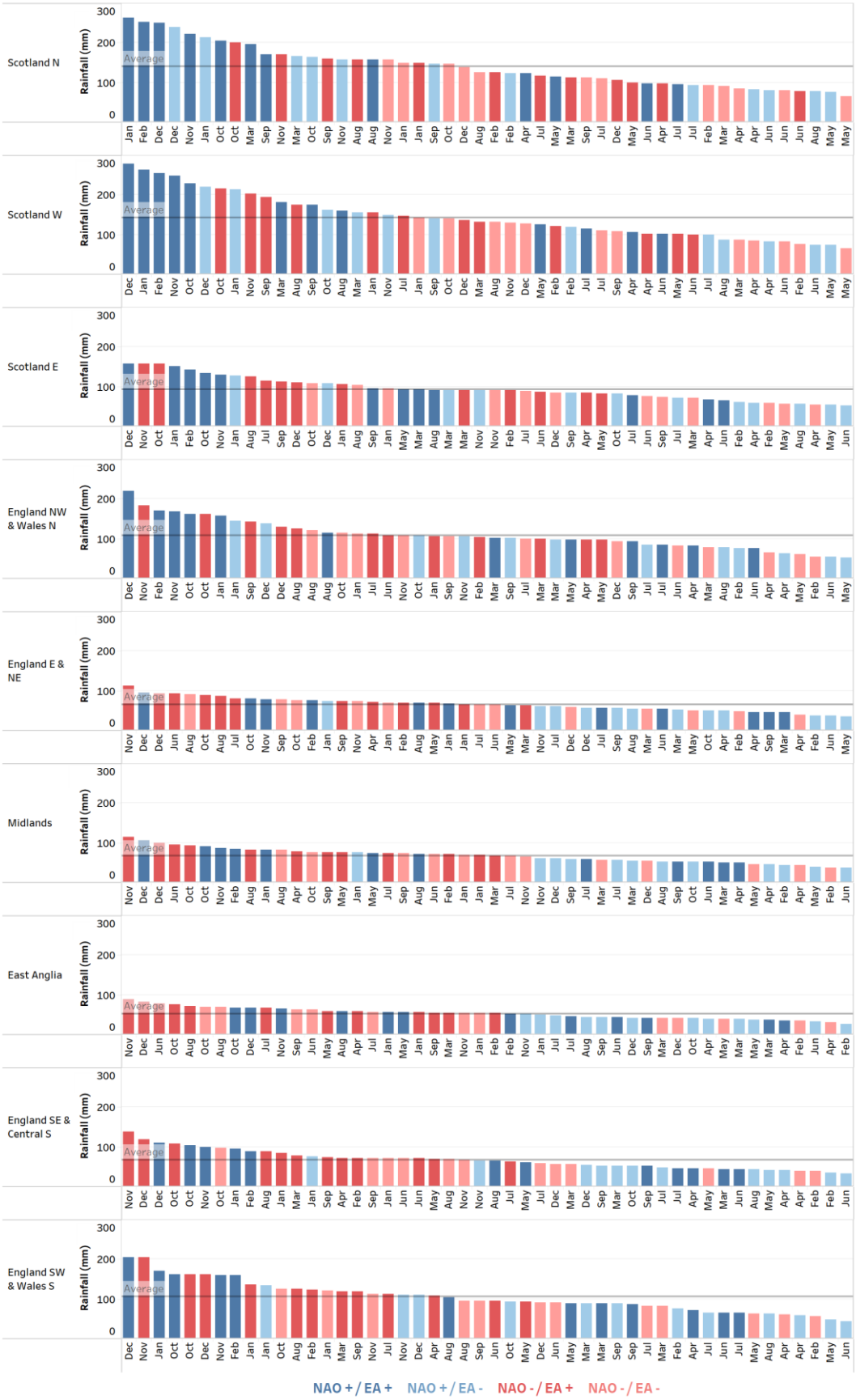

***Figure 4**: As per Figure 3, however, with the monthly NAO/EA phase combinations ranked in descending order based on the spatially averaged rainfall value. The average line on the individual graphs represents the annual (12-month) average rainfall for the Climate District.*

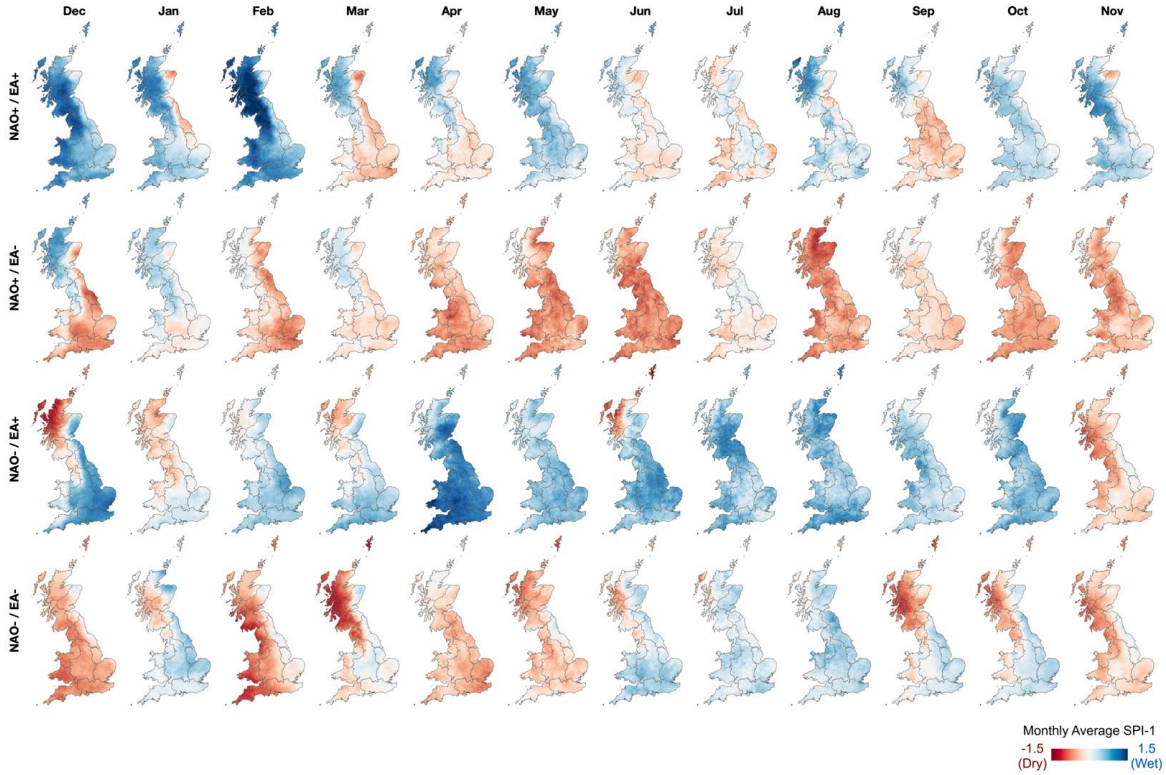

***Figure 5**: Average monthly SPI-1 values under different phase combinations of the NAO and EA.*

***Figure 6**: Scatter plots of the NAO and EA indices for the winter (DJF) months with points symbolised based on the Climate District average SPI-1 value. Quadrants with majority red/blue points indicate a drying/wetting tendency associated with that NAO/EA phase combination.*

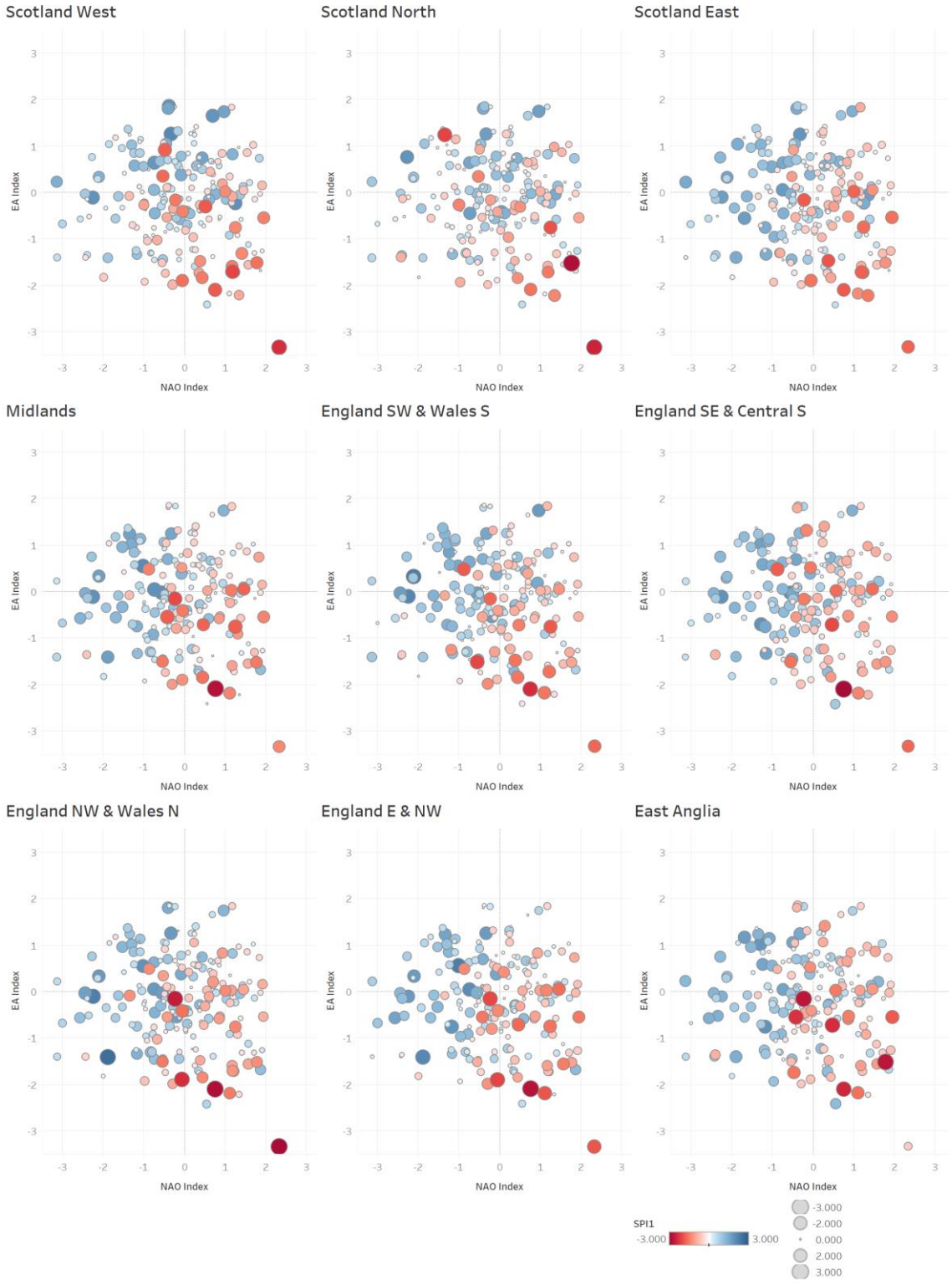

***Figure 7**: As per Figure 6; however showing the NAO and EA indices for the summer (JJA) months.*

In the southern districts, such as East Anglia or England SW and Wales S, the months with the highest average rainfall also occur during late autumn and winter, but in association with EA+ phases (Figure 5, Figure 6 and Figure 7). For example, the five wettest months on average in East Anglia all occur under a phase combination of NAO− and EA+ conditions, and the nine wettest months on average (exceeding 150 mm) in England SW and Wales S occur when the

EA is in a positive phase (Figure 4). Drier than average conditions in the southern and central climate districts are typically associated with EA− phases during the winter months (Figure 5, Figure 6 and Figure 7).

These findings suggest that during winter the NAO has a stronger influence on average wet/dry conditions in the northern and western regions, whilst the EA has a stronger influence on the central, southern and eastern regions. On average, wetter conditions across the country occur when both teleconnections are in a positive phase, and the driest average conditions when both are in a negative phase (Figure 5). Combinations of NAO/EA in opposing phases result in more marked spatial differences in wet/dry conditions between the north-west and south-east regions during winter (Figure 5).

In most Climate Districts, the months with the lowest average monthly rainfall (50–100 mm) occur in late spring and throughout summer and are generally associated with EA− phases and NAO+ phases (Figure 4). During the summer months both teleconnections have a more spatially consistent influence on rainfall than in winter. Typically, the driest summer months are associated with a combination of EA− and NAO+ phases (Figure 5), convergent with the inverse NAO/SPI-1 correlations presented in Figure 2. Wetter average conditions are associated with a combination of EA+ and NAO− phases (Figure 5). For example, average summer monthly rainfall is approximately half the depth under EA−/NAO+ phases as under EA+/NAO− phases in the England SW and Wales S Climate District (Figure 3). Smaller differences in wet/dry signals are found in the summer months when both teleconnections are in the same phase (Figure 5).

The convergence of the evidence presented in Figure 3, Figure 4, Figure 5, Figure 6 and Figure 7 allows us to consider how the NAO and EA interact to influence average monthly regional rainfall spatial distribution and volume in Great Britain. As with the correlation analysis in Figure 2, the relative influence of the two teleconnections clearly varies in space and time. In the northern Climate Districts of Scotland North and West, the months with the highest average monthly rainfall occur during late autumn and winter and are clearly associated with NAO+ phases (Figure 5), with average monthly rainfall exceeding 200 mm (Figure 3). The highest average rainfall volumes are found in these regions when both the NAO and EA are in positive phases (Figure 4). Drier average conditions occur in the north-west when the NAO is in a negative phase, with average monthly rainfall in the region of 100–150mm; approximately half the average monthly rainfall as under NAO+ phases (Figure 3). In these two Climate Districts the NAO has a notable influence on average wet/dry conditions during winter.

SPI-1 Threshold Frequency Analysis

Figure 8 and Figure 9 show the percentage of time (Figure 1) the very wet (SPI-1 > 1.5) and extremely wet (SPI-1 > 2.0) SPI-1 class thresholds are exceeded for each calendar month

across the study period. Figure 10 and Figure 11 show the percentage of time that severely dry (SPI-1< −1.5) and extremely dry (SPI-1 < −2.0) thresholds are exceeded.

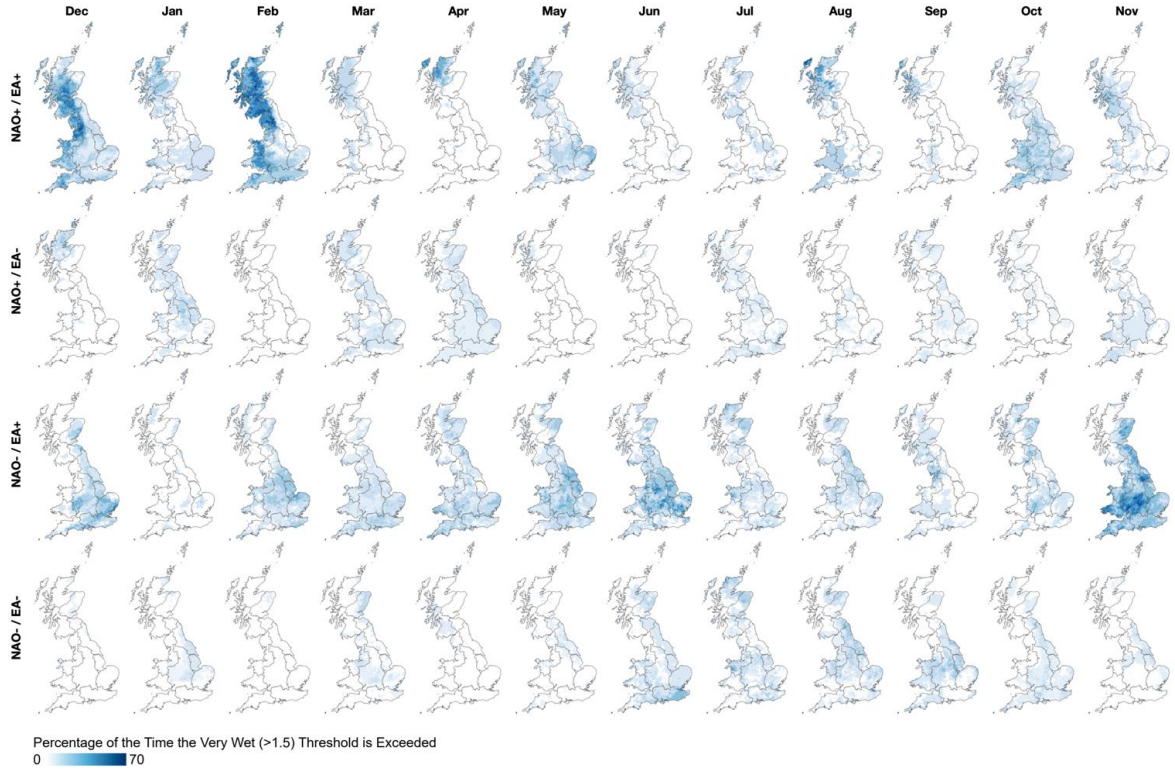

Figure 8: *Percentage of time the very wet (SPI-1 > 1.5) SPI-1 class threshold is exceeded under different phase combinations of the NAO and EA.*

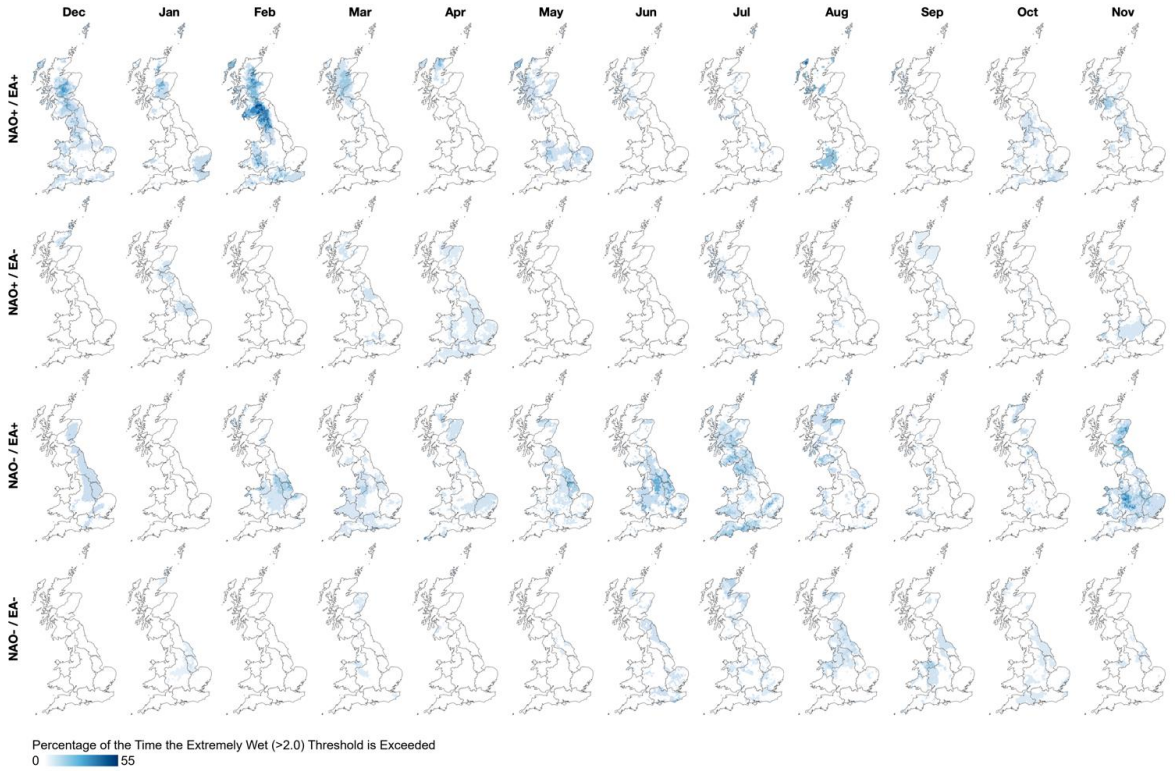

Figure 9: *As per Figure 7 but for the extremely wet (SPI-1 > 2.0) SPI-1 class.*

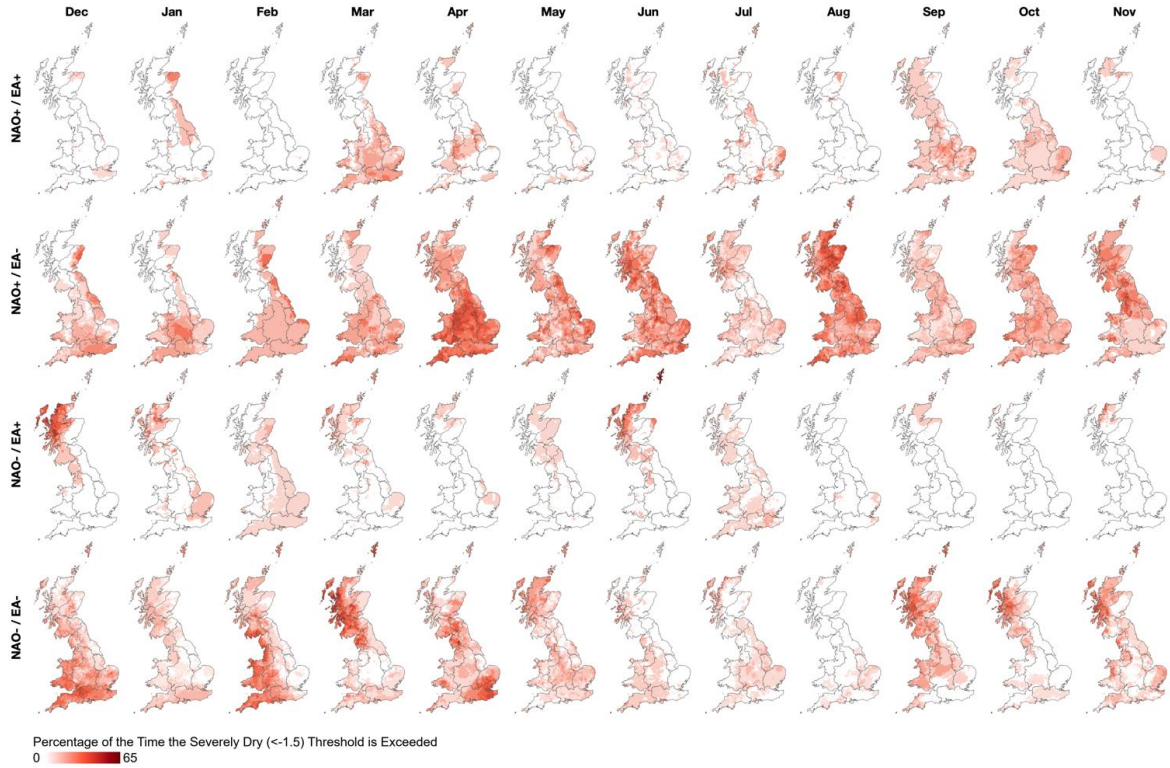

Figure 10: *As per Figure 7 but for the severely dry (SPI-1 < −1.5) SPI-1 class.*

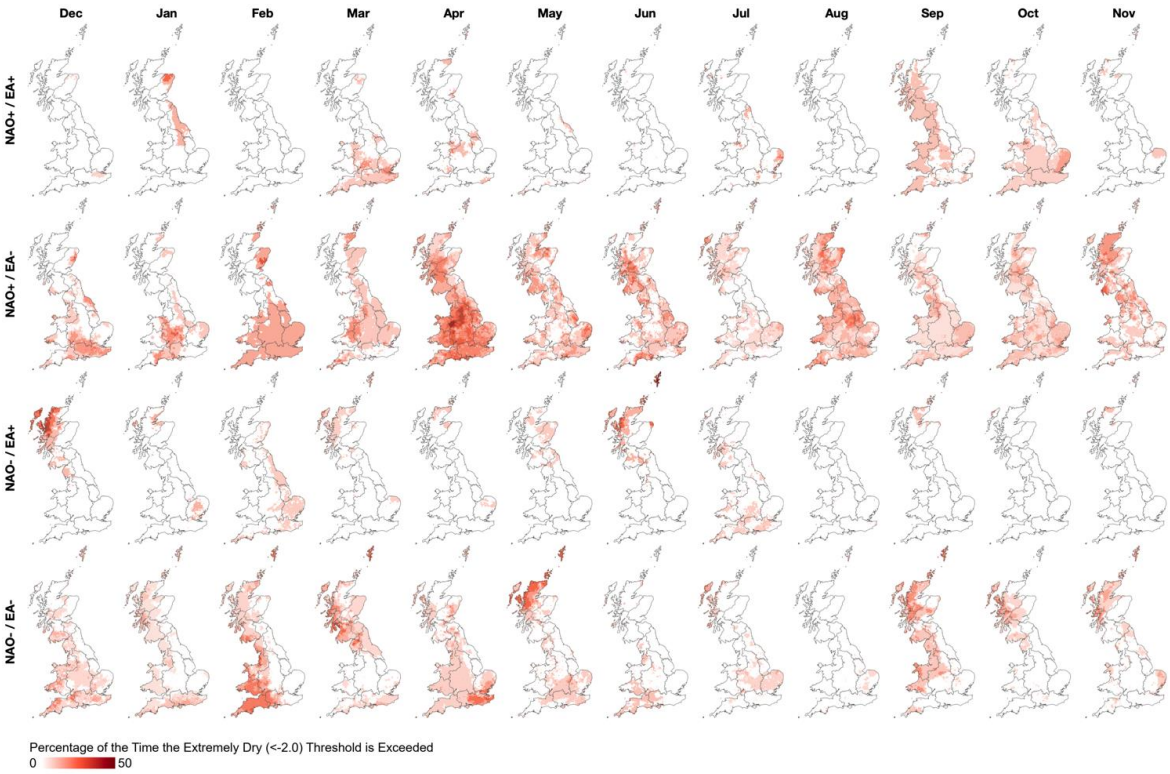

Figure 11. *As per Figure 7 but for the extremely dry (SPI-1 < −2.0) SPI-1 class.*

The SPI-1 class frequency analysis shows spatio-temporal variability in the extent of wet/dry extremes relative to the combination phases of the NAO and EA teleconnections. Figure 8 and Figure 9 show that during the winter months the north-western areas have a higher incidence

of very/extremely wet/dry conditions when both the NAO and EA are in a positive phase. Wetter conditions throughout the year are more likely in the southern, eastern and central regions when the EA is in a positive phase. In the summer months the phase combination of NAO− and EA+ is most likely to result in very wet conditions across most Climate Districts. The occurrence of very/extremely wet conditions in the summer months with NAO+ and EA− phases is very low.

Conversely, opposite patterns in the spatio-temporality of severe and extreme dry events are shown in Figure 10 and Figure 11. In the winter months there is a high incidence of severely dry conditions in the north-west under NAO− phases, independent of the phase of the EA. Meanwhile severely dry conditions have a higher frequency of occurrence in the southern regions when the EA is negative, a pattern which is present in most calendar months. In the summer months, the phase combination of NAO+ and EA− phases has the highest incidence of severe/extreme dry conditions across Great Britain. In the summer months, the incidence of severe/extreme dry conditions in other phase combinations is considerably less. These findings regarding the spatio-temporal variability in the occurrence of wet/dry extremes corroborate the correlation and average rainfall/SPI-1 analyses discussed above and demonstrate the combined role of both teleconnections in influencing the spatial distribution and frequency of wet/dry extremes.

Discussion

This study used high-resolution gridded rainfall datasets for Great Britain to map the spatially variable rainfall signatures of the NAO and EA atmospheric-oceanic circulations, contributing to research exploring the effect of and interactions between these two North Atlantic teleconnections.

Our correlation and analyses of high-resolution gridded rainfall and SPI-1 datasets presents a new understanding of the spatially variable influences of the NAO and EA on rainfall depth and distribution in Great Britain. During winter, we find that the NAO has a strong influence on regional rainfall in the north-western areas, with significant wet/dry conditions associated with NAO +/− phases (Figure 8, Figure 9, Figure 10 and Figure 11), a general relationship identified in previous research (Wilby et al. 1997; Burt & Howden 2013; Afzal et al. 2015; Rust et al. 2018; West et al. 2019b). The effect of the EA in the north-western area during winter appears to be more limited. Conversely the southern, central and eastern regions show a stronger relationship between wet/dry events and the phase of the EA, with wetter conditions in these areas associated with EA+ conditions (Figure 8 and Figure 9), and drier conditions EA− (Figure 10 and Figure 11).

The typical NAO-rainfall response in Great Britain is often noted as being along a NW/SE gradient during the winter months, with opposing wet/dry responses observed in these two

regions (West et al. 2019b; 2021a). Our findings suggest that this spatially variable response is potentially dependent on the phase and strength of the EA, with the opposing NW/SE rainfall responses being conditional on whether the EA is in the same or opposite phase to the NAO (Figure 5). Less distinctive spatial differences in the relative influence of the NAO and EA were found in the summer months, with the NAO in particular having a more spatially homogenous signature (Folland et al. 2009; Hall & Hanna 2018; West et al. 2019b). The more spatially consistent rainfall signatures in the summer months may be associated with greater convective, rather than orographic, rainfall generation (Burt & Howden 2013; West et al 2019b; 2021a). The wet/dry directionality of the rainfall response to the NAO is also inverted during the summer as the positive winter correlations become negative (Figure 2). These spatio-temporally variable effects of the NAO and EA were found in average rainfall/SPI-1 values (Figure 3, Figure 4, Figure 5, Figure 6 and Figure 7) and the analysis of extreme wet/dry event occurrence (Figure 8, Figure 9, Figure 10 and Figure 11).

Our analyses exploring the interaction between the phases of both the NAO and EA reveal the two teleconnections can either enhance or moderate the regional rainfall influence of each. For example, when both teleconnections are in a positive phase during the winter months, generally higher rainfall averages were found (Figure 5) and the occurrence of very/extremely wet conditions was high across the country (Figure 8 and Figure 9), although most notably in the north-west. Moore et al. (2013) explored the combined effect of NAO/EA phases on winter mean SLP across the North Atlantic region (see their Figure 6); NAO+/EA+ phases result in a southwesterly movement and strengthening of the Icelandic Low, with lower SLP extending over the North Atlantic and Great Britain, increasing the likelihood of higher rainfall. Conversely under NAO−/EA− phases the Icelandic Low dipole experiences higher than average SLP, resulting in an extended area of higher pressure over Great Britain (Moore et al. 2013), producing drier conditions. When the NAO and EA are in opposing +/− phases this results in a northeasterly movement of the two dipoles and a more marked difference in SLP between Iceland and the Azores (Moore et al. 2013). This manifests in our analysis as a clear NW/SE rainfall signature across Great Britain (Figure 5).

In our analysis, the combination of NAO+ and EA− phases results in the driest average conditions during the summer months (Figure 5) and the highest probably of severe dry conditions occurring (Figure 10). Conversely NAO− phases were found to be typically associated with wetter conditions (Figure 5). Folland et al. (2009) identified that a positive summer NAO is associated with a northward movement of the North Atlantic storm track, and easterly winds bringing warm air from continental Europe. Conversely, a negative summer NAO is associated with a southward movement of the storm track (Folland et al. 2009) resulting in higher rainfall across Great Britain.

Our analyses also show how the EA can have a moderating effect on the regional NAO-rainfall response. For example, during the summer months more diluted rainfall signatures (Figure 5) and lower occurrence rates of wet/dry extremes (Figure 8, Figure 9, Figure 10 and Figure 11) were found when both the NAO and EA were in the same phase. This may be associated with the effect of the summer NAO N/S movement of the storm track (Folland et al. 2009) being either moderated or enhanced by the EA (as is the case during the winter months (Moore et al. 2013)).

West et al. (2021a) analysed the spatio-temporal variability in the regional rainfall response to the NAO in Great Britain, finding that whilst more consistent responses were found in the north-west during winter, in the southern, central and eastern regions more wet/dry variability can be observed. Based on the results presented in this study, we suggest that some of this wet/dry variability is potentially associated with the phase and strength of the EA, which has consistent positive correlations with SPI-1 values in the southern and central regions throughout the year (Figure 2). Comas-Bru and McDermott (2014) suggest that through a combination of both the NAO and EA we may be able to describe winter climate variability more accurately; our analyses support this observation and highlight that this is also true in the summer months.

The findings of this study also have implications for the inclusion of monthly and seasonal NAO forecasts in water management decision making, which is potentially limited due to NAO-rainfall response variability (Rust et al. 2021b). Whilst NAO forecasts may contain useful information for the north-western areas during the winter months, they are likely to be less useful in the south (West et al. 2021a). This implies that even highly accurate NAO forecasts are not enough to fully predict regional rainfall across Great Britain (Hall & Hanna 2018). Our analyses reveals that the phase and strength of the EA might, to an extent, explain NAO-rainfall response variability. EA indices might therefore serve as a useful addition to regional hydrometeorological forecasting research, and predictions of both the NAO and EA several months in advance might be of practical use to water resource managers. However, as far as we are aware, no EA forecasting skill improvements have been reported in recent years, as has been the case with the winter NAO (Athanasiadis et al. 2020; Smith et al. 2020).

In this study we used monthly modelled teleconnection indices from NOAA (NOAA 2021a) to quantity the NAO and EA, with positive/negative phases defined by a threshold of ±0.25. It is important to note that there is no fixed approach to defining the phases of atmospheric circulations (Hurrell & Deser 2009), and there is scope for future work to examine the sensitivity of the rainfall signatures identified in this study to the method of phase definition. There is also scope for future research to apply the high-resolution rainfall products used in this study to examine the influence of and interactions between other atmospheric-oceanic circulations not considered in this analysis, which may include the Scandinavian Pattern (Bueh

& Nakamura 2007; Comas-Bru & McDermott 2014; Zubiate et al 2017) and East Atlantic/West Russia Pattern (Krichak & Alpert 2005; Ionita 2014; Lim 2015) which have also been associated with variability in European climate. There is also scope to explore at a high resolution the influence of phases of the NAO/EA on the location and strength of the Icelandic Low and Azores High meridional dipoles, and how the relationship between the NAO/EA and rainfall might have changed over time, especially given the winter EA index positive trend which has been found in some studies (Mikhailova & Yurovsky 2016).

Conclusion

This study used high-resolution gridded rainfall and SPI-1 datasets to map the monthly rainfall signatures of the North Atlantic Oscillation (NAO) and East Atlantic Pattern (EA) in Great Britain, with the aim of contributing to research exploring the interaction between these two atmospheric-oceanic circulations. Our findings show that the influence of the two teleconnections varies in space and time with distinctive signatures observed in both average rainfall/SPI-1 values and wet/dry extremes. In the winter months our analyses show the strong influence of the NAO on average monthly rainfall and extreme wet/dry events in the north-western regions of Great Britain. Meanwhile, in the southern, central and eastern regions stronger EA-rainfall relationships were present, which is significant given that these regions have been reported as having more variable NAO-rainfall responses in previous research. In the summer months we find that opposing +/− phases of the NAO and EA indices produce stronger wet/dry signatures, with average conditions when the two teleconnections are in the same phase being more diluted, resulting in a lower probability of wet/dry extremes.

Our findings suggest both the NAO and EA have a prominent influence on regional rainfall distribution and volume in Great Britain, which has implications for the use of teleconnection forecasts in water management decision making. We conclude that accounting for both NAO and EA influences will lead to an enhanced understanding of both historic and future spatial distribution of monthly precipitation.

Appendix

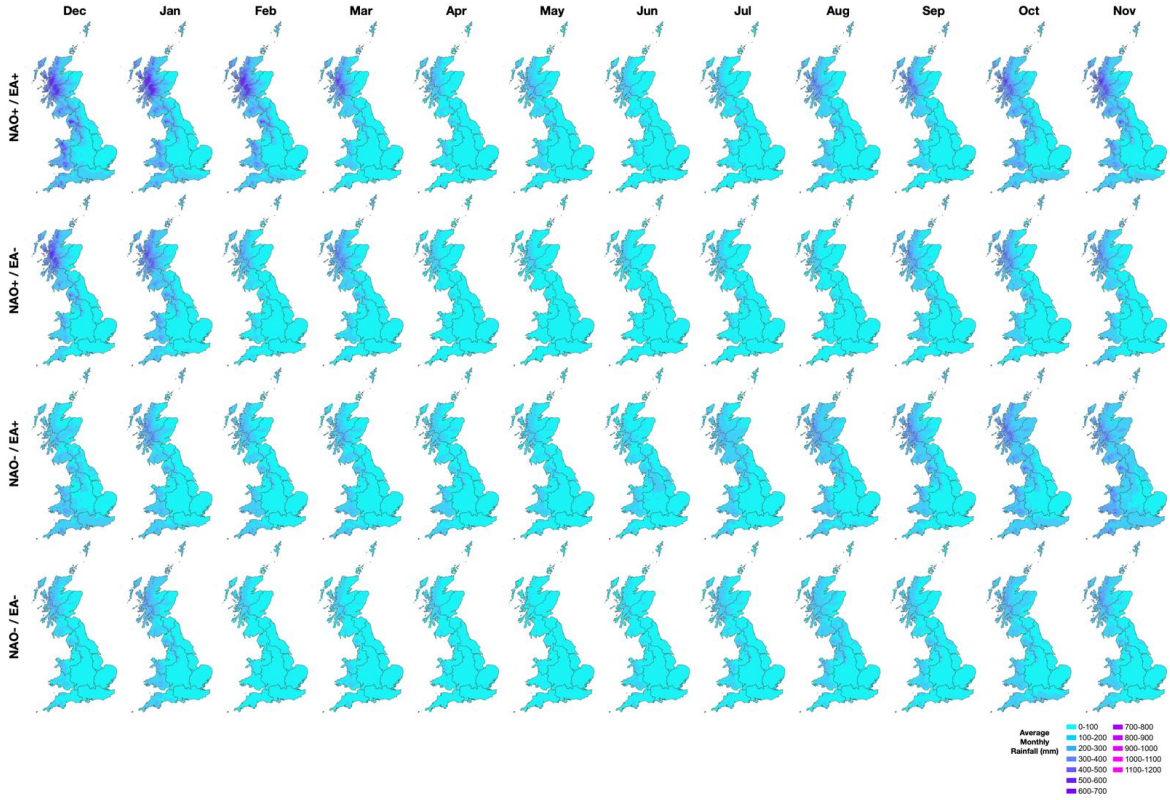

Figure A1: *Maps of average monthly rainfall (based on the CEH GEAR dataset) under different phase combinations of the NAO and EA.*

Paper 6: The Influence of the North Atlantic Oscillation & East Atlantic Pattern on Drought in British Catchments

Citation: West, H., Quinn, N. & Horswell, M. (2022). The Influence of the North Atlantic Oscillation & East Atlantic Pattern on Drought in British Catchments. Frontiers in Environmental Science, Vol.10, 754597.

Published: 17th March 2022.

Contributions: Following the spatial analyses in Paper 5, there was an opportunity to undertake further research into the relationships between NAO/EA and drought conditions as part of a Special Section in Frontiers (co-led by NQ). HW led on this analysis with support from NQ and MH. HW produced the first draft of the paper which was shared for feedback with NQ and MH.

Changes to Original Paper:

- No changes have been made between this version and that published in March 2022.

Abstract

Drought events are influenced by a combination of both climatic and local catchment characteristics. In Great Britain the North Atlantic Oscillation (NAO) has long been recognised as the leading mode of climate variability, and studies have also noted the role of the East Atlantic Pattern (EA) as a secondary mode. This study aimed to develop an understanding of the combined influence of the NAO and EA on rainfall distribution and magnitude and the variable nature of meteorological to hydrological drought propagation. Initially, this study explores correlations between teleconnection indices and standardised precipitation and streamflow indices for 291 catchments across Great Britain, before focusing on nine case study catchments for further analysis. For each case study catchment, we use quantile regression and an analysis of drought frequency to explore the combined influence of the NAO and EA on drought conditions. Through a convergence of evidence from these analyses we make three observations. Firstly, in the winter months both the NAO and EA exert an influence on drought conditions, however there is spatial variability in the relative influence of the NAO and EA; the NAO has a stronger influence in the north-west, whilst the EA has a stronger influence in the southern and central regions. Secondly, in the summer months, less distinctive spatial differences were found, with higher probability of drought conditions under NAO+ phases, which however can be enhanced or moderated by the EA. Finally, as a result of catchment characteristics there is spatio-temporal variability in the propagation of meteorological to hydrological drought. Our findings suggest that by considering the NAO and

EA in combination, we can better describe climate and drought variability. We conclude by noting the potential implications our study has on the role of monthly teleconnection forecasts in water management decision making in Great Britain, and acknowledge the current limitations associated with incorporating such understanding.

Introduction

Drought is a significant hydrometeorological hazard which can have severe socio-economic and environmental impacts (Nagarajan 2010). Recent work has continued to advance our understanding of drought events, their spatio-temporal propagation through the hydrological cycle, and their impacts (Parry et al. 2016; Van Loon et al. 2016; Barker et al. 2016; 2019; Parsons et al. 2019; Tanguy et al. 2021). Droughts are typically classified on the basis of underlying physical processes and environmental/socio-economic impacts. These include meteorological drought (low precipitation), soil moisture or agricultural drought (low soil moisture), hydrological drought (low discharge and groundwater), and socio-economic drought (where there is a substantial impact on water resources affecting society) (Wilhite and Glantz 1985; Van Loon 2015). Conceptually these 'drought types' have a sequential progression over time from meteorological to hydrological (and socio-economic) drought.

The spatiality of drought events is complex in Britain, as is the propagation of rainfall to flows within catchments. Distinctive differences in both rainfall and flow regimes have been found between the north-western and south-eastern areas of the country which are related to a range of climatological and hydrological variables (Burt & Howden 2013; Folland et al. 2015; Chiverton et al, 2015; Barker et al. 2016; Rust et al. 2018; West et al. 2019b; 2022a; Svensson & Hannaford, 2019). Tanguy et al. (2021) identify NW/SE differences in the characteristics of meteorological drought events in Britain (see Figure 1 of Tanguy et al. 2021). Notably, when examined with short rainfall accumulation periods, shorter and less severe droughts were found in the north-western areas, whilst longer and more severe droughts were found in the south-eastern areas. Although it should be noted that using longer rainfall accumulation periods resulted in less distinctive differences between the NW and SE (Tanguy et al. 2021).

Spatial patterns in the propagation of meteorological to hydrological drought is further complicated as it is influenced by both climate and catchment characteristics (Van Loon & Laaha 2015). Barker et al. (2016) found that streamflow in the NW is sensitive to short meteorological droughts, such as those identified by Tanguy et al. (2021), due to the highly responsive nature of catchments in this region (Chiverton et al. 2015). Meanwhile low flows in the southern and eastern parts of the country are more strongly related to rainfall deficits over longer time periods due to their catchment characteristics and baseflow dominance (Barker et al. 2016).

Droughts are inherently driven by climatic processes, and for Great Britain and most of northern and western Europe, the North Atlantic Oscillation (NAO) atmospheric-oceanic circulation has long been identified as the leading mode of climate variability (Rodwell et al. 1999; Sweeney & O'Hare 1992; Hurrell & Van Loon 1997). The NAO is defined by two meridional diploes - the Icelandic Low and Azores High/Anticyclone. When the sea level pressure (SLP) difference between these two locations is greater than average the NAO is said to be in a positive phase (NAO+), whilst a weaker than average SLP difference represents a negative phase (NAO-) (Hurrell et al. 2003). Significant correlations have been reported between North Atlantic Oscillation Indices (quantitative measures of the phase and magnitude of the NAO - NAOI) and rainfall in Britain. For example, significant positive correlations have been found in the north-west of the country during winter (Wilby et al. 1997; Fowler & Kilsby 2002; Afzal et al. 2015; Rust et al. 2018) and West et al. (2019b) report significant increases/decreases in winter rainfall (200-300mm) in the north-west associated with NAO+/- phases, relative to when the NAO is in a weak neutral state (defined as half the standard deviation plus/minus the long term mean of the NAOI (Berton et al. 2017)). Generally, winter correlations are weaker, and there is greater variability in the NAO-rainfall response, in the southern and eastern areas (Rust et al. 2018; West et al. 2021a).

The influence of the NAO is typically reported as being weaker in the summer months compared to winter (Folland et al. 2009). However spatially consistent rainfall responses to the NAO have been observed in summer across Great Britain, although these correlations are typically negative and weaker (Folland et al. 2009; Hall & Hanna 2018; West et al. 2019b). It should be noted however that summer correlations between the NAO and rainfall can vary depending on the calculation method of the chosen NAOI (Pokorná & Huth 2015; West et al. 2019b).

The East Atlantic Pattern (EA) has also been acknowledged to have an impact on European climate and has been referred to as a southward shifted NAO-like pattern (Comas-Bru & McDermott 2014; Mikhailova & Yurovsky 2016). The EA is noted as having a well-defined monopole at approximately 55°N; 20–35°W (Barnston & Livezry 1987; Moore & Renfrew 2012; Comas-Bru & McDermott 2014; Mellado-Cano et al. 2019), the SLP conditions at which have the potential to influence the location and strength of the NAO dipoles (Moore et al. 2011). Studies have noted that the phase and magnitude of the EA also influences rainfall spatial distribution and volume across Europe, and consequently by using a combination of the NAO and EA we may be able to describe winter climate variability more accurately (Comas Bru & McDermott 2014; Mellado-Cano et al. 2020). In Great Britain, positive correlations have been found between the EA and rainfall, which are typically stronger in the southern and central regions (Casanueva et al. 2014; Hall & Hanna 2018; West et al. 2021b).

As described above, north-west/south-east differences have been reported when exploring drought characteristics and propagation in Britain (Barker et al. 2016; Tanguy et al. 2021). Similar NW/SE spatio-temporal patterns have been found when exploring the propagation of NAO-driven rainfall deviations to streamflow in catchments (Burt & Howden 2013; Rust et al. 2021a). Catchments in the north-west are more sensitive to NAO-rainfall deviations, whilst catchments in the southern regions are less susceptible due to their geology, terrain and landcover characteristics which moderate flows (West et al. 2022a). Spatially and temporally variable NAO signals have also been detected in groundwater levels across aquifers in Britain (Lavers et al. 2015; Rust et al. 2019) and fluvial water temperatures (Wilby & Johnson 2020). As far as we are aware, no study has explored at similar large scales the propagation of EA-rainfall signatures.

The above discussion describes the complex interplay between climate and hydrological systems, which manifests in spatio-temporal variability in rainfall, flow responses, and subsequent drought characteristics and propagation, generally along a N/S or NW/SE gradient in Britain. This study aims to bring together understandings of the influence of the NAO and EA on rainfall distribution and magnitude, and the variable nature of meteorological to hydrological drought (i.e. rainfall-streamflow) propagation. In doing so we present new insights into the influence of these two teleconnections on drought in British catchments and how this varies in space and time.

Developing our understanding of the potential effect of the NAO on low rainfall conditions, and how these deficits propagate through catchments, may help us to improve water management decision making and prepare for potential drought events. Forecasting skill for the winter NAO has improved in recent years (Baker et al. 2017; Parker et al. 2019; Athanasiadis et al. 2020; Smith et al. 2020), and there is increasing potential to include the NAO as a factor in monthly streamflow forecasting/modelling (UK Hydrological Outlook 2020; Donegan et al. 2021). However, we acknowledge further work is required to understand how teleconnection forecasting might be fully utilised given the spatio-temporal variability in NAO-rainfall responses (West et al. 2021a; Rust et al. 2021b), and we are unaware of any similar forecasting skill improvements having been reported for the EA.

Methods

Data

Standardised indicators are commonly used for monitoring a range of different hydrometeorological/hydrological variables, such as precipitation, evapotranspiration, streamflow and groundwater (Bachmair et al. 2016). Standardised indicators are effective for hydrological monitoring as they are scaled in relation to local wetness/dryness (relative to a standard or baseline period) and can be calculated over a range of months (the accumulation

period). For drought monitoring and assessment in particular, standardised indicators have been used in wide range of research and applications (Hannaford et al. 2011; Bachmair et al. 2016; Huang et al. 2017; Dhurmea et al. 2019; Yeh 2019; Parsons et al. 2019; Mehr et al. 2020).

In this study we use two standardised indicators: The Standardised Precipitation Index (SPI) and Standardised Streamflow Index (SSI), both of which have been used in drought research in Great Britain (Barker et al. 2016; 2019). Both timeseries were downloaded from the UK Centre for Ecology and Hydrology (Tanguy et al. 2017; Barker et al. 2018) for the period Jan 1950-Nov 2015. The SPI and SSI datasets are calculated using interpolated historic rainfall (Met Office 5km rainfall grids) and reconstructed streamflow datasets (UKCEH – Smith et al. 2018). The rainfall was fitted to a Gamma Distribution whilst a Tweedie Distribution was used for streamflow (Tanguy et al. 2017; Barker et al. 2018). Both have a common standard period of 1961-2010 and were calculated using a one-month accumulation period (SPI-1 and SSI-1). Positive SPI-1/SSI-1 values indicate higher mean monthly rainfall/flows relative to the 1961-2010 standard period, whilst negative values indicate lower mean monthly rainfall/flows. The SSI-1 data were downloaded for 291 catchments across Britain which vary in geography, size and physical characteristics. The SPI-1 data for each of these 291 catchments were derived by area-weighting the national 5km gridded SPI-1 dataset.

The NOAA Climate Prediction Centre calculates monthly indices for a range of atmospheric-oceanic circulations, including the NAO and EA (NOAA 2021a). The CPC use a modelling approach based on a rotated principal component analysis (RCPA) to calculate their monthly teleconnection indices (after Barnston & Livezry 1987), avoiding any limitations with using indices directly calculated using in-situ SLP measurements (Pokorná & Huth 2015). The teleconnection indices from the CPC have been used in studies exploring the impact of atmospheric-circulations on low rainfall and drought conditions globally (Irannezhad et al. 2015; Huang et al. 2017; Abiy et al. 2019; Amini et al. 2020; Onate-Valdivieso et al. 2020; Hassan & Nayak 2021). Monthly NAO and EA indices were download for the period Jan 1950-Nov 2015 (NOAA 2021a).

The first analytical stage of this study (correlation and quantile regression) explores the relationship between each of the two teleconnections and meteorological/hydrological drought. In these initial analyses the NAO and EA are treated individually. Later analysis, quantifying the frequency of different drought severities, explores the interaction between the NAO and EA and the combined effect of different teleconnection phases.

Monthly NAOI-Rainfall and NAOI-Flow Correlation Analyses

The first stage of this research sought to examine the influence of the NAO and EA on catchment rainfall (quantified by the SPI-1) and streamflow (quantified by the SSI-1), and how

their respective influence changes in space and time across the 291 catchments. Spearman correlation coefficients were calculated between the two teleconnection indices and SPI-1 and SSI-1 values for each catchment and calendar month, over the period Jan 1950-Nov 2015. Distinctive spatio-temporal differences were observed across the correlation results, representing the general influence of each of the two teleconnections.

Case Study Catchments

To develop a more detailed understanding of the combined effect of the NAO and EA on meteorological drought, and how rainfall deficits propagate through to hydrological drought, nine case study catchments were selected for further analysis. One catchment from each of the Met Office Climate Districts was chosen to ensure a spatially representative sample across Great Britain. The Climate Districts represent areas of relatively homogeneous climate and have been used in similar research (Wilby et al. 1997; Simpson & Jones 2014; West et al. 2019b). The catchments were chosen as they vary not only geographically, but also represent a range of physical characteristics such as size, terrain and geology. The representativeness of the nine case study catchments was evaluated using a similarity analysis (described below). Figure 1 presents the nine case study catchments and Table 1 summarises their key physical and hydrological characteristics.

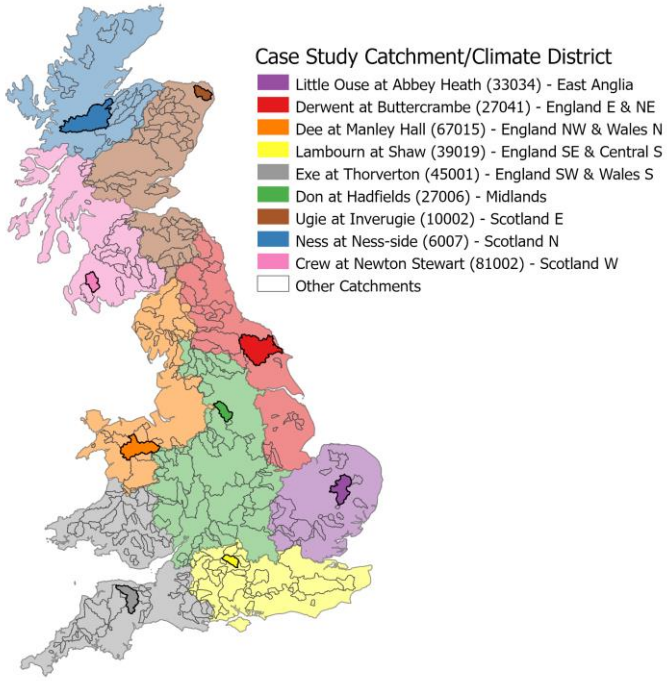

***Figure 1**: Location of the nine case study catchments. Shading indicates the Met Office Climate Districts for Great Britain. Numbers in brackets are the Catchment ID from the UK National River Flow Archive.*

Table 1: Summary of case study catchment characteristics (data from the UK National River Flow Archive).

Catchment (NRFA ID)	Climate District	Average Annual Rainfall (1961-1990) (mm)	Elevation (mAOD)	Landcover (% Coverage)	Bedrock Geology Permeability (% Coverage) (HP = High Permeability, MP = Mixed Permeability, LP = Low Permeability)	Size (km^2)	Base Flow Index
Ness at Ness-side (6007)	Scotland N	1765	• Min = 7 • Max = 1109.6	• Woodland = 16.97 • Arable = 1.22 • Grassland = 13.33 • Mountain/Heath/Bog = 61.58 • Urban = 0.06	• HP Bedrock = 0 • MP Bedrock = 9.82 • LP Bedrock = 90.18	1839.1	0.61
Cree at Newton Stewart (81002)	Scotland W	1757	• Min = 5.2 • Max = 843	• Woodland = 49.09 • Arable = 0.33 • Grassland = 39.73 • Mountain/Heath/Bog = 9.05 • Urban = 0.76	• HP Bedrock = 0 • MP Bedrock = 0 • LP Bedrock = 100	368	0.28
Ugie at Inverugie (10002)	Scotland E	812	• Min = 9.5 • Max = 233.7	• Woodland = 11.35 • Arable = 43.89 • Grassland = 34.59 • Mountain/Heath/Bog = 8.49 • Urban = 1.56	• HP Bedrock = 0 • MP Bedrock = 2.44 • LP Bedrock = 97.56	325	0.64
Exe at Thorverton (45001)	England SW & Wales S	1249	• Min = 27.6 • Max = 516.8	• Woodland = 14.97 • Arable = 12.85 • Grassland = 66.71 • Mountain/Heath/Bog = 2.76 • Urban = 2.37	• HP Bedrock = 0 • MP Bedrock = 15.65 • LP Bedrock = 84.35	600.9	0.5
Dee at Manley Hall (67015)	England NW & Wales N	1367	• Min = 28.10 • Max = 878.2	• Woodland = 17.51 • Arable = 1.23 • Grassland = 62.96 • Mountain/Heath/Bog = 14.87 • Urban = 1.00	• HP Bedrock = 0 • MP Bedrock = 4.48 • LP Bedrock = 89.30	1013.2	0.54
Little Ouse at Abbey Heath (33034)	East Anglia	607	• Min = 8.10 • Max = 94.60	• Woodland = 15.33 • Arable = 63.25 • Grassland = 16.33 • Mountain/Heath/Bog = 0 • Urban = 5.03	• HP Bedrock = 99.73 • MP Bedrock = 0.27 • LP Bedrock = 0	688.5	0.8
Don at Hadfields Weir (27006)	Midlands	1014	• Min = 32.3 • Max = 543.4	• Woodland = 15.66 • Arable = 6.17 • Grassland = 35.64 • Mountain/Heath/Bog = 18.83 • Urban = 20.23	• HP Bedrock = 0 • MP Bedrock = 43.38 • LP Bedrock = 0	373	0.49
Lambourn at Shaw (39019)	England SE & Central S	736	• Min = 72.4 • Max = 260.3	• Woodland = 10.26 • Arable = 53.72 • Grassland = 30.27 • Mountain/Heath/Bog = 0.10 • Urban = 2.40	• HP Bedrock = 97.33 • MP Bedrock = 0 • LP Bedrock = 0	243.1	0.97

Derwent at Buttercrambe (27041)	England E & NE	765	• Min = 9.50 • Max = 453.2	• Woodland = 15.43 • Arable = 41.46 • Grassland = 26.76 • Mountain/Heath/Bog = 12.11 • Urban = 3.10	• HP Bedrock = 2.68 • MP Bedrock = 51.45 • LP Bedrock = 44.16	1586	0.7

Similarity analysis (Esri 2022a) was used to assess the representativeness of each of the nine case study catchments in terms of their rainfall and flow responses to the NAO and the EA. This analysis gives an indication of how similar their meteorological and hydrological drought characteristics might be to the other 290 catchments, both within and beyond their associated Climate District. The similarity analysis algorithm was first applied to the two NAO and EA SPI-1 correlation time series for each of the nine case study catchments, and secondly to the NAO and EA SSI-1 correlation time series. The algorithm first standardises the selected correlation coefficients for each catchment - this standardisation uses a z-score transformation where the mean of all of the coefficients is subtracted from each value and divided by the standard deviation. This standardised value is then subtracted from the coefficients of the case study catchment, the difference squared and totalled, creating a similarity index (Esri 2022a). Using this index, the 290 catchments were ranked from most to least similar and mapped.

Spatial autocorrelation in the similarity rank values was assessed using the Global Morans I statistic. The Global Morans I evaluates whether the spatial distribution of similarity rank values across the 290 catchments (not including the case study catchment) is more clustered or dispersed than would be expected in a random spatial distribution of the same values (Esri 2022b). The Global Morans I statistic requires a conceptualisation of how each catchment is spatially related to its neighbours. Due to the variability in the size of each catchment (Esri 2022c), a fixed distance band threshold which maximises spatial autocorrelation within the similarity rank values was used (Esri 2022b; 2022c). This was a distance of 50km from the geometric centroid of each catchment.

We undertook two separate analyses to investigate the influences of the NAO and the EA individually on meteorological drought conditions, and how this propagates to hydrological drought within each of the nine case study catchments, firstly using quantile regression analysis, and secondly drought severity frequency analysis.

Quantile Regression Analysis

A standard generalised linear regression model would assume that the NAO or EA have an equal influence on both wet and dry conditions (high/low rainfall and flows). The use of a quantile regression model allows for an assessment of the relationship between each teleconnection index and low (negative) SPI-1/SSI-1 values at different quantile levels, allowing for a more complete understanding of the influence of the teleconnection on low rainfall and flow conditions in the case study catchments (Amini et al. 2020).

We performed quantile regression using 99 quantiles between the NAO and EA indices and the catchment SPI-1 and SSI-1 values. We extracted the quantile regression coefficients for SPI-1/SSI-1 quantiles below 0.2 (Amini et al. 2020), which equated to standardised index values <-1 in all cases. This analysis was undertaken for both winter (DJF) and summer months (JJA). This allowed for an assessment of the nature and strength of the winter/summer relationship between the two teleconnections and meteorological (low SPI-1) and hydrological (low SSI-1) drought in the case study catchments.

Drought Severity Frequency Analysis

The second stage of this research moved beyond looking at the individual effect of the NAO and EA and explored their combined influence. A frequency analysis quantifying the relationship between the phase of the two teleconnections and low SPI-1 and SSI-1 values was undertaken, which compliments the correlation and quantile regression analyses above. For the winter (DJF) and summer months (JJA) we plotted the NAO and EA indices and examined the associated spatio-temporal patterns in low (negative) SPI-1 and SSI-1 values. We also calculated the frequency of mild (0 > index < -1), moderate (-1 > index < -1.5) and severe (index < -1.5) drought (McKee et al. 1993) under different combinations of NAO and EA phases.

As in previous research (e.g. Comas-Bru and McDermott 2014; Berton et al. 2017; West et al. 2021a), the monthly teleconnection index values were classified. Months with teleconnection index values >0.25 were classified as positive phases, whilst months with index values <-0.25 were classified as negative phases. Months with index values falling between these two thresholds were classified as neutral phases. This classification produces nine possible combinations of NAO and EA phases. Phase frequency analysis allowed us to then assess the influence of the combined teleconnections on drought conditions for each of the nine case study catchments, and to identify any associated seasonal and spatial trends.

Results

The first stage of the research explored the individual effect of the NAO and EA on rainfall and flows using correlation and regression analyses. Figure 2 presents the analysis of monthly correlation between the NAO and SPI-1 and SSI-1 values for 291 catchments across Great Britain. The NAO has strong positive correlations between both the SPI-1 and SSI-1 in catchments in the north-western region during the winter months (DJF). In the southern and eastern catchments weaker correlations are found, although these catchments do show stronger negative NAO SPI-1/SS-1 correlations in the spring (MAM). During the summer months (JJA) more spatially consistent negative correlations are found, however differences in the SPI-1 and SSI-1 correlation time series are more pronounced. In the southern and eastern areas, catchments show stronger negative correlations between the NAO and SPI-1 than SSI-1.

Autumn months (SON) are also marked by negative correlations and a transitioning back to the winter north-west/south-east pattern described above. The spatio-temporal correlation patterns indicate that in the winter months NAO- phases have an influence on meteorological drought conditions in the north-western catchments, which propagates through to hydrological drought in streamflow. In the summer months the effect of the phase of the NAO is reversed, with negative correlations indicating that NAO+ phases have a stronger meteorological drought control. However, the propagation of these negative NAO SPI-1 correlations to SSI-1 correlations varies spatially (West et al. 2022a), indicating that the propagation of monthly NAO-driven meteorological drought to hydrological drought is more limited.

Figure 2: Monthly correlations between the NAO and SPI-1/SSI-1 for the 291 catchments across Great Britain. Note the difference between the significant positive correlations in the NW during winter (DJF), compared to the more spatially homogenous negative correlations in summer (JJA).

Figure 3 shows the comparable correlation monthly time series between the EA and catchment SPI-1 and SSI-1 values. Notable spatio-temporal differences between the monthly NAO time series (Figure 2) and the EA SPI-1/SSI-1 correlations were found. In the winter months (DJF) positive EA correlations are present across most of Great Britain, although coefficients generally strengthen from north to south. These positive correlations persist into the spring (MAM). The summer months (JJA) are also marked by mostly positive correlations, although of a weaker strength than in the winter months. The positive relationship of the EA index with catchment SPI-1 and SSI-1 values indicates that EA- phases are likely to be associated with meteorological drought conditions, which as with the NAO correlations, variably propagate to hydrological drought conditions.

***Figure 3**: Monthly correlations between the EA and SPI-1/SSI-1 for the 291 catchments across Great Britain. Note the difference in strength between the positive correlations in the during winter (DJF) compared to the slightly weaker correlations in summer months (JJA).*

Figure 4 presents the monthly correlation analyses in Figures 2 and 3 for the nine case study catchments. The spatio-temporal patterns across the correlations in the case study catchments align with the above discussion. For example, in the winter months the Ness and Crew in the north-west show strong positive correlations between the NAO and SPI-1, whilst the Exe in the south has stronger winter correlations between the EA and SPI-1. As outlined above the NAO correlations are reversed in the summer months, with the majority of case study catchments showing negative correlations. Meanwhile the EA generally remains positively correlated with both SPI-1 and SSI-1 throughout the year. The moderation of rainfall-streamflow propagation is also exemplified in Figure 4 by the Lambourn catchment as it shows a stronger correlation between the EA and SPI-1 than the EA and SSI-1.

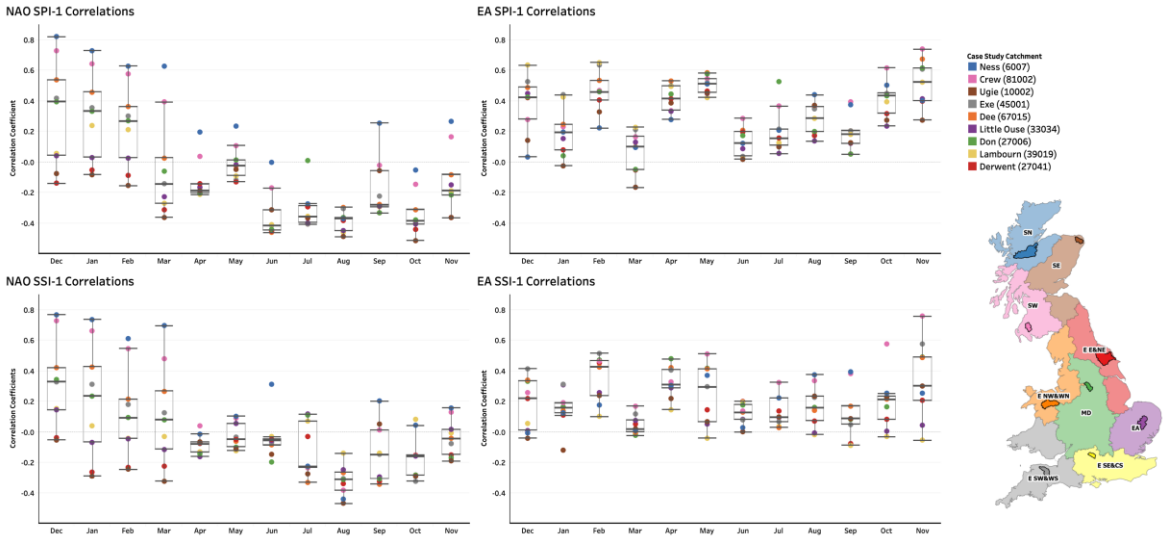

***Figure 4**: Monthly correlation analyses between the NAO/EA and catchment SPI-1 and SSI-1 values for the nine case study catchments.*

Similarity Analysis

Figures 5 and 6 present the results of the similarity analysis between the various correlation time series for the case study catchments. In both figures the catchment is highlighted in yellow, with the remaining 290 catchments ranked from most similar to least similar. Catchments with lower values indicate those which have a greater similarity in their individual NAO and EA monthly correlation time series (mapped in full in Figures 2 and 3) to those of the case study catchment. Catchments with higher values indicate those which have monthly correlation time series which are less similar to the case study catchment.

Figures 5 and 6 show that each case study catchment is generally well representative of its respective Climate District (Figure 1) in terms of the correlation between the two teleconnections and SPI-1 and SSI-1 values. For example, Figure 5 shows that the Ness and Crew catchments in Scotland North and Scotland West are generally representative of correlations between the two teleconnections and SPI-1 for catchments in the north-western

area, and the Exe and Lambourn represent catchments in the south-west and central southern areas of Britain well.

Table 2 presents the results of the Global Morans I statistic for each of the similarity rank datasets mapped in Figures 5 and 6; where the z-score is positive and p-value significant, the similarity rank values are more clustered than would be expected if the underlying spatial processes were random (Esri 2022b). Our results show that this is the case for all 18 (two per case study catchment) similarity rank value datasets. The Morans I Index provides an indication as to the strength of the spatial autocorrection, with higher values indicating greater clustering of similarity rank values.

Across all nine case study catchments, the Morans I Index (Table 2) was found to be greater for the SPI-1 correlation similarity rank values than for the SSI-1 similarity rank values, although it should be noted that the SSI-1 values were still spatially autocorrelated, albeit with a weaker strength. For example, in Figure 5, for the Exe catchment we can see higher SPI-1 similarity rank values across the south-west and southern central areas, indicating more similar teleconnection SPI-1 correlations. Whilst in Figure 6 the similarity rank values for the SSI-1 correlations for the same area are more spatially variable. This is likely a result of the characteristics of catchments which may moderate rainfall-flow propagation, such as geology, terrain and landcover (Chiverton et al. 2015; Barker et al. 2016; West et al. 2022a).

***Figure 5**: Similarity analysis results based on the NAO/EA SPI-1 correlation time series mapped in Figures 2 and 3. The case study catchment is highlighted in yellow. Catchments with lower values indicate those which have greater similarity in their NAO/EA monthly correlations to those of the case study catchment. Catchments with higher values indicate those which have NAO/EA correlations which are less similar.*

***Figure 6**: As per Figure 5, but showing the results of the similarity analysis based on the NAO/EA SSI-1 correlation time series.*

***Table 2**: Results of the Global Morans I statistical analysis for the similarity rank values mapped in Figures 5 and 6. Where the z-score is positive and p-value significant then the similarity rank values are more clustered than would be expected if the underlying spatial processes were random. The Morans I Index indicates the strength of the similarity rank value clustering.*

Catchment	Correlation Similarity Rank Values	Morans I Index	z-score	p-value
Ness at Ness-side (6007)	SPI-1	0.735	26.34	0.005
	SSI-1	0.623	22.31	0.005
Cree at Newton Stewart (81002)	SPI-1	0.782	27.98	0.005
	SSI-1	0.763	27.32	0.005
Ugie at Inverugie (10002)	SPI-1	0.847	29.03	0.005
	SSI-1	0.753	25.81	0.005
Exe at Thorverton (45001)	SPI-1	0.874	31.25	0.005
	SSI-1	0.629	22.56	0.005
Dee at Manley Hall (67015)	SPI-1	0.776	27.79	0.005
	SSI-1	0.673	24.13	0.005
Little Ouse at Abbey Heath (33034)	SPI-1	0.845	30.29	0.005
	SSI-1	0.794	28.48	0.005
Don at Hadfields Weir (27006)	SPI-1	0.785	28.05	0.005
	SSI-1	0.588	21.05	0.005
Lambourn at Shaw (39019)	SPI-1	0.868	31.07	0.005
	SSI-1	0.719	25.75	0.005
Derwent at Buttercrambe (27041)	SPI-1	0.827	29.61	0.005
	SSI-1	0.791	28.28	0.005

Quantile Regression Analysis

Figure 7 presents the results of the quantile regression analysis between the teleconnection indices and the SPI-1 and SSI-1 values for the nine case study catchments. Figure 7 shows the coefficients for quantiles <0.2. These results give an indication of the direction (sign) and strength of the statistical relationship between the NAO and EA indices and meteorological and hydrological drought conditions (i.e. low SPI-1 and SSI-1 values) in the case study catchments.

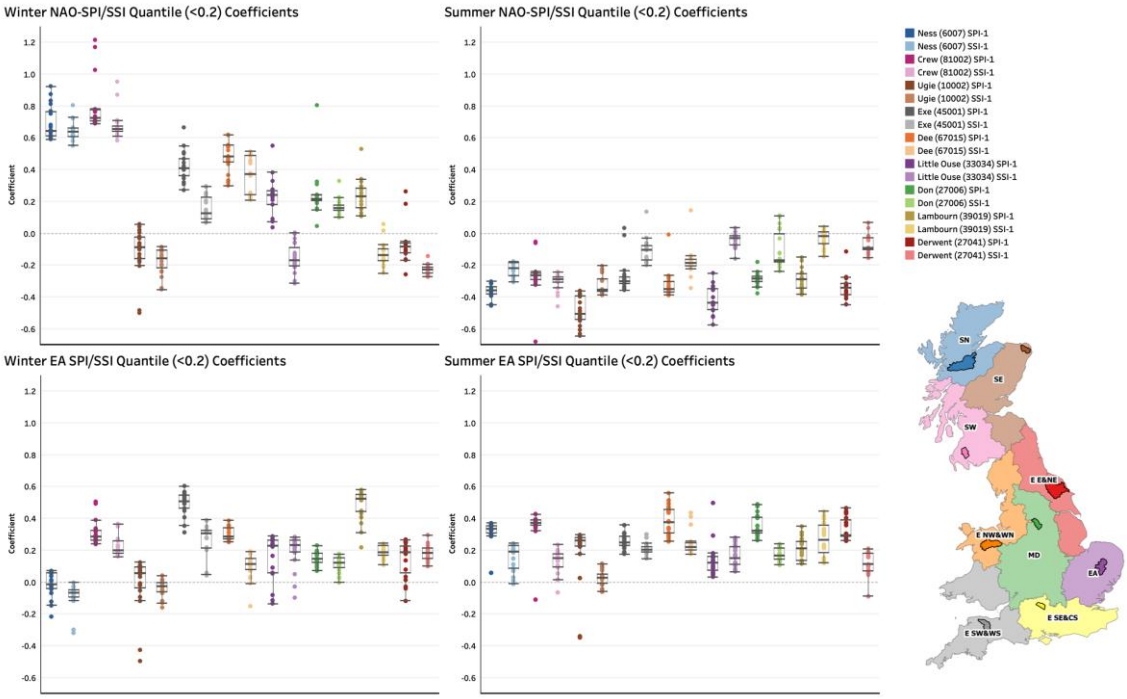

***Figure 7**: Extracted quantile coefficients between the NAO/EA indices and SPI-1/SSI-1 values. Coefficients were extracted for quantiles <0.2, the range of these quantile coefficients is represented in this figure as box plots.*

As with the monthly correlation analyses (Figures 2 and 3) the quantile regression coefficients for low SPI-1/SSI-1 values demonstrate the relative influences of the NAO and EA on drought conditions, which varies in space (across the country) and time (across the seasons). Catchments in the north-west (the Ness and Crew) have a very strong positive relationship between the NAO and low SPI-1 values, indicating that NAO- conditions result in meteorological droughts in these catchments. Similar relationships are observed in these catchments between the NAO and SSI-1 values. This highlights the responsive nature of catchments in this region; meteorological droughts propagate through the catchments resulting in hydrological drought. Case study catchments in the southern and central regions of Great Britain show weaker positive relationships between the NAO and drought conditions, however the EA has an equal, and in some cases such as the Exe stronger, positive EA-drought relationship.

As discussed in relation to the correlations in Figure 4, the quantile regression analysis evidences the moderating effect of catchment characteristics in limiting the propagation of meteorological to hydrological drought. For example, the Lambourn in the winter EA plot in

Figure 7 – where a moderately strong positive relationship between the EA and meteorological drought is not replicated with the comparable SSI-1 coefficients.

The extracted summer quantile coefficients further corroborate the monthly correlation analyses in Figure 4. The NAO has a weaker negative summer relationship with low SPI-1 values which is generally consistent across the case study catchments; suggesting that NAO+ phases, to an extent, influence summer meteorological drought. The EA retains its positive relationship, suggesting EA- phases may produce meteorological drought conditions in summer. For both teleconnections the propagation of summer meteorological to hydrological drought varies in space and time which we suggest is related to the characteristics of the catchment and the extent to which these moderate rainfall-flow propagation.

Drought Severity Frequency Analysis

In this stage of the research, we moved beyond quantifying the individual effect of the two teleconnections to examine the combined influence of NAO and EA phases. Figure 8 shows seasonal plots for winter (DJF) and summer (JJA) of the NAO and EA indices for each case study catchment. Each point represents one month and is coloured based and the catchment SPI-1 value, and sized per the SSI-1 value. A large red point therefore indicates both meteorological (low SPI-1) and hydrological drought (low SSI-1) conditions, whilst a small red point suggests meteorological drought conditions, but less severe or no hydrological drought.

Figure 9 shows the percentage occurrence of dry/low flow conditions (negative SPI-1 and SSI-1 values) under each of the NAO/EA phase combinations for the winter and summer months. Figure 10 shows the distribution of these occurrences across mild, moderate and severe drought classes.

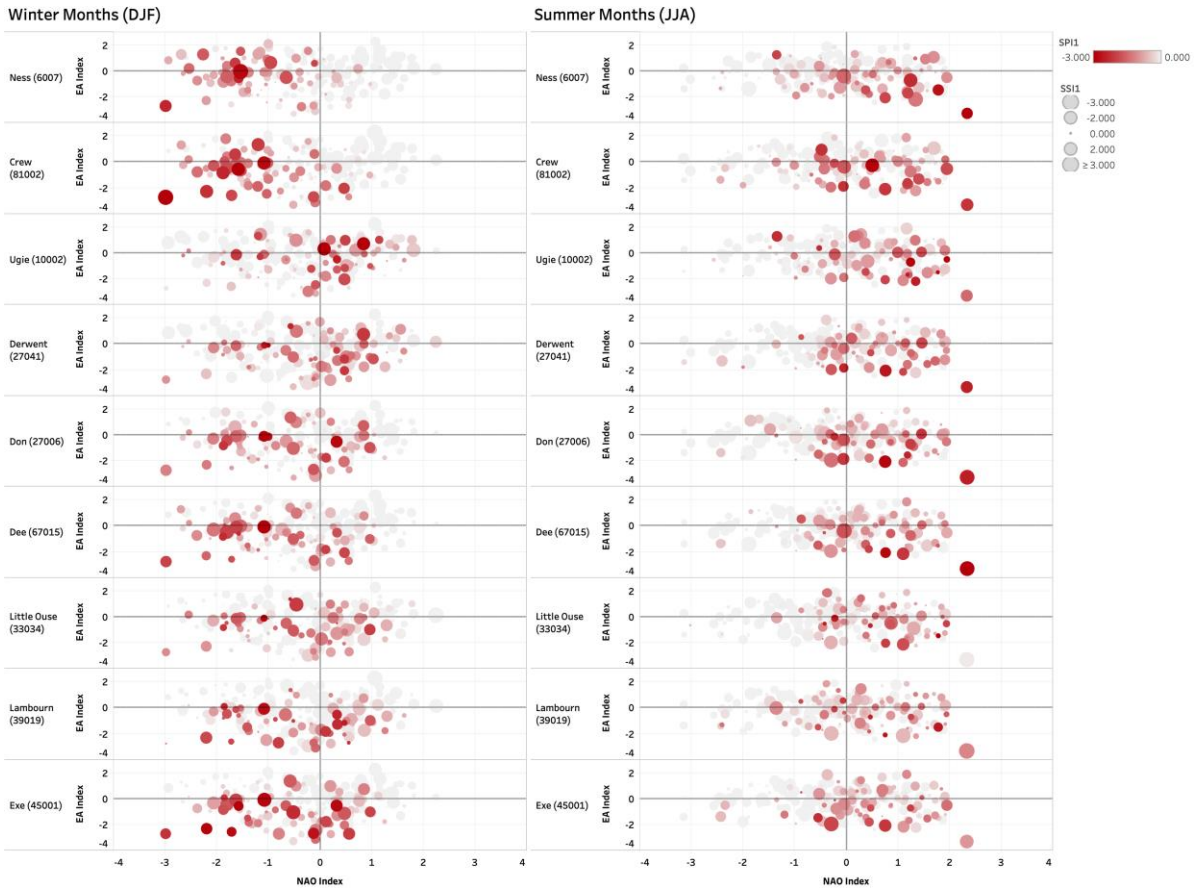

***Figure 8**: Seasonal teleconnection index plots for winter (DJF) and summer (JJA). The points are coloured by the catchment SPI-1 value, whilst the size represents the SSI-1 value. Large red points indicate both meteorological and hydrological drought, whilst a small red point suggests meteorological, but not hydrological, drought.*

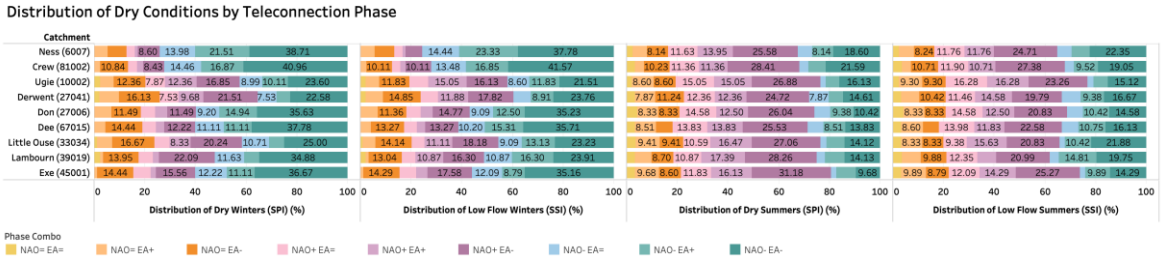

***Figure 9**: Distribution of dry events (negative SPI-1 and SSI-1 values) under different phase combinations of the NAO and EA for the winter and summer months. Values represent the percentage of time dry events occur under the different phase combinations.*

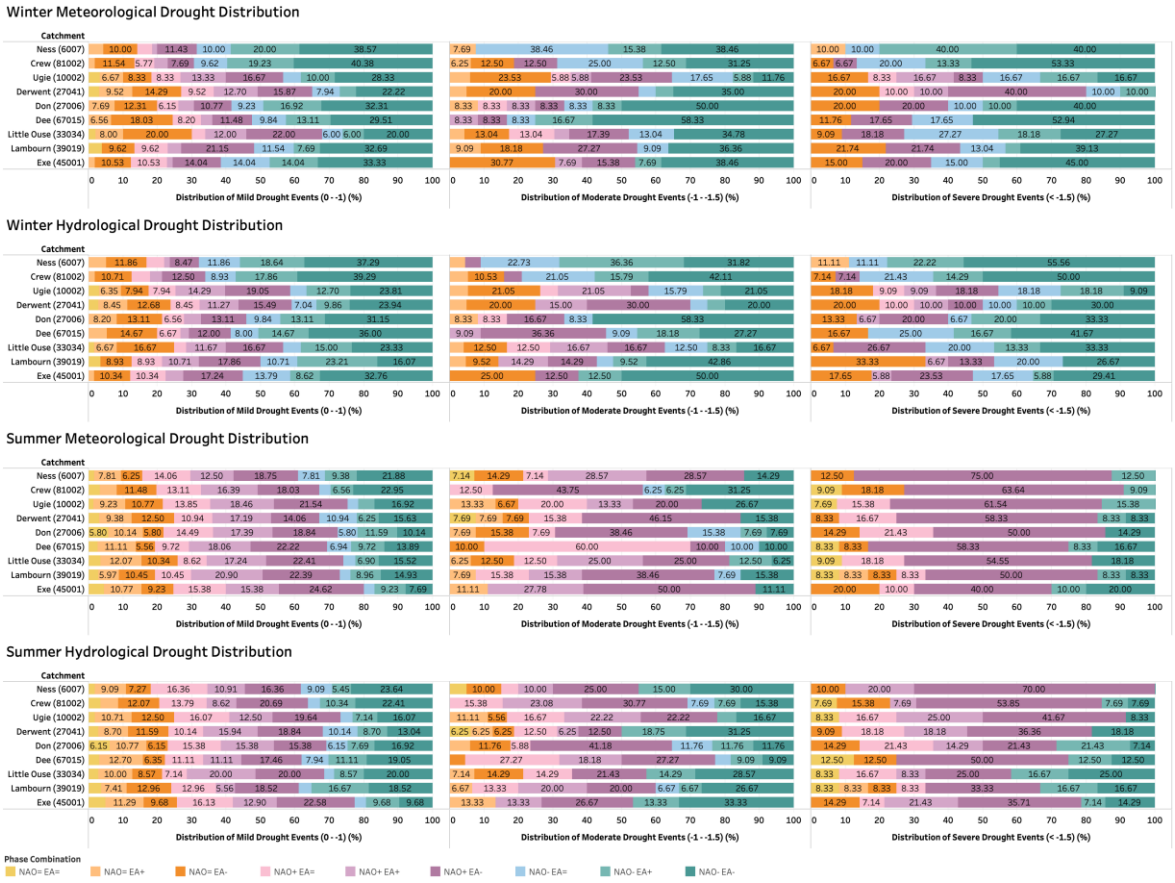

***Figure 10**: Distribution of mild (0 > index < -1), moderate (-1 > index < -1.5) and severe (index < -1.5) droughts under phases combinations of NAO and EA. Values represent the percentage of time drought events of different severities occur under the different phase combinations.*

Analysis of the teleconnection indices (Figure 8) and drought severity frequency analysis (Figures 9 and 10) support the correlation and regression analyses (Figures 4 and 7), revealing distinctive spatio-temporal patterns in the relative influence of the NAO and EA on drought conditions in the case study catchments. Notably the occurrence of dry events when both the NAO and EA are in a weak neutral state is very low (Figure 9), highlighting the importance of the phases of the NAO and EA on the occurrence of drought in the case study catchments.

The climate districts of Scotland North and Scotland West are represented in this analysis by the Ness and Crew catchments. Figures 8-10 highlight the clear influence the NAO has on meteorological and hydrological drought conditions in these two catchments as explained by the quantile regression analysis, with NAO- phases being clearly associated with drought conditions. The effect of the EA during winter in these catchments, and north-western Scotland generally, appears to be limited. For example, in the Ness catchment during winter 68.57% of mild and 90% of severe meteorological droughts occur when the NAO is in a negative phase, independent of the phase of the EA (Figure 10). The occurrence of drought events in these catchments when the NAO is in a positive phase is minimal, with no severe meteorological droughts in the Ness associated with NAO+ phases. The occurrence of hydrological droughts in these two catchments also show a strong relationship with NAO- phases (Figures 9 and 10).

In the summer months the direction of the relationship between the NAO and drought is reversed, with low rainfall/flow conditions being associated with NAO+ phases (Figure 9). Differences in the occurrences of the mild and severe drought severity classes under different phase combinations of the NAO and EA are more notable in the summer months (Figure 10). These differences are associated with the phase of the EA, suggesting that the teleconnection has a moderately stronger influence in the summer, relative to the winter months. Mild drought conditions can be associated with a larger range of NAO and EA phase combinations (Figure 10), possibly because of higher temperatures and other hydrometeorological factors/variables (Van Loon 2015) not considered in this study. However severe meteorological drought conditions in the Ness catchment only occur when the EA is also in a negative phase, and 91% of severe droughts in the Crew are associated with EA- conditions (Figure 10). Similar relationships between the phase of the NAO and EA and hydrological drought occurrence are also observed in the Ness and Crew.

Less clear teleconnection-drought patterns are found in the Ugie catchment in Scotland East, however Figure 8 does suggest a weak relationship between drought conditions and NAO+ phases, but with greater variability than the influence of the NAO in Scotland North and Scotland West during winter as described above. Drought conditions have a similar frequency of occurrence under different NAO/EA phase combinations (Figures 9 and 10). However as in the Ness and Crew catchments, in the summer months meteorological droughts have a higher frequency of occurrence when the NAO is in a positive phase, with severe meteorological droughts associated with a combination of NAO+ and EA- conditions.

The southern and central areas of Great Britain show notably different teleconnection-drought patterns to the northern/north-western catchments. The Exe catchment, representing the England South-West and Wales South Climate District, shows a stronger relationship between the EA and winter drought conditions than it does for the NAO. For example, 80% of severe meteorological droughts during winter in the Exe are associated with EA- phases (Figure 10). A very small proportion of severe meteorological droughts in the Exe are associated with a positive phase of the EA. In contrast, summer meteorological droughts have a higher rate of occurrence under NAO+ conditions. 70% of severe meteorological drought events in the Exe occur under NAO+ conditions, the majority of which are also associated with EA- phases (Figure 10).

Whilst in the Exe catchment the influence of the teleconnections on both meteorological and hydrological drought is relatively similar (Figure 9), the Lambourn catchment, representing the England South East and Central South Climate District, illustrates the role of catchment characteristics in moderating drought propagation. In terms of meteorological drought, the Lambourn has similar EA drought relationships to the Exe (demonstrated by the similarity analysis in Figure 5). However, there is a weaker teleconnection-drought relationship with

flows (SSI-1). The occurrence of hydrological drought is more evenly distributed across the different phase combinations of the NAO and EA (Figures 9 and 10), indicating that catchment characteristics, in the case of the Lambourn highly permeable bedrock (Table 1), limits the propagation of meteorological to hydrological drought.

Catchments in the eastern districts, the Little Ouse and Derwent, show teleconnection-drought relationships similar to the Exe and Lambourn. In the Little Ouse catchment, for example, meteorological droughts have a higher rate of occurrence under EA- conditions during winter, with 62% of dry events being associated with EA- phases (Figure 9). Summer drought relationships are also similar, for example 58.3% of severe summer meteorological droughts are associated with a combination of EA- and NAO+ phases in the Derwent (Figure 10).

Winter meteorological droughts in the Midlands and England North West and Wales North Climate Districts, represented by the Don and Dee catchments, are influenced more clearly through a combination of the NAO (which generally has a greater influence in the north-western areas) and the EA (which generally has a stronger southern influence). Winter meteorological droughts in these case study catchments are associated with both NAO- and EA- phases (Figures 8 and 9). In the Dee for example, 83.34% of severe meteorological droughts in winter are associated with NAO- phases, however half of these are also associated with EA- conditions (Figure 10). Propagation to hydrological drought in the Dee is relatively clear, possibly due to low permeability bedrock and steep topography (Table 1). EA- phases have an association with droughts in these catchments during the summer months, in combination with NAO+ phases for the more severe drought classes (Figure 10).

Discussion

This study aimed to explore the relative influence of the NAO and EA on meteorological drought in British catchments, and whether these rainfall deficits propagate to hydrological drought. We examine both the individual effect of the NAO and EA through correlation and regression analyses, and the frequency of drought events of varying severities under different NAO and EA phase combinations. Based on the convergence of evidence across the results of this study we make three main observations which will be discussed in turn.

The first observation relates to the variable influence of both the NAO and EA during the winter (DJF) months. Our analyses highlight that the NAO has a strong influence on meteorological drought conditions in the north-western catchments during winter, as found in previous correlation-based studies (Wilby et al. 1997; Rust et al. 2018; West et al. 2019b). In these catchments NAO- phases are generally associated with meteorological droughts, shown by the Crew and Ness (Figures 8 and 9). When the NAO is in a negative phase the SLP difference between the Icelandic Low and Azores High is weaker than normal resulting in a more northerly jet stream, which in turn limits the movement of low pressure systems north-westerly

across the Atlantic region (Hurrell et al. 2003). This results in low rainfall over the north-western regions of Britain (West et al. 2019b). In the southern, eastern and central areas the NAO has a less consistent influence on rainfall (West et al. 2021a), however strong positive correlations with the EA were found in these areas (Figures 3 and 4). In the southern catchments, the Exe, Lambourn and Little Ouse, meteorological droughts are generally more associated with EA- conditions (Figures 8 and 9). These findings suggest that NAO- and EA- conditions result in the driest winter conditions nationally with the NAO has a stronger meteorological drought influence in the north-western areas, whereas the EA has more influence in the southern and central areas. Moore et al. (2013) analysed the effect of the phase of the EA on the strength and location of the NAO dipoles, finding that NAO-/EA- phase combinations results in higher than average SLP at the Icelandic Low action point, and an extended area of high pressure in the region producing drier conditions.

Our second observation relates to the differences in the summer months (JJA) compared to the spatial variability described above for winter. In the summer, the NAO has a more spatially homogenous influence on rainfall in Great Britain and correlations are of the opposite sign to those in the north-west during winter (Hall & Hanna 2018, West et al. 2019). NAO+ phases have been associated with drier summer conditions, as the North Atlantic storm track is shifted northerly, and easterly winds bring warm continental air from Europe (Folland et al. 2009). The correlation coefficients mapped in Figure 3 and quantile regression results in Figure 7 show that the effect of the EA during summer is weaker than during winter, however a positive relationship is still present for most of the 291 catchments. During the summer months there is a higher frequency of drought occurrence under NAO+ conditions across all nine case study catchments (Figure 9). However, differences in drought severity are associated with the phase of the EA, with severe meteorological droughts having a higher frequency of occurrence under a combination of NAO+ and EA- phases (Figure 10). This suggests that the phase of the EA can enhance (notably EA- conditions) or moderate drought conditions associated with summer NAO+ phases. As far as we are aware no study has yet mapped the influence of EA phases on the NAO dipoles and North Atlantic storm track during the summer months. However, if the NAO+/EA- phase combination during summer results in a similar strengthening of the Azores High as is the case in winter (Moore et al. 2013), then this may potentially explain the more extreme dry conditions found under this phase combination in this study.

Our final observation relates to the propagation of meteorological to hydrological drought, a process influenced by both climate and catchment characteristics (Van Loon & Laaha 2015; Barker et al. 2016). Our analyses show spatio-temporal differences between the two teleconnections influence on meteorological and hydrological drought; we interpret these differences as being a function of the geography and characteristics of catchments, such as terrain, geology and landcover. In the winter in the north-west the rainfall deficits as a result of

NAO- phases propagate to streamflow resulting in hydrological drought. Catchments in the north-west are responsive to rainfall due to topographic and geological characteristics (Chiverton et al. 2015) and so short meteorological droughts in this area (as identified by Tanguy et al. 2021) quickly propagate to low flows. Our analyses also identify cases where there is limited meteorological to hydrological drought propagation, particularly in catchments in the southern and central regions. For example, in the Lambourn catchment which is underlain with highly permeable bedrock (Table 1), a notably stronger EA-drought relationship was identified with rainfall than with flows (Figures 7 and 9). We suggest that some catchments, depending on their geography and characteristics, are potentially more resilient to drought propagation, with the influence of the NAO and EA on both rainfall and streamflow varying in space and time due to catchment characteristics (West et al. 2022a). However, we acknowledge that this observation is based on our interpretation of the difference in meteorological and hydrological drought occurrence in our analyses, and we have not undertaken an analysis explicitly quantifying the effect of catchment characteristics.

In recent years our ability to predict the NAO several months in advance has improved, especially during the winter months (Baker et al. 2017; Athanasiadis et al. 2020; Smith et al. 2020). This study demonstrates that this improved predictive ability might be useful in water resource management planning. For example, if several months in advance of winter the NAO was forecast to be in a strong negative phase, water authorities could prepare for a higher probability of meteorological and hydrological drought onset in the highly responsive catchments in the north-west.

However, NAO predictive skill has largely only improved during its stronger winter phases, and as far as we are aware, no improvements have been made in EA prediction. This has implications for regional forecasting and the inclusion of teleconnection indices in water management decision making. This is especially true in the southern, central and eastern regions where our analysis demonstrates the clear influence of the EA on meteorological and, more variably, hydrological drought conditions, particularly in the summer months where the phase of the EA can enhance or lessen drought severity associated with NAO+ phases. Our analysis therefore supports the findings of Hall & Hanna (2018), who suggest that even highly accurate NAO forecasts might have a limited role in water management decision making especially in the southern, central and eastern areas of Great Britain, and Comas-Bru & McDermott (2014), who suggest that a combination of both the NAO and EA may be able to explain (hydro)climatic variability more accurately.

In this study we have used relatively new long-term historic datasets for rainfall and flows (Tanguy et al., 2017; Barker et al., 2018) to explore associations between the NAO and EA on monthly drought conditions in British catchments. There is scope to utilise these datasets and the analytical approaches used in this study to explore how the NAO/EA-drought relationship

has changed over time and might change in the future with climate change, especially given the positive EA index trend identified in studies (Mikhailova and Yurovsky 2016). Further in this study we have explored a specific monthly drought scenario relating to the monthly teleconnection indices (NOAA 2021a). As the SPI/SSI datasets used in this study have indices published over longer accumulation periods (representing different drought duration/severity) there is potential to explore the association between teleconnections and rainfall/flows over different periods of time. Future research might also explore the association of drought conditions in catchments with other atmospheric-oceanic circulations such as the Scandinavian Pattern and East Atlantic/West Russia Pattern for which monthly indices are modelled by NOAA (NOAA 2021a) and rainfall correlations have been found across the North Atlantic and European region (Krichak and Alpert 2005; Comas-Bru and McDermott 2014).

Conclusions

This study aimed to explore the influence of the NAO and EA North Atlantic teleconnections on meteorological drought in British catchments, and the extent to which these rainfall deficits propagate through catchments resulting in hydrological drought. Based on evidence from our analyses we highlight three main observations from this study:

1. During the winter months there is spatial variability in the relative influence of the NAO and EA on drought conditions, with NAO- phases resulting in higher drought probability in the north-western areas (regardless of EA phase), and EA- phases being associated with higher drought probability in the southern and central areas.
2. There is less spatial variation in the relative influence of the NAO and EA during the summer months, with drought conditions associated with NAO+ phases across most catchments. Although we find that the phase of the EA can moderate or enhance this, with severe meteorological droughts being associated with a combination of NAO+ and EA- phases.
3. There is spatio-temporal variability in the propagation of meteorological to hydrological drought, with streamflow in catchments in the north-west typically being more responsive to rainfall deficits, whilst catchments in the southern and central regions have higher hydrological drought resilience.

Our study has implications relating to the role of monthly teleconnection forecasts in water management decision making in Great Britain, however, we acknowledge the current limitations associated with incorporating such understanding.

Summary of the Research Undertaken

This final chapter reflects on how each of the papers presented in this thesis address the research objectives and summarises the contribution to knowledge presented in this thesis. Table 1 maps the objectives against key findings from the published articles, which are expanded on in the following commentary.

***Table 1**: Mapping the Research Objectives against the key findings across the six published articles.*

Research Objective	Paper	Key Findings
1. Quantify the influence of the NAO on rainfall and streamflow across long-term (50-100 years) historic spatio-temporal signatures.	• **Paper 1**: Regional Rainfall Response to the North Atlantic Oscillation in Great Britain. • **Paper 2**: Spatio-Temporal Propagation of North Atlantic Oscillation (NAO) Rainfall Deviations to Streamflow in British Catchments.	• NAO-rainfall signatures are sensitive to the chosen NAOI (and its calculation method). • There is a clear winter north-west and south-east divide in rainfall and streamflow signatures related to NAO phase. • The NAO has an effect on summer rainfall and flows, which is more spatially consistent across the country.
2. Investigate the extent to which catchment characteristics moderate circulation-rainfall deviations propagating to streamflow.	• **Paper 2**: Spatio-Temporal Propagation of North Atlantic Oscillation (NAO) Rainfall Deviations to Streamflow in British Catchments.	• Catchments in the north-west have more consistent NAO-rainfall and NAO-flow correlations, compared to catchments in the southern/central regions. • Catchments in the north-west are generally steep and have impermeable geologies, thus flows are more responsive to NAO-rainfall deviations. • Catchments in the southern and central areas are flat, vegetated and have permeable geologies, making them more resilient to NAO-rainfall deviations.
3. Assess long-term variability in monthly NAO-rainfall signatures.	• **Paper 3**: Spatio-Temporal Variability in North Atlantic Oscillation Monthly Rainfall Signatures in Great Britain.	• During the winter the north-west has a statistically significant and more consistent NAO-rainfall response. • The southern and eastern regions have a more variable NAO-rainfall response over time.

		• There is greater NAO-rainfall response variability across the country during the summer.
4. Assess the influence of a range of other circulations on rainfall and evaluate the relative importance of the NAO over space and time.	• **Paper 4**: The Spatio-Temporal Influence of Atmospheric Circulations on Monthly Precipitation in Great Britain.	• Each of the five atmospheric circulations analysed has a spatio-temporally variable influence on monthly rainfall. • The analysis highlights that the NAO only partially explains precipitation variability, especially in the southern regions and during summer. • Significant explanatory power is gained by looking at atmospheric circulations in combination, in particular the EA has a secondary (and at times dominant) influence.
5. Assess the explanatory potential of atmospheric circulation combinations for the British hydroclimate and explore the implications for water/environmental management decision making.	• **Paper 5**: Monthly Rainfall Signatures of the North Atlantic Oscillation & East Atlantic Pattern in Great Britain. • **Paper 6**: The Influence of the North Atlantic Oscillation & East Atlantic Pattern on Drought in British Catchments.	• The north-west has strong NAO-rainfall-flow relationships, whilst the EA has more influence in the southern/central areas. • In the summer opposing phases of the NAO and EA produce more extreme wet/dry signatures. • The phase of the EA can moderate or enhance the rainfall effect of the NAO, especially in terms of drought severity. • By considering the NAO and EA in combination we can better explain rainfall and flow variability which may have water resource management implications if circulation forecasting continues to improve.

1. Quantify the influence of the NAO on rainfall and streamflow across long-term (50-100 years) historic spatio-temporal signatures.

The first research aim was to understand the influence of the NAO by quantifying long-term rainfall and streamflow signatures. Paper 1 explored regional rainfall relationships, whilst Paper 2 identified streamflow relationships across a large number of catchments (n=291). Paper 1 used high resolution CEH GEAR and SPI datasets to quantify rainfall deviations under NAO Positive and Negative phases at a monthly scale between 1900-2015. Correlations were

calculated for the Met Office Climate Districts using two different NCAR NAO Indices – one derived from station-measured SLP data, and one modelled principal component (PC) based index.

Key findings from Paper 1 include the observation of clear winter rainfall signatures associated with Positive and Negative phases of the NAO, with greater rainfall deviations under NAO+/- phases relative to neutral conditions (>100mm in some areas) in the north-west of the country. Opposite but less extreme rainfall deviations (<50mm) were found in the south-east. Relationships with summer rainfall were also observed, although the spatiality of the rainfall signatures was more consistent across Great Britain, and opposite to the wet/dry NAO phase response of the north-west during winter.

This work represented the first national scale, monthly NAO-rainfall assessment undertaken for a long time period; addressing limitations in previous research relating to short data record length, non-spatially continuous station-based rainfall observations, and a restriction to only exploring relationships during the winter months.

Paper 2 continues to develop an understanding of the influence of the NAO on UK hydroclimate. The first section of this paper uses long-term modelled streamflow and SSI datasets are used to assess NAO-flow relationships for 291 catchments across a long historic time period (1900-2015). Similar spatio-temporal relationships between the NAO and streamflow were found; where during winter catchments in the north-west see significantly higher flows under NAO+ conditions, and significantly decreased flow under NAO- conditions. In some north-western catchments flows are as much as doubled under NAO+ compared to NAO-. Less discernible differences in flows between the two NAO phases were found in the southeast. This work also found NAO-flow summer relationships, however as with rainfall the wet/dry response is the opposite of that during winter.

This work represented the first spatially and temporally large-scale analysis of the sub-annual influence of the NAO on streamflow in Britain, and like Paper 1 addresses limitations from previous NAO-flow studies relating to scale, resolution and limited data availability.

2. **Investigate the extent to which catchment characteristics moderate circulation-rainfall deviations propagating to streamflow.**

The second aim of this research sought to investigate the extent to which catchment characteristics, such as terrain, landcover and geology, might moderate the propagation of circulation-rainfall deviations to streamflow. This aim was addressed in Paper 2, where following an exploration of NAO-rainfall and NAO-flow relationships within catchments, these two sets of signatures were compared using space-time clustering analysis.

There were strong positive correlations (r=0.6-0.8) between the NAO index and both rainfall and streamflow in catchments in the north-west, suggesting that NAO-rainfall deviations quickly propagate through to flows. Catchments in this region are generally steep, high elevation, and have high low permeability bedrock coverage making them less able to moderate NAO-rainfall deviations during winter. In summer NAO-rainfall linkages are also observed (r=-0.4 - -0.6), however for many catchments in the central and southern regions these NAO-rainfall relationships are not fully replicated in flows (r=0 - -0.4). Catchments in these regions are generally flat, low-lying and have highly permeable geologies, suggesting that these characteristics moderate NAO-rainfall-flow propagation during the summer.

Similar spatio-temporal patterns in the moderating effect of catchment characteristics were found in Paper 6 which explores the extent to which NAO and EA induced meteorological droughts propagate to hydrological droughts. This work found spatio-temporal variability in the propagation of drought with catchments in the southern and central region having high hydrological drought resilience.

This work presents new evidence of the variable nature of the propagation of circulation-rainfall linkages to flows due to the moderating effect of catchment characteristics.

3. Assess long-term variability in monthly NAO-rainfall signatures.

Whilst previous studies have reported variability in NAO-rainfall signatures, none have quantified this at high resolution. Paper 3 addresses this knowledge gap and presents a novel application of space-time analyses to understand the variability in NAO-rainfall signatures at a high spatial (5 km) and temporal (monthly) resolution across Great Britain.

The analysis confirmed the presence of statistically significant NAO-rainfall spatial signatures across Great Britain and that some regions, such as the north-west during winter, show a relatively high level of consistency in the rainfall response to the phase of the NAO over time. For example some areas in the north-west show a >70% likelihood of significant wet/dry conditions related to the phase of the NAO. In other words, the NAO consistently results in significant increases/decreases in rainfall in this region across the period 1900-2015.

However, as well as areas of significant and consistent NAO-rainfall responses, this work also revealed greater long-term variability in NAO-rainfall relationships across the central, southern and eastern areas of Britain. In these regions, NAO phases generally result in more variable rainfall responses over time – in some areas the likelihood of significant wet/dry conditions under both phases of the NAO is almost equal. In summary, the analyses revealed that whilst typical and consistent NAO-rainfall signatures can be quantified across the year, there is also significant NAO-rainfall response variability over time.

This work involved novel application of GIS-based space-time analyses and quantifies for the first time the consistency/variability in monthly NAO-rainfall signatures over a long historic time period (1900-2015).

4. **Assess the influence of a range of other circulations on rainfall and evaluate the relative importance of the NAO over space and time.**

Paper 3 concluded that variability in regional rainfall response to the NAO may be associated with the concurrent phase and magnitude of other atmospheric circulations across the North Atlantic and European region, especially across the central, southern and eastern areas of Britain. Paper 4 presents an analysis exploring the relationship between different circulations and monthly SPI-1 across the IHU Groups of Great Britain. Circulation-rainfall relationships were explored for the NAO, EA, SCA, EAWR and POL, separately and in combination, for the period 1950-2015. Monthly circulation indices from NOAA were used in this analysis which resulted in a shorter historic period than was used in Papers 1-3. The period 1950-2015 is the longest time overlap between the NOAA circulation index and CEH datasets.

The effect of each circulation was explored both individually, using monthly univariate regression, and in combination using multiple regression. These analyses highlight the influence of each circulation and establish that the NAO only partially explains precipitation variability – especially in the southern regions and during the summer months, where circulations such as the EA also have an importance influence. In the majority of regions R^2 values of the multivariate model considering all circulations was considerably higher (R^2=0.6-0.8) than the comparative univariate models

This work represented the first high resolution analysis quantifying the influence of a range of atmospheric circulations on rainfall, highlighting that there is significant explanatory value in looking beyond the NAO when seeking to understand hydroclimatic variability in Great Britain.

5. **Assess the explanatory potential of atmospheric circulation combinations for the British hydroclimate and explore the implications for water/environmental management decision making.**

Paper 4 concludes that by looking at a range of different atmospheric circulations we may be able to explain precipitation variability more accurately. The regression analysis undertaken highlights the NAO and EA as being the primary and secondary influences. Papers 5 and 6 build on this understanding and present new evidence of the combined effect of the NAO and EA on monthly precipitation (Paper 5) and drought conditions (Paper 6).

Paper 5 sought to identify the effect of the NAO and EA (and their interaction) on monthly rainfall patterns across Great Britain by using high resolution datasets to map NAO/EA spatio-temporal rainfall signatures across a 65-year period (1950-2015). These analyses revealed key patterns in the spatio-temporal influence of each circulation. In the winter months the NAO was found to have a strong influence on rainfall and extremes in the north-western regions, whilst in the southern and central regions stronger EA-rainfall relationships were present (r=0.4-0.8). The paper also explored how rainfall patterns vary when the NAO and EA are in the same/opposing phase. Notably, in the summer months opposite phases of the NAO and EA resulted in stronger and spatially consistent wet/dry signatures (SPI +/- 1.5).

Importantly the findings of this work suggest that both the NAO and EA have a prominent influence on regional rainfall distribution and volume in Great Britain, concluding that accounting for both circulations may lead to an improved understanding of spatial distributions of monthly precipitation.

Paper 6 continues to develop the high resolution understanding of the individual and combined influence of the NAO and EA by exploring circulation-drought relationships at a catchment scale. In this paper an assessment of both meteorological (SPI) and hydrological (SSI) droughts was undertaken. This represented the first study quantifying the influence of both circulations on drought, at a monthly scale, across a large number of catchments (n=291).

Through a convergence of evidence from correlation, quantile regression and an analysis of drought frequency/severity under different NAO/EA phase combinations, three observations were made. Firstly, this work found that the NAO and EA exert strong influences on drought during winter. However, as with the rainfall signatures from Paper 5, there is spatial variability in the relative influence of the NAO and EA; with the NAO having a stronger north-west influence, and the EA having a stronger influence in the southern and central regions. Secondly, this work found less distinctive spatial differences during summer, and a higher probability of drought conditions under NAO+ phases. However, the severity of summer drought is partially dependent on the phase of the EA as concurrent opposing phases of the NAO/EA produced more extreme conditions. For example in the majority of case study catchments NAO+/EA- concurrent phases are associated with >50% of severe meteorological drought occurrences (SPI<-1.5).

Figures 1 and 2 synthesise the key spatial signatures of the NAO and EA across a range of scales used variably in the six papers presented in this thesis (Met Office Climate Districts, IHU Areas and Catchments) for the winter (DJF) and summer (JJA) months between 1950-2015. They highlight that both the NAO and EA have an impact on precipitation and river flows which varies across space and time.

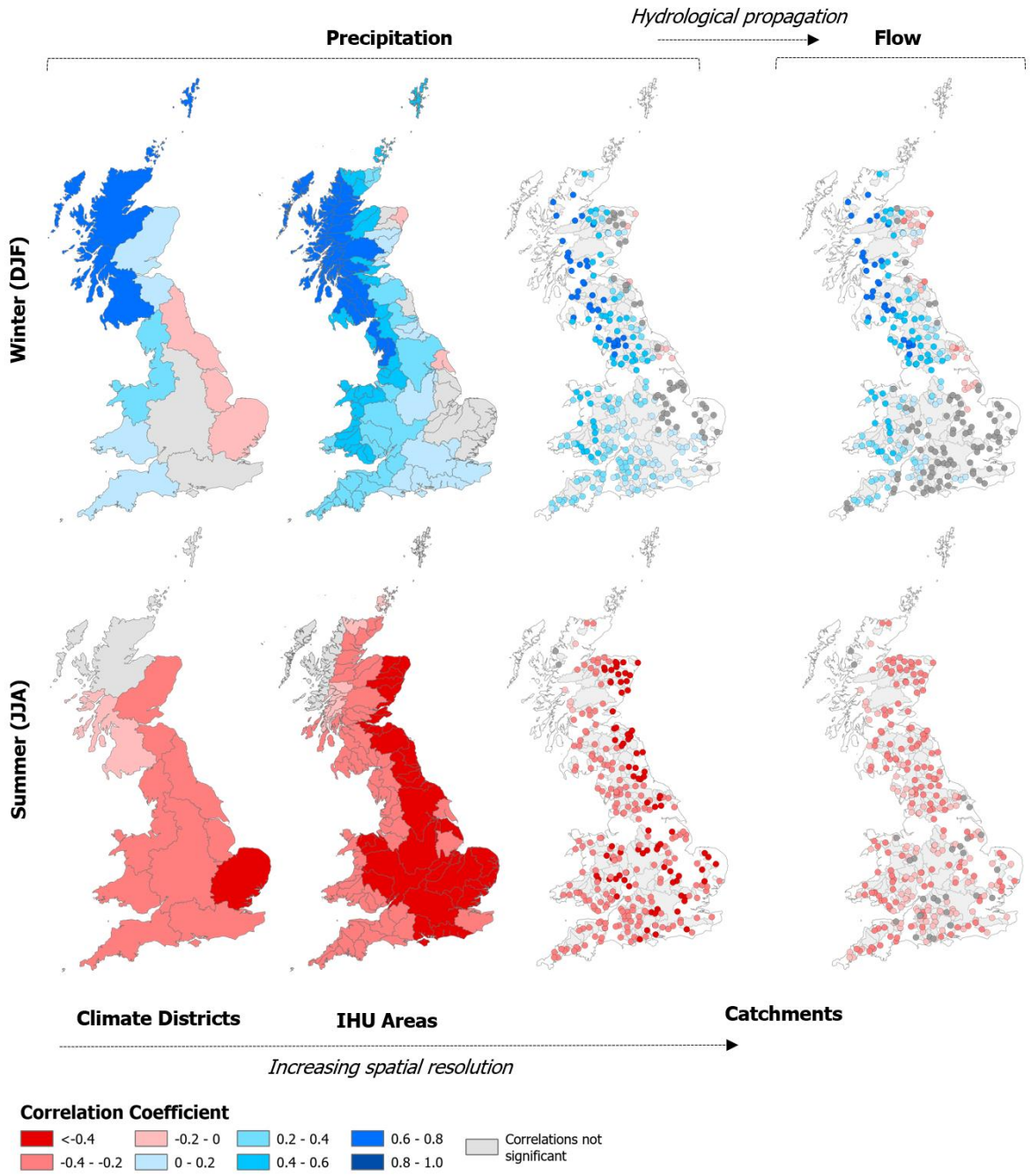

***Figure 1**: Summary of the relationship between the NAO and precipitation (SPI-1) and flow (SSI-1) for the winter and summer months across a range of scales. To produce this figure Spearman correlations were calculated between the NOAA NAO index and SPI-1 for each spatial unit between 1950-2015. Correlations not significant following FDR p-value adjustment are not shown (see details below).*

During the winter months the NAO has a spatially distinctive association with precipitation across scales. Stronger positive correlations occur in the north-west and weaker (sometimes negative/non-significant) correlations are found in the south in winter. In the north-western catchments these rainfall deviations propagate to flows. Meanwhile in southern catchments a greater number of non-significant correlations are found due to the moderating effect of catchment characteristics (see Paper 2). During the summer months the NAO has a more spatially consistent negative association with precipitation across spatial scales, which as in the case in winter variably propagates to flows.

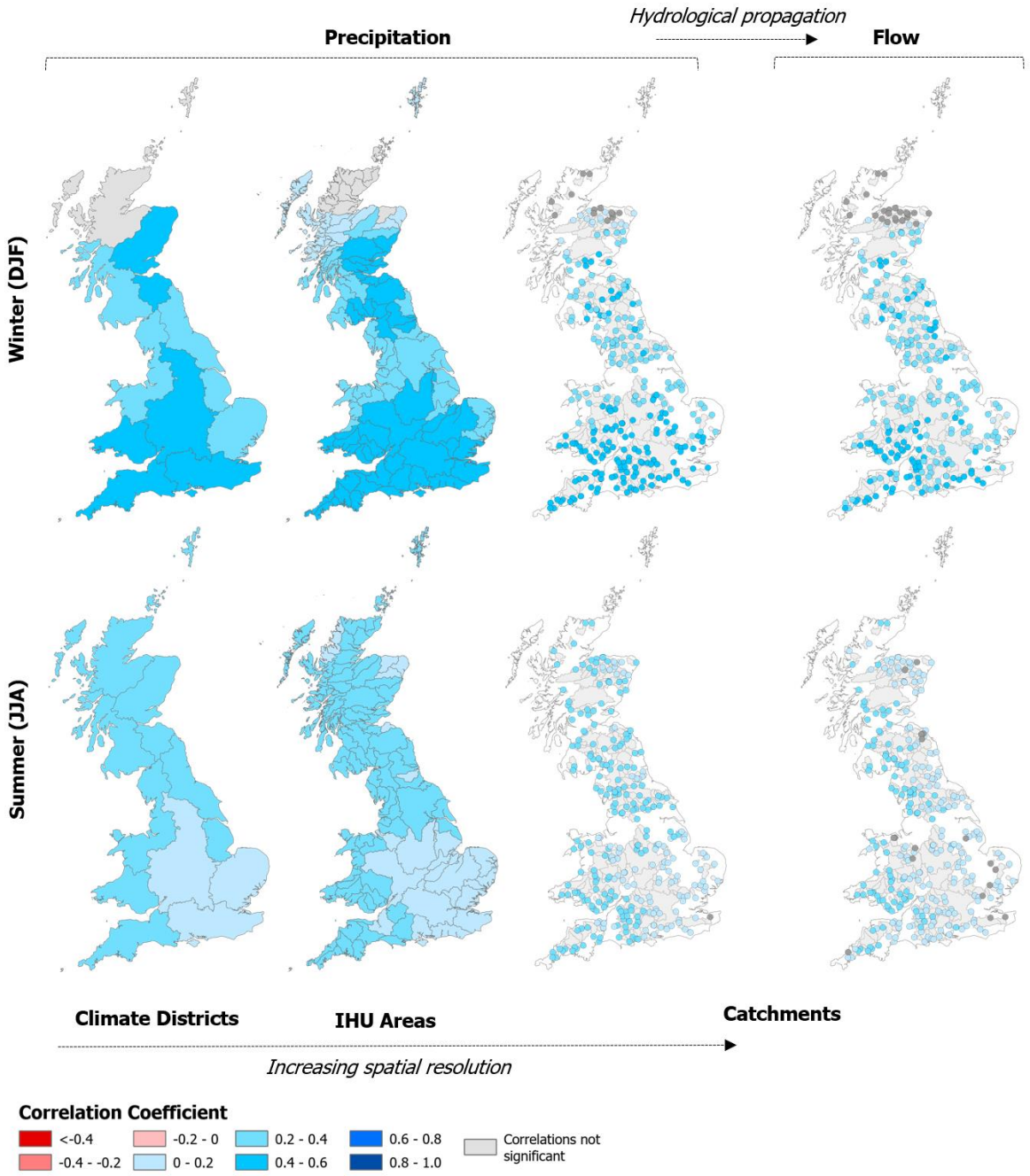

***Figure 2**: Summary of the relationship between the EA and precipitation (SPI-1) and flow (SSI-1) for the winter and summer months across a range of scales. To produce this figure Spearman correlations were calculated between the NOAA EA index and SPI-1 for each spatial unit between 1950-2015. Correlations not significant following FDR p-value adjustment are not shown (see details below).*

Correlations between the EA and precipitation and flows generally remain positive across the various spatial and temporal scales shown in Figure 2. In the winter months these are typically stronger in the southern and central regions of Great Britain. However during summer correlations are more consistent and generally moderately weaker than during winter. As with the NAO flow signatures in Figure 1 some EA-rainfall signatures do not propagate to flows for some catchments in the central, southern and eastern regions, which is likely produced by a moderating effect of catchment characteristics.

The signatures shown in Figures 1 and 2 have potential implications for the inclusion of atmospheric circulation indices in water resource and environmental management as seasonal forecasts of atmospheric circulations have potential to aid in decision making practices (Wilby et al. 2004). Research into the development of weather generators for water companies has included both winter and summer indices for the NAO, and also the EA index (Serinaldi & Kilsby 2012; Dawkins et al. 2022).

Our ability to predict the winter NAO in advance has continuously improved (Athanasiadis et al. 2020; Smith et al. 2020). However, variability in NAO-rainfall signatures (Paper 3) suggest that NAO forecasts alone may not be enough to accurately predict regional rainfall (Hall & Hanna 2018). Whilst NAO forecasts may by useful for the north-western areas during winter, they are likely to be less so in the south. Papers 4-6 highlight that the EA might, to an extent, better explain precipitation variability in these regions, and would be a more useful climate predictor. EA indices might therefore be a useful addition to regional hydrometeorological forecasting. In a positive development in this regard, Thornton et al. (2023) recently reported that the EA may be predictable in late autumn/early winter. Combined improved predictive skill for both the NAO and EA might have potential benefits and applications in water resource management practice (Table 2).

Table 2: Summary of findings which have potential water resource management implications.

Region	Winter	Summer
North-West	• The phase and strength of the NAO has a strong association with precipitation and flows (in steep and impermeable catchments) and therefore has a strong influence on water resources in the NW. • NAO+/- results in significant wet/dry conditions and high/low flows. • The EA has a weak/non-significant influence on water resources.	• The effect of the NAO in the NW is weaker than during winter and therefore has a lesser influence on water resources. • The EA also has a weak influence on water resources.
Midlands	• The NAO and EA have a moderately strong relationship with rainfall which generally propagates to flow.	• NAO/EA rainfall influence is stronger than the flow relationship. Persistent NAO/EA phases at the seasonal/annual scale may therefore be required for flow deviations and a greater impact on water resources. • NAO+/- results in dry/wet conditions and low/high (inverse to the relationship in the NW during winter). • Whilst the NAO is the primary influence, the phase of the EA can enhance/moderate the severity of dry conditions (Paper 6).
East Coast	• The NAO has a weak/non-significant influence on water resources. • The EA has a moderately strong association with precipitation and flow potentially indicating its greater influence on water resources.	
Central and South-East	• The NAO has a weak association with precipitation. Propagation to flow is limited by catchment characteristics (e.g. permeable geology and flat terrain).	

	Persistent strong NAO phases (seasonal-annual scales) may have a more notable influence on water resources. • EA has a strong association with precipitation and flows suggesting a greater influence on water resources than the NAO at a monthly scale. • EA+/- results in wet/dry conditions.	
South-West	• Both the EA and NAO have a moderately strong relationship with rainfall which generally propagates to flow. • Both circulations may therefore have an influence on water resources at the monthly scale. • Circulation +/- phases results in wet/dry conditions.	

However, NAO predictive skill has only improved during its stronger winter phases and predictions at a monthly timescale represent a current predictability gap (Kent et al. 2022). Further whilst have improvements in EA prediction have been recently reported, climate models currently underestimate the strength and predictability of the EA (Thornton et al. 2023). Dawkins et al. (2022) also note a limitation of their rainfall generator, which includes the NAO and EA as climatic drivers, is the use of observed rather than forecasted circulation indices.

These current limitations of circulation forecasting have implications for the inclusion of atmospheric circulation indices in water management practices. This is especially true in the southern, central and eastern regions where this research clearly demonstrates the effect the EA has on meteorological and, more variably depending on catchment characteristics, hydrological conditions, particularly during summer where the phase of the EA can influence drought severity driven by NAO+ conditions. This research has also highlighted that exploring signatures at a monthly scale is important given intra-seasonal variability, suggesting that the current monthly-scale NAO predictability gap (Kent et al. 2022) mentioned above is limiting from a practical perspective.

The conclusions presented regarding the potential of including circulation forecasts in water management supports the findings of Hall and Hanna (2018), who suggest that currently even highly accurate sole NAO forecasts might have a limited role in water management decision making, and Comas-Bru and McDermott (2014), who propose by looking at the NAO and EA in combination allows us to more accurately be able to explain (hydro)climatic variability.

Additional Analysis

This section presents the results of additional analysis not published in one of the research papers presented in this Thesis, but which do however compliment the analysis and help to address the aims and objectives of the research.

Correlation Significance Analysis

Additional analysis explored the statistical significance of the correlations reported in Papers 1,2,5 and 6. To account for the possibility of Type I errors influencing the results the False Discover Rate (FDR) p-value correction was undertaken for the NAO and EA correlations reported in Figure 2 of Paper 5 (following the method of Benjamini-Hochberg (1995)). An FDR of 0.2 was used in this analysis. The FDR method was used rather than the more traditional Bonferroni correction as FDR is less conservative and results in the removal of fewer significant results (Haynes 2013). This analysis is shown in Figures 3 and 4. Any IHU areas not meeting the FDR adjusted significance level are not mapped.

Figures 3 and 4 show that for most months' correlations between the NAO/EA and SPI remain significant with the FDR adjusted p-value filter (i.e. where IHU areas not meeting the significance threshold are not mapped). The distinctive seasonality in the correlation strength and direction noted above (Figures 1 and 2) remain – for example the strong positive winter correlation with the NAO in the north-western regions and the generally consistent positive relationship between the EA and SPI across most of the country throughout the year. The use of the FDR adjusted p-value does result in some months showing few significant correlations between the circulations and monthly SPI, such as March and May for the NAO correlations and June and July for the EA. However, this does not significantly alter the conclusions in Papers 1,2,5 and 6.

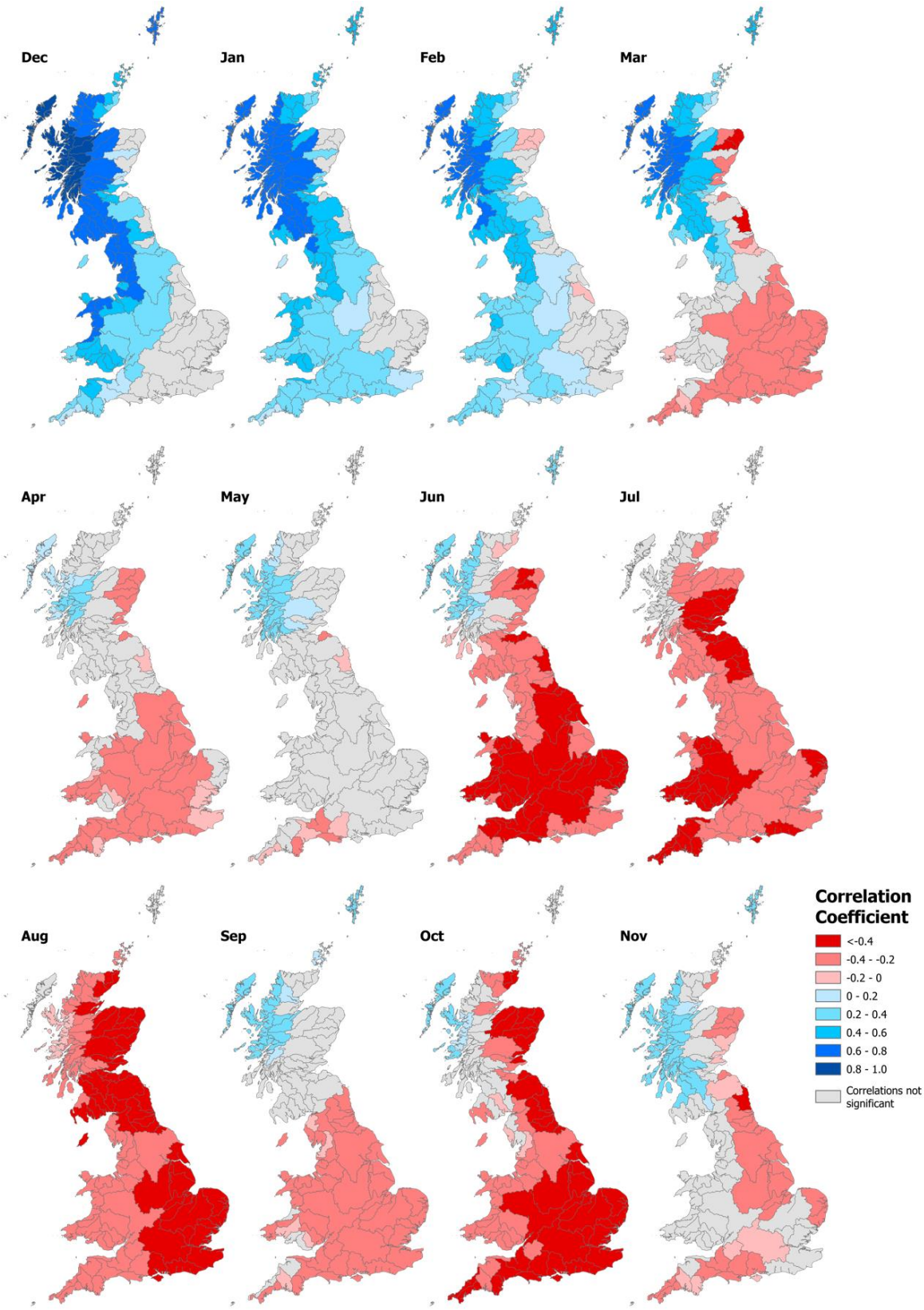

Figure 3: Monthly correlation coefficients for the period January 1950–December 2015 between the NOAA NAO teleconnection index and IHU SPI-1 values. Correlations which do not meet the FDR correction significance test are not mapped (grey IHU areas).

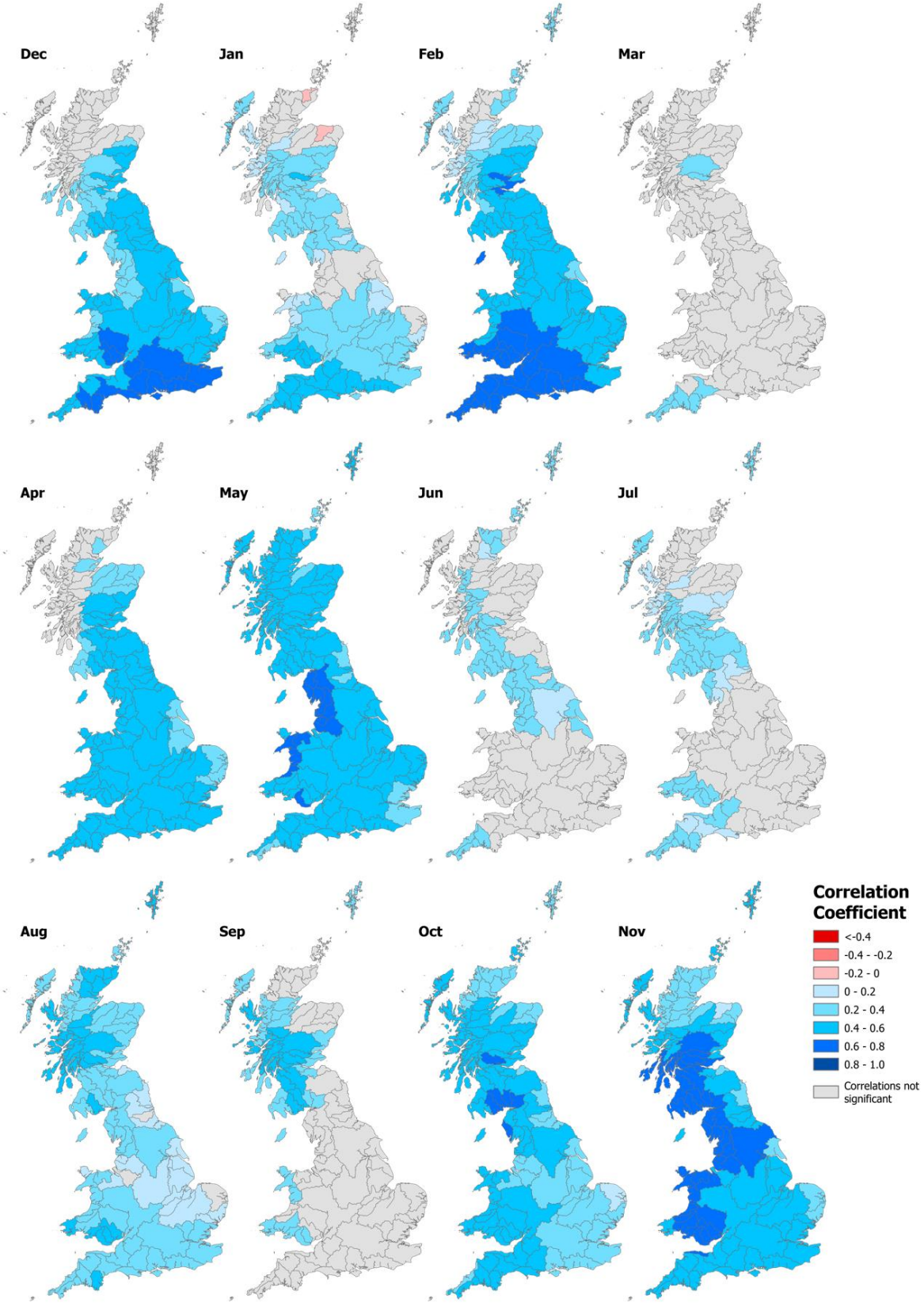

Figure 4: *Monthly correlation coefficients for the period January 1950–December 2015 between the NOAA EA teleconnection index and IHU SPI-1 values. Correlations which do not meet the FDR correction significance test are not mapped (grey IHU areas).*

Stationarity Analysis

Additional analysis has also been undertaken to explore the extent to which the correlation coefficients between the NAO and EA are stationary (i.e., consistent over time). To explore these temporal trends correlation coefficients have been mapped at decadal intervals between the NAO/EA and SPI for the IHU Areas. This analysis is presented in Appendix A.

The time series correlations shown in Appendix A generally show that in most instances where significant correlations exist (after FDR p-value adjustment) the strength and direction of the relationship between the NAO/EA and IHU Area SPI-1 remains relatively consistent over time. For example in Figure A1 positive relatively strong correlations exist between the NAO and SPI-1 in north-west Scotland during winter, and in Figure A3 negative correlations persist over time in the more southern regions. Likewise for the EA, there are temporally consistent positive correlations between the NOAA EA index and SPI-1 (Figures A5-A8).

Potential Uncertainties

This section highlights some of the potential uncertainties arising in the analyses presented in the six papers. Table 3 outlines sources of uncertainty and provides an assessment of the potential impact this has on the results of this research.

***Table 3**: Sources of potential uncertainty in this research.*

Factor	Assessment	Potential Uncertainty
Dataset Uncertainties		
Gridded Estimates of Aerial Rainfall (GEAR) (Tanguy et al. 2016)	Medium impact	• GEAR is an interpolated dataset and so the accuracy of the modelled estimates is sensitive to the number of, and distance between, observed rainfall values. If a given 1km pixel is >100km from an observation, then no interpolated value is published (Tanguy et al. 2016). • As an estimate of the quality of the modelled estimate a distance grid is provided alongside the GEAR rainfall estimates (Keller et al. 2015). • To assess the impact of this the distance grids for from 1900-2015 are presented in Appendix B at 25-year intervals. These show that rainfall grids pre-1925 have a higher number of missing estimates due to the 100km threshold being exceeded. This is largely confined to northern/western Scotland. Post-1925 the number of observations increases, and later in the time series the majority of Great Britain has a low distance to the closest rainfall observation decreasing the level of uncertainty. • This has been rated as medium impact due to the missing observations in the earlier rainfall grids, which increase uncertainty in the earlier analyses presented in Paper 1. Paper 5 also uses GEAR but from 1950 onwards where the number of missing observations is very low.

Gridded Standardised Precipitation Index (SPI) (Tanguy et al. 2017)	Low impact	• As the SPI is calculated using the Met Office rainfall grids, there is less historic variability in the interpolation process due to the addition of a greater number of historic rainfall records: the Met Office 5km rainfall grids are a combination of UKCP09 data (1910-1959 and 2001-2011), Met Office daily grids (1960-2000), Met Office updates (2012-2015) and new data from the Met Office recovered as part of the Historic Droughts project (1862-1909) (Tanguy et al. 2017). • Rated as low impact due to the increased number of observations in the early years of analysis presented in Papers 1-3 (1900 onwards).
Historic Modelled Daily Flows for Great Britain (Smith et al. 2018)	Low-medium impact	• The historic daily flows used in this research were generated by the GR4J model and have been found to provide good flow representations (Smith et al. 2019). • To assess this in the context of this research additional analysis was undertaken to compare observed flows from the NRFA for the nine case study catchments used in Paper 6. • For each catchment flow duration curves were created showing the observed flow (Appendix C), the best performing model run of the 500 ensembles (used in this research) and the minimum/maximum flow values from across the 500 ensembles. • This additional analysis highlights that the historic GR4J modelled flows provide a good representation of the flows in the catchment. However model performance appears to be consistently poorer for higher/peak flows across the nine catchments (<5th percentile). • Uncertainty has been assessed as low-medium impact in relation to the use of this dataset to derive NAO-flow signatures as general flow representation is good. However, for any additional research exploring peak flow-circulation relationships further assessment would be needed regarding the suitability of the GR4J modelled flows.
Standardised Streamflow Index (SSI) (Barker et al. 2018)	Low-medium impact	• The SSI data was derived using the best performing model run of the 500 ensembles from the historic modelled daily flows and so is subject to the same potential uncertainties.
Methodological Uncertainties		
Phase definition method	Medium-high impact	• Papers 1-3 used long historic time series of NAO Indices (1900-2015) from NCAR. As such the teleconnection phase definition approach used by Berton et al. (2017) (half the standard deviation plus/minus the long-term mean) was used. • Papers 4-6 drew on the NOAA circulation indices which have a shorter record length (1950-2015). When the Berton et al. (2017) approach was applied to this time series this resulted in some months with a limited number of observations. As such a

		threshold approach of -0.25 and 0.25 was used for each index to define negative and positive phases respectively. • The approach to defining positive and negative phases for each index is essentially arbitrary and there is no unform approach in the literature. • Using +/- 0.25 provided a relatively consistent sample for each month and phase combination (Figure 1 in Paper 5). • Further analysis could be undertaken to understand how the set threshold for phase definition influences the circulation-hydroclimate signatures. A higher threshold would strengthen the rainfall signatures, however based on current data would result in fewer observations for each NAO/EA monthly combination (histograms for the NOAA NAO and EA indices can be found in Appendix D).
Conceptualisation of spatial relationships	Low impact	• The spatial statistical approaches in Papers 3 and 6 require the definition of how features within the dataset are related spatially (for example neighbours can be defined within a fixed-distance or whether there is feature contiguity). • The decision on which spatial relationship approach to use in the calculation of these measures can have an impact on the subsequent results. • This has been rated as low impact however as guidance is provided by software developers on which spatial relationship definition to use for a given data structure (Esri 2022c).

Opportunities for Future Research

There are opportunities to continue to develop our understanding of the relationship between atmospheric circulations and hydroclimate in both Great Britain and across the North Atlantic/European region. Future research might have the following aims:

- Assess at a high spatio-temporal resolution the relationship between the NAO, EA and other circulations on peak and annual maximum flows. Given the higher error/uncertainty identified in the previous section for the historic flows derived from the GR4J model, other modelled flow datasets might be used for such research, for example flows from the DECIPHeR model (Coxon et al. 2019). The DECIPHeR model has performed well in the wetter north-western catchments of Britain (Coxen et al. 2019), which is significant given the strong regional NAO-flow relationships identified in this region. There may also be potential to draw on the CAMELS-GB database which collates observed flows alongside various meteorological variables for 671 British catchments (Coxon et al. 2020).
- Further assess the (non)stationarity in the relationships between atmospheric circulations and precipitation/flow, potentially employing methods reviewed by Slater et al. (2021).

Future work may investigate how the relationship between the NAO/EA and rainfall might have changed over time, especially given the winter EA index positive trend which has been found in some studies (Mikhailova & Yurovsky 2016).

- Assess the predictive value of atmospheric circulation indices for regional rainfall and flows.
- Evaluate the sensitivity of rainfall/flow relationships to different phase-definition approaches.
- Song et al. (2023) identified that westward movement of the NAO dipoles influences climate over mid-latitude Asia. Future work may assess the influence of the location and strength of the Icelandic Low and Azores High meridional dipoles across the year, using the space-time analyses from Paper 3 and 60km UKCP18 SLP data (Met Office Hadley Centre 2018a), or NCAR Reanalysis data (NCAR 2023), and how this influences UK/European climate.
- Assess how the interaction between the NAO and EA might affect NAO-snowfall/-wind relationships found in previous research (Spencer & Essery 2016; Zubiate et al. 2017), using UKCP18 gridded datasets (Met Office Hadley Centre 2019).
- Investigate the relationship between atmospheric circulations and storm surge simulation data from UKCP18 for coastal waters (Met Office Hadley Centre 2018b).
- Investigate the association with UK Hydroclimate and atmospheric-oceanic systems not considered in this research. For example, the El-Nino Southern Oscillation (ENSO) has been attributed to weather patterns around Britain (Wilby 1993) and has been found to potentially influence the phase of the NAO and Atlantic Multidecadal Oscillation (Zhang et al. 2019). Future research could explore whether ENSO is related to the EA and how these in combination (alongside the NAO) influence UK hydroclimate. This could be analysed through mediation analysis to explore whether the relationship between a given circulation and rainfall is influenced (mediated) by a secondary circulation index.

Additionally, future research might seek to explore how to effectively integrate atmospheric circulation index forecasts in water and environmental management to aid decision making processes (Wilby et al. 2004). However, at present there are limitations to pursuing this given the spatio-temporal variability in NAO rainfall signatures found in this research (Paper 3) and the lack of accurate monthly teleconnection forecasts for multiple circulations (Papers 4-6). Nevertheless, recent advances in the predictability of the NAO and EA (Smith et al. 2020; Thornton et al. 2023) show positive progress in this area, and if forecasting research continues to improve there may be greater opportunities to incorporate circulation indices in water management in the future.

References

Abiy, A.Z., Melesse, A.M. & Abtew, W. (2019). Teleconnection of regional drought to ENSO, PDO and AMO: Southern Florida and the Everglades. *Atmosphere*, Vol.10(6), 295.

Afzal, M., Gagnon, A.S. & Mansell, M.G. (2015). Changes in the variability and periodicity of precipitation in Scotland. *Theoretical and Applied Climatology*, 119, 135-159.

Almendra-Martín, L., Martinez-Fernandez, D., Piles, M., Gonzalez-Zamora, A., Benito-Verdugo, P. & Gaona, J. (2022). Influence of atmospheric patterns on soil moisture dynamics in Europe. *Science of the Total Environment*, Vol.846, 157537.

Amini, M., Ghadami, M., Fathian, F. & Modarres, R. (2020). Teleconnections between oceanic-atmospheric indices over Iran using quantile regressions. *Hydrological Sciences Journal*, Vol.65, 2286-2295.

Athanasiadis., P.J., Yeager, S., Kwon, Y-O., Bellucci, A., Smith, D.W. & Tibaldi, S. (2020). Decadal predictability of North Atlantic blocking and the NAO. *Npj Climate and Atmospheric Science*, Vol.3(20).

Bachmair, S., Stahl, K., Collins, S., Hannaford, J., Acreman, M., Svoboda, M., Knutson, C., Smith, K.H., Wall, N., Fuchs, B., Corssman, N.D. & Overton, I.C. (2016). Drought indicators revisited: The need for wider consideration of environment and society. *WIREs Water*, Vol.3, 516-536.

Baker, L.H., Shaffrey, L.C. & Scaife, A.A. (2017). Improved seasonal predication of UK regional precipitation using atmospheric circulation. *International Journal of Climatology*, Vol.35(51), 437-453.

Balling, R.C. Jr. & Goodrich, G.B. (2011). Interannual variations in the local spatial autocorrelation of tropospheric temperatures. *Theoretical and Applied Climatology*, Vol.103, 451-457.

Barker, L.J., Hannaford, J., Chiverton, A. & Svensson, C. (2016). From meteorological to hydrological drought using standardised indicators. *Hydrology and Earth System Sciences*, Vol.20, 2483-2505.

Barker, L.J., Smith, K.A., Svensson, C., Tanguy, M. & Hannaford, J. (2018). Historic Standardised Streamflow Index (SSI) using Tweedie distribution with standard period 1961-2010 for 303 UK catchments (1891-2015). *NERC Environmental Information Data Centre*, https://doi.org/10.5285/58ef13a9-539f-46e5-88ad-c89274191ff9.

Barker, L.J., Hannaford, J., Parry, S., Smith, K.A., Tanguy, M. & Prudhomme, C. (2019). Historic hydrological droughts 1891-2015: Systematic characterisation for a diverse set of catchments across the UK. *Hydrology and Earth System Sciences*, Vol.23, 4583-4602.

Barnston, A.G. & Livezey, R.E. (1987). Classification, seasonality and persistence of low-frequency atmospheric circulation patterns. *Monthly Weather Review*, Vol.115, 1083-1126.

Bednorz, E., Czernecki, B., Tomczyk, A.M. & Półrolniczak, M. (2018). If not NAO then what? Regional circulation patterns governing summer air temperatures in Poland. *Theoretical and Applied Climatology*, Vol.136, 1325-1337.

Bednorz, E. & Tomczyk, A.M. (2021). Influence of macroscale and regional circulation patterns on low- and high-frequency sea level variability in the Baltic Sea. *Theoretical and Applied Climatology*, Vol.144, 115-125.

Bell, V.A., Davies, H.N., Kay, A.L., Brookshaw, A. & Scaife, A.A. (2017). A national-scale seasonal hydrological forecast system: Development and evaluation over Britain. *Hydrology and Earth System Sciences,* Vol.21, 4681-4691.

Benjamini, Y. & Hochberg, Y. (1995). Controlling the false discovery rate: A practical and powerful approach to multiple testing. *Journal of the Royal Statistical Society: Series B (Methodological)*, Vol.57(1). 289-300.

Beranová, R. & Huth, R. (2008). Time variations of the effects of circulation variability modes on European temperature and precipitation in winter. *International Journal of Climatology*, Vol.28(2), 139-158.

Berton, R., Driscoll, C.T. & Adamowski, J.F. (2017). The near-term prediction of drought and flooding conditions in the north-eastern United States based on extreme phases of AMO and NAO. *Journal of Hydrology*, Vol.553, 130-141.

Bonsccorso, B., Cancelliere, A. & Rossi, G. (2015). Probabilistic forecasting of drought class transitions in Sicily (Italy) using Standardised Precipitation Index and North Atlantic Oscillation Index. *Journal of Hydrology,* Vol.526, 136-150.

Bower, D., Hannah, D.M. McGregor, G.R. (2004). Techniques for assessing the climate sensitivity of river flow regimes. *Hydrological Processes*, Vol.18, 2515-2543.

Brayshaw, D.J., Hoskins, B. & Black, E. (2010). Some physical drivers of changes in the winter storm tracks over the North Atlantic and Mediterranean during the Holocene. *Philosophical Transactions of the Royal Society of London A: Mathematical, Physical and Engineering Sciences*, Vol.366(1931), 5185-5223.

Bueh, C. & Nakamura, H. (2007). Scandinavian pattern and its climatic impact. *Quarterly Journal of the Royal Meteorological Society*, Vol.133, 2117-2131.

Burningham. H. & French, J. (2013). Is the NAO winter index a reliable proxy for wind climate and storminess in northwest Europe? *International Journal of Climatology*, Vol. 33, 2036-2049.

Burt, T. & Howden, N. (2013). North Atlantic Oscillation amplifies orographic precipitation and river flow in upland Britain. *Water Resources Research*, Vol.49, 3504-3515.

Caroletti, G.N., Coscarelli, R. & Caloiero, T. (2021). A sub-regional approach to the influence analysis of teleconnection patterns in Calabria (southern Italy). *International Journal of Climatology*, Vol.41, 4574-4586.

Casanueva, A., Rodriguez-Puebla, C., Frias, M.D. & Gonzalez-Reviriego, N. (2014). Variability of extreme precipitation over Europe and its relationships with teleconnection patterns. *Hydrology and Earth System Sciences*, Vol.18, 709-725.

Chen, M., Papadikis, K. & Jun, C. (2021). An investigation on the non-stationarity of flood frequency across the UK. *Journal of Hydrology*, Vol.597, 126309.

Chiverton, A., Hannaford, J., Holman, I., Corstanje, R., Prudhomme, C., Bloomfield, J. & Hess, T.M. (2015). Which catchment characteristics control the temporal dependence structure of daily river flows. *Hydrological Processes*, Vol.29, 1353-1369.

Chun, K.P., Dieppois, B., Qing, H., Sidibe, M., Eden, J., Paturel, J.-E., Mahe, H., Rouche, N., Klaus, J. & Conway, D. (2021). Identifying drivers of streamflow extremes in West Africa to inform a nonstationary predication model. *Weather and Climate Extremes*, Vol.33, 100346.

Clark, R.T., Bett, P.E., Thornton, H.E. & Scaife, A.A. (2017), Skillful seasonal predictions for the European energy industry. *Environmental Research Letters*, Vol.12, 024002.

Comas-Bru, L. & McDermott, F. (2014), Impacts of the EA and SCA patterns on European twentieth century NAO-winter climate relationship. *Quarterly Journal of the Royal Meteorological Society*, Vol.140, 354-363.

Coxon G., Freer, J., Lane, R., Dunne, T., Knoben, W.J.M., Howden, N.J.K., Quinn, N., Wagener, T. & Woods, R. (2019). DECIPHeR v1: Dynamic flexEs and ConnectIvity for Predications of HydRology. *Geoscientific Model Development*, Vol.12(6), 2285-2306.

Coxon, G., Addor, N., Bloomfield, J., Freer, J., Fry, M., Hannaford, J., Howden, N.J.K., Lane, R., Medlinda, L., Robinson, E.L., Wagener, T. & Woods, R. (2020). CAMELS-GB: Hydrometeorological time series and landscape attributes for 671 catchments in Great Britain. *Earth System Science Data*, Vol.12(4), 2459-2483.

Dawkins, L.C., Osborne, J.M., Economou, T., Darch, G.J.C. & Stoner, O.R. (2022). The Advanced Meteorology Explorer: A novel stochastic gridded daily rainfall generator. *Journal of Hydrology*, Vol.607, 127478.

De Luca, P., Hillier, J.K., Wilby, R.L., Quinn, N. & Harrigan, S. (2017). Extreme multi-basin flooding linked with extra-tropical cyclones. *Environmental Research Letters*, Vol.12, 114009.

del Rio, S., Herrero, L., Pinto-Gomes, C. & Penas, A. (2011). Spatial analysis of mean temperature trends in Spain over the period 1961-2006. *Global Planetary Change*, Vol.78(102), 65-75.

Dhurmea, K.R., Boojhawon, R. & Rughooputh, S.D.D.V. (2019). A drought climatology for Mauritius using the standardized precipitation index. *Hydrological Sciences Journal*, Vol.64(2), 227-240.

Donegan, S., Murphy, C., Harrigan, S., Broderick, C., Golian, S., Knight, J., Matthews, T., Prudhomme, C., Quinn, D.F., Scaife, A.A., Stringer, N. & Wilby, R.L. (2021). Conditioning ensemble streamflow prediction with the North Atlantic Oscillation improves skill at longer lead in times. *Hydrology and Earth System Sciences*, Vol.25, 4159-4183.

Esri (2020). *Space-time cluster analysis* [ONLINE]. Available at: https://pro.arcgis.com/en/pro-app/tool-reference/spatial-statistics/space-time-analysis.htm. Accessed 06/08/2020.

Esri (2021). Hot Spot Analysis (Getis-Ord Gi*) [ONLINE]. Available at: https://pro.arcgis.com/en/pro-app/latest/tool-reference/spatial-statistics/hot-spot-analysis.htm. Accessed 04/02/2021.

Esri (2022a). Similarity Search [ONLINE]. Available at: https://pro.arcgis.com/en/pro-app/latest/tool-reference/spatial-statistics/similarity-search.htm. Accessed 07/05/2021.

Esri (2022b). Spatial autocorrelation (Global Morans I) [ONLINE]. Available at: https://pro.arcgis.com/en/pro-app/latest/tool-reference/spatial-statistics/spatial-autocorrelation.htm. Accessed 11/05/2021.

Esri (2022c). Modelling spatial relationships [ONLINE]. Available at: https://pro.arcgis.com/en/pro-app/latest/tool-reference/spatial-statistics/modeling-spatial-relationships.htm#GUID-729B3B01-6911-41E9-AA99-8A4CF74EEE27. Accessed 24/07/2021.

Folland, C.K., Knight, J., Linderholm, H.W., Fereday, D., Ineson, S. & Hurrell, J.W. (2009). The summer North Atlantic Oscillation: past, present and future. *Journal of Climate*, Vol.22, 1082-1103.

Folland, C.K., Hannaford, J., Bloomfield, J., Kendon, M., Svensson, C., Marchant, B.P. & Wallace, E. (2015). Multi-annual droughts in the English lowlands: A review of their

characteristics and climate drivers in the winter half-year. *Hydrology and Earth System Sciences*, Vol.19, 2353-2375.

Fowler, H.J. & Kilsby, C.G. (2002). Precipitation and the North Atlantic Oscillation: A study of climatic variability in Northern England. *International Journal of Climatology*, Vol.22, 843-866.

Gao, N., Bueh, C., Xie, Z. & Gong, Y. (2019). A novel identification of the Polar/Eurasia Pattern and its weather impact in May. *Journal of Meteorological Research*, Vol.33, 810-825.

Garner, G., Hannah, D. & Watts, G. (2017). Climate change and water in the UK: recent scientific evidence for past and future change. *Progress in Physical Geography*, Vol.41(2), 154-170.

Getis, A. & Ord, J.K. (2010). The Analysis of Spatial Association by Use of Distance Statistics. *Geographical Analysis*, Vol.24, 189-206.

Hall, R.J. & Hanna, E. (2018). North Atlantic circulation indices: links with summer and winter temperature and precipitation and implications for seasonal forecasting. *International Journal of Climatology*, Vol.38(S1), 660-677.

Hannaford, J., Lloyd-Hughes, B., Keef, C., Parry, S. & Prudhomme, C. (2011). Examining the large-scale spatial coherence of European drought using regional indicators of precipitation and streamflow drought. *Hydrological Processes*, Vol.25, 1146-1162.

Hassan, W.U. & Nayak, M.A. (2021). Global teleconnections in droughts caused by oceanic and atmospheric circulation patterns. *Environmental Research Letters,* Vol.16, 014007.

Hayes W. (2013). Benjamini–Hochberg Method. In: Dubitzky, W., Wolkenhauer, O., Cho, KH., Yokota, H. (eds) *Encyclopedia of Systems Biology*. Springer, New York, NY. https://doi.org/10.1007/978-1-4419-9863-7_1215.

Herceg-Bulić, I. & Kucharski, F. (2014). North Atlantic SSTs as a link between wintertime NAO and the following spring climate. *Journal of Climate*, Vol.27(1), 186-201.

Huang, S., Li, P., Huang, Q., Leng, G., Hou, B. & Ma, L. (2017). The propagation from meteorological to hydrological drought and its potential influence factors. *Journal of Hydrology*, Vol.547, 184-195.

Hurrell, J.W. (1995). Decadal trends in the North Atlantic Oscillation: Regional temperatures and precipitation. *Science*, Vol.269, 676-679.

Hurrell, J.W. & Deser, C. (2009). North Atlantic climate variability: the role of the North Atlantic Oscillation. *Journal of Marine Systems*, Vol.78, 28-41.

Hurrell, J.W. & Van Loon, H. (1997). Decadal variations in climate associated with the North Atlantic Oscillation. *Climatic Change*, Vol.36(3-4), 301-326.

Hurrell, J.W., Kushnir, Y., Ottersen, G. & Visbeck, M. (2003). An overview of the North Atlantic Oscillation. In Hurrell, J.W., Kushnir, Y., Ottersen, G. & Visbeck, M. (eds.), *The North Atlantic Oscillation: Climate Significance and Environmental Impact*. AGU Geophysical Monograph Series, Vol.134, American Geophysical Union: Washington.

Ionita, M. (2014). The impact of the East Atlantic/Western Russia pattern on the hydroclimatology of Europe from mid-winter to late spring. *Climate*, Vol.2, 295-309.

Irannezhad, M., Torabi Haghigi, A., Chen, D. & Kløve, B. (2015). Variability in dryness and wetness in central Finland and the role of teleconnection patterns. *Theoretical and Applied Climatology*, Vol.122(3-4), 471-486.

Jones, M.R., Blenkinsop, S., Fowler, H.J. & Kilsby, C.G. (2014). Objective classification of extreme rainfall for the UK and updated estimates of trends in regional extreme rainfall. *International Journal of Climatology*, Vol.34, 751-765.

Jung, T., Hilmer M., Ruprecht, E., Kleppek, S., Gulev, S.K. & Zolina, O. (2003). Characteristics of the recent eastward shift of interannual NAO variability. *Journal of Climate*, Vol.16, 3371-3382.

Keller, V.D.J., Tanguy, M., Prosdocimi, I., Terry, J.A., Hitt, O., Cole, S.J., Fry, M., Morris, D.G. & Dixon, H. (2015). CEH-GEAR: 1km resolution daily and monthly areal rainfall estimates for the UK for hydrological and other applications. *Earth Systems Science and Data*, Vol.7, 143-155.

Kendon, E.J., Roberts, N.M., Fowler, H.J., Roberts, M.J., Chan, S.C. & Senior, C.A. (2014). Heavier summer downpours with climate change revealed by weather forecast resolution model. *Nature Climate Change*, Vol.4, 570-576.

Kendon, M., McCarthy, M., Jevrejeva, S., Matthews, A. & Legg, T. (2018). State of the UK climate 2017. *International Journal of Climatology*, Vol.38(S2), 1-35.

Kent, C., Scaife, A.A. & Dunstone, N. (2022). What potential for improving sub-seasonal predications of the winter NAO. *Atmospheric Science Letters*, https://doi.org/10.1002/asl.1146.

Kingston, D.G., Lawler, D.M. & McGregor, G.R. (2006). Linkages between atmospheric circulation, climate and streamflow in the North Atlantic: Research prospects. *Progress in Physical Geography*, Vol.30(2), 143-174.

Kingston, D.G., McGregor, G.R., Hannah, D.M. & Lawler, D.M. (2007). Large-scale climatic controls on New England river flow. *Journal of Hydrometeorology*, Vol.8(3), 367-379.

Kingston, D.G., Hannah, D.M., Lawler, D.M. & McGregor, G.R. (2009). Climate-river-flow relationships across montane and lowland environments in northern Europe. *Hydrological Processes*, Vol.23, 985-996.

Kingston, D.G., Fleig, A.K., Tallaksen, L.M. & Hannah, D.M. (2013). Ocean-atmosphere forcing of summer streamflow drought in Great Britian. *Journal of Hydrometeorology*, Vol.14(1), 331-344.

Kingston, D.G., Stagge, J.H., Tallaksen, L.M. & Hannah, D.M. (2015). European-scale drought: understanding connections between atmospheric circulation and meteorological drought indices. *Journal of Climate*, Vol. 28(2), 505-516.

Kosanic, A., Harrison, S., Anderson, K. & Kavcic, I. (2014). Present and historical climate variability in South West England. *Climatic Change*, Vol.124, 221-237.

Kral, F., Fry, M. & Dixon, H. (2015). Integrated Hydrological Units of the United Kingdom. *NERC Environmental Information Data Centre.* https://doi.org/10.5285/f1cd5e33-2633-4304-bbc2-b8d34711d902.

Krichak, S.O. & Alpert, P. (2002). Decadal trends of main Eurasian oscillations and the Mediterranean precipitation. *Theoretical and Applied Climatology*, Vol.72, 209-220.

Krichak, S.O. & Alpert, P. (2005). Decadal trends in the East Atlantic-West Russian pattern and Mediterranean precipitation. *International Journal of Climatology*, Vol.25, 183-192.

Laize, C.L.R. & Hannah, D.M. (2010). Modification of climate-river-flow associations by basin properties. *Journal of Hydrology*, Vol.389(1-2), 186-204.

Lavers, D., Prudhomme, C. & Hannah, D.M. (2010). Large-scale climate, precipitation and British river flows: Identifying hydrological connections and dynamics. *Journal of Hydrology*, Vol.395(3-4), 242-255.

Lavers, D., Hannah, D.M. & Bradley, C. (2015). Connecting large-scale atmospheric circulation, river flow and groundwater levels in a chalk catchment in southern England. *Journal of Hydrology*, Vol.523, 179-189.

Lim, Y-K. (2015). he East Atlantic/West Russia (EA/WR) teleconnection in the North Atlantic: Climate impact and relation to Rossby wave propagation. *Climate Dynamics*, Vol.44, 3211-3222.

Ord, J.K. & Getis, A. A. (1995). Local Spatial Autocorrelation Statistics: Distributional Issues and an Application. *Geographical Analysis*, Vo.27, 286-306.

Maidens, A., Knight, J.R. & Scaife, A.A. (2021). Tropical and stratospheric influence in winter atmospheric circulation patterns in the North Atlantic sector. *Environmental Research Letters*, Vol.16, 024035.

McKee, T.B., Doesken, N.J. & Kleist, J. (1993). The relationship of drought frequency and duration to time scales. *Eighth Conference on Applied Climatology*, January 17-22 1993, Anaheim, California, USA.

Mehr, A.D., Sorman, A.U., Kahya, E. & Afshar, M.H. (2020). Climate change impacts on meteorological drought using SPI and SPEI: A case study of Ankara, Turkey. *Hydrological Sciences Journal*, Vol.65(2), 254-268.

Mellado-Cano, J., Barriopedro, D., Garcia-Herrera, R., Trigo, R.M. & Hernandez, A. (2019). Examining the North Atlantic Oscillation, East Atlantic Pattern jet variability since 1685. *Journal of Climate*, Vol.32, 6285-6298.

Mellado-Cano, J., Barriopedro, D., Garcia-Herrera, R., Trigo, R.M. (2020). New observation insights into the atmospheric circulation over the Euro-Atlantic sector since 1685. *Climate Dynamics*, Vol.54, 823-841.

Met Office (2016). *Is UKCP09 still an appropriate tool for Adaption Planning?* [ONLINE]. Available at: http://ukclimateprojections.metoffice.gov.uk/media.jsp?mediaid=88738&filetype=pdf. Accessed 03/05/2018.

Met Office Hadley Centre (2018a). *UKCP18 Global Projections at 60km Resolution for 1900-2100* [ONLINE]. Available at: https://catalogue.ceda.ac.uk/uuid/97bc0c622a24489aa105f5b8a8efa3f0. Accessed 31/03/2022.

Met Office Hadley Centre (2018b). UKCP18 Simulations of Sea Surface Elevation for UK Waters [ONLINE]. Available at: https://catalogue.ceda.ac.uk/uuid/5fcae68057ea43259d0a4530d34e4ba5?jump=related-anchor. Accessed 31/03/2022.

Met Office Hadley Centre (2019). UKCP18 Convection-Permitting Model Projections for the UK at 2.2km resolution [ONLINE]. Available at: https://catalogue.ceda.ac.uk/uuid/ad2ac0ddd3f34210b0d6e19bfc335539. Accessed 31/03/2022.

Mikhailova, N.V. & Yurovsky, A.V. (2016). The East Atlantic Oscillation: mechanism and impact on the European climate in winter. *Physical Oceanography*, Vol.2016, 25-33.

Moore, G.W.K., Pickart, R.S. & Renfrew, I.A. (2011). Complexities in the climate of the subpolar North Atlantic: A case study from the winter of 2007. *Quarterly Journal of the Royal Meteorological Society*, Vol.137, 757-767.

Moore, G.W.K. & Renfrew, I.A. (2012). Cold European winters: Interplay between the NAO and East Atlantic mode. *Atmospheric Science Letters*, Vol.13, 1-8.

Moore, G.W.K., Renfrew, I.A. & Pickart, R.S. (2013). Multidecadal variability of the North Atlantic Oscillation. *Journal of Climate*, Vol.26(8), 2453-2466.

Moulds, S., Slater, L.J., Dunstone, N.J. & Smith, D.M. (2022). Skillful decadal flood predication. *Geophysical Research Letters*, Vol.50(3), e2022GL100650.

Nagarajan, R. (2010). *Drought Assessment*, Springer; Science and Business Media.

National Center for Atmospheric Research (NCAR) (2020). Hurrell North Atlantic Oscillation (NAO) Index (PC-Based) [ONLINE]. Available at: https://climatedataguide.ucar.edu/climate-data/hurrell-north-atlantic-oscillation-nao-index-pc-based. Accessed 30/6/2020.

National Center for Atmospheric Research (NCAR) (2023). NCEP-NCAR Reanalysis 1 [ONLINE]. Available at: https://psl.noaa.gov/data/gridded/data.ncep.reanalysis.html. Accessed 25/02/2023.

NOAA (2021a) Climate Prediction Centre - Northern Hemisphere Teleconnections [ONLINE]. Available at: https://www.cpc.ncep.noaa.gov/data/teledoc/telecontents.shtml. Accessed 18th Jan 2022.

NOAA (2021b) Climate Prediction Centre – East Atlantic Pattern [ONLINE]. Available at: https://www.cpc.ncep.noaa.gov/data/teledoc/ea.shtml. Accessed 17th March 2021.

Onate-Valdivieso, F., Uchuari, V. & Onate-Paladines, A. (2020). Large-scale climate variability patterns and drought: A case study in South-America. *Water Resources Management*, Vol.34, 2061-2079.

Palin, E.J., Scaife, A.A., Wallace, E., Pope, E.C.D., Arribas, A. & Brookshaw, A. (2016). Skillful seasonal forecasts of winter disruption to the UK transport system. *Journal of Applied Meteorology and Climatology*, Vol.55, 325-344.

Parker, T., Woollings, T., Weisheimer, A., O'Reilly, C., Baker, L. & Shaffrey, L. (2019). Seasonal predictability of the winter North Atlantic Oscillation from a Jet Stream perspective. *Geophysical Research Letters*, Vol.46(16), 10159-100167.

Parry, S., Prudhomme, C., Wilby, R.L. & wood, P.J. (2016). Drought termination: concept and characterisation. *Progress in Physical Geography*. Vol.40(6), 743-767.

Phillips, I.D., McGregor, G.R., Wilson, C.J., Bower, D. & Hannah, D.M. (2003). Regional climate and atmospheric circulation controls on the discharge of two British rivers 1984-97. *Theoretical and Applied Climatology*, Vol.76, 141-164.

Pokorná, L. & Huth, R. (2015). Climate impacts of the NOA are sensitive to how the NAO is defined. *Theoretical and Applied Climatology*, Vol.119(3-4), 639-652.

Rodwell, M.J., Rowell, D.P. & Folland, C.K. (1999). Oceanic forcing of the wintertime North Atlantic Oscillation and European climate. *Nature*, Vol.398, 320-323.

Rodrigo, F.S. (2021). Exploring combined influences of seasonal East Atlantic (EA) and North Atlantic Oscillation (NAO) on the temperature-precipitation relationship in the Iberian Peninsula. *Geosciences*, Vol.11, 211.

Rogerson, P.A. (2014). *Statistics for Geographers* (4th Edition). SAGE Publications: London.

Rust, W., Holman, I., Corstanje, R., Bloomfield, J. & Cuthbert, M. (2018). A conceptual model for climatic teleconnection signal control on groundwater availability in Europe. *Earth-Science Reviews*, Vol.177, 164-174.

Rust, W., Holman, I., Bloomfield, J., Cuthbert, M. & Corstanje, R. (2019). Understanding the potential of climate teleconnections to project future groundwater drought. *Hydrology and Earth System Sciences*, Vol.23, 3233-3245.

Rust, W., Cuthbert, M., Bloomfield. J., Corstanje, R., Howden, N. & Holman, I. (2021a). Exploring the role of hydrological pathways in modulating North Atlantic Oscillation (NAO) teleconnection periodicities from UK rainfall to streamflow. *Hydrology and Earth System Sciences*, Vol.25, 2223-2237.

Rust, W., Bloomfield, J., Cuthbert, M., Corstanje, R. & Holman, I. (2021b). Non-stationary control of the NAO on European rainfall and its implications for water resources management. *Hydrological Processes*, Vol.35(3), e14099.

Scaife, A.A., Arribas, A., Blockley, E., Blookshaw, A., Clark, R.T., Dunstone, N., Eade, R., Fereday, D., Folland, C.K., Gordon, M., Hermanson, L., Knight, J.R., Lea, D.J., MacLachlan, C., Maidens, A., Martin, M., Peterson, A.K., Smith, D., Vellinga, M., Wallace, E., Waters, J. & Williams, A. (2014). Skillful long-range prediction of European and North American winters. *Geophysical Research Letters*, Vol.41, 2514-2519.

Scott, L. & Warmerdam, N. (2021). Extended Crime Analysis with ArcGIS Spatial Statistics Tools [ONLINE]. Available at: https://www.esri.com/news/arcuser/0405/ss_crimestats1of2.html. Accessed 04/02/2021.

Serinaldi, F. & Kilsby, C.G. (2012). A modular class of multisite monthly rainfall generators for water resource management and impact studies. *Journal of Hydrology*, Vol.464-465, 528-540.

Sibley, A. (2010). Analysis of extreme rainfall and flooding in Cumbria 18-20 November 2009. *Weather*, Vol.65(11), 287-292.

Simpson, I.R. & Jones, P.D. (2014). Analysis of UK precipitation extremes derived from Met Office gridded data. *International Journal of Climatology*, Vol.34, 2438-2449.

Slater, L.J., Anderson, B., Buechel, M., Dadson, S., Han, S., Harrigan, S., Kelder, T., Kowal, K., Lees, T., Matthews, T., Murphy, C. & Wilby, R.L. (2021). Nonstationary weather and water extremes: a review of methods for their detection, attribution and management. *Hydrology and Earth System Sciences*, Vol.25, 3897-3955.

Smith, D.M., Scaife, A.A., Eade, R. & Knight, J.R. (2016). Seasonal to decadal predication of the winter North Atlantic Oscillation: emerging capability and future prospects. *Quarterly Journal of the Royal Meteorological Society*, Vol.142, 611-617.

Smith, D.M., Scaife, A.A., Eade, R., Athanasisadis, P., Bellucci, A., Bethke, I., Bilbao, R., Borchert, L.F., Caron, L.-P., Counillon, F., Danabasoglu, G., Delworth, T., Doblas-Reyes, F.J., Dunstone, J., Estella-Perez, V., Flavoni, S., Hermanson, L., Keenlyside, N., Kharin, V., Kimoto, M., Merryfield, W.J., Mignot, J., Mochizuki, T., Modali, K., Monerie, P.-A., Muller, W.A., Nicoli, D., Ortega, P., Pankatz, K., Pohlmann, H., Robson, J., Ruggieri, P., Sospedra-Alfonso, R., Swingedouw, D., Wang, Y., Wild, S., Yeager, S., Yang, X. & Zhang, L. (2020). North Atlantic climate far more predicable than models imply. *Nature*, Vol.583, 796-800.

Smith, K.A., Tanguy, M., Hannaford, J. & Prudhomme, C. (2018). Historic reconstructions of daily river flow for 303 UK catchments (1891-2015). *NERC Environmental Information Data Centre.* https://doi.org/10.5285/f710bed1-e564-47bf-b82c-4c2a2fe2810e.

Smith, K.A., Stringer, N., Tanguy, M., Eastman, M., Dadson, S. & Knight, J. (2019). Improving winter ensemble streamflow prediction in the UK using North Atlantic Oscillation analogues. *European Geosciences Union General Assembly*, April 7-12 2019, Vienna, Austria.

Smith, K.A., Barker, L.J., Tanguy, M., Parry, S., Harrigan, S., Legg, T.P., Prudhomme, C. & Hannaford, J. (2019). A multi-objective ensemble approach to hydrological modelling in the UK: An application to historic drought reconstruction. *Hydrology and Earth System Sciences*, Vol.23, 3247-3268.

Song, X., Yin, Z. & Zhang, Y. (2023). Subseasonal reversals of winter surface air temperature in mid-latitude Asia and the roles of westward-shift NAO. *Environmental Research Letters*, DOI 10.1088/1748-9326/acb787.

Spencer, M. & Essery, R. (2016). Scottish snow cover dependence on the North Atlantic Oscillation index. *Hydrology Research*, Vol.47(3), 619-629.

Stagge, J.H., Tallaksen, L.M., Gudmundsson, L., Van Loon, A.F. & Stahl, K. (2015). Candidate distributions for climatological drought indices (SPI and SPEI). *International Journal of Climatology*, Vol.35(13), 4027-4040.

Sun, J. & Wang, H. (2012). Changes of the connection between the summer North Atlantic Oscillation and the East Asian summer rainfall. *Journal of Geophysical Research*, Vol.117, D08110.

Svensson, C. & Hannaford, J. (2019). Oceanic conditions associated with Euro-Atlantic high pressure and UK drought. *Environmental Research Communications*, Vol.1, 101001.

Sweeney, J.C. & O'Hare, G.P. (1992). Geographical variations in precipitation yields and circulation types in Britain and Ireland. *Transactions of the Institute of British Geographers*, Vol.17(4), 448-463.

Tanguy, M., Dixon, H., Prosdocimi, I., Morris. D.G. & Keller, V.D.J. (2016). Gridded estimates of daily and monthly areal rainfall for the United Kingdom (1890-20150 [CEH GEAR]. *NERC Environmental Information Centre*. doi:10.5285/33604ea0-c238-4488-813d-0ad9ab7c51ca.

Tanguy, M., Fry, M., Svenssson, C. & Hannaford. (2017a). Historic gridded Standardized Precipitation Index for the United Kingdom 1862-2015 (generated using gamma distribution with standard period 1961-2010 v4. *NERC Environmental Information Centre*. doi:10.5285/233090b2-1d14-4eb9-9f9c-3923ea2350ff.

Tanguy, M., Fry, M., Svensson, C. & Hannaford, J. (2017b). Historic Standardized Precipitation Index time series of IHU Groups (1862-2015). *NERC Environmental Information Centre*. https://doi.org/10.5285/a01e09b6-4b40-497b-a139-9369858101b3.

Tanguy, M., Haslinger, K., Svensson, C., Parry, S., Barker, L.J., Hannaford, J. & Prudhome, C. (2021). Regional differences in spatiotemporal drought characteristics in Great Britain. *Frontiers in Environmental Science*, Vol.9, 639-649.

Thornton, H.E., Smith, D., Scaife, A.A. & Dunstone, N. (2023). Seasonal Predictability of the East Atlantic Pattern in Late Autumn and Early Winter. *Geophysical Research Letters*, Vol.50(1), e2022GL100712.

Trigo, I.F. (2006). Climatology and interannual variability of storm-tracks in the Euro-Atlantic sector: A comparison between ERA-40 and NCEP/NCAR reanalysis. *Climate Dynamics*, Vol.36(2-3), 127-143.

Tsanis, I. & Tapoglou, E. (2019). Winter North Atlantic Oscillation impact on European precipitation and drought under climate change. *Theoretical and Applied Climatology*, Vol.135, 323-330.

UK Hydrological Outlook. (2020). UK Hydrological Outlook December 2020 [ONLINE]. Available at: http://www.hydoutuk.net/files/2816/0743/4122/2020_12_HO_Complete.pdf. Accessed 14/12/2020.

Uvo, C.B., Foster, K. & Olsson, J. (2021). The spatio-temporal influence of atmospheric teleconnection patterns on hydrology in Sweden. *Journal of Hydrology: Regional Studies,* Vol.34, 100782.

Van Loon, A.F. (2015). Hydrological drought explained. *WIREs Water*, Vol.2(4), 359-392.

Van Loon, A.F. & Laaha, G. (2015). Hydrological drought severity explained by climate and catchment characteristics. *Journal of Hydrology*, Vol.526, 3-14.

Van Loon, A.F., Stahl, K., Di Baldassarrre, G., Clark, J., Rangecroft, S., Wanders, N., Gleeson, T., Van Dijk, A.I.J.M., Tallaksen, L.M., Hannaford, J., Uijlenhoet, R., Teuling, A.J., Hannah, D.M., Sheffield, J., Svoboda, M., Verbeiren, B., Wagener, T. & Van Lanen, H.A.J. (2016). Drought in a human-modified world: reframing drought definitions, understanding and analysis approaches. *Hydrology and Earth System Sciences*, Vol.20, 3631-3650.

Varouchakis, E.A., Corzo, G.A., Karatzas, G.P. & Kotsopoulou, A. (2018). Spatio-temporal analysis of annual rainfall in Crete, Greece. *Acta Geophysica*, Vol.66(3), 319-328.

Visbeck, M.H., Hurrell, J.W., Polvani, L. & Cullen, H.M. (2001). The North Atlantic Oscillation: past, present and future. *Proceedings of the National Academy of Sciences of the United States of America*, Vol.98(23), 12876-12877.

Wallace, J.M. & Gutzler, D.S. (1981). Teleconnections in the geopotential height field during the Northern Hemisphere winter. *Monthly Weather Review*, Vol.109, 784-812.

Watts, G., Hannah, D.M. & Watkinson, A. (2015). Introduction to the special issue on the impact of climate change on water in the UK. *Progress in Physical Geography*, Vol.39(1), 3-5.

Wedgbrow, C.S., Wilby, R.L. & Fox, H.R. (2005). Experimental seasonal forecasts of low summer flows in the River Thames, UK, using expert systems. *Climate Research*, Vol.28, 133-141.

Weisheimer, A., Schaller, N., O'Reilly, C., MacLeod, D.A. & Palmer T. (2017). Atmospheric seasonal forecasts of the twentieth century: multi-decadal variability in predictive skill of the winter North Atlantic Oscillation (NAO) and their potential value for extreme event attribution. *Quarterly Journal of the Royal Meteorological Society*, Vol.143, 917-926.

West, H., Quinn, N. & Horswell, M. (2019a). A space-time geostatistical approach to exploring the stationarity of North Atlantic Oscillation driven wet/dry conditions in Great Britain. *European Geosciences Union General Assembly*, April 7-12 2019, Vienna, Austria.

West, H., Quinn, N. & Horswell, M. (2019b). Regional rainfall responses to the North Atlantic Oscillation across Great Britain. *Hydrology Research*, Vol.50(6), 1549-1563.

West, H., Quinn, N. & Horswell, M. (2019c). Spatial variations in the relationship between precipitation and streamflow in Great Britain. *International Union of Geodesy and Geophysics General Assembly*, July 10 2019, Montreal, Canada.

West, H., Quinn, N. & Horswell, M. (2021a). Spatio-Temporal Variability in North Atlantic Oscillation Monthly Rainfall Signatures in Great Britain. *Atmosphere*, Vol.12(6), 763.

West, H., Quinn, N. & Horswell, M. (2021b), Monthly rainfall signatures of the North Atlantic Oscillation and East Atlantic Pattern in Great Britain. *Atmosphere*, Vol.12(11), 1533.

West, H., Quinn, N. & Horswell, M. (2022a). Spatio-temporal propagation of North Atlantic Oscillation (NAO) rainfall deviations to streamflow in British catchments. *Hydrological Sciences Journal*, Vol.67(5), 676-688.

West, H., Quinn, N. & Horswell, M. (2022b). The influence of the North Atlantic Oscillation and East Atlantic Pattern on drought in British catchments. *Frontiers in Environmental Science,* doi: 10.3389/fenvs.2022.754597.

Wilby, R.L. (1993). Evidence of ENSO in the synoptic climate of the British Isles since 1880. *Weather*, Vol.48(8), 234-239.

Wilby, R.L., O'Hare, G. & Barnsley, N. (1997). The North Atlantic Oscillation and British Isles climate variability. *Weather*, Vol.52(9), 266-276.

Wilby, R.L., Wedgbrow, C.S. & Fox, H.R. (2004). Seasonal predictability of the summer hydrometeorology of the River Thames, UK. *Journal of Hydrology*, Vol.295(1-4), 1-16.

Wilby, R.L. & Quinn, N. (2013). Reconstructing multi-decadal variations in fluvial flood risk using atmospheric circulation patterns. *Journal of Hydrology*, Vol.487, 109-121.

Wilby, R.L. & Johnson, M.F. (2020). Climate Variability and Implications for Keeping Rivers Cool in England. *Climate Risk Management*, Vol.30, 100259.

Wilhite, D.A. & Glantz, M.H. (1985). Understanding the drought phenomenon: The role of definitions. *Water International*, Vol.10(3), 111-120.

Woollings, T., Czuchnicki, C. & Franzke, C. (2014). Twentieth century North Atlantic jet variability. *Quarterly Journal of the Royal Meteorological Society*, Vol.140(680), 783-791.

Wrzesinski, D. & Paluszkiewicz, R. (2011). Spatial differences in the impact of the North Atlantic Oscillation on the flow of rivers in Europe. *Hydrology Research*, Vol.42(1), 30-39.

Yeh, H-F. (2019). Using integrated meteorological and hydrological indices to assess drought characterisation in southern Taiwan. *Hydrology Research*, Vol.50(3), 901-914.

Zhang, W., Mei, X., Geng, X., Turner, A.G. & Jin, F.F. (2019). A non-stationary ENSO-NAO relationship due to AMO modulation. *Journal of Climate*, Vol.32(1), 33-43.

Zubiate, L., McDermott, F., Sweeney, C. & O'Malley, M. (2017). Spatial variability in winter NAO-wind speed relationships in western Europe linked to concomitant states of the East Atlantic and Scandinavian patterns. *Quarterly Journal of the Royal Meteorological Society*, Vol.143, 552-562.

Appendix

Appendix A: Decadal Correlation Time Series

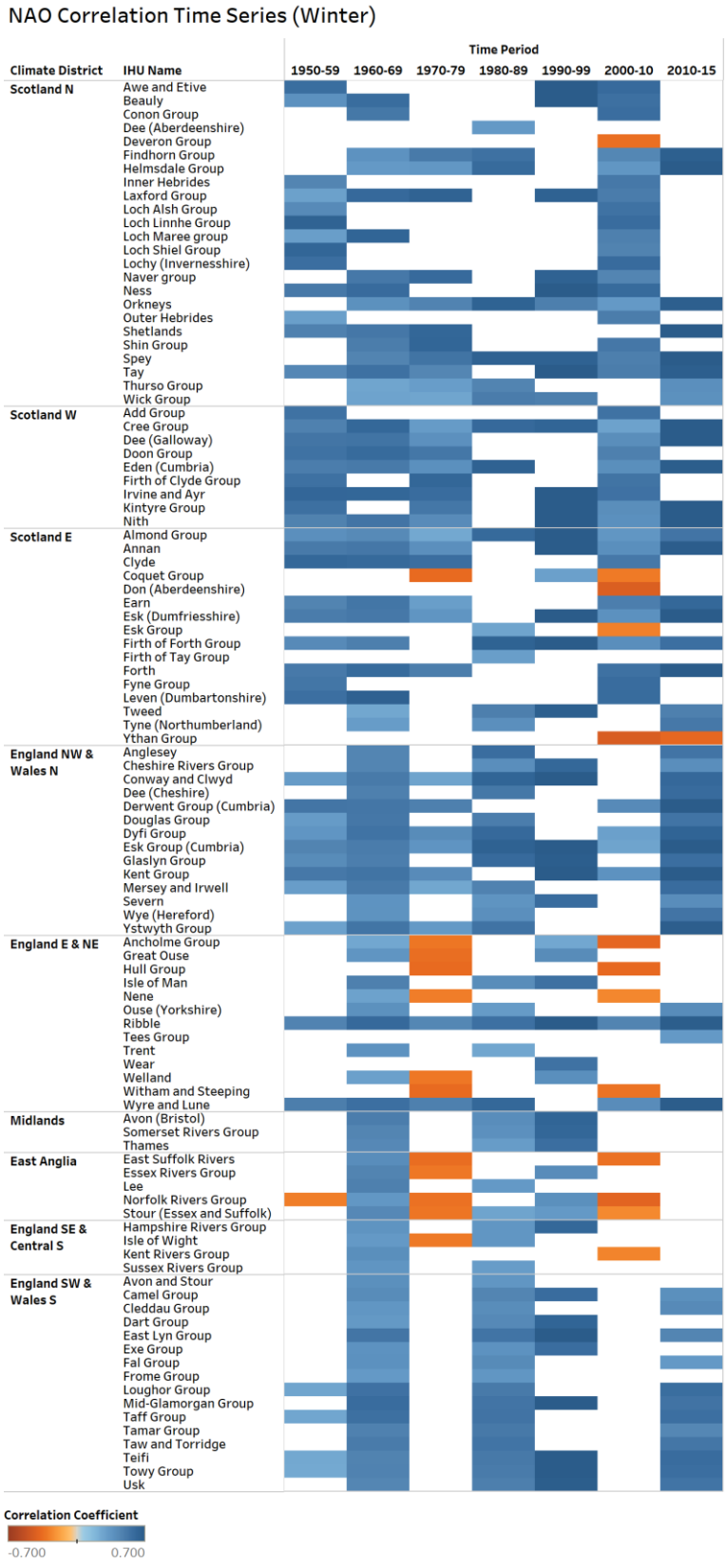

***Appendix A1**: Winter correlation time series between the NAO and SPI-1 for IHU Areas. Correlations which are not significant (after p-value adjustment using the FDR approach) are not shown.*

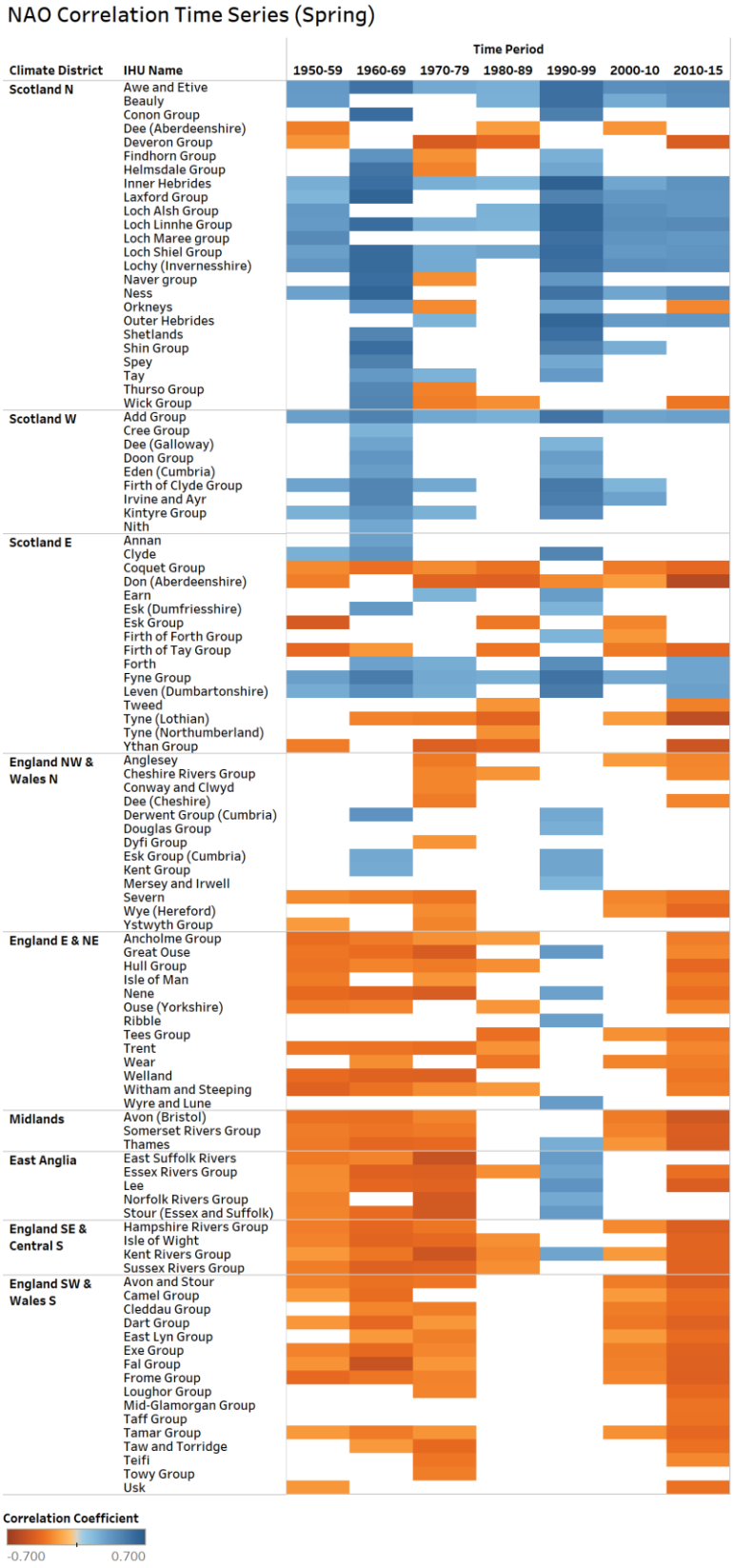

***Appendix A2**: Spring correlation time series between the NAO and SPI-1 for IHU Areas. Correlations which are not significant (after p-value adjustment using the FDR approach) are not shown.*

***Appendix A3**: Summer correlation time series between the NAO and SPI-1 for IHU Areas. Correlations which are not significant (after p-value adjustment using the FDR approach) are not shown.*

***Appendix A4**: Autumn correlation time series between the NAO and SPI-1 for IHU Areas. Correlations which are not significant (after p-value adjustment using the FDR approach) are not shown.*

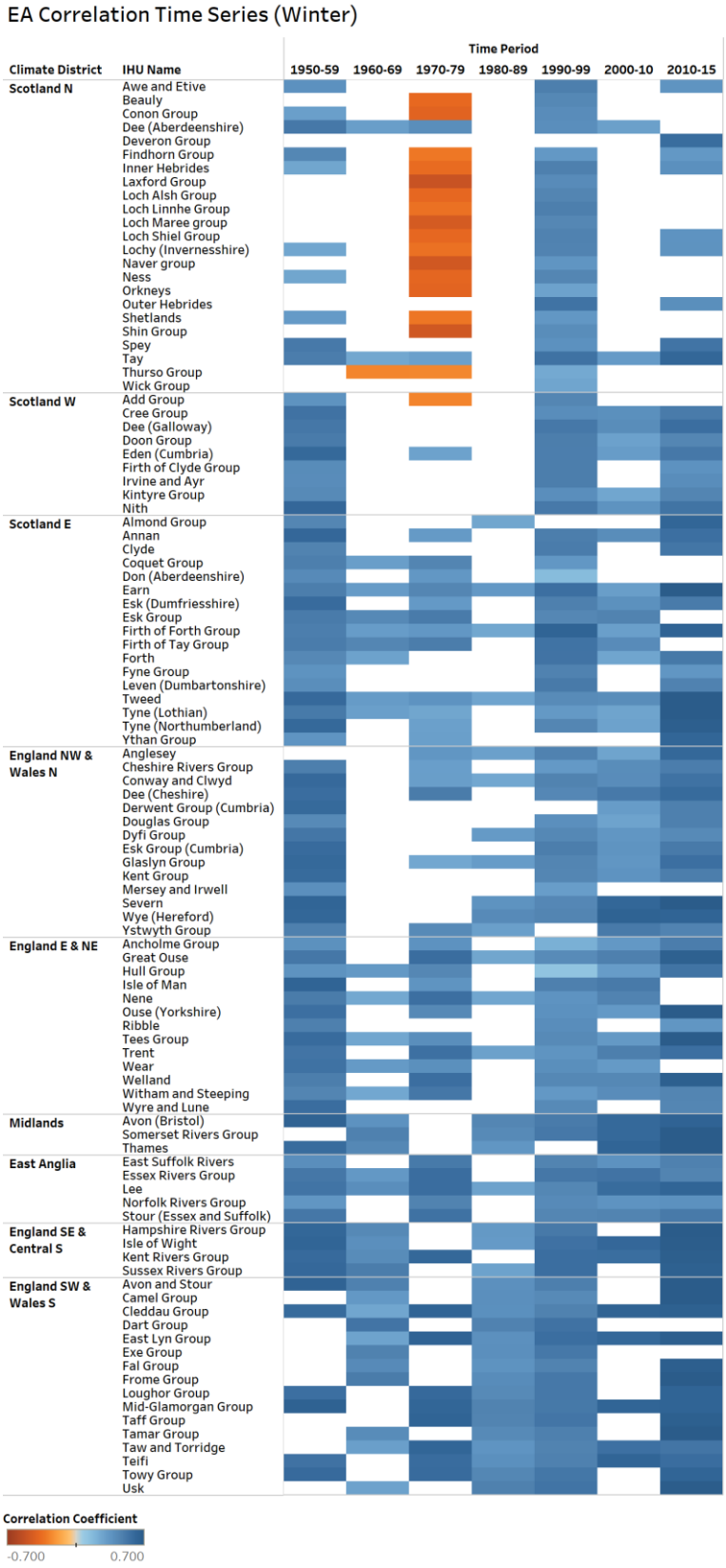

***Appendix A5**: Winter correlation time series between the EA and SPI-1 for IHU Areas. Correlations which are not significant (after p-value adjustment using the FDR approach) are not shown.*

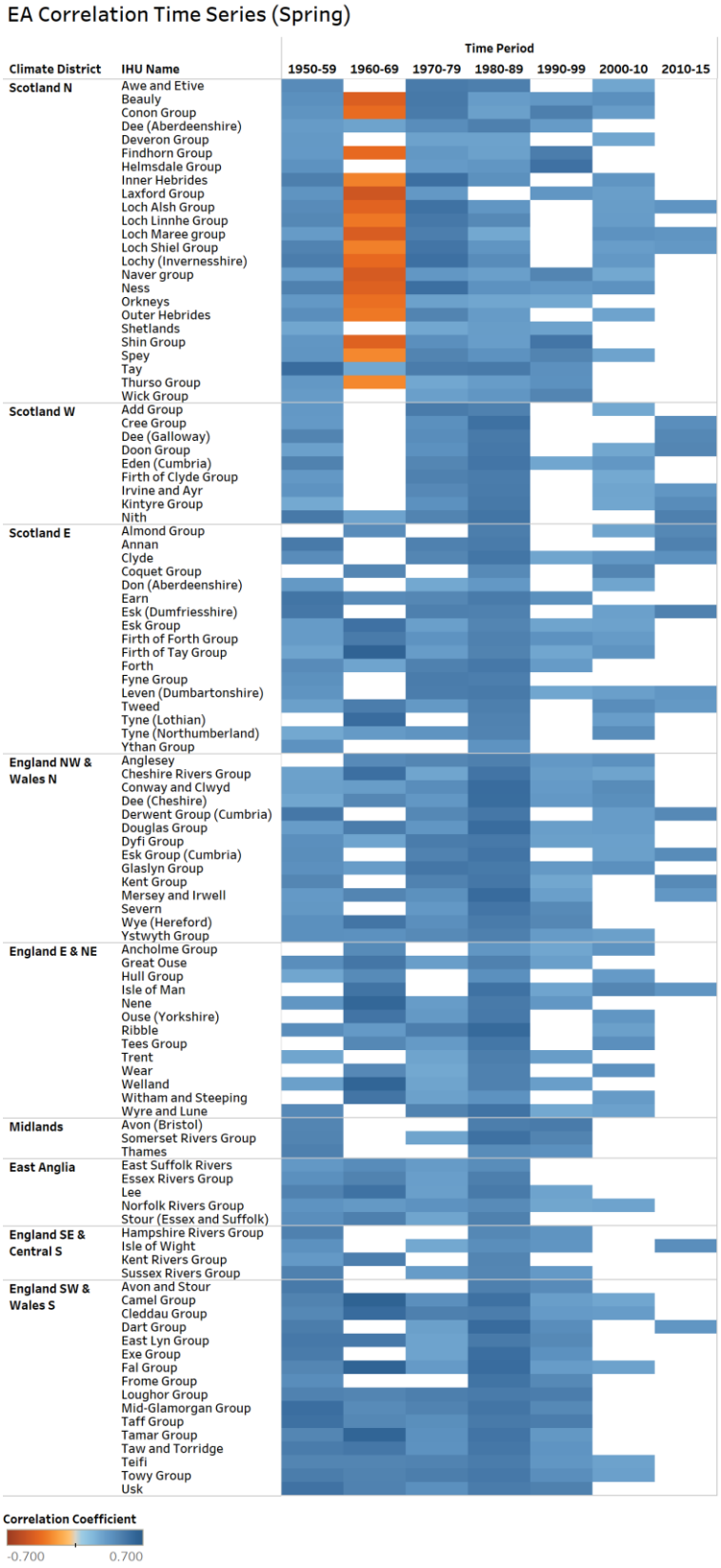

***Appendix A6**: Spring correlation time series between the EA and SPI-1 for IHU Areas. Correlations which are not significant (after p-value adjustment using the FDR approach) are not shown.*

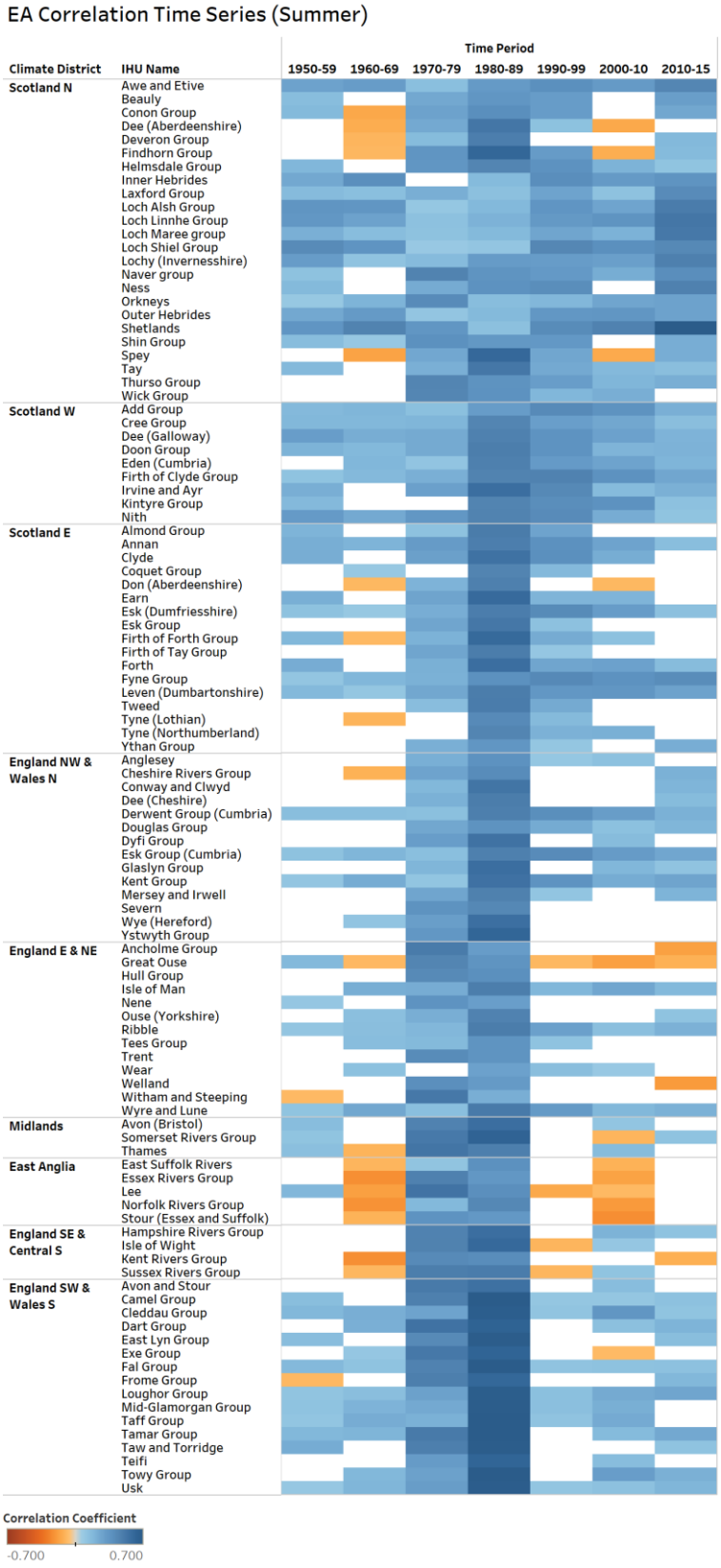

***Appendix A7**: Summer correlation time series between the EA and SPI-1 for IHU Areas. Correlations which are not significant (after p-value adjustment using the FDR approach) are not shown.*

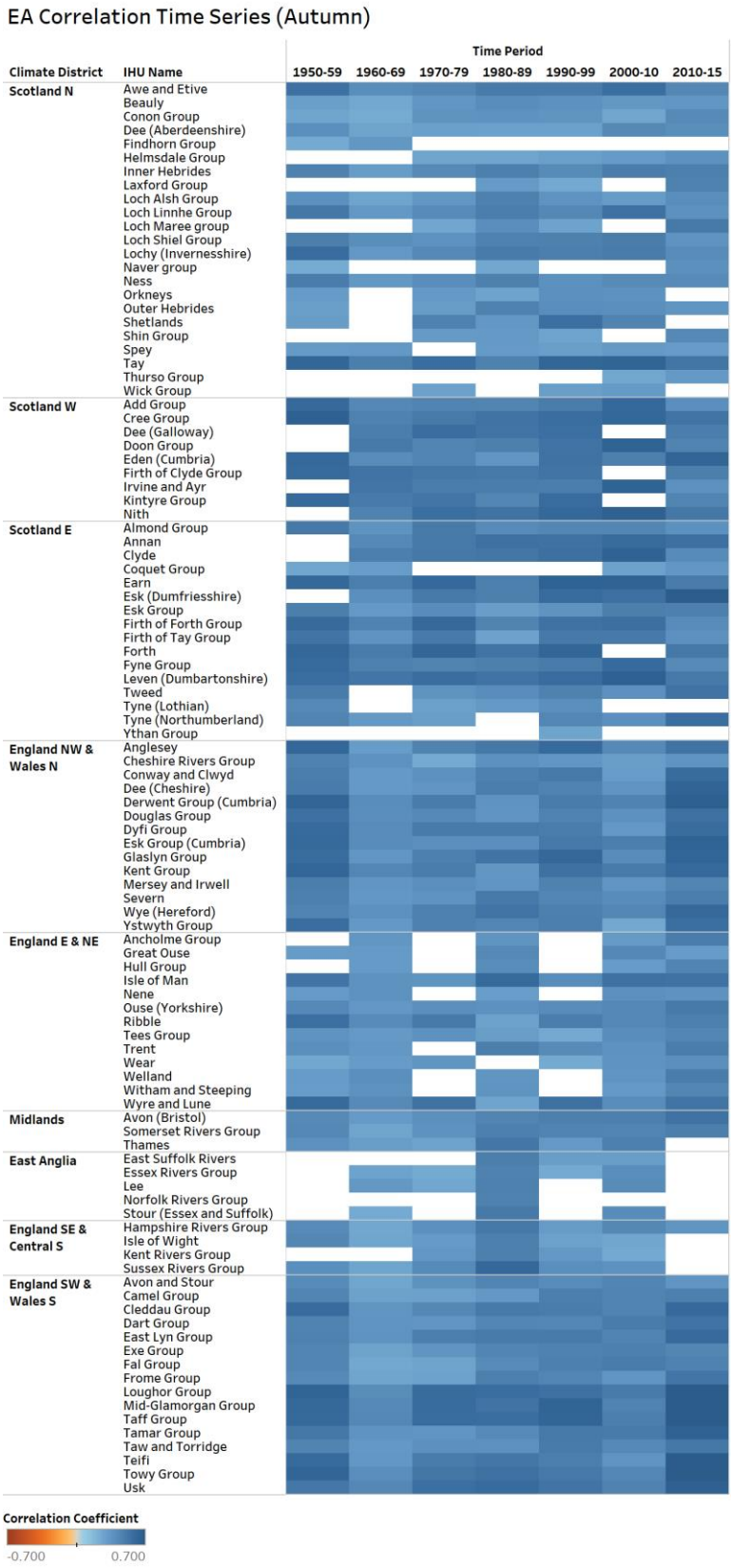

***Appendix A8**: Autumn correlation time series between the EA and SPI-1 for IHU Areas. Correlations which are not significant (after p-value adjustment using the FDR approach) are not shown.*

Appendix B: GEAR Distance Grids

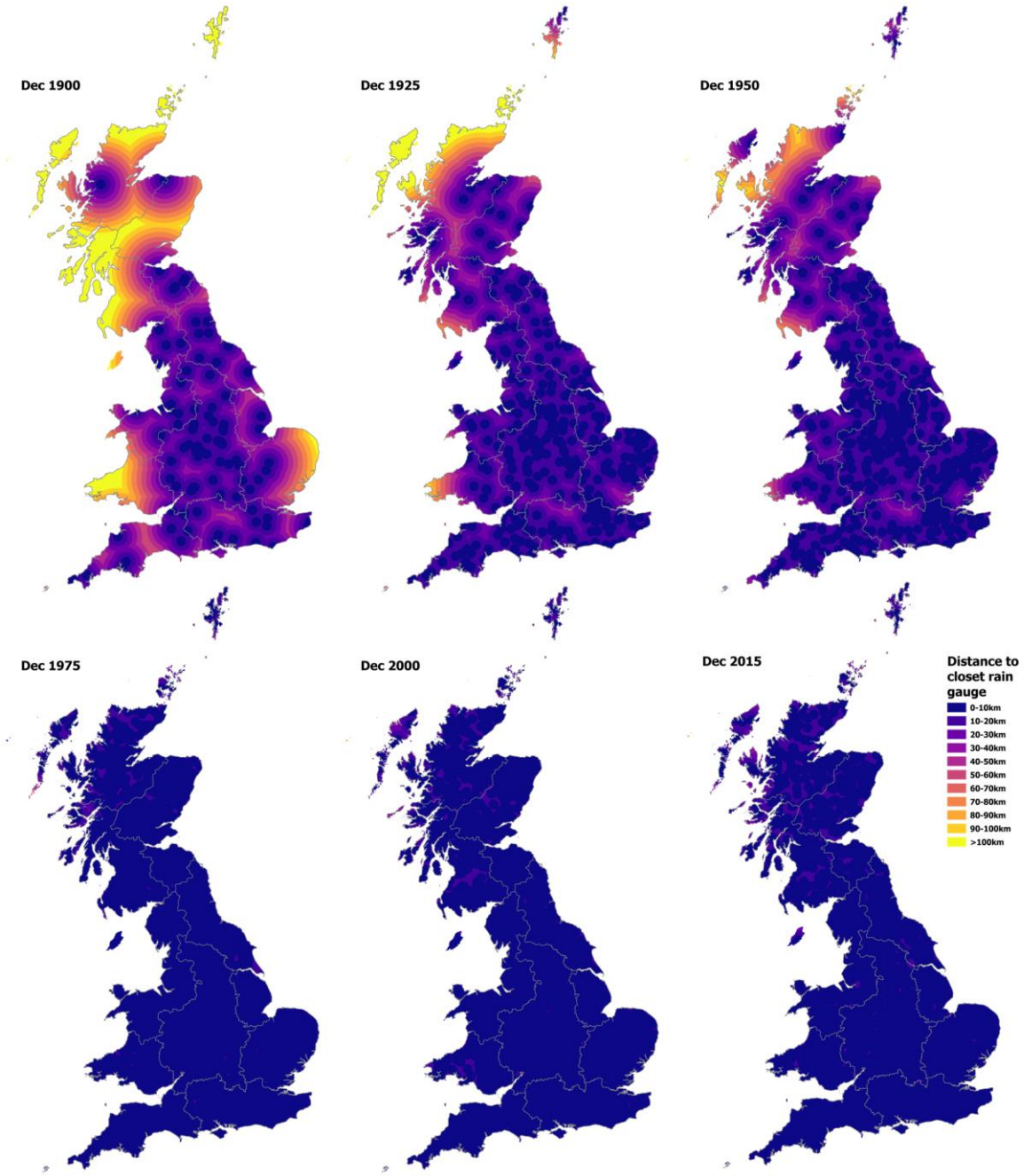

***Appendix B**: Maps showing the distance to the nearest rainfall observation/gauge used in the GEAR interpolation process at 25-year intervals for December (Tanguy et al. 2016). Pixels greater than 100km (marked in yellow) from an observation are not estimated due to the high uncertainty.*

Appendix C: Assessing Accuracy of Historic Modelled Flows

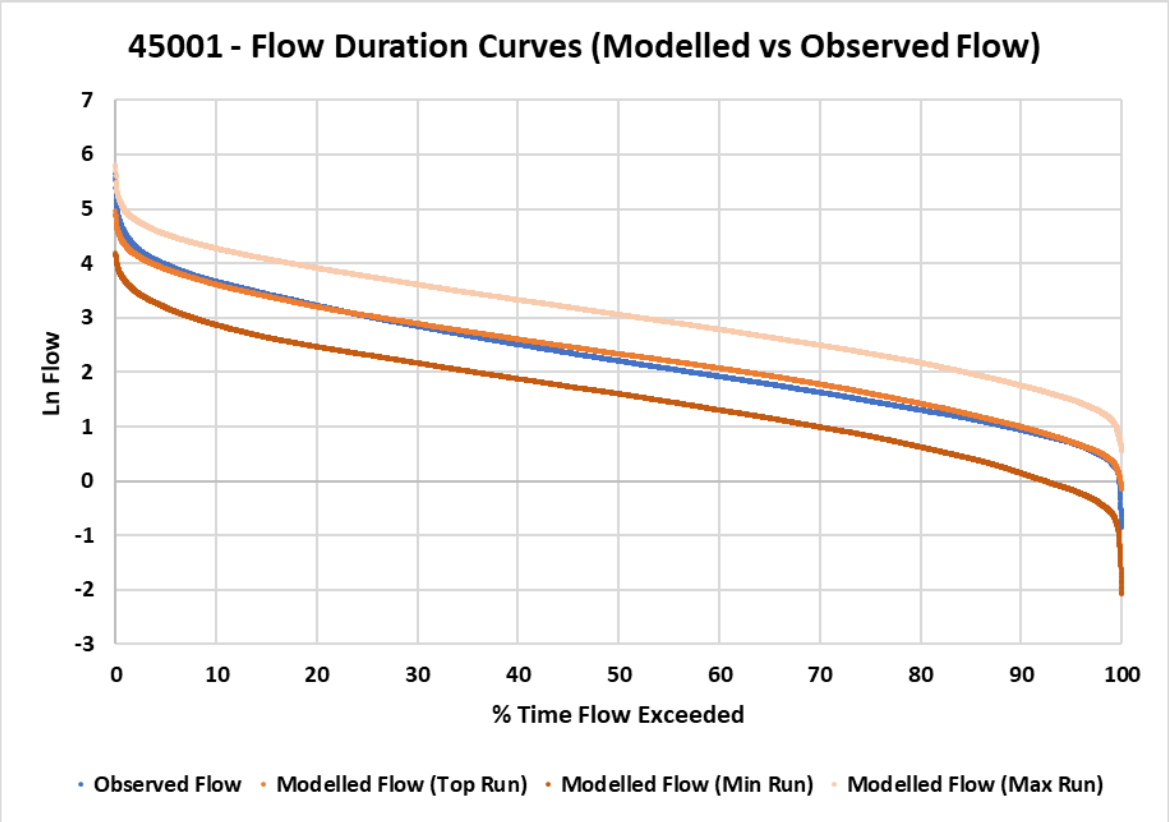

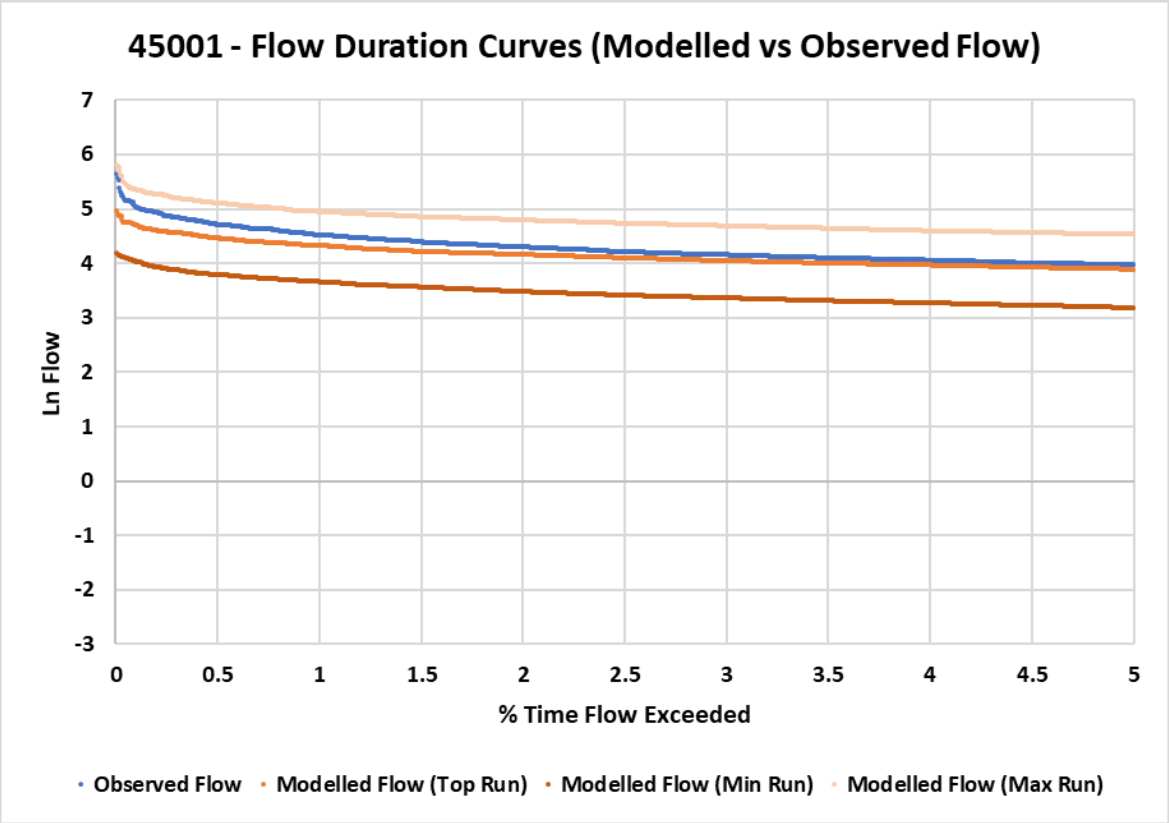

***Appendix C1**: Flow duration curve for the Exe (45001) showing the observed flow (NRFA), the top (best) performing run of 500 ensembles, and the minimum/maximum flow estimates (Smith et al. 2018). Flow values shown with a natural log transformation.*

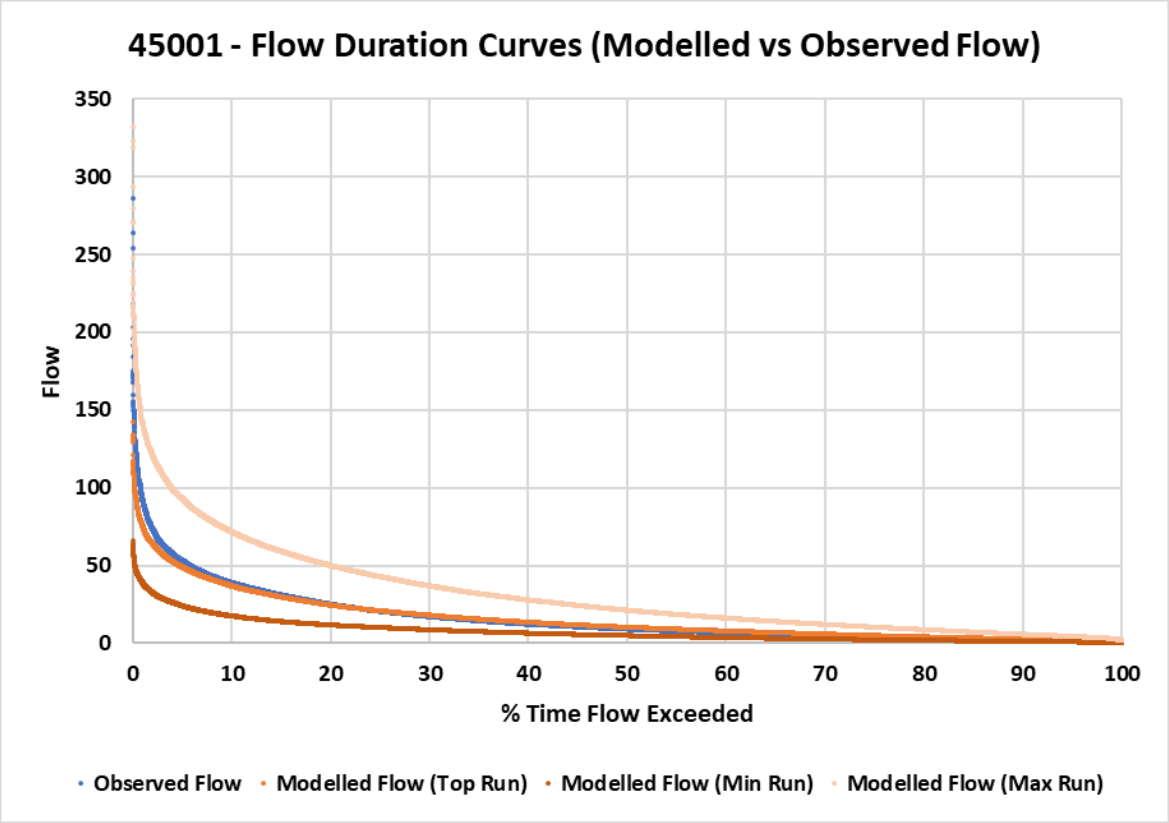

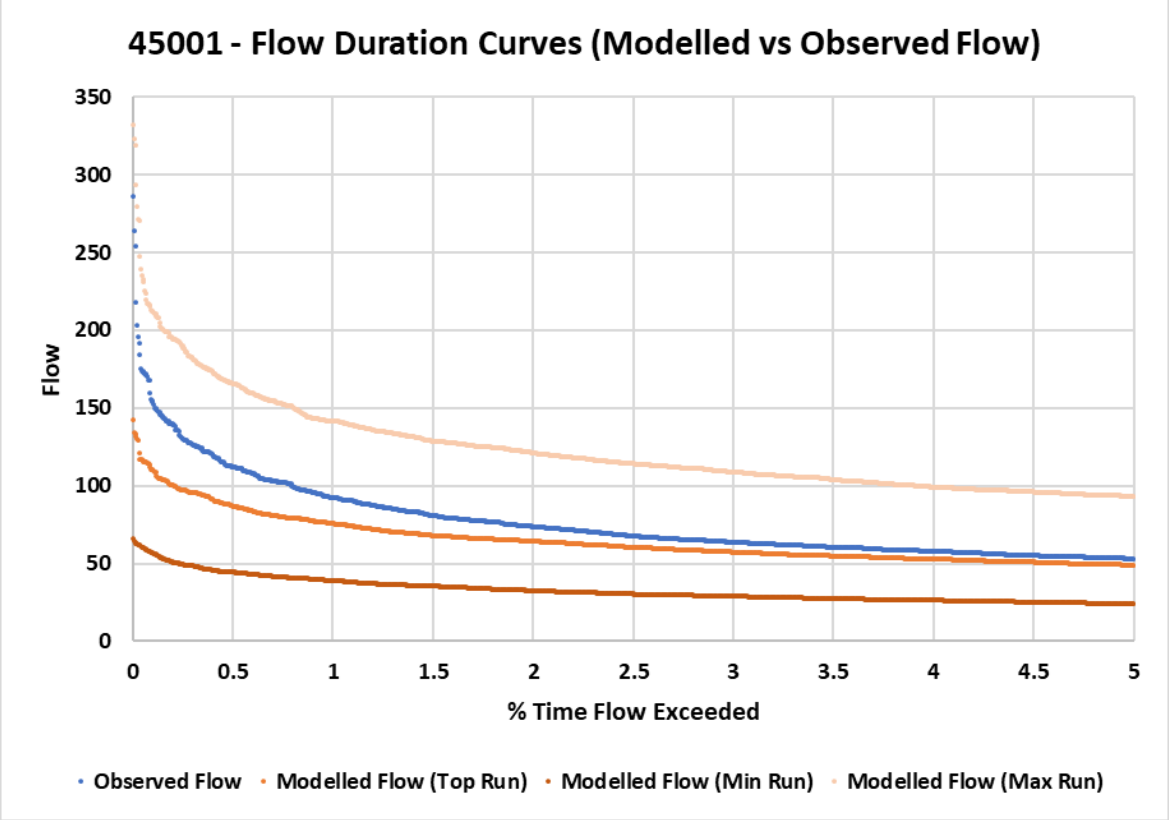

Appendix C2: Flow duration curve for the Exe (45001) showing the observed flow (NRFA), the top (best) performing run of 500 ensembles, and the minimum/maximum flow estimates (Smith et al. 2018).

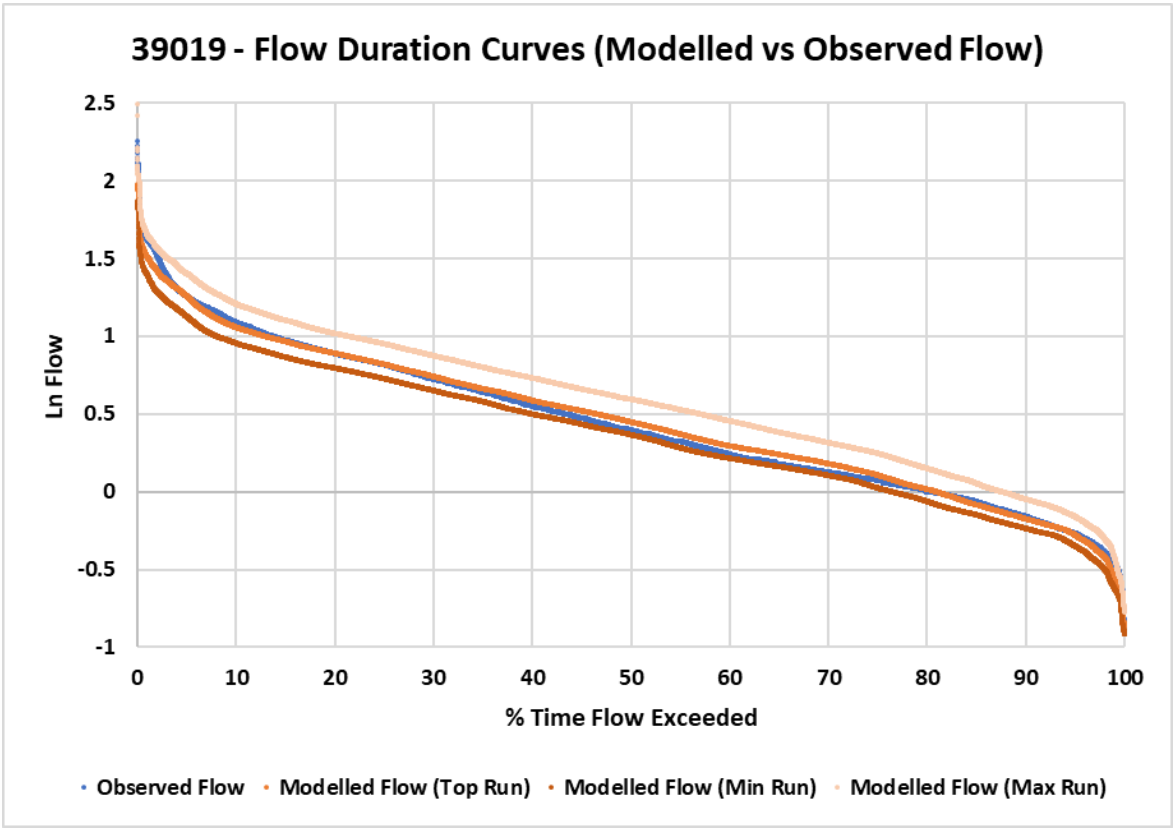

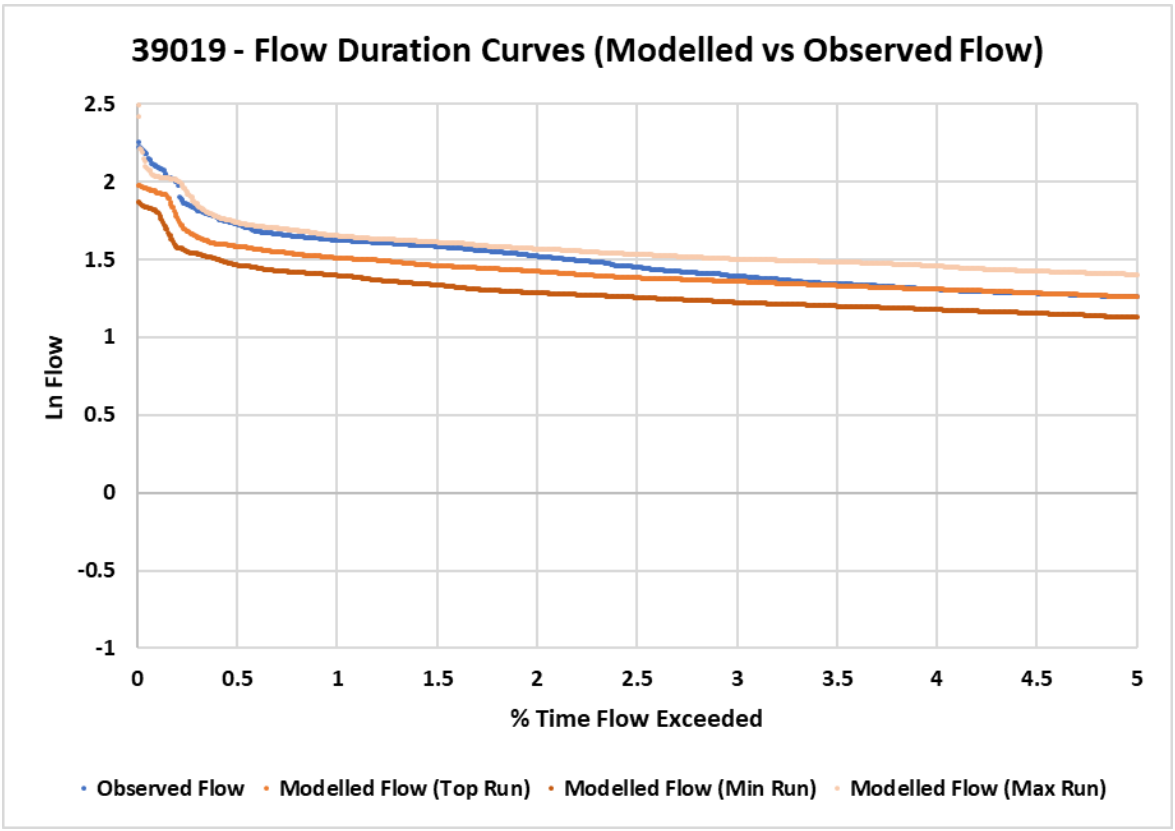

Appendix C3: Flow duration curve for the Lambourn (39019) showing the observed flow (NRFA), the top (best) performing run of 500 ensembles, and the minimum/maximum flow estimates (Smith et al. 2018). Flow values shown with a natural log transformation.

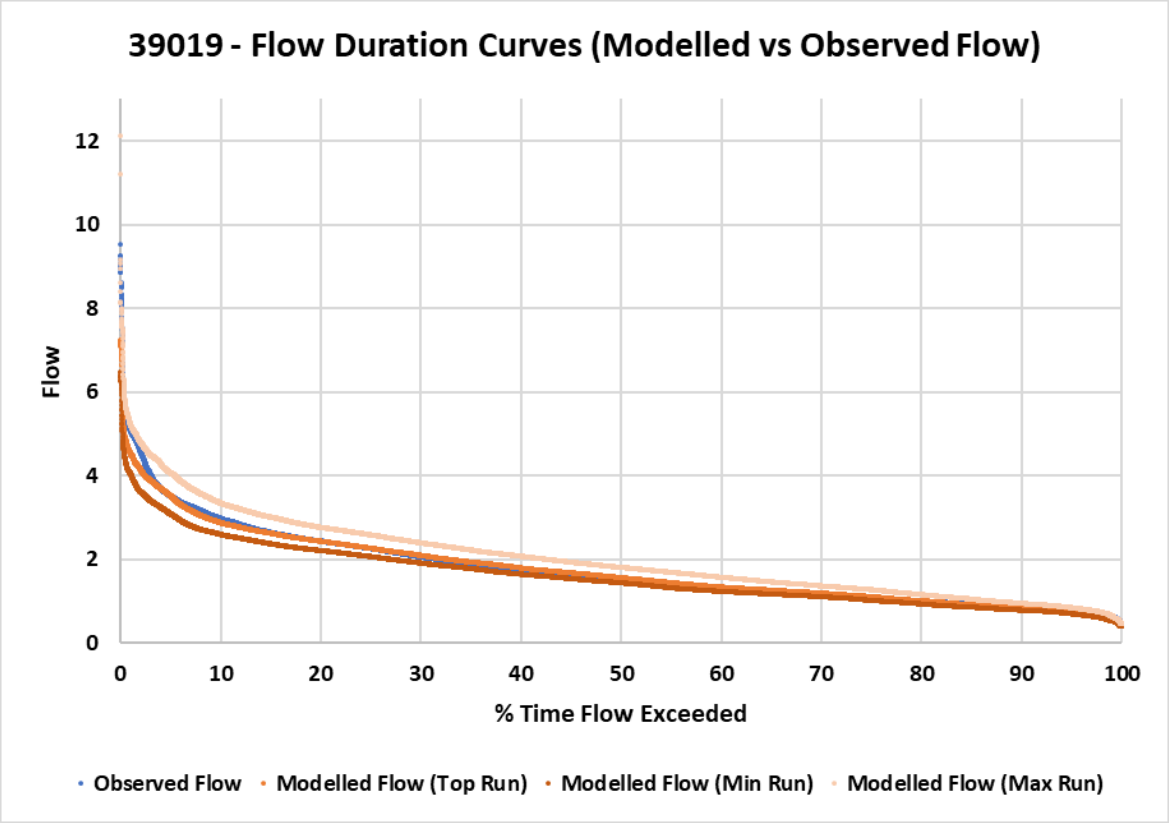

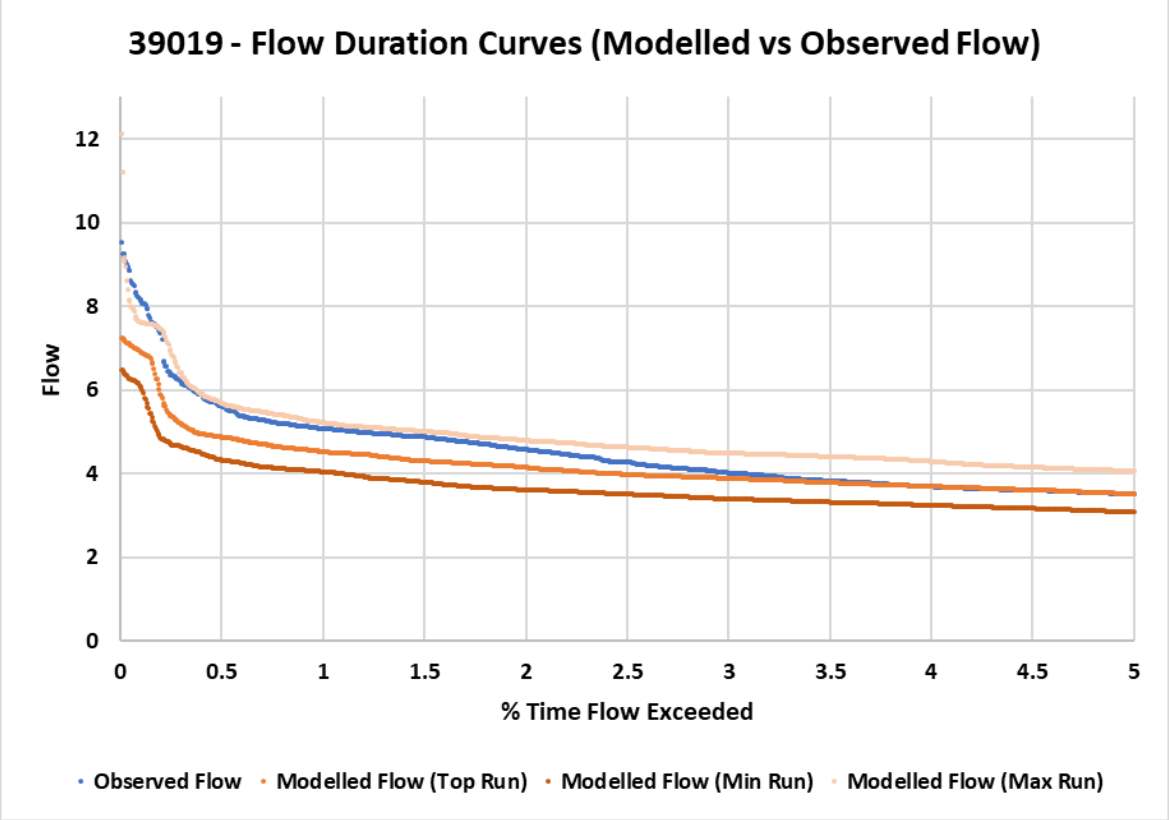

Appendix C4: Flow duration curve for the Lambourn (39019) showing the observed flow (NRFA), the top (best) performing run of 500 ensembles, and the minimum/maximum flow estimates (Smith et al. 2018).

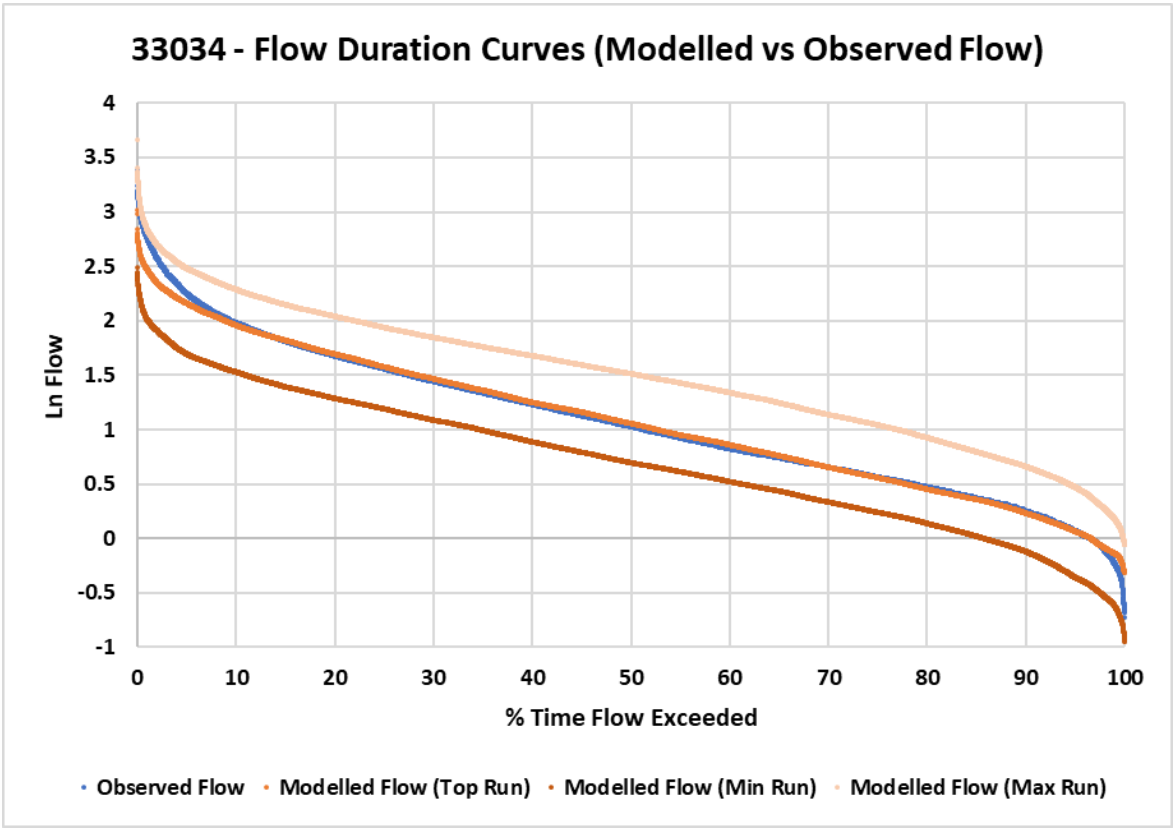

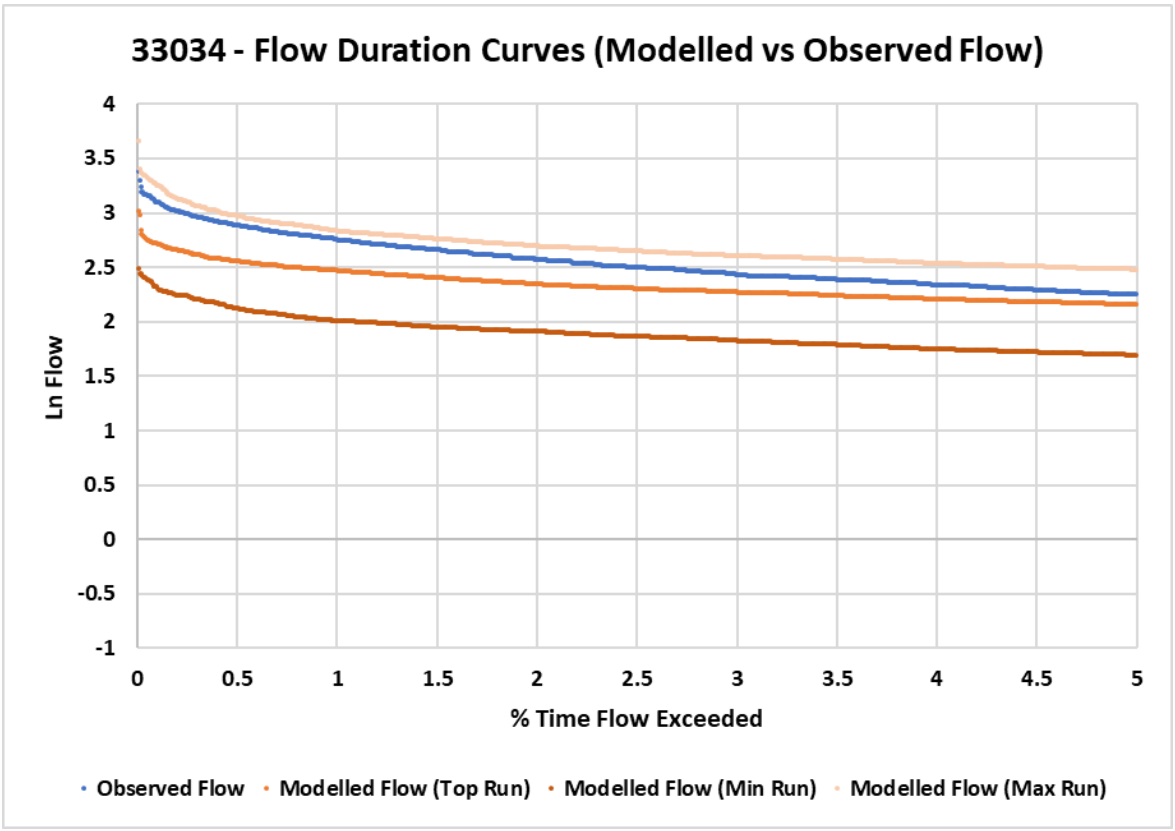

Appendix C5: Flow duration curve for the Little Ouse (33034) showing the observed flow (NRFA), the top (best) performing run of 500 ensembles, and the minimum/maximum flow estimates (Smith et al. 2018). Flow values shown with a natural log transformation.

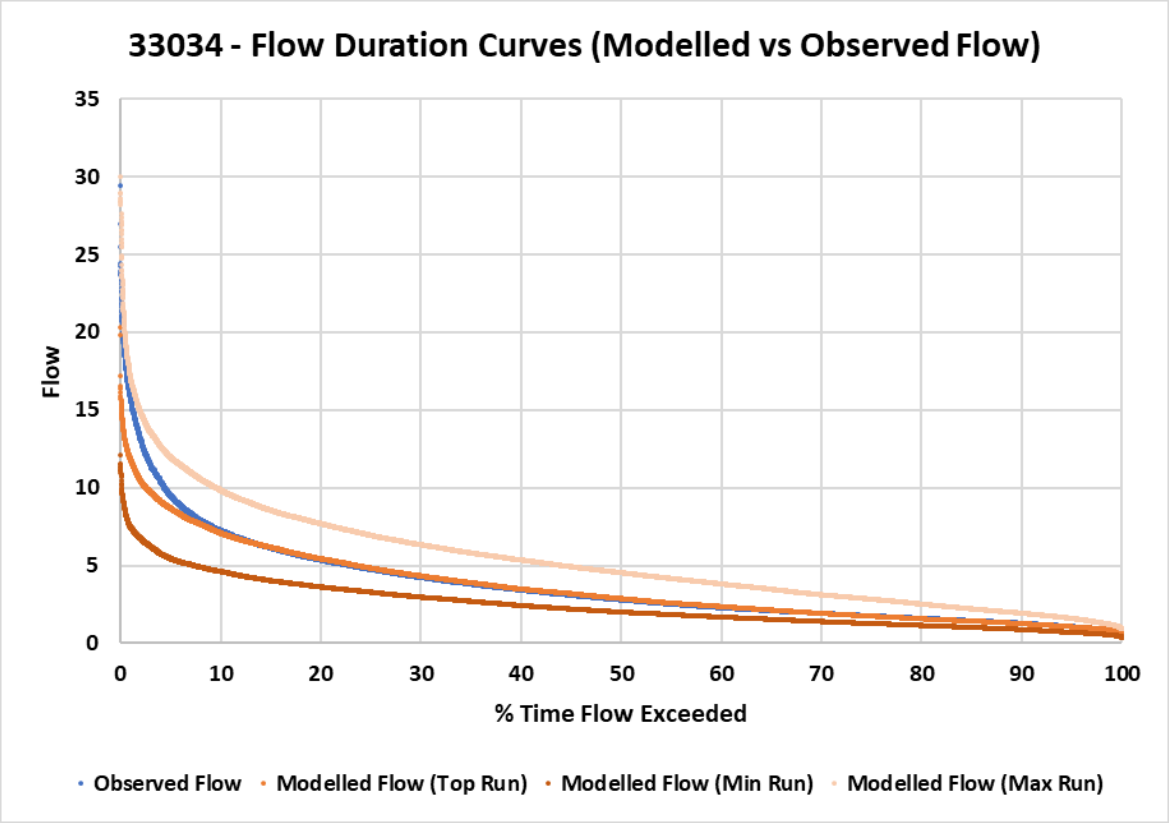

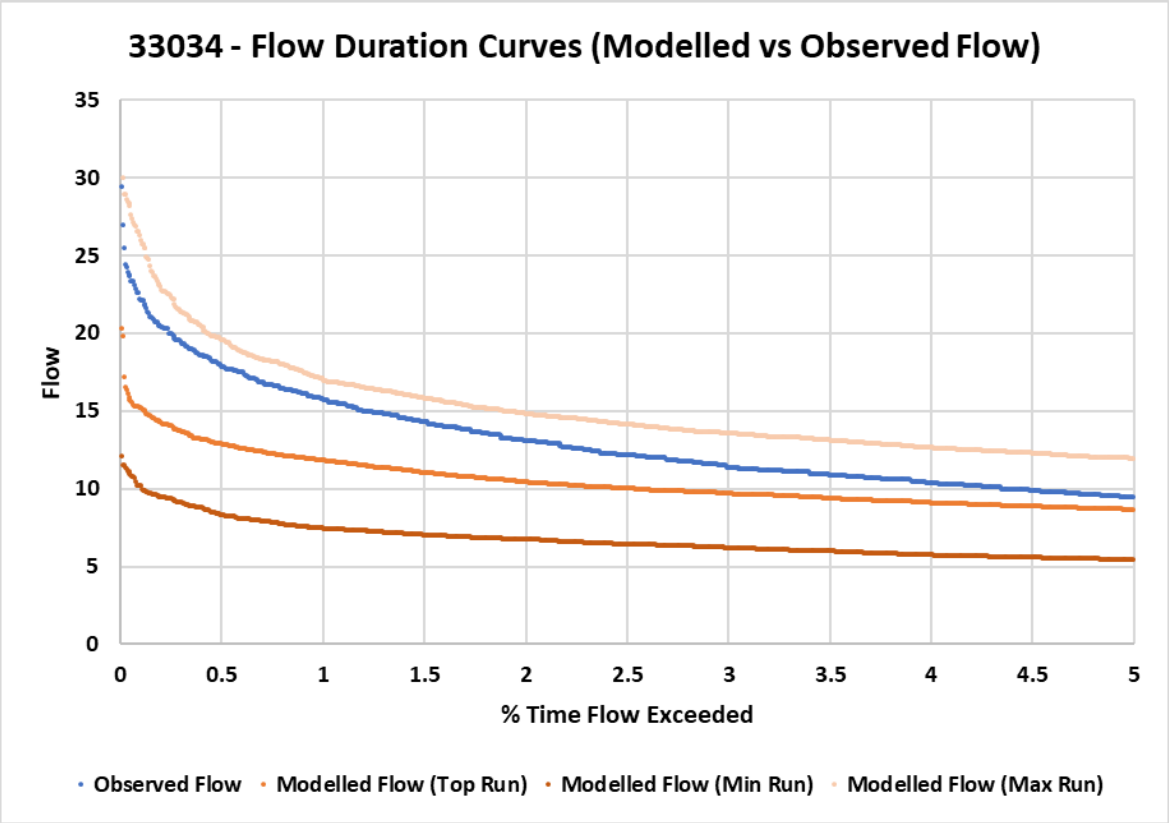

Appendix C6: Flow duration curve for the Little Ouse (33034) showing the observed flow (NRFA), the top (best) performing run of 500 ensembles, and the minimum/maximum flow estimates (Smith et al. 2018).

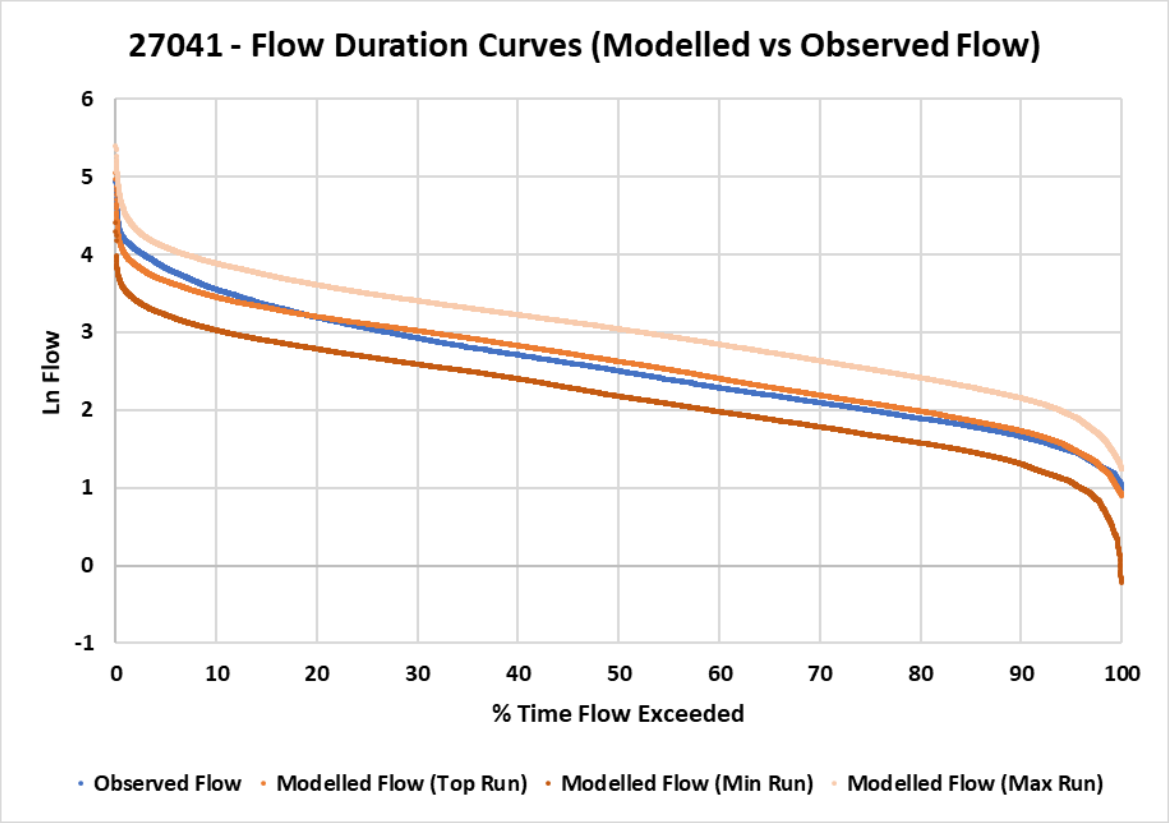

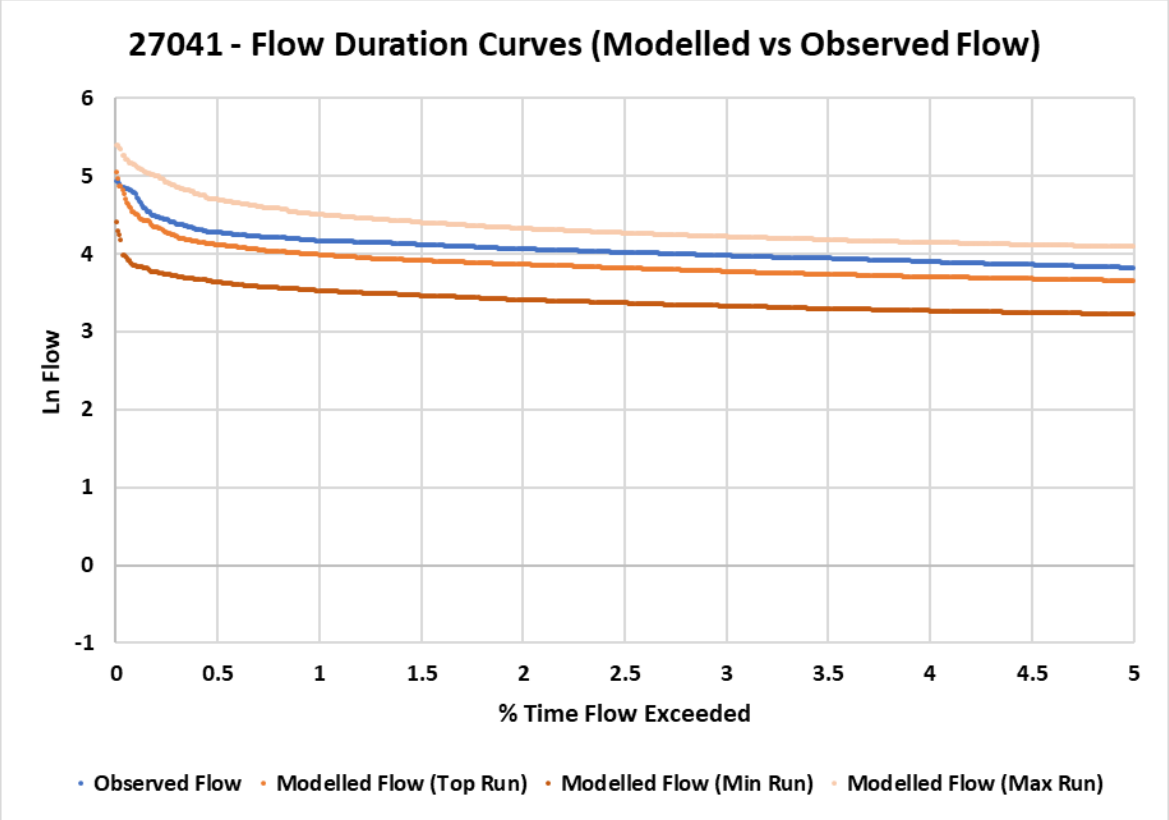

***Appendix C7**: Flow duration curve for the Derwent (27041) showing the observed flow (NRFA), the top (best) performing run of 500 ensembles, and the minimum/maximum flow estimates (Smith et al. 2018). Flow values shown with a natural log transformation.*

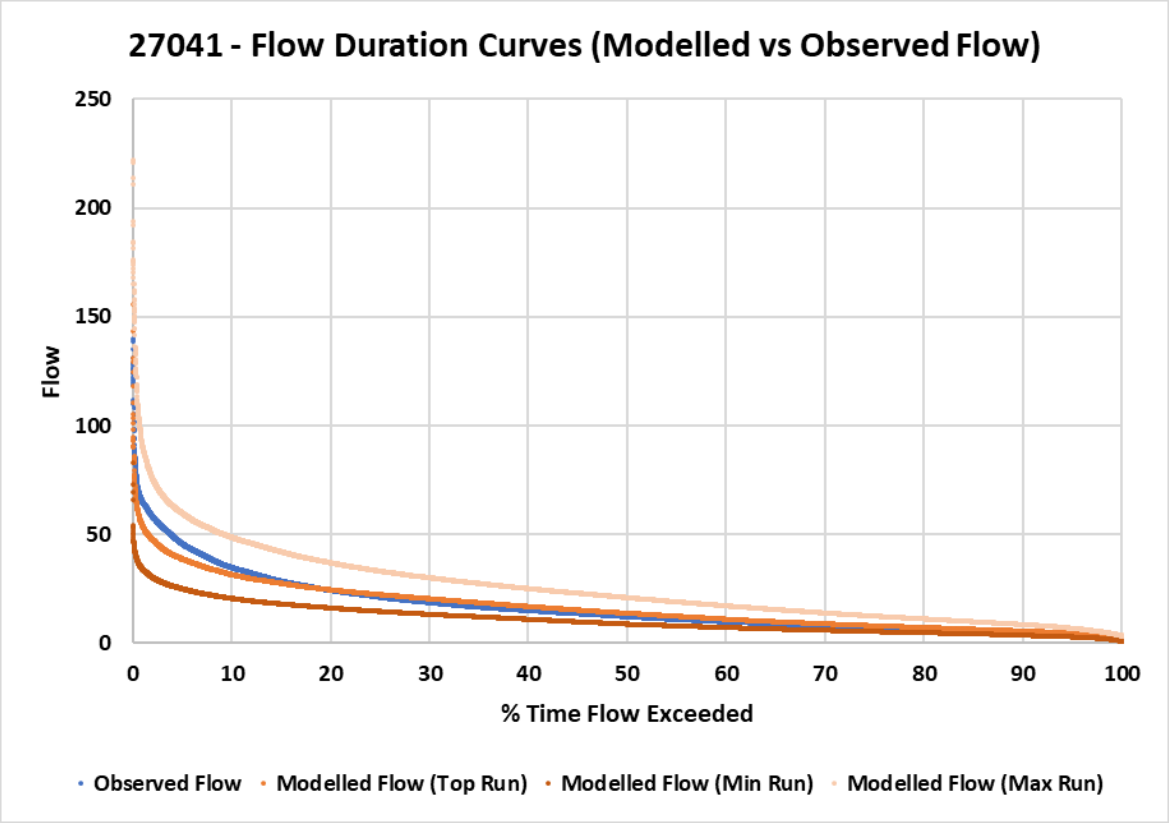

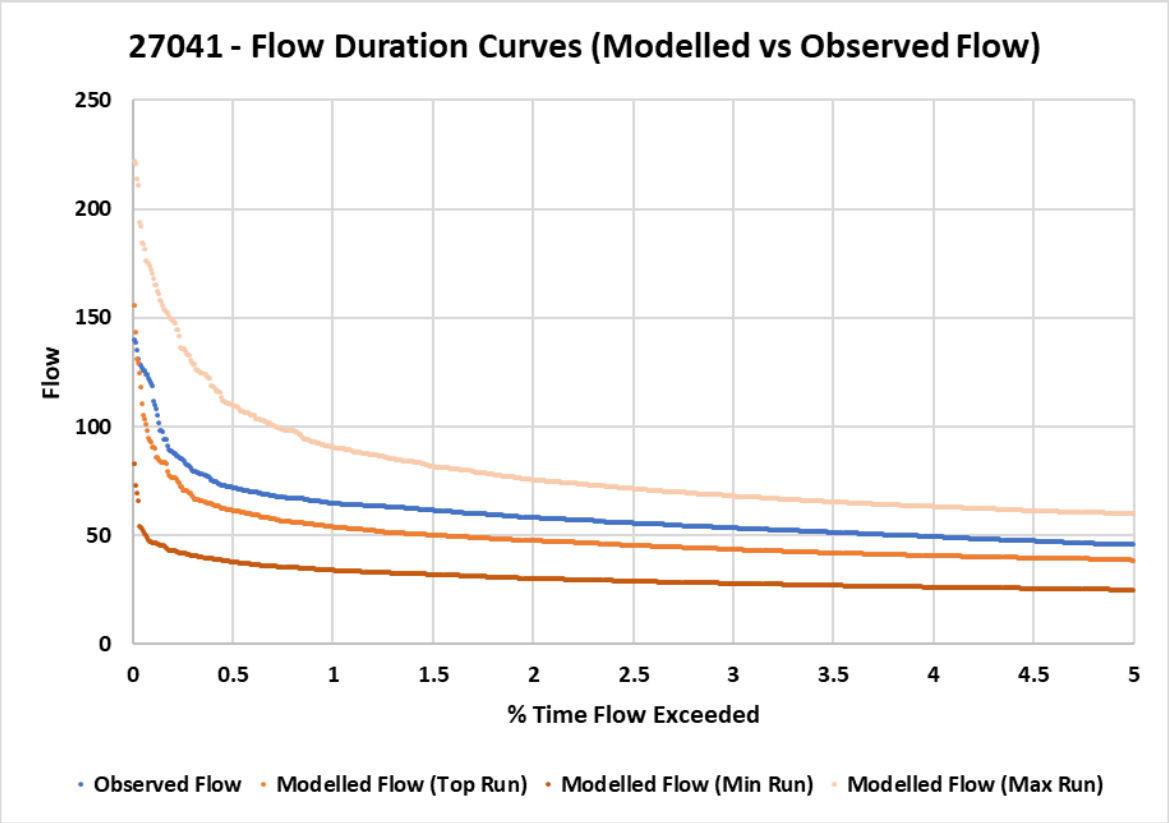

Appendix C8: Flow duration curve for the Derwent (27041) showing the observed flow (NRFA), the top (best) performing run of 500 ensembles, and the minimum/maximum flow estimates (Smith et al. 2018).

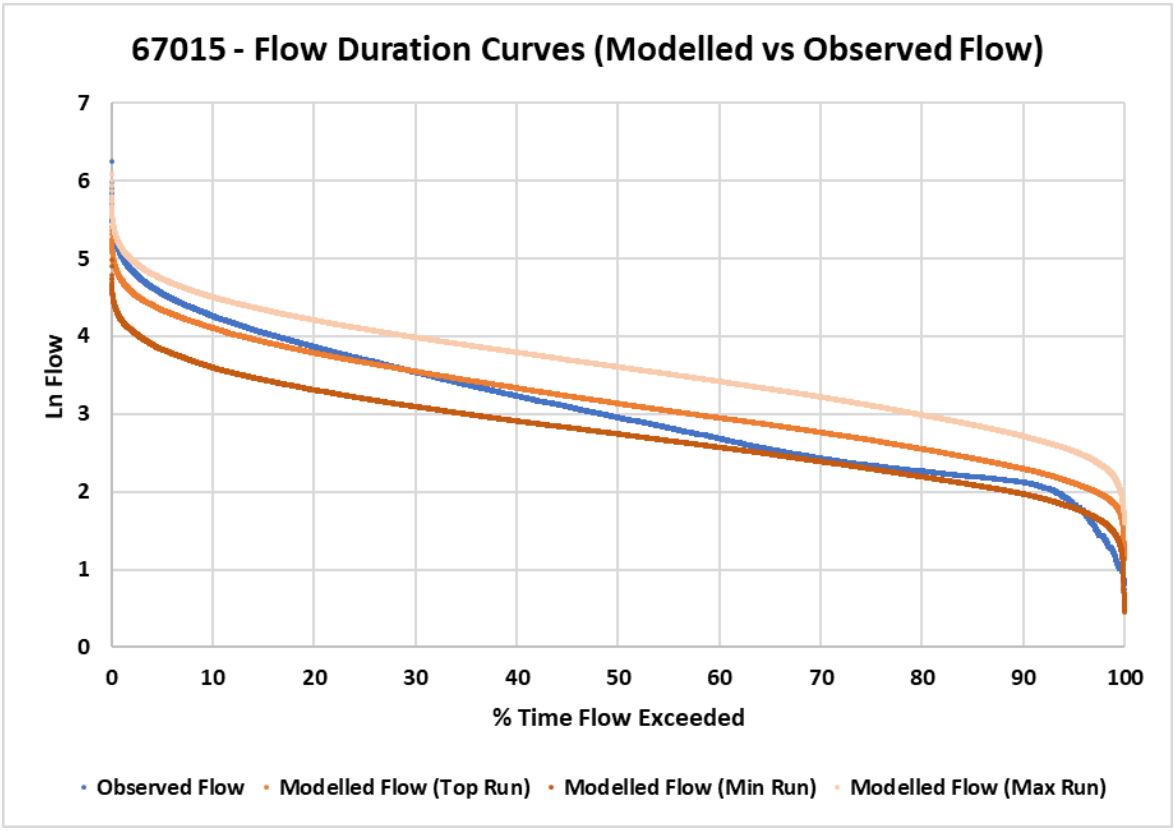

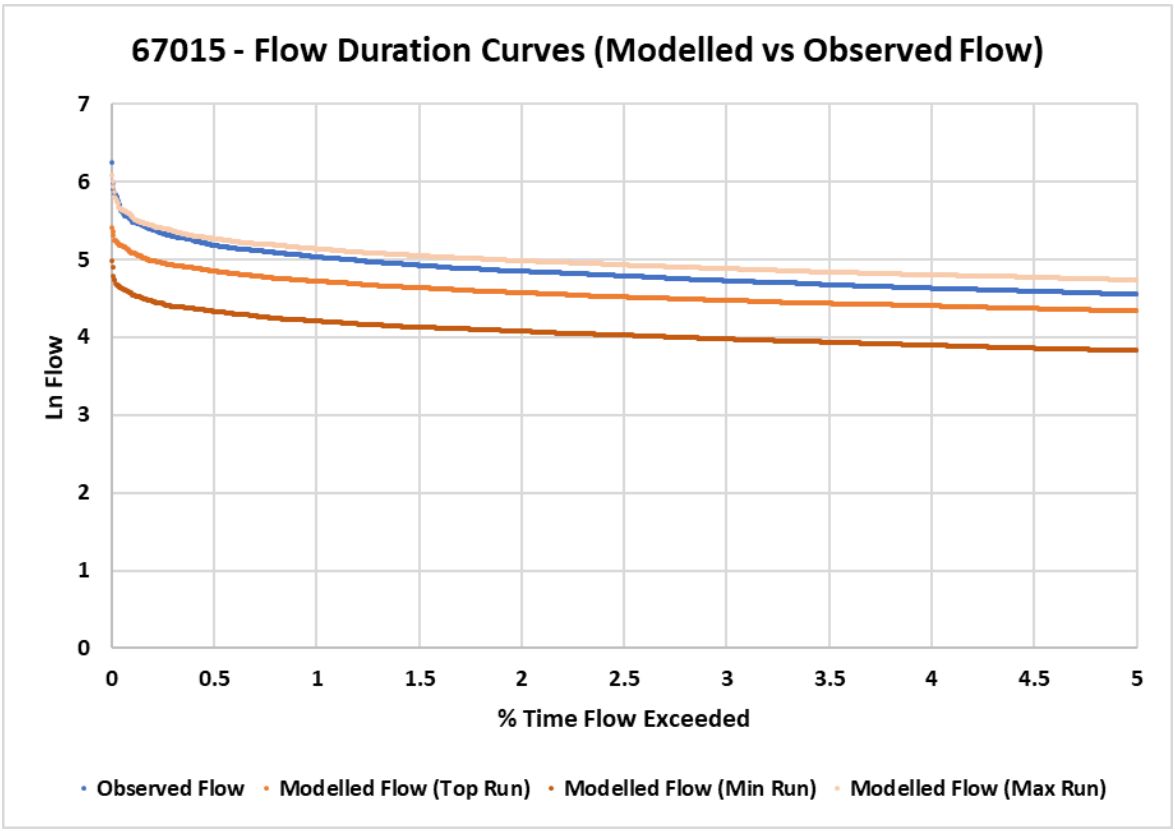

Appendix C9: Flow duration curve for the Dee (67015) showing the observed flow (NRFA), the top (best) performing run of 500 ensembles, and the minimum/maximum flow estimates (Smith et al. 2018). Flow values shown with a natural log transformation.

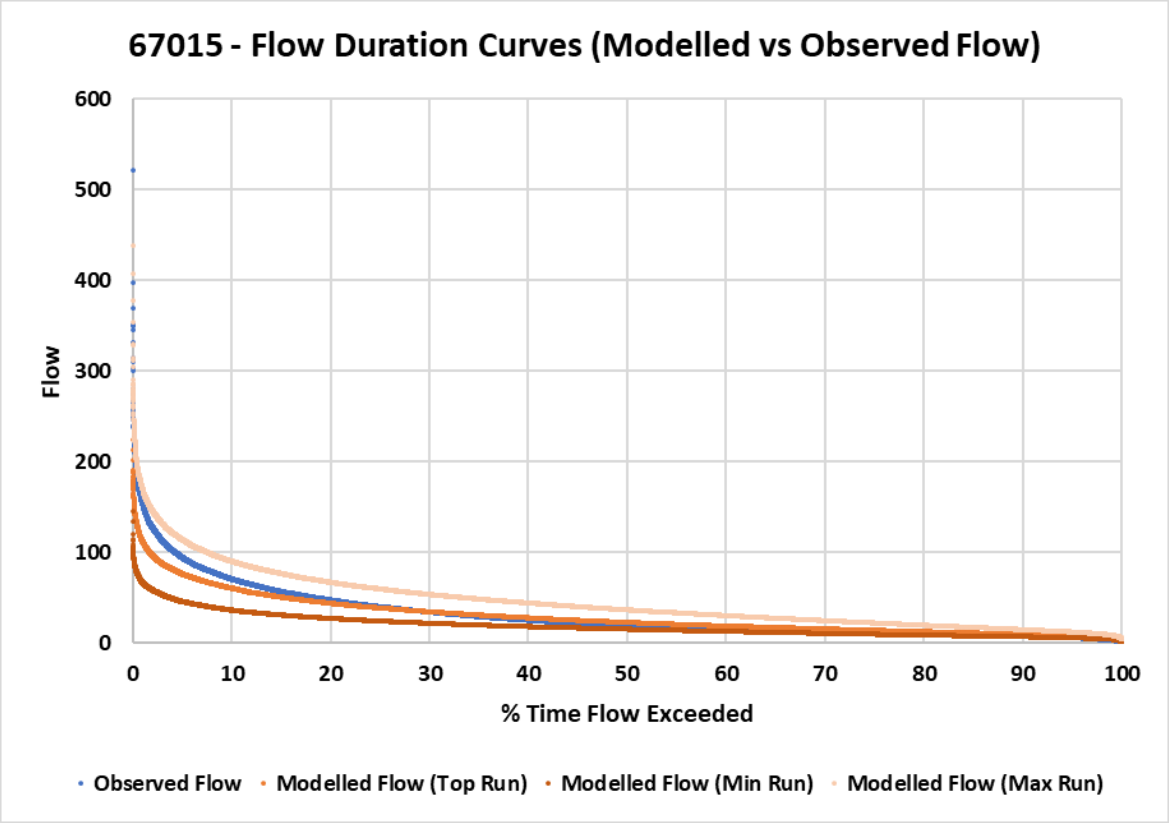

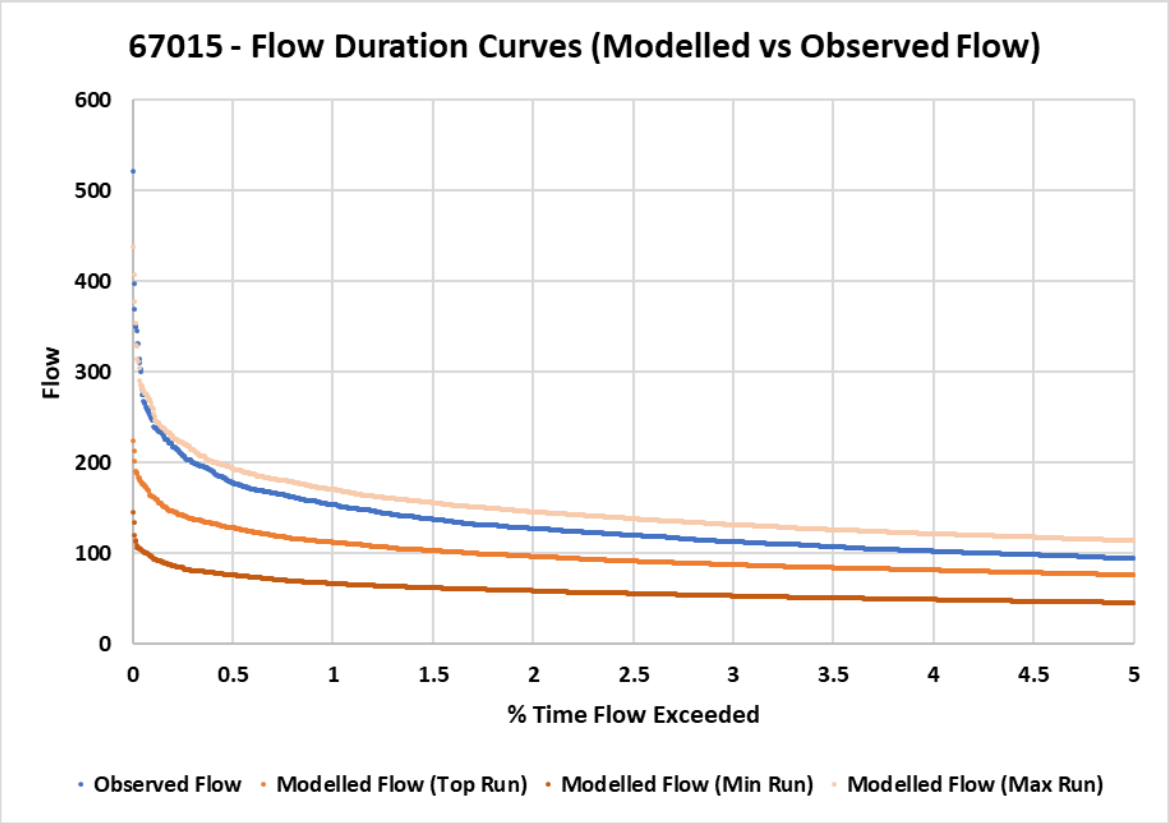

Appendix C10: Flow duration curve for the Dee (67015) showing the observed flow (NRFA), the top (best) performing run of 500 ensembles, and the minimum/maximum flow estimates (Smith et al. 2018).

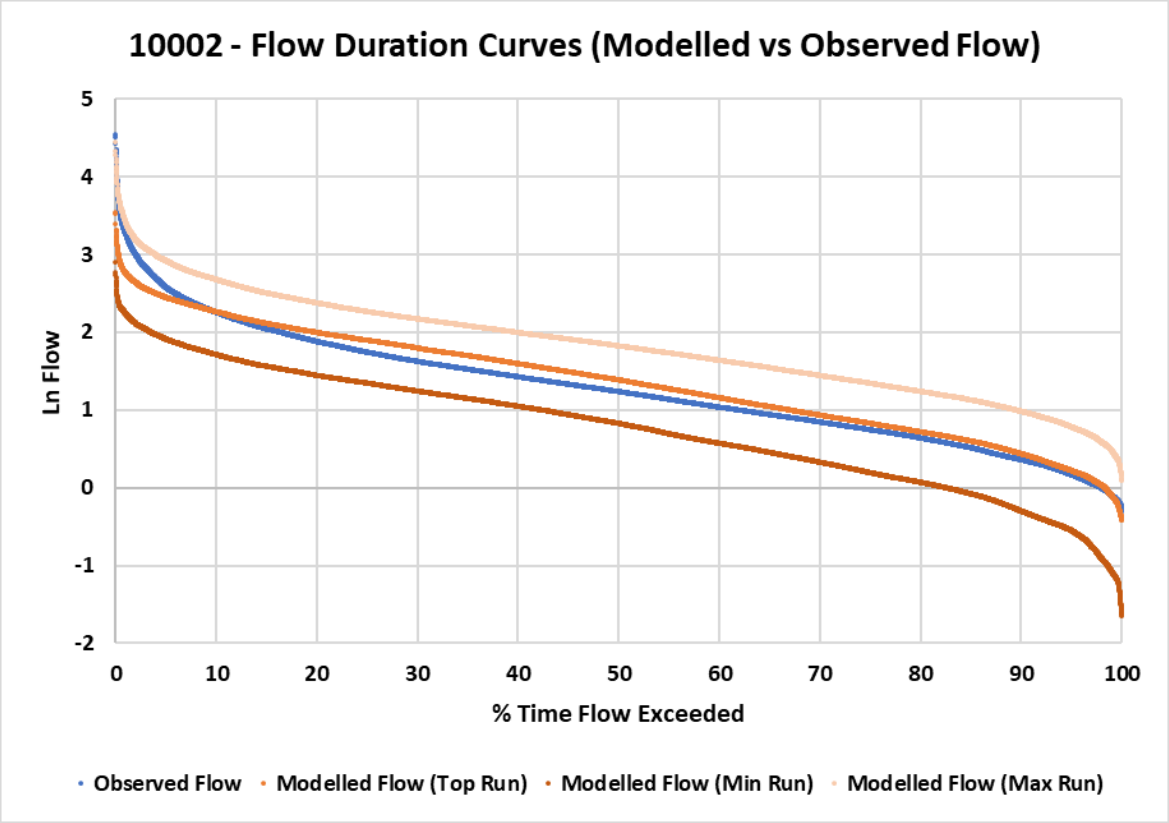

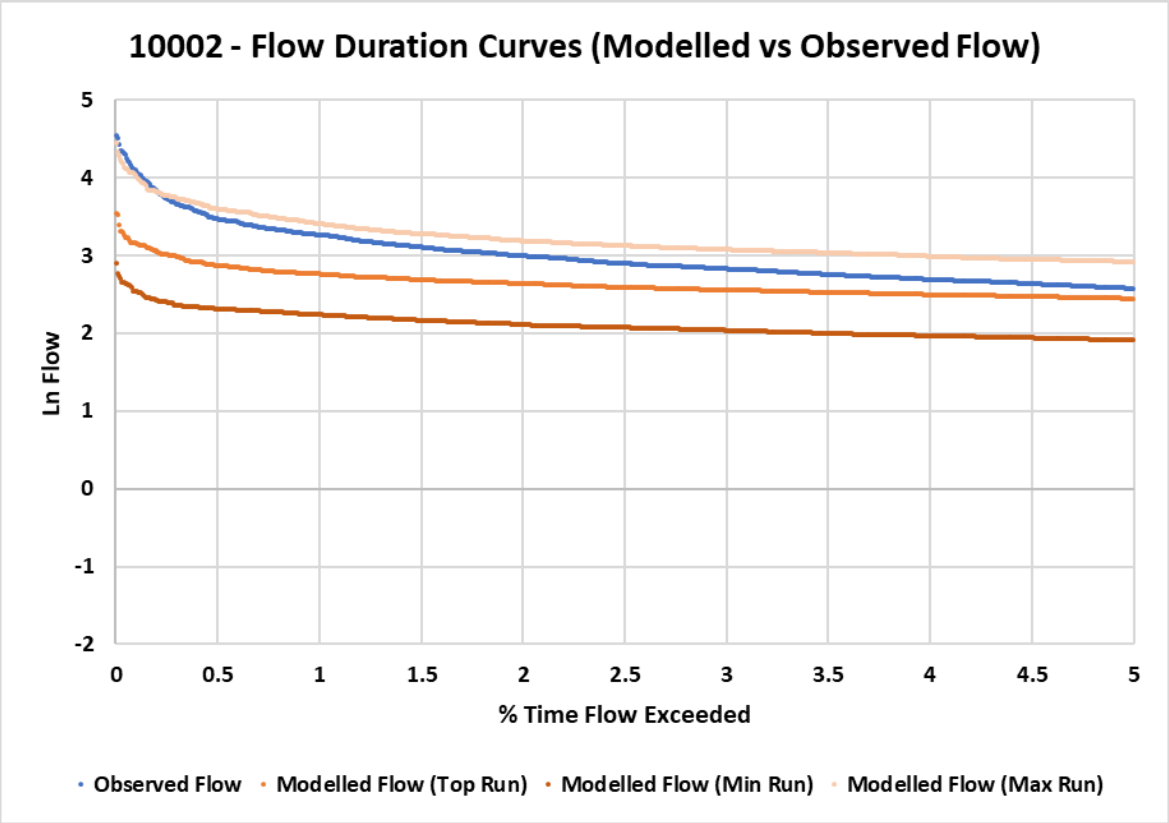

***Appendix C11**: Flow duration curve for the Ugie (10002) showing the observed flow (NRFA), the top (best) performing run of 500 ensembles, and the minimum/maximum flow estimates (Smith et al. 2018). Flow values shown with a natural log transformation.*

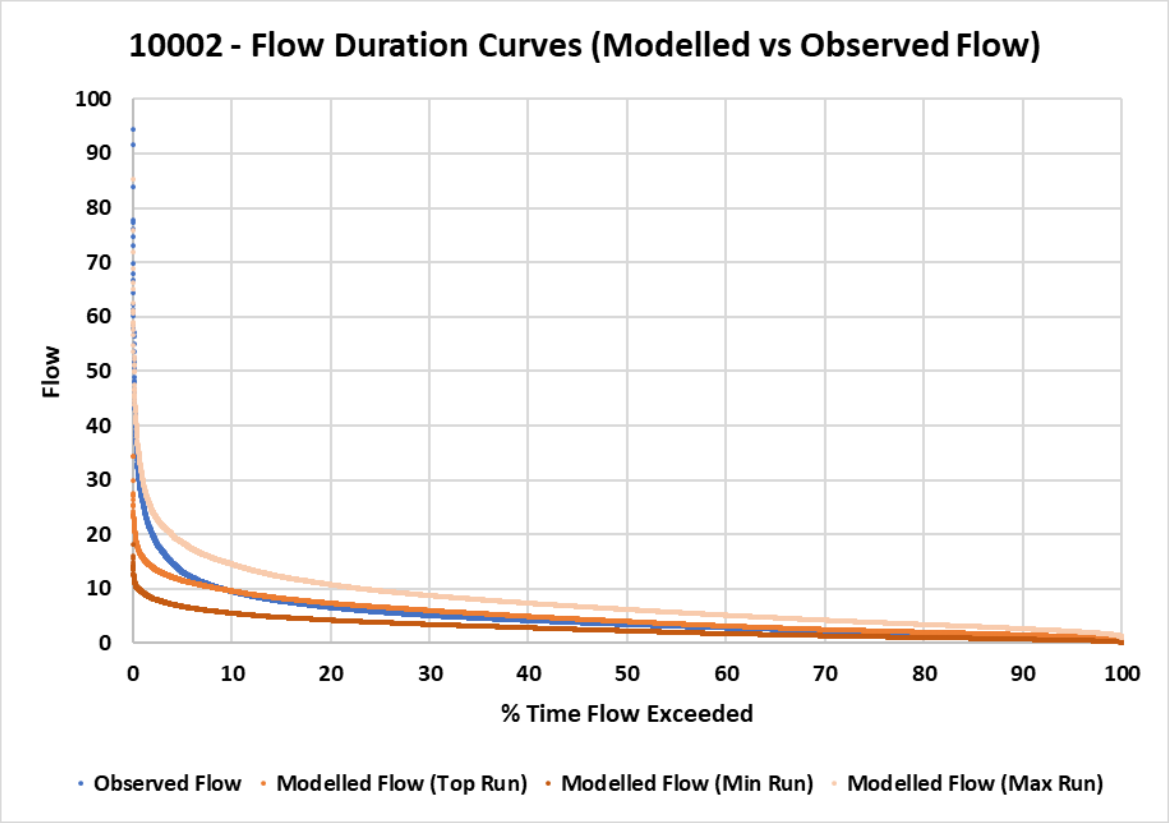

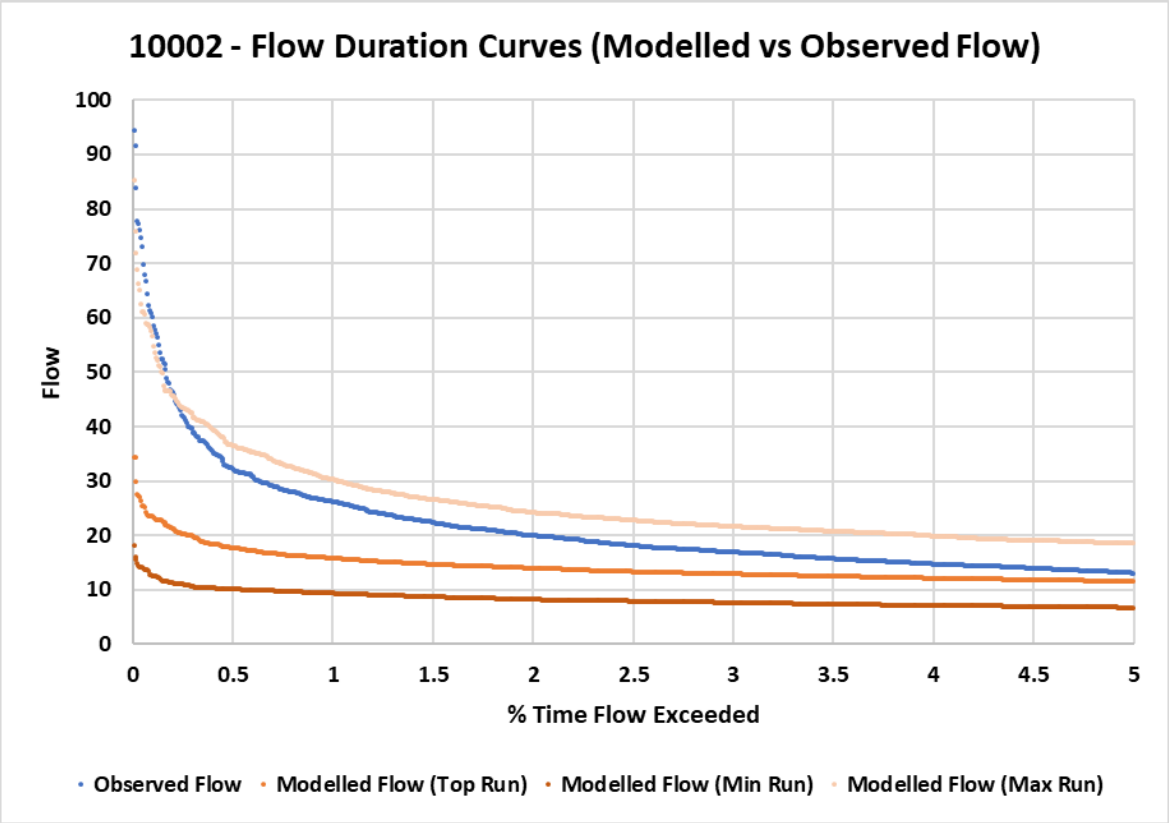

***Appendix C12**: Flow duration curve for the Ugie (10002) showing the observed flow (NRFA), the top (best) performing run of 500 ensembles, and the minimum/maximum flow estimates (Smith et al. 2018).*

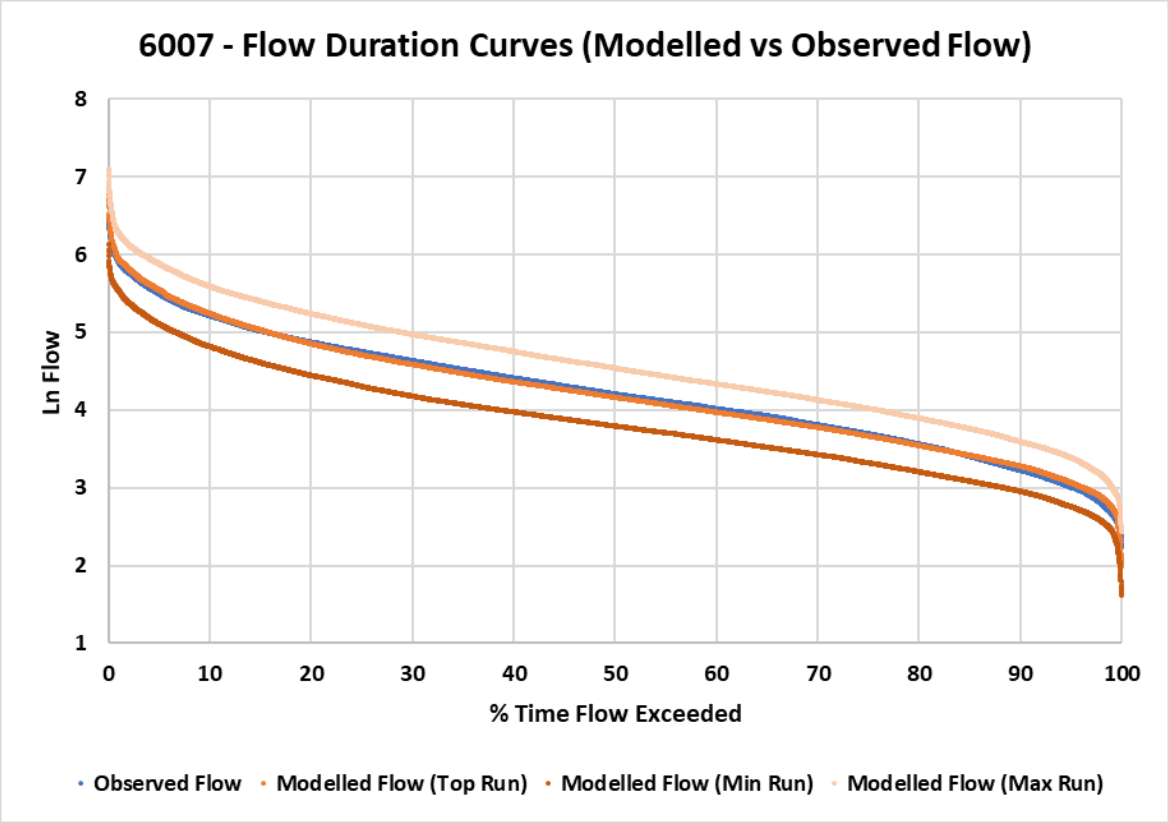

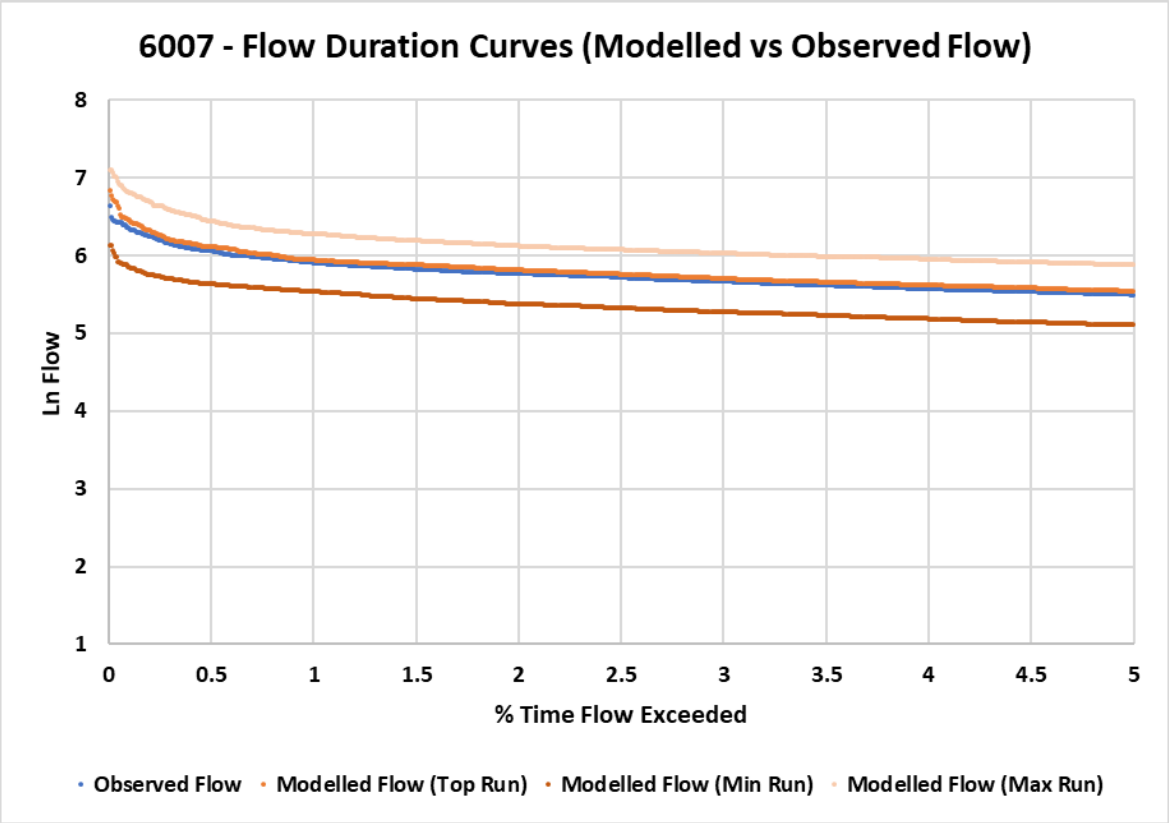

Appendix C13: Flow duration curve for the Ness (6007) showing the observed flow (NRFA), the top (best) performing run of 500 ensembles, and the minimum/maximum flow estimates (Smith et al. 2018). Flow values shown with a natural log transformation.

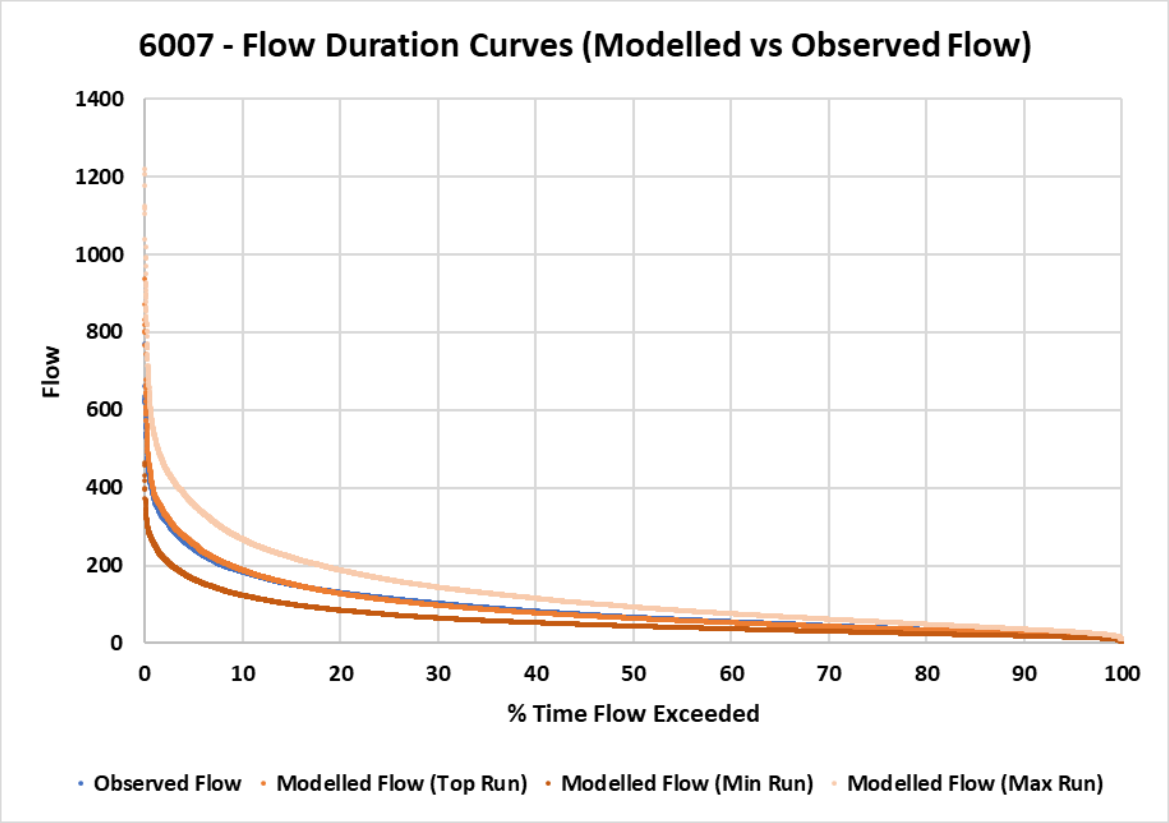

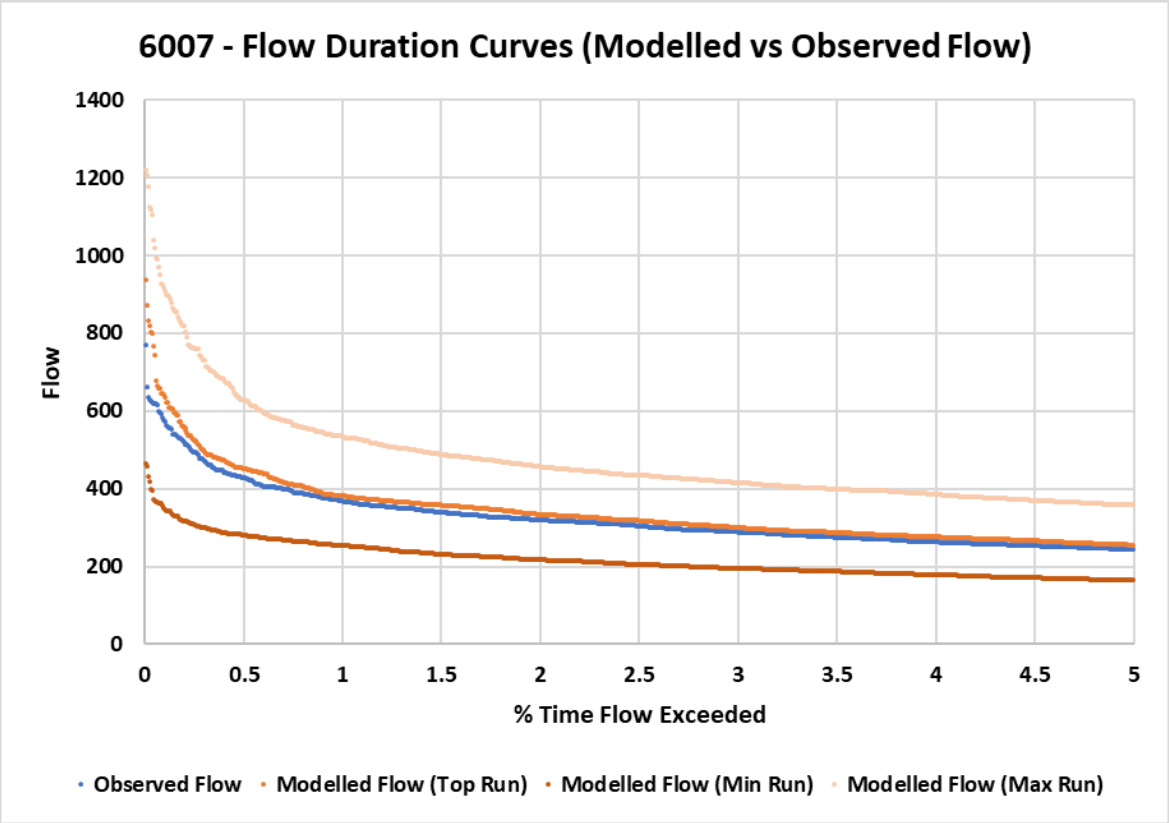

Appendix C14: Flow duration curve for the Ness (6007) showing the observed flow (NRFA), the top (best) performing run of 500 ensembles, and the minimum/maximum flow estimates (Smith et al. 2018).

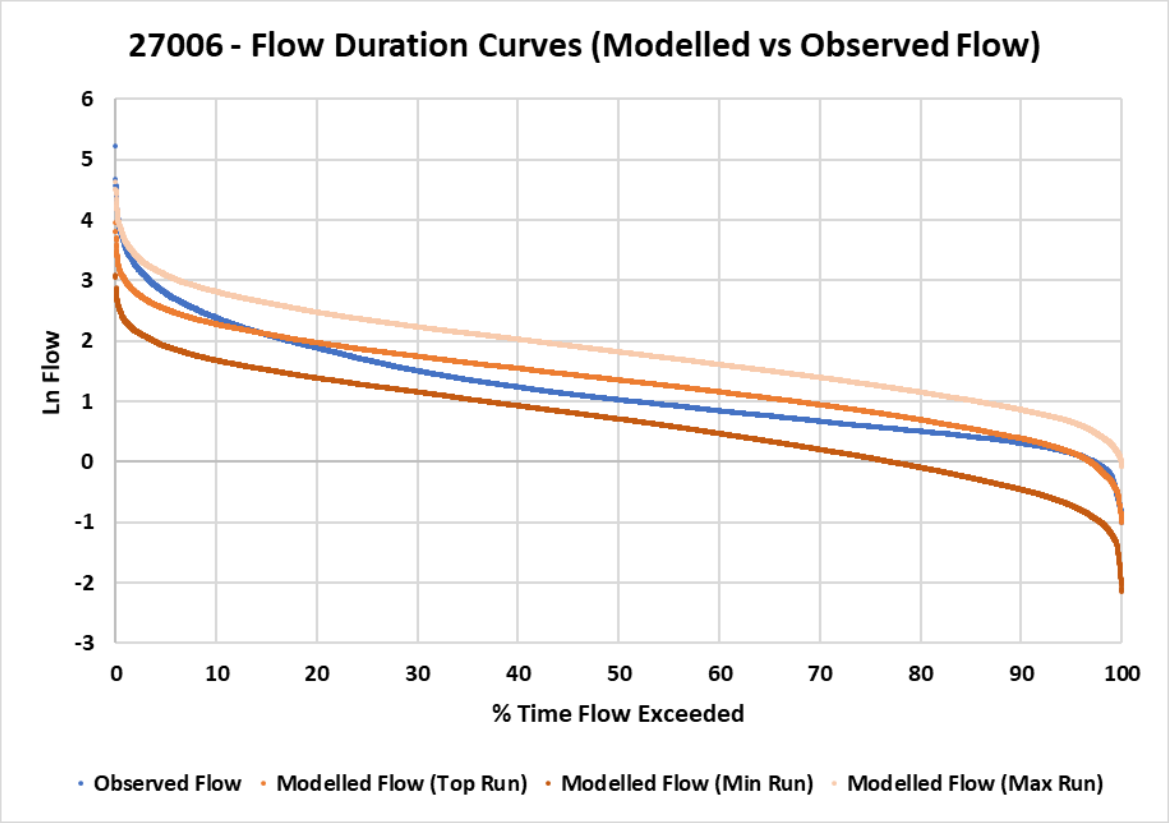

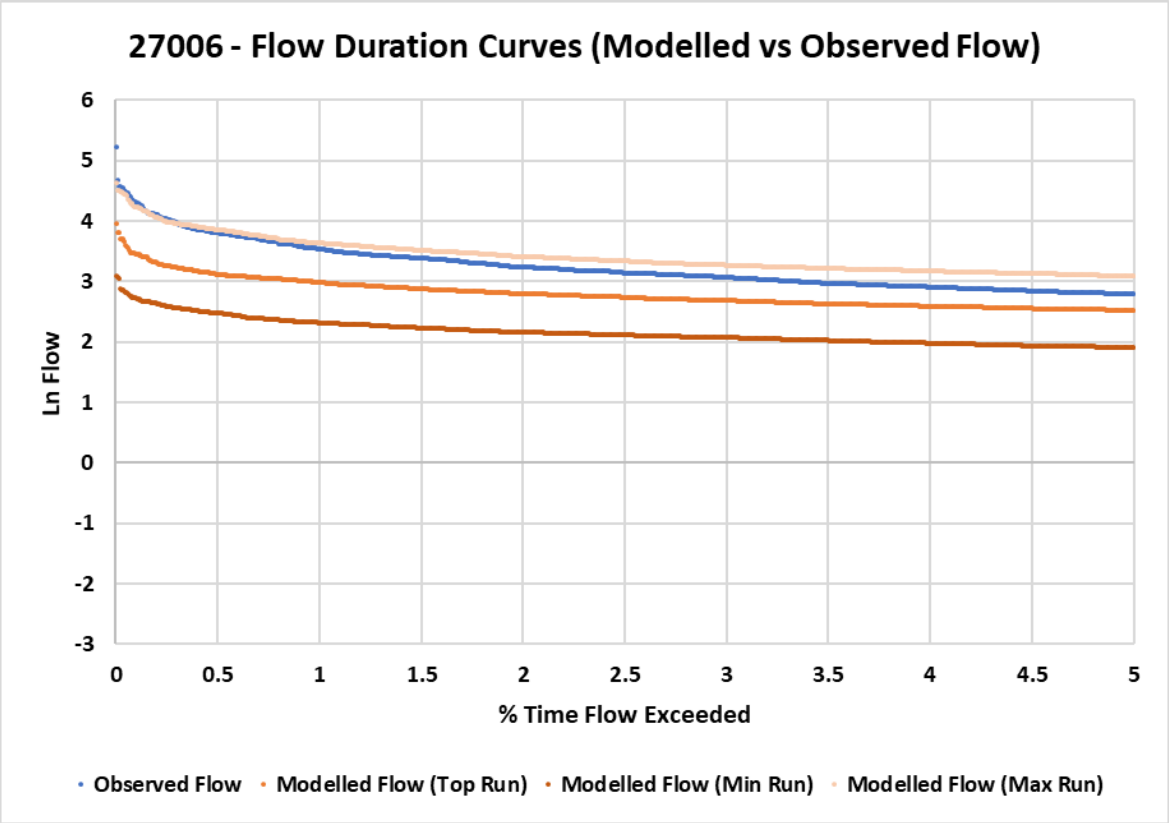

***Appendix C15**: Flow duration curve for the Don (27006) showing the observed flow (NRFA), the top (best) performing run of 500 ensembles, and the minimum/maximum flow estimates (Smith et al. 2018). Flow values shown with a natural log transformation.*

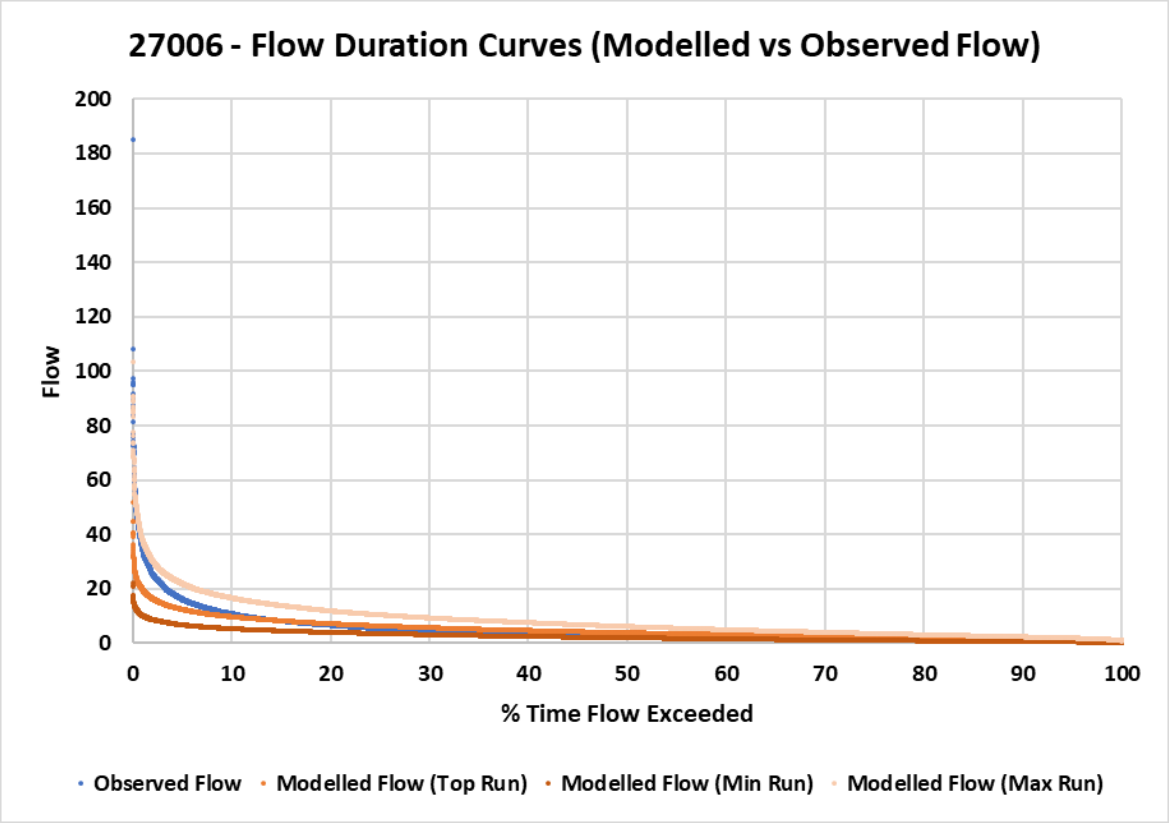

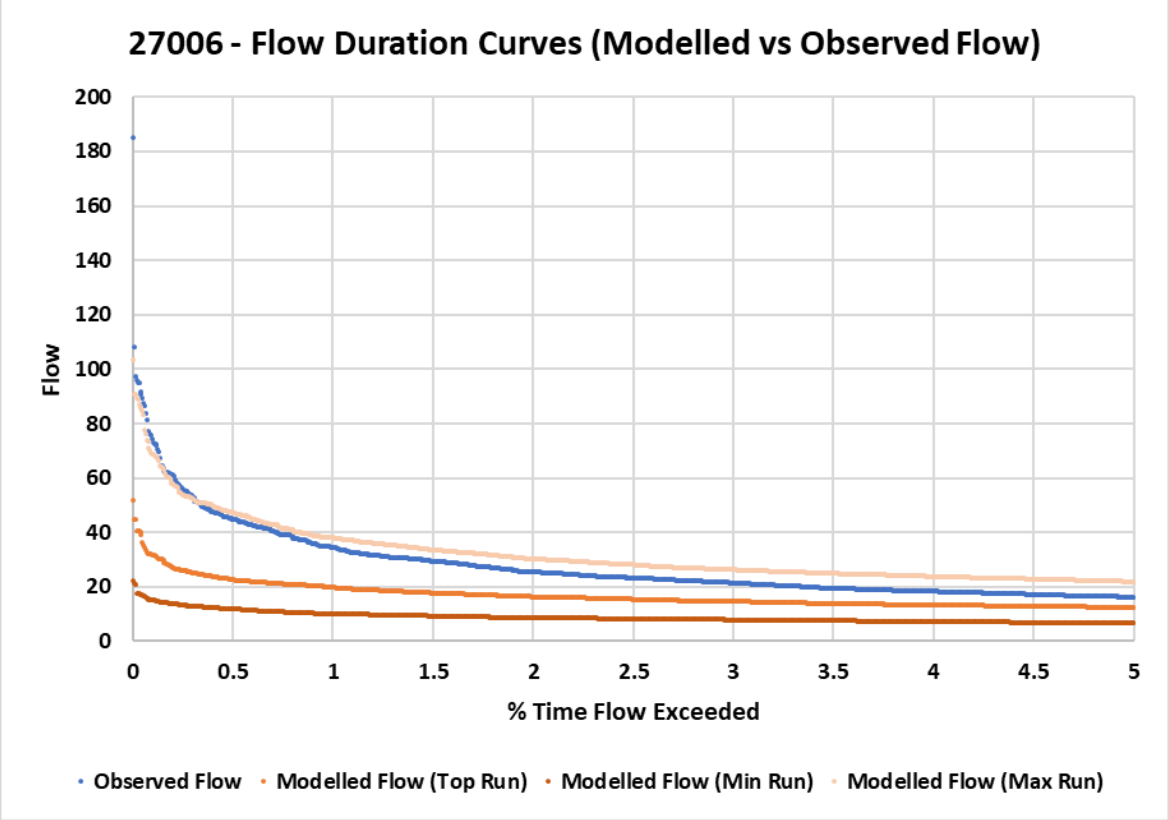

Appendix C16: Flow duration curve for the Don (27006) showing the observed flow (NRFA), the top (best) performing run of 500 ensembles, and the minimum/maximum flow estimates (Smith et al. 2018).

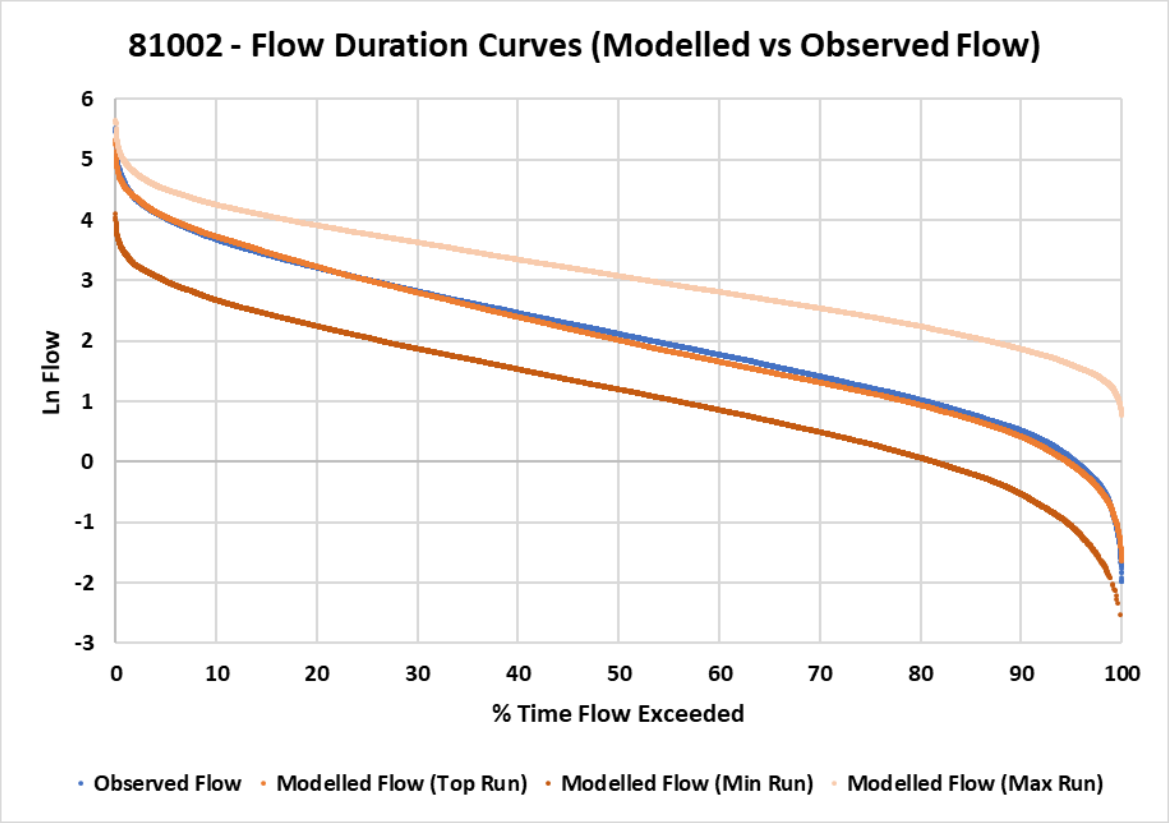

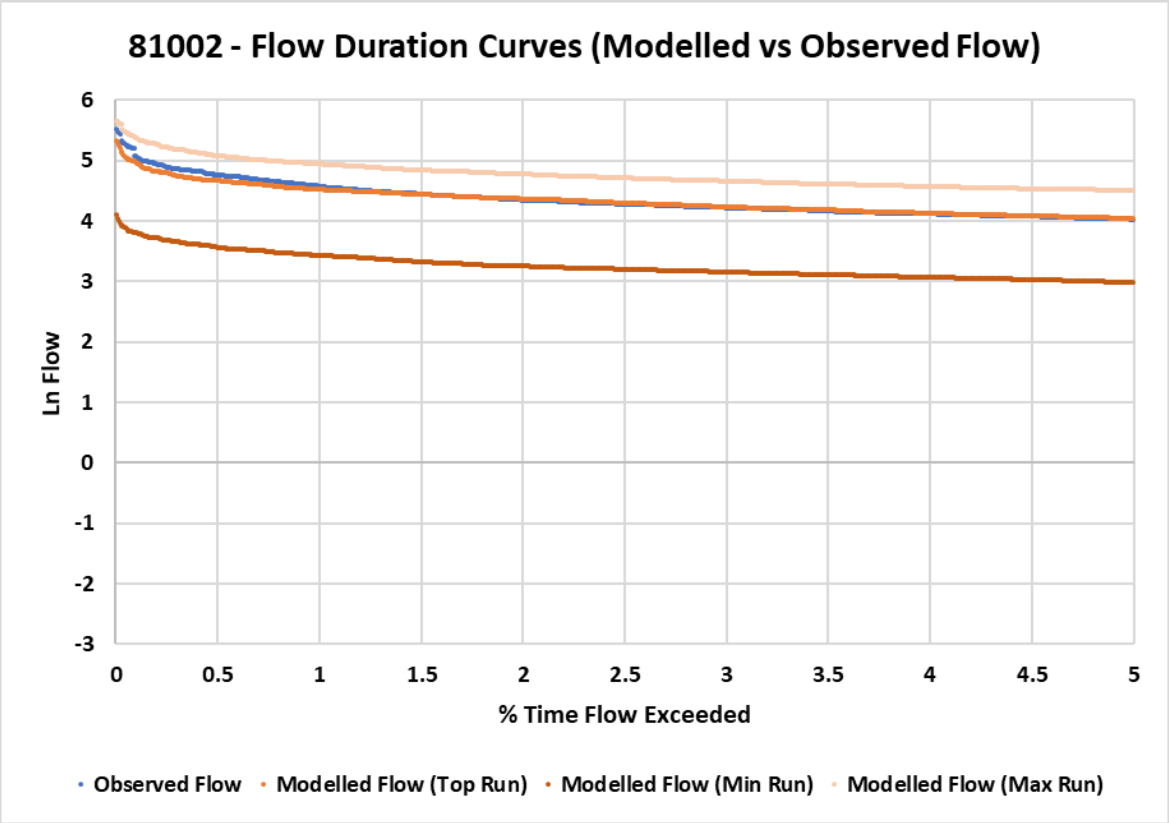

***Appendix C17**: Flow duration curve for the Cree (81002) showing the observed flow (NRFA), the top (best) performing run of 500 ensembles, and the minimum/maximum flow estimates (Smith et al. 2018). Flow values shown with a natural log transformation.*

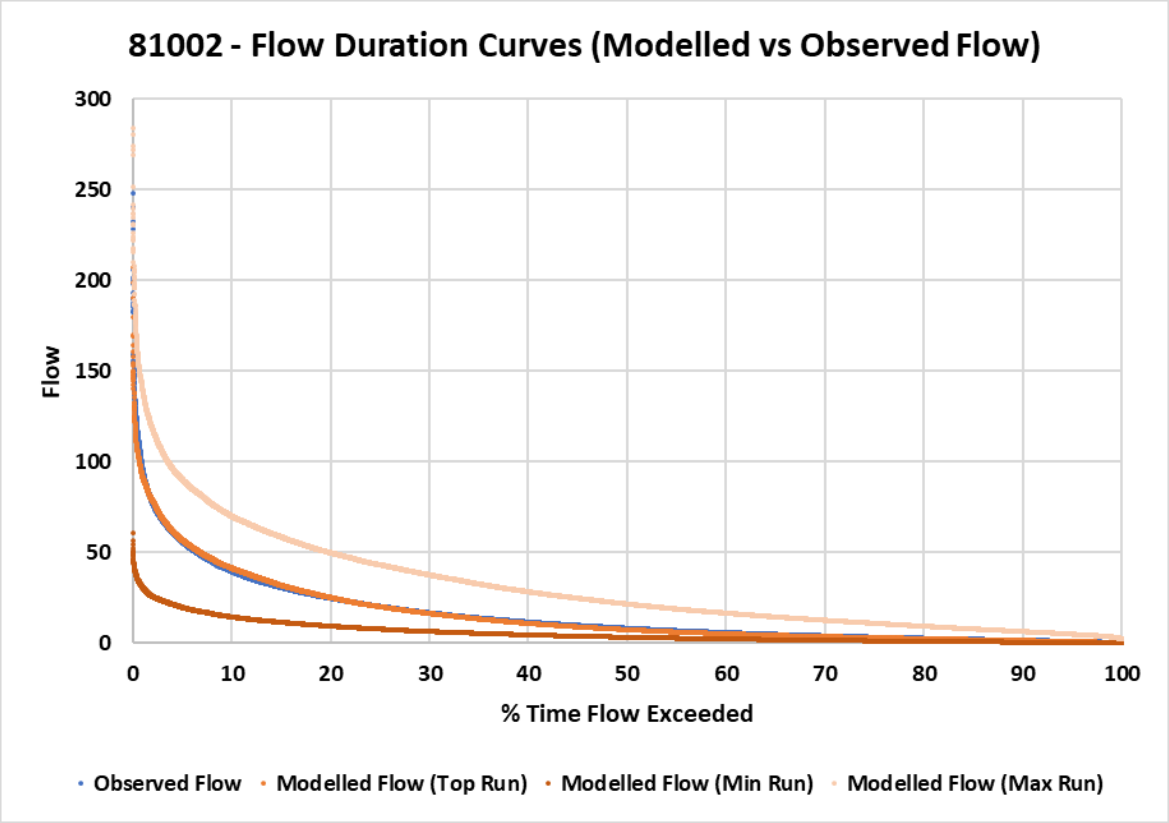

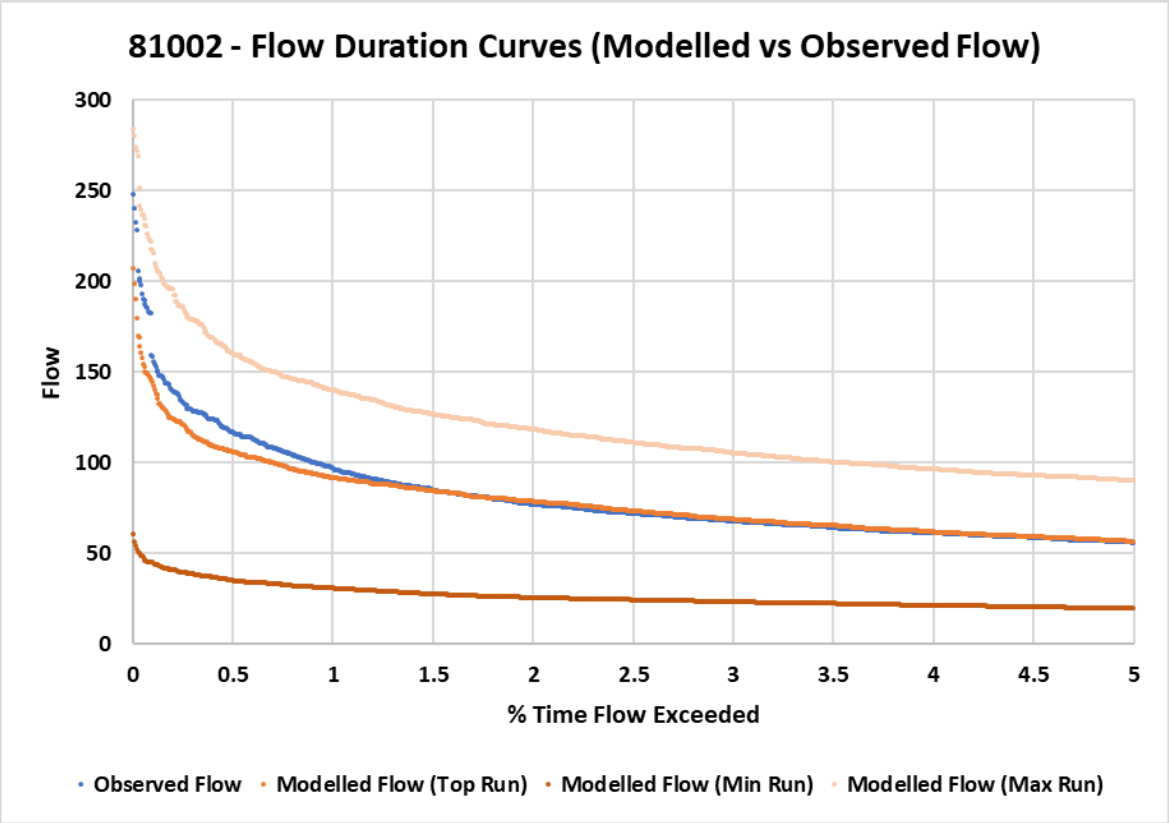

Appendix C18: Flow duration curve for the Cree (81002) showing the observed flow (NRFA), the top (best) performing run of 500 ensembles, and the minimum/maximum flow estimates (Smith et al. 2018).

Appendix D: Circulation Index Histograms

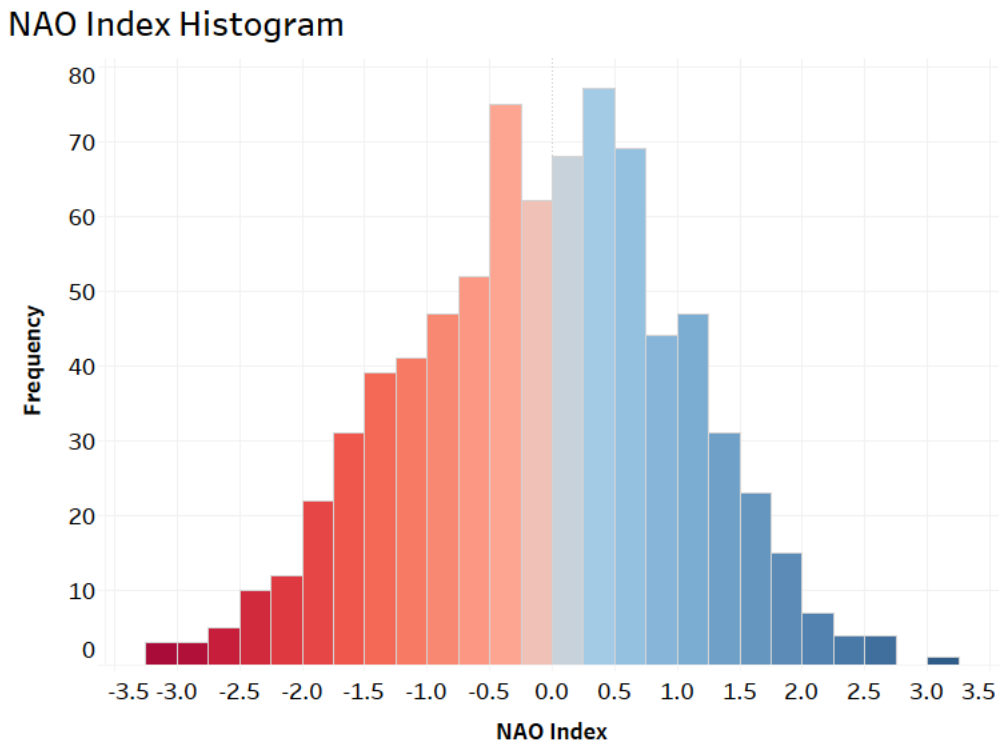

Appendix D1: *Histogram of the NOAA NAO Index (NOAA 2021a)*

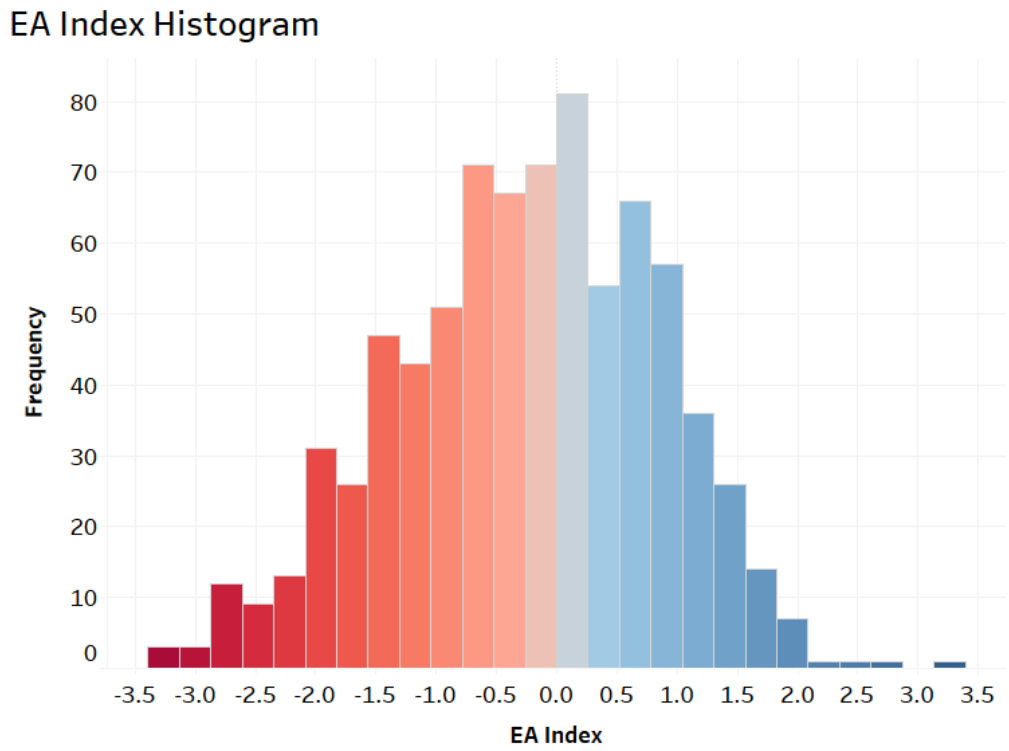

Appendix D2: *Histogram of the NOAA EA Index (NOAA 2021a)*